

***"Chlorochromatium aggregatum"* – molecular basis of  
a bacterial symbiosis**

Dissertation  
der Fakultät für Biologie  
der Ludwig-Maximilians-Universität München

vorgelegt von

**Kajetan Vogl**  
aus München

München  
im Dezember 2007

1. Gutachter: Prof. Dr. Jörg Overmann, LMU München
2. Gutachter: Prof. Dr. Anton Hartmann, LMU München

Tag des Promotionskolloquiums: 18.02.2008

## Publications originating from this thesis

### Chapter 2:

**Vogl K**, Glaeser J, Pfannes KR, Wanner G, Overmann J (2006) *Chlorobium chlorochromatii* sp. nov., a symbiotic green sulfur bacterium isolated from the phototrophic consortium "*Chlorochromatium aggregatum*". Arch Microbiol 185:363-372

### Chapter 3:

**Vogl K**, Dreßen M, Wenter R, Schlickerrieder M, Overmann J (2007) Identification and analysis of four candidate symbiosis genes from "*Chlorochromatium aggregatum*", a highly developed bacterial symbiosis. Submitted

### Chapter 4:

Wanner G, **Vogl K**, Overmann J (2007) Ultrastructural characterization of the prokaryotic symbiosis in "*Chlorochromatium aggregatum*". manuscript

### Chapter 5:

Kanzler BEM, Pfannes KR, **Vogl K**, Overmann J (2005) Molecular characterization of the nonphotosynthetic partner bacterium in the consortium "*Chlorochromatium aggregatum*". Appl Environ Microbiol 71:7434-7441

### Chapter 6:

Pfannes KR, **Vogl K**, Overmann J (2007) Heterotrophic symbionts of phototrophic consortia: members of a novel diverse cluster of *Betaproteobacteria* characterized by a tandem *rrn* operon structure. Environ Microbiol 9:2782-94

## **Contributions of the Co-authors**

### **Chapter 2:**

Dr. Jens Glaeser generated an enrichment culture containing the epibiont of “*Chlorochromatium aggregatum*” and a heterotrophic bacterium. He also performed the DGGE.

Kristina Pfannes determined the salinity optimum and the cell surface hydrophobicity of the epibiont. She did the KOH-string test and the gram-staining and extracted the pigments of the epibiont.

Prof. Dr. Gerhard Wanner carried out the electron microscopy.

### **Chapter 3:**

Martina Müller and Martina Schlickerieder made the disaggregation studies of “*Chlorochromatium aggregatum*”.

Roland Wenter performed the long range RT-PCR of Cag\_1919.

### **Chapter 4:**

Kajetan Vogl cultivated the phototrophic consortia and *Chlorobium chlorochromatii*. He discussed the results and wrote the manuscript together with Prof. Dr. Wanner.

### **Chapter 5:**

Kajetan Vogl developed the experimental strategy to get the 16S rRNA sequence of the central bacterium together with Prof. Dr. Overmann. He established the design of specific probe and FISH with helper oligonucleotides with Cont-995 and instructed the diploma student Birgit Kanzler in these methods.

### **Chapter 6:**

Kajetan Vogl developed the new cultivation approach of phototrophic consortia.

I hereby confirm the above statements

Kajetan Vogl

Prof. Dr. Jörg Overmann

---

**Table of contents**

	<b>Page</b>
<b>Chapter 1</b>	<b>1</b>
Introduction	
<b>Chapter 2</b>	<b>19</b>
<i>Chlorobium chlorochromatii</i> sp. nov., a symbiotic green sulfur bacterium isolated from the phototrophic consortium " <i>Chlorochromatium aggregatum</i> "	
Abstract	20
Introduction	21
Material and Methods	22
Results and Discussion	28
References	38
<b>Chapter 3</b>	<b>41</b>
Identification and analysis of three candidate symbiosis genes from " <i>Chlorochromatium aggregatum</i> ", a highly developed bacterial symbiosis	
Summary	42
Introduction	43
Results	44
Discussion	57
Experimental Procedures	62
References	69
<b>Chapter 4</b>	<b>75</b>
Ultrastructural elements of the prokaryotic symbiosis in " <i>Chlorochromatium aggregatum</i> "	
Abstract	76
Introduction	77
Material and Methods	78
Results	80
Discussion	89
References	95

<b>Chapter 5</b>	Molecular characterization of the non-photosynthetic partner bacterium in the consortium “ <i>Chlorochromatium aggregatum</i> ”	<b>99</b>
	Abstract	100
	Introduction	101
	Material and Methods	102
	Results and Discussion	109
	References	118
<b>Chapter 6</b>	Heterotrophic symbionts of phototrophic consortia: members of a novel diverse cluster of <i>Betaproteobacteria</i> characterized by a tandem <i>rrn</i> operon structure	<b>123</b>
	Summary	124
	Introduction	125
	Results and Discussion	127
	Experimental Procedures	141
	References	146
<b>Chapter 7</b>	Discussion	<b>153</b>
<b>Chapter 8</b>	Summary	<b>169</b>

**I. Danksagung****II. Lebenslauf**

# Introduction

## Symbiotic relationships

Living together of two different species of organisms independent on the outcome of the interaction was defined as symbiosis by de Bary (1879). Symbiosis can therefore be seen as a long-term interaction between organisms that ranges from mutualistic to pathogenic associations. Mostly the term “symbiosis” is used for interactions where at least one organism benefits from the other. Two kinds of cooperation can be distinguished: commensalism and mutualism. In a commensal relationship one individual benefits but not the other. In mutual interaction both partners benefit with a range from only marginal support to absolute mutual dependence.

## Symbiosis of bacteria with eukaryotes

Many symbioses involve prokaryotes which are associated with eukaryotes. For symbiosis between microbes and animals, several model systems have been developed and full genome sequences of symbionts are available. Examples are the genomes of *Buchnera* sp., *Wigglesworthia* sp., *Sodalis glossinidius*, *Vibrio fischeri* and *Photorhabdus luminescens* (Moran 2006). *Buchnera aphidicola* is a symbiont of aphids and provides them with essential amino acids. African tsetse flies harbor *Wigglesworthia* sp., *Sodalis glossinidius*. *Sodalis glossinidius* has three type III secretion systems and *Wigglesworthia* supplies the flies with vitamins and cofactors. *Vibrio fischeri* lives in specialized light organs of *Euprymna scolopes*. The light produced by *Vibrio fischeri* uses *Euprymna scolopes* for counterlighting to reduce its visibility to predators (Dale and Moran 2006; Moran 2006). *Photorhabdus luminescens* shows a mutual and virulent behavior during his life-cycle. *Photorhabdus* colonizes the intestinal tract of young nematodes with infect insect hosts. The bacteria are released into the blood of the insects. *Photorhabdus* then kills the insects and converts the insect body into food source for nematodes and reinfects young nematodes. Genes for the production of bioactive compounds were found in the genome of *Photorhabdus luminescens* (Moran 2006; Goodrich-Blair and Clarke 2007). Among the symbioses between bacteria and plant, the root nodule symbiosis of rhizobia and legumes is well understood. The bacterial symbionts fix molecular dinitrogen and provide reduced nitrogen for plant growth. The plant provides photosynthates in form of dicarboxylic acid, particularly malate and succinate (Lodwig and Poole 2003) and a microaerobic niche for the oxygen-sensitive nitrogenase. Both partners can be manipulated genetically and genome

sequence information is available. Genome sequences of the symbiotic nitrogen fixing bacteria *Bradyrhizobium japonicum*, *Mesorhizobium loti*, *Rhizobium leguminosarum* bv. *viciae* and *Sinorhizobium meliloti* are accessible via the webpage of DOE Joint genome institute (<http://www.jgi.doe.gov/>) and for *Medicago truncatula* TIGR *Medicago truncatula* Genome Project provides access to sequence information.

### **Bacteria-bacteria interaction**

In contrast to interactions between prokaryotes and eukaryotes, interspecies interactions between prokaryotic cells have been studied mainly with respect to syntrophic cooperations (Schink 2002). Syntrophic cooperations comprise anaerobic degradation of amino acids and sugars where energetical restrictions do not necessarily force the partner organisms into strict interdependencies because one of both can run the fermentation process on its own. Methanogenic degradation of electron-rich substrates like fatty acids, alcohols and aromatics where hydrogen acts predominantly as electron carrier between oxidative and reductive metabolic processes are further examples for syntrophic cooperations. Due to energy limitation, with only fractions of an ATP unit synthesized per substrate molecule metabolized, the cooperation is intensified by close proximity of the partner cells (Schink 1997; Schink 2002). A stable syntrophic association was also observed for green sulfur bacteria and sulfur- and sulfate-reducing bacteria (Pfennig 1980). Here, sulfur compounds act as electron carrier. Sulfide is oxidized by the green sulfur bacteria to sulfur or sulfate, which is subsequently reduced back by sulfur- and sulfate-reducing bacteria generating sulfide. The syntrophy via the sulfur cycle allows both bacteria to grow together with the same efficiency like a single bacterial species (Pfennig 1980).

### **Green sulfur bacteria**

Green sulfur bacteria (*Chlorobiaceae*) are anoxygenic and obligately photoautotrophs. They occur in the chemocline of stratified lakes where light reaches sulfide-containing water layers (van Gemerden and Mas 1995). The cells are characterized by spherical, ovoid, straight, or curved shapes and a gram-negative cell wall. All species lack flagella and are non-motile with the exception of *Chloroherpeton thalassium* whose cells are long unicellular filaments, highly flexible, and motile by gliding. Green and brown pigmented *Chlorobiaceae* can be distinguished. The brown species contain bacteriochlorophyll (BChl) *e* and, with the exception of the epibiont of "*Pelochromatium roseum*" (Glaeser *et al.* 2002), the carotenoids isorenieratene and  $\beta$ -

isorenieratene as the major light-harvesting pigments. Green-colored species contain bacteriochlorophyll *c* or *d* and chlorobactene and OH-chlorobactene as the main carotenoids (Imhoff 1995; Overmann 2001). All green sulfur bacteria have small amounts of BChl *a*. The photosynthetic apparatus comprise a type I reaction center, the Fenna-Matthews-Olson (FMO) protein and chlorosomes. Chlorosomes are 70-180 nm long and 30-60 nm wide ovoid bodies, which contain the photosynthetic pigments and are attached to the cytoplasmic face of the cellular membrane (Cohen-Bazire *et al.* 1964; Staehelin *et al.* 1978). Green sulfur bacteria have highly similar physiological capacities. Sulfur compounds (sulfide, sulfur or sometimes thiosulfate), H<sub>2</sub> or ferrous iron are used as electron donors and they grow photoautotrophically with CO<sub>2</sub> as sole carbon source. Carbon is fixed by the reverse tricarboxylic acid cycle and they photoassimilate a number of simple organic substrates like acetate or pyruvate in the presence of both sulfide and bicarbonate. Most strains require vitamin B<sub>12</sub> as growth factor. Most strains become light saturated at 10  $\mu\text{mol}\cdot\text{m}^{-2}\cdot\text{s}^{-1}$  (daylight fluorescence tubes), while growth becomes inhibited at intensities above 200  $\mu\text{mol}\cdot\text{m}^{-2}\cdot\text{s}^{-1}$  (Overmann 2001). Green sulfur bacteria form a tight phylogenetic group, separated from the eubacterial radiation (Fig.1) (Gibson *et al.* 1985). They are divided into four genera and 14 species (Imhoff 2003).

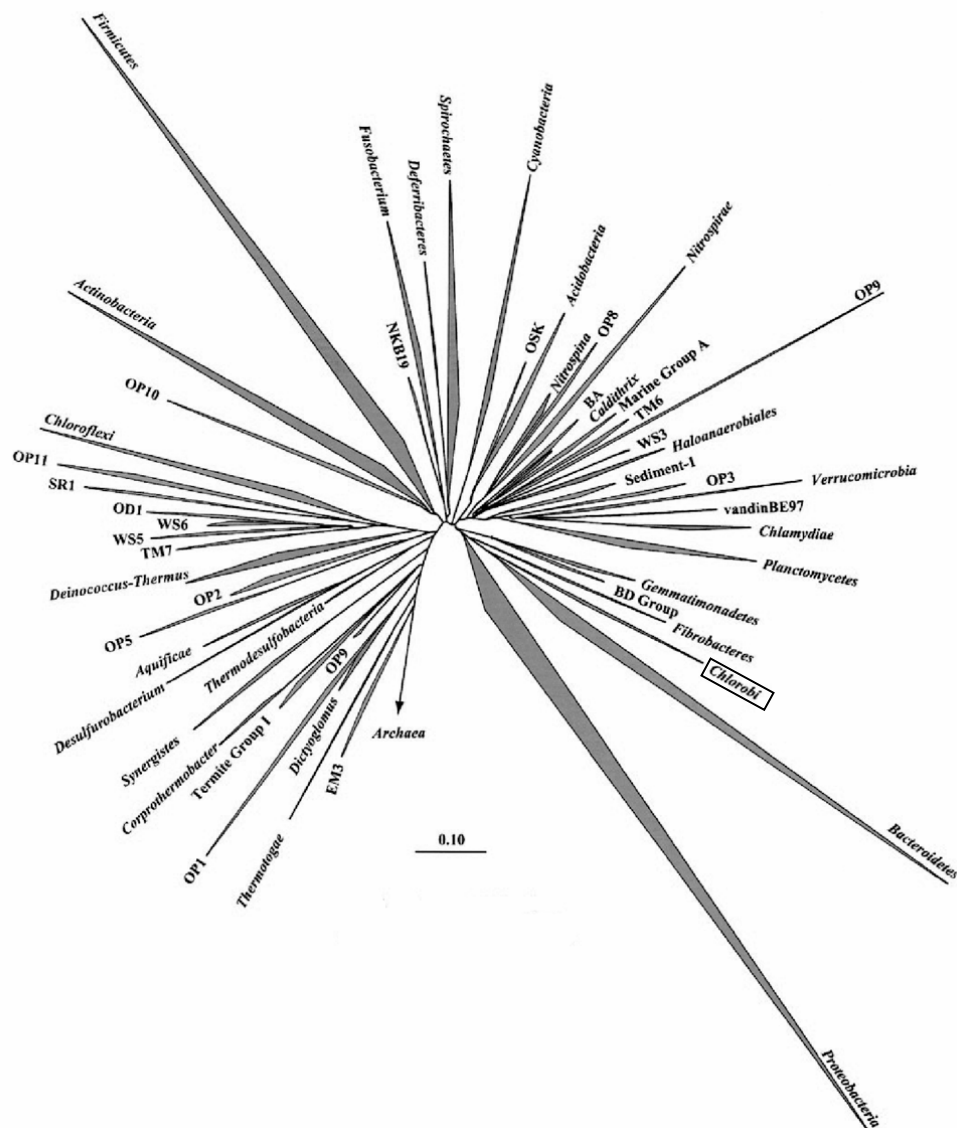


**Figure 1.** Phylogenetic tree of *Bacteria* showing established phyla (italicized Latin names) and candidate phyla described previously (Hugenholtz *et al.* 1998; Rappe and Giovannoni 2003; Harris *et al.* 2004) with the November 2003 ARB database (<http://arb-home.de>) (Ludwig *et al.* 2004) with 16,964 sequences that are >1,000 bp. The vertex angle of each wedge indicates the relative abundance of sequences in each phylum; the length of each side of the wedge indicates the range of branching depth found in that phylum. The group of *Chlorobiaceae* is highlighted with a box (adapted from Handelsman 2004).

## Phototrophic consortia

Particular green sulfur bacteria occur in symbiotic associations. These highly organized associations between green sulfur bacteria and a chemotrophic proteobacterium are called phototrophic consortia. In most cases a motile rod-shaped bacterium is surrounded by 13-69 green sulfur bacteria, so called epibionts (Fröstl and Overmann 1998; Overmann 2001; Overmann and Schubert 2002; Overmann 2005). In 1906, Lauterborn first described phototrophic consortia namely "*Chlorochromatium aggregatum*". Buder (1914) first mentioned that phototrophic consortia consist of a central colorless polar flagellated cell and many peripheral green cells. Since these first descriptions, eight morphologically different types of phototrophic consortia with a motile rod shaped central bacterium were found. These are "*C. aggregatum*" (Lauterborn 1906; Fröstl and Overmann 2000), "*Chlorochromatium glebulum*" (Skuja 1957; Fröstl and Overmann 2000), "*Chlorochromatium magnum*" (Fröstl and Overmann 2000), "*Chlorochromatium lunatum*" (Abella *et al.* 1998), "*Pelochromatium roseum*" (Lauterborn 1913; Tuschak *et al.* 1999), "*Pelochromatium roseo-viride*" (Gorlenko and Kusnezov 1972), "*Pelochromatium latum*" (Glaeser and Overmann 2004), "*Pelochromatium selenoides*" (Abella *et al.* 1998). They are differentiated on the basis of the color (green or brown), the cellular morphology and number of epibionts and the overall shape of consortia (Overmann 2005). Furthermore two non-flagellated morphotypes of phototrophic consortia "*Chloroplana vacuolata*" (Dubinina and Kuznetzov 1976) and "*Cylindrogloea bacterifera*" (Perfiliev 1914; Skuja 1957) were discovered. They contain gas vesicles and are immotile. Phototrophic consortia occur in many freshwater lakes worldwide at depths with low light intensities and low concentrations of sulfide (Overmann *et al.* 1998; Glaeser and Overmann 2004). There is a great diversity of phototrophic consortia in the natural environment and they show a nonrandom distribution and seem to be only slowly dispersed over long geographic distances (Glaeser and Overmann 2004). Phototrophic consortia can amount to two-thirds of the total bacterial biomass of the chemocline of lakes indicating an ecological relevance (Gasol *et al.* 1995). To date phototrophic consortia represent the most highly developed association between non-related bacteria. Fröstl and Overmann (1998) obtained a highly enriched culture of "*C. aggregatum*" (Fig. 2) from Lake Dagow through skillful chemotaxis experiments.

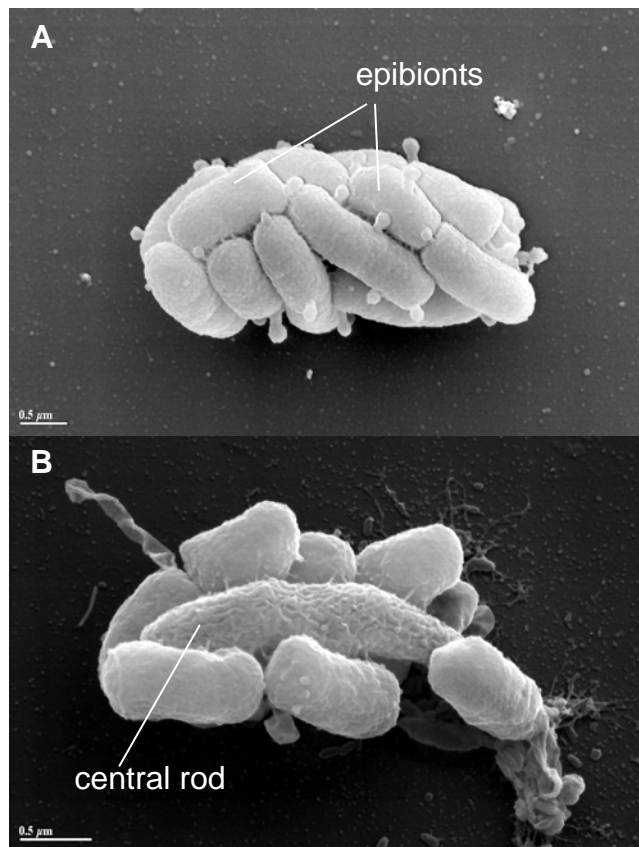


**Figure 2.** Scanning electron photomicrographs of “*Chlorochromatium aggregatum*“. **A** Intact consortium after fixation with 2% glutardialdehyde. The outer layer of epibionts covers the central bacterium. **B** “*C. aggregatum*” without fixation after exposure to air. Partial disaggregation lead to the uncovering of the central rod-shaped bacterium.

Initial fluorescence *in situ* hybridization (FISH) analysis revealed that the central rod of “*C. aggregatum*” from Lake Dagow as well as the central rod of “*C. magnum*” from Lake Echo belongs to the *Betaproteobacteria* (Fröstl and Overmann 2000). Phylogenetic analysis of the nearly complete 16S rRNA sequence showed that the central bacterium represents a so far isolated phylogenetic lineage related to *Rhodoferrax* sp., *Polaromonas vacuolata*, and *Variovorax paradoxus* within the family *Comamonadaceae* (Kanzler *et al.* 2005). Since all known sulfate reducing bacteria belong to the *Deltaproteobacteria* or to the low GC Gram-positive bacteria, an internal sulfur cycle between sulfide and elemental sulfur as physiological basis of the symbiosis (Pfennig 1980) seems to be unlikely. Phylogenetic affiliation of the epibiont by FISH showed that they belong to the green sulfur bacteria (Tuschak *et al.* 1999). The epibionts of phototrophic consortia represent unique 16S rRNA sequence types and form several distinct phylogenetic clusters (Fröstl and Overmann 2000; Glaeser and Overmann 2004). The epibionts oxidize sulfide photosynthetically like non symbiotic green sulfur bacteria (Fröstl and Overmann 1998).

Furthermore the epibionts of “*P. roseum*” assimilated  $\text{H}^{14}\text{CO}_3^-$  in a light-dependent manner and their  $\Delta\delta^{13}\text{C}$  values of the esterifying alcohols (tetradanol, farnesol, hexadecanol) of its bacteriochlorophyll molecules demonstrated that the epibiont grew photoautotrophically *in situ* like non-symbiotic green sulfur bacteria (Glaeser and Overmann 2003a). Several independent experimental observations indicated a rapid signal transfer between the epibionts and the central bacterium of phototrophic consortia. Epibionts of the same consortium were of the equal size and showed a nonrandom frequency distribution. The cell division of all epibionts took place synchronously and parallel to that of the central rod indicating a highly coordinated process (Overmann *et al.* 1998). “*C. aggregatum*” shows a scotophobic behavior. They accumulated at wavelength that correspond to the absorption maximum of BChl *c* of the immotile epibiont. Since phototrophic consortia are motile by the flagellated colorless central bacterium, a specific signal transfer must occur between the epibionts sensing the light and the motile central rod (Fröstl and Overmann 1998). A further example for signal transfer in phototrophic consortia was noticed in “*P. roseum*” in natural samples. Consortia were chemotactically attracted by sulfide and 2-oxoglutarate. The uptake of 2- $^{14}\text{C}$ (U)-oxoglutarate was monitored by microautoradiography and revealed that 2-oxoglutarate is utilized in the presence of light and sulfide but not if either light or sulfide were absent. Since the epibiont by itself is unable to use 2-oxoglutarate, the incorporation of 2-oxoglutarate by the central bacterium seem to be regulated by the metabolic state of the epibionts (Glaeser and Overmann 2003b). Since “*Chlorochromatium aggregatum*” can be cultivated in the laboratory, the genome of the epibiont *Chlorobium chlorochromatii* has been completely sequenced (<http://img.jgi.doe.gov/>) and the sequencing of the central rod is in progress. Accordingly phototrophic consortia can serve as a model for symbiosis between non-related prokaryotes. They will allow studies of mechanisms of cell-to-cell signaling, coordination of cell division and cell-to-cell contact and to study the coevolution of non-related bacteria.

### **Interaction of bacteria via signal exchange**

Bacteria communicate with each other via chemical signal molecules like  $\gamma$ -butyrolactones, quinolones, amino acids, oligopeptides, N-acyl homoserine lactones (AHL), autoinducer-2 (AI-2) and possibly other molecules (Bassler 2002). Three classes of molecules that serve for chemical signaling in bacteria are well known: oligopeptides, AHLs and the LuxS/AI-2 class.

### Signal exchange in gram positive bacteria

Gram-positive bacteria mainly use oligopeptides for signaling. The oligopeptide range from 5 to 17 amino acids and typically a preprotein is synthesized that is then proteolytically cleaved into an active signal peptide and exported from the cell. They are often posttranslationally modified by the incorporation of lactone and thioacetone groups, lanthionines and isoprenyl groups (Camilli and Bassler 2006; Keller and Surette 2006). Membrane-bound two-component signaling proteins receive the oligopeptide signals and signal transduction is mediated by a phosphorylation cascade that influences the activity of a DNA-binding transcriptional regulatory protein. The oligonucleotide signals are highly specific (Bassler 2002).

### Signal exchange in gram negative bacteria

A typical Gram-negative bacteria signal molecule is the acyl homoserine lactone. AHLs share a homoserine lactone moiety, but different acyl side chains are incorporated into the signal molecule. AHLs are synthesized from S-adenosylmethionine and particular fatty acyl chains by acyl-acyl carrier proteins and LuxI-type AHL synthases (Waters and Bassler 2005; Camilli and Bassler 2006; Keller and Surette 2006). Many AHLs cross membranes freely and typically the AHL signal is detected in the cytoplasm by a member of the LuxR family of transcriptional regulators. LuxR-AHL complexes bind DNA promoter elements and activate the transcription of target genes. The specificity of the LuxR-AHL interaction is ensured by the acyl binding pocket in the LuxR protein which is highly selective for the acyl chain of its cognate AHL molecule (Bassler 2002; Camilli and Bassler 2006).

### Interspecies signal exchange

In contrast to the specific AHL and peptide signals, which are used for intraspecies cell-cell communication, the LuxS/AI-2 system seems to be a universal interspecies chemical language (Bassler 2002). This pathway exists in both Gram-positive and Gram-negative bacteria and was found in over 55 species (Vendeville *et al.* 2005). The enzyme LuxS has a further role in the metabolism of bacteria. AI-2 is generated as a byproduct of the S-adenosylmethionine, the main methyl donor in bacteria, metabolism. Two distinct structures of AI-2 were determined. The AI-2 of *Vibrio harveyi* is (2S,4S)-2-methyl-2,3,3,4-tetrahydroxytetrahydrofuran-borate and forms a complex with the receptor LuxP. In *Salmonella typhimurium*, the AI-2 is a (2R,4S)-2-methyl-2,3,3,4-tetrahydroxytetrahydrofuran and is bound by LsrB (Waters and Bassler 2005). The signal

transduction occurs by a phosphorylation cascade. There are many examples showing that bacteria respond to chemical substances that are produced by other organisms like crosstalk between AHL signal between *Pseudomonas aeruginosa* and *Burkholderia cepacia* in cystic-fibrosis and the communication of gram-positive bacteria of the oropharyngeal flora and *P. aeruginosa* via AI-2. However there are no conclusive examples of communication systems that have specifically evolved for interspecific interactions (Keller and Surette 2006). Phototrophic consortia are probably a suitable model, to search for an evolved interspecific communication system.

### **Cellular adhesion**

The repeat region of RTX (repeats in toxin) toxins mediates protein-target cell interaction (Lally *et al.* 1999). Generally, RTX toxins are typically found in Gram-negative pathogenic bacteria. Members of the RTX toxin family are cytolytic toxins, metallo-dependent proteases, lipases and nodulation-associated proteins (Welch 1995). The names are based on the fact that all members of the protein family contain six to 40 repetitions of a glycine- and aspartate-rich nonapeptide motif, which includes a GGXGXD consensus motif, in the carboxy-terminal half of the protein (Czuprynski and Welch 1995). The crystal structure of the alkaline protease of *Pseudomonas aeruginosa* turn out that  $\text{Ca}^{2+}$  ions are bound by the repeated GGXGXD sequence motif within a so called parallel beta roll motif (Baumann *et al.* 1993). Calcium is critical for the biological activity of RTX toxins. In general the RTX toxin operon consists of four genes in the transcriptional order C, A, B, and D. The A gene codes for the structural protein whereas the three remaining genes (B, C, and D) flanking the A gene are required for transporting and activating the RTX toxin (Czuprynski and Welch 1995). To become biological active, the RTX toxins have to be modified posttranslationally by fatty acid acylation. The modification depends on an acyl carrier protein and the C gene product. The gene products of the genes B and D are required for the transport of the RTX toxin (Lally *et al.* 1999). In contrast to other exoprotein groups the RTX toxins are not synthesized as a precursor with a cleavable amino-terminal signal sequence. They are secreted with a noncleavable C-terminal signal peptide that is recognized by the secretory apparatus of the B and D proteins (Braun *et al.* 1993). In general RTX toxins contain two domains. The three-dimensional structure of the alkaline protease of *P. aeruginosa* revealed a N-terminal proteolytic domain and a C-terminal calcium binding domain with glycine- and aspartate-rich nonapeptide motif forming a parallel beta roll motif (Baumann *et al.* 1993). Cytolytic RTX toxins have four hydrophobic regions which may be involved in pore

forming in target cells at the N-terminal region and also the nonapeptide motif at the C-terminal region (McWhinney *et al.* 1992). The C-terminal glycine/aspartate-rich RTX repeat region present in all RTX toxins is necessary for binding to the target cell (Ludwig *et al.* 1998; El-Azami-El-Idrissi *et al.* 2003) and  $\text{Ca}^{2+}$  ions are crucial for cell binding (Ludwig *et al.* 1998; Knapp *et al.* 2003). These two domains are separable (Cruz *et al.* 1990) and the catalytic domain is not required for cell binding (El-Azami-El-Idrissi *et al.* 2003).

### **Approach for dissecting the molecular basis of interaction**

A frequently problem in biological research is the discovery and characterization of specifically induced genes or genes specific for a certain organism. Also in this project, a major interest is the identification of symbiosis-specific properties of *Chl. chlorochromatii* CaD. A powerful method to tackle this problem was developed from Straus and Ausubel 1990 called genomic subtraction. The principle of subtraction hybridization is the removal of nucleic acid sequences from one strain which are homologous with sequences from another strain. The nucleic acid to be subtracted is hybridized with an excess of subtractor DNA. Those sequences specific for a strain that have not hybridized are then separated from the mixture. With this subtraction hybridization and shot-gun sequencing a symbiotic loci in *Rhizobium* was identified (Perret *et al.* 1994). A limitation of this method was that it worked poorly for obtaining low abundance transcripts. This problem was overcome by suppression subtractive hybridization. The method is based on suppression PCR and combines normalization and subtraction in a single procedure. The genomic DNA sample that contains the sequence of interest is called “tester” and the reference DNA sample is called “driver”. Tester and driver DNAs are hybridized and the remaining unhybridized DNAs represent tester-specific sequences. Genomic DNA from the tester and driver are digested with an appropriate restriction enzyme. The tester DNA fragments are then divided into two samples and ligated with two distinct adaptors. Each sample is first hybridized with an excess of driver DNA. During this first hybridization, tester molecules that match driver molecules mostly form driver-tester heterohybrids and are eliminated from the single strand (ss) fraction. Furthermore, the ss DNAs in the tester fraction are significantly enriched for tester-specific sequences, as nontarget sequences present in both tester and driver form heterodimers. The reannealing process is more effective for abundant molecules due to the second order kinetics of hybridization. Therefore the concentration of low and high abundant molecules become approximately equal. During the second hybridization the two samples are mixed

without denaturing and the remaining equalized and subtracted ss tester DNAs can reassociate and form new hybrids. A second portion of driver DNA was added to further enrich tester-specific sequences. Due to the adaptor and PCR primer structure exponential amplification can only occur in tester-tester heterohybrids (Fig. 3) (Diatchenko *et al.* 1996; Gurskaya *et al.* 1996). The suppression subtractive hybridization was also optimized for bacterial genomes and was used to identify bacterial strain specific genes. This was mainly done for pathogen bacterial strains which were subtracted from apathogen strains like for example for *Helicobacter pylori* (Akopyantis *et al.* 1998), *Burkholderia cepacia* (Parson *et al.* 2003) and *Haemophilus influenza* (Smoot *et al.* 2002). In addition, this method was used to identify niche-specific genes in marine *Synechococcus* isolates (Jones *et al.* 2006). Suppression subtractive hybridization turned out to be an appropriate method to analyze the complex microbial community like the microorganisms in the rumen (Galbraith *et al.* 2004).

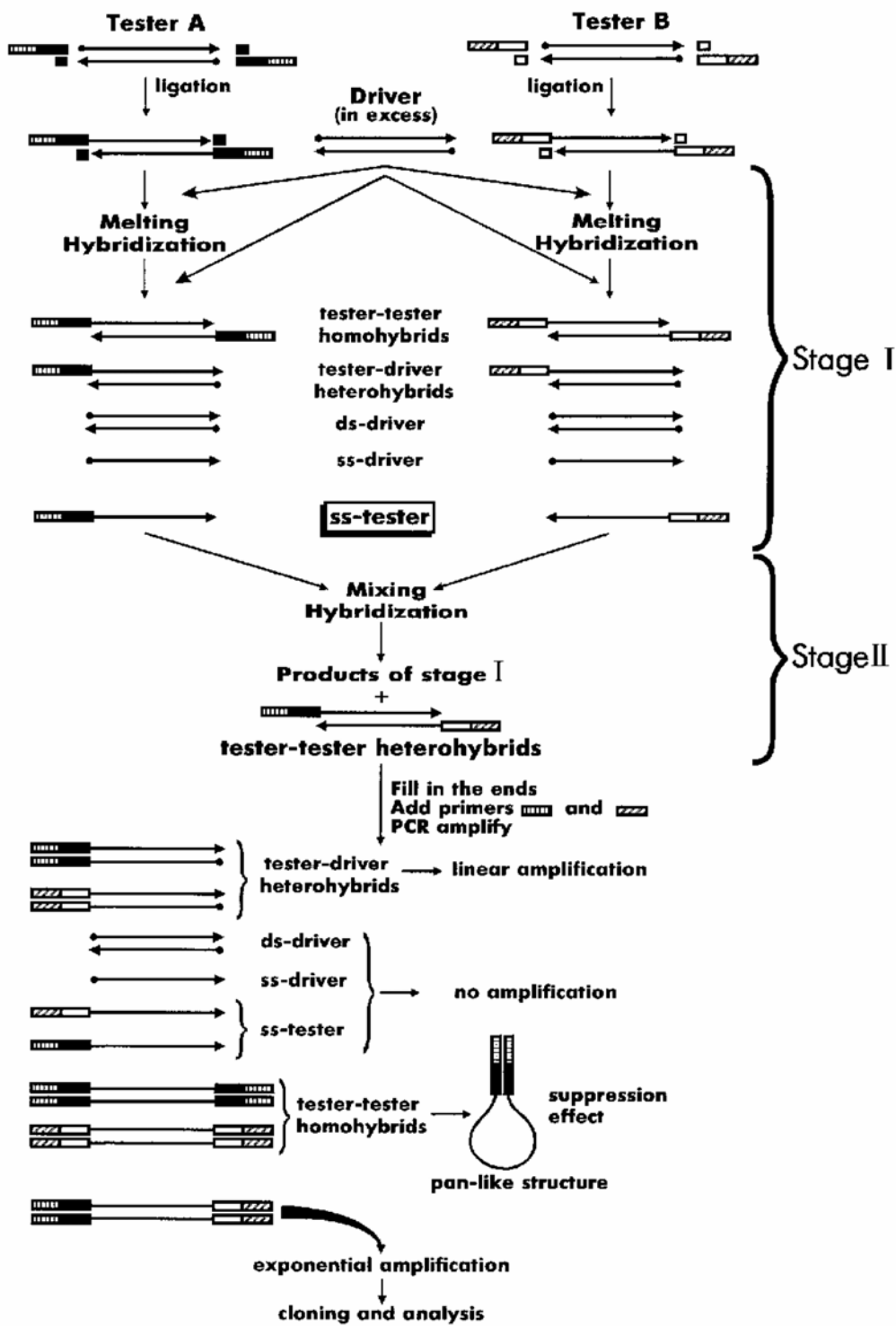


**Figure 3.** Schematic diagram of equalizing cDNA subtraction procedure with the use of PCR suppression effect. Solid and open boxes represent the inner parts of Adapter 1 and Adapter 2, respectively. Vertical and inclined hatched boxes represent the outer parts of Adapter 1 and Adapter 2, respectively. (From Gurskaya *et al.* 1996)

## Goals of the study

Previous research on phototrophic consortia showed that they are ecologically relevant (Gasol *et al.* 1995) and can serve as a model for prokaryotic interaction (Overmann 2005). Several independent experiments suggest a rapid signal transfer within phototrophic consortia concerning cell division (Overmann *et al.* 1998), response to light (Fröstl and Overmann 1998), and regulation of the metabolism (Glaeser and Overmann 2003b). In contrast, little knowledge exists about the basis of the symbiosis between the epibiont and the central bacterium. As basis for the symbiosis, an internal sulfur cycle was proposed (Pfennig 1980). Since the phylogenetic affiliation of the central bacterium revealed that it belongs to the *Betaproteobacteria* (Fröstl and Overmann 2000; Kanzler *et al.* 2005), an internal sulfur cycle in phototrophic consortia seems to be unlikely. Goal of the present work was to identify symbiosis relevant properties of the epibiont. Therefore a physiological, a molecular, and a morphological approach were chosen. First, to gain more insights into the physiological basis of symbiosis, the epibiont of “*Chlorochromatium aggregatum*” was to be isolated in pure culture. The epibiont was known to belong to the green sulfur bacteria (Tuschak *et al.* 1999) and to grow photoautotrophically *in situ* like free-living green sulfur bacteria (Glaeser and Overmann 2003a). The pure culture of the epibiont of “*C. aggregatum*” allows to study the physiology of the epibiont in detail and to assess particular physiological properties of symbiotic green sulfur bacteria. It is also possible to answer the question if the symbiosis is an obligate one. Second, based on the close phylogenetic relationship between all green sulfur bacteria (Imhoff 1995), subtractive hybridization of DNA from the epibiont of “*C. aggregatum*” against a collection of 16 free-living strains was performed to examine the molecular basis of symbiosis. Since the major difference between the 16 free-living strains and the epibiont is the symbiotic state of the latter, suppression subtractive hybridization against non-symbiotic green sulfur bacteria should recover genes involved in symbiosis. Third, initial electron microscopy studies revealed a specific adhesion structure in the epibiont and a distinct structure in the central bacterium (Müller 2003). Detailed electron microscopic examinations were performed to elucidate the morphological basis of symbiosis.

## References

- Abella CA, Cristina XP, Martinez A, Pibernat I, Vila X (1998) Two new motile phototrophic consortia: “*Chlorochromatium lunatum*” and “*Pelochromatium selenoides*”. Arch Microbiol 169:452-459
- Akopyants NS, Fradkov A, Diatschenko L, Hill JE, Siebert PD, Lukyanov SA, Sverdlov ED, Berg DE (1998) PCR-based subtractive hybridization and differences in genes among strains of *Helicobacter pylori*. Proc Natl Acad Sci USA 95:13108-13113
- Bassler BL (2002) Small talk: cell-to-cell communication in bacteria. Cell 109:421-424
- Baumann U, Wu S, Flaherty KM, McKay DB (1993) Three-dimensional structure of the alkaline protease of *Pseudomonas aeruginosa*: a two-domain protein with a calcium binding parallel beta roll motif. EMBO J 12:3357-3364
- Braun V, Schönherr R, Hobbie S (1993) Enterobacterial hemolysins: activation, secretion and pore formation. Trends Microbiol 1:211-216
- Buder J (1914) *Chloronium mirabile*. Berichte deutsche botanische Gesellschaft 31:80-97
- Camilli A, Bassler BL (2006) Bacterial small-molecule signaling pathways. Science 311:1113-1116
- Cohen-Bazire G, Pfennig N, Kunizawa R (1964) The fine structure of green bacteria. J Cell Biol 22:207-225
- Cruz WT, Young R, Chang YF, Struck DK (1990) Deletion analysis resolves cell-binding and lytic domains of the *Pasteurella* leukotoxin. Mol Microbiol 4:1933-1939
- Czuprynski CJ, Welch RA (1995) Biological effects of RTX toxins: the possible role of lipopolysaccharide. Trends Microbiol 3:480-483
- Dale C, Moran NA (2006) Molecular interactions between bacterial symbionts and their hosts. Cell 126:453-465
- De Bary A (1879) Die Erscheinung der Symbiose. Naturforschung Versammlung Cassel
- Diatchenko L, Lau YFC, Campell AP, Chenchik A, Moqadam F, Huang B, Lukyanov S, Lukyanov K, Gurskaya N, Sverdlov ED, Siebert PD (1996) Suppression subtractive hybridization: a method for generating differentially regulated or tissue-specific cDNA probes and libraries. Proc Natl Acad Sci USA 93:6025-6030
- Dubinina GA, Kuznetsov SI (1976) The ecological and morphological characteristics of microorganisms in Lesnaya Lamba (Karelia). Int Rev Ges Hydrobiol 61:1-19
- El-Azami-El-Idrissi M, Bauches C, Loucka J, Osicka R, Sebo P, Ladant D, Leclerc C (2003) Interaction of *Bordetella pertussis* adenylate cyclase with CD11b/CD18. J Biol Chem 278:38514-38521
- Fröstl J, Overmann J (1998) Physiology and tactic response of “*Chlorochromatium aggregatum*”. Arch Microbiol 169:129-135
- Fröstl J, Overmann J (2000) Phylogenetic affiliation of the bacteria that constitute phototrophic consortia. Arch Microbiol 174:50-58
- Galbraith EA, Antonopoulos DA, Withe BA (2004) Suppressive subtractive hybridization as a tool for identifying genetic diversity in an environmental metagenome: the rumen as a model. Environ Microbiol 6:928-937

- Gasol JM, Jürgens K, Massana R, Calderón-Paz JI, Pedrós-Alió C (1995) Mass development of *Daphnia pulex* in a sulphide-rich pond (Lake Cisó). *Arch Hydrobiol* 132:279-296
- Gibson J, Ludwig W, Stackebrandt E, Woese CR (1985) The phylogeny of the green photosynthetic bacteria: Absence of a close relationship between *Chlorobium* and *Chloroflexus*. *Syst Appl Microbiol* 6:152-156
- Glaeser J, Bañeras L, Rütters H, Overmann J (2002) Novel bacteriochlorophyll *e* structures and species-specific variability of pigment composition in green sulfur bacteria. *Arch Microbiol* 177:475-485
- Glaeser J, Overmann J (2003a) Characterization and in situ carbon metabolism of phototrophic consortia. *Appl Environ Microbiol* 69:3739-3750
- Glaeser J, Overmann J (2003b) The significance of organic carbon compounds for *in situ* metabolism and chemotaxis of phototrophic consortia. *Environ Microbiol* 5:1053-1063
- Glaeser J, Overmann J (2004) Biogeography, evolution, and diversity of epibionts in phototrophic consortia. *Appl Environ Microbiol* 70:4821-4830
- Goodrich-Blair H, Clarke DJ (2007) Mutualism and pathogenesis in *Xenorhabdus* and *Photorhabdus*: two roads to the same destination. *Mol Microbiol* 64:260-268
- Gorlenko VM, Kuznetsov SI (1972) Vertical distribution of phototrophic bacteria in the Kononér Lake of the Mari ASSR. *Microbiol* 40:651-652
- Gurskaya NG, Diatchenko L, Chenchik A, Siebert PD, Khaspekov GL, Lukyanov KA, Vagner LL, Ermolaeva OD, Lukyanov SA, Sverdlov ED (1996) Equalizing cDNA subtraction based on selective suppression of polymerase chain reaction: cloning of Jurkat cell transcripts induced by phytohemagglutinin and phorbol 12-myristal 13-acetate. *Anal Biochem* 240:90-97
- Handelsman J (2004) Metagenomics: application of genomics to uncultured microorganisms. *Microbiol Mol Biol Rev* 68:669-685
- Harris JK, Kelley ST, Pace NR (2004) New perspective on uncultured bacterial phylogenetic division OP11. *Appl Environ Microbiol* 70:845-849
- Hugenholtz P, Goebel BM, Pace NR (1998) Impact of culture-independent studies on the emerging phylogenetic view of bacterial diversity. *J Bacteriol* 180:4765-4774
- Imhoff JF (1995) Taxonomy and physiology of phototrophic purple bacteria and green sulfur bacteria. In: Blankenship RE, Madigan MT, Bauer CE (eds) *Anoxygenic photosynthetic bacteria*. Kluwer Academic Publishers, Dordrecht, The Netherlands, pp 1-15
- Imhoff JF (2003) Phylogenetic taxonomy of the family *Chlorobiaceae* on the basis of the 16S rRNA and *fmo* (Fenna-Matthews-Olsen protein) gene sequence. *Int J Syst Evol Microbiol* 53:941-951
- Jones H, Ostrowski M, Scanlan DJ (2006) A suppression subtractive hybridization approach reveals niche-specific genes that may be involved in predator avoidance in marine *Synechococcus* isolates. *Appl Environ Microbiol* 72:2730-2737
- Kanzler BEM, Pfannes KR, Vogl K, Overmann J (2005) Molecular characterization of the nonphotosynthetic partner bacterium in the consortium "*Chlorochromatium aggregatum*". *Appl Environ Microbiol* 71:7434-7441
- Keller L, Surette MG (2006) Communication in bacteria: an ecological and evolutionary perspective. *Nature Rev Microbiol* 4:249-258

- Knapp O, Maier E, Polleichtner G, Masin J, Sebo P, Benz R (2003) Channel formation in model membranes by the adenylate cyclase toxin of *Bordetella pertussis*: Effect of calcium. *Biochemistry* 42:8077-8084
- Lally ET, Hill RB, Kieba IR, Korostoff J (1999) The interaction between RTX toxins and target cells. *Trends Microbiol* 7:356-361
- Lauterborn R (1906) Zur Kenntnis der sapropelischen Flora. *Allg Bot Z* 12:196-197
- Lodwig E, Poole P (2003) Metabolism of *Rhizobium* bacteroids. *Crit Rev Plant Sci* 22:37-78
- Ludwig A, Jarchau T, Benz R, Goebel W (1988) The repeat domain of *Escherichia coli* haemolysin (Hyl A) is responsible for its Ca<sup>2+</sup>-dependent binding to erythrocytes. *Mol Gen Genet* 214:553-561
- Ludwig W, Strunk O, Westram R, Richter L, H. Meier, Yadhukumar, Buchner A, Lai T, Steppi S, Jobb G, Forster W, Brettske I, Gerber S, Ginhart AW, Gross O, Grumann S, Hermann S, Jost R, König A, Liss T, Lussmann R, May M, Nonhoff B, Reichel B, Strehlow R, Stamatakis A, Stuckmann N, Vilbig A, Lenke M, Ludwig T, Bode A, Schleifer KH (2004) ARB: a software environment for sequence data. *Nucleic Acids Res* 32:1363-1371
- McWhinney DR, Cang YF, Young RY, Struck DK (1992) Separable domains define target cell specificities of an RTX hemolysin from *Actinobacillus pleuropneumoniae*. *J Bacteriol* 174:291-297
- Moran NA (2006) Symbiosis. *Curr Biol* 16:866-871
- Müller M (2003) Physiologie und Morphologie von phototrophen Konsortien. Diplomarbeit LMU München
- Overmann J (2001) Phototrophic consortia: a tight cooperation between non-related eubacteria. In: Seckbach J (ed) *Symbiosis. Mechanisms and model systems*. Kluwer Academic Publ, Dordrecht, pp 239-255
- Overmann J (2001a) Green sulfur bacteria. In: Boone DR, Castenholz RW, Garrity GM (eds) *Bergey's Manual of Systematic Bacteriology* 2nd ed. Springer, New York, pp 601-605
- Overmann J (2005) Symbiosis between non-related bacteria in phototrophic consortia. In: Overmann J (ed) *Molecular basis of symbiosis. Progress in Molecular Subcellular Biology*, Springer-Verlag, Berlin Heidelberg, pp 21-37
- Overmann J, Schubert K (2002) Phototrophic consortia: model systems for symbiotic interrelations between prokaryotes. *Arch Microbiol* 177:201-208
- Overmann J, Tuschak C, Fröstl J, Sass H (1998) The ecological niche of the consortium "*Pelochromatium roseum*". *Arch Microbiol* 169:120-128
- Parson YN, Banasko R, Detsika MG, Duangsonk K, Rainbow L, Hart CA, Winstanley C (2003) Suppression-subtractive hybridization reveals variations in gene distribution amongst the *Burkholderia cepacia* complex, including the presence in some strains of a genomic island containing putative polysaccharide production genes. *Arch Microbiol* 179:214-223
- Perret X, Fellay R, Bjourson AJ, Cooper JE, Brenner S, Broughton WJ (1994) Subtraction hybridization and shot-gun sequencing: a new approach to identify symbiotic loci. *Nucleic Acids Res* 22:1335-1341
- Perviliev BV (1914) On the theory of symbiosis of *Chlorochromatium aggregatum* Lauterb. (*Chloronium mirabile* Buder) and *Cylindrogloea bacterifera* nov. gen., nov. spec. (in Russian). *I Microbiol Petrogr* 1:222-225

- Pfennig N (1980) Syntrophic mixed cultures and symbiotic consortia with phototrophic bacteria: a review. In: Gottschalk G, Pfennig N, Werner (eds) Anaerobes and anaerobic infections. Fischer, Stuttgart New York, pp 127-131
- Rappe MS, Giovannoni SJ (2003) The uncultured microbial majority. *Annu Rev Microbiol* 57:369-394
- Schink B (1997) Energetics of syntrophic cooperation in methanogenic degradation. *Microbiol Mol Biol Rev* 61:262-280
- Schink B (2002) Synergistic interactions in the microbial world. *Antonie Leeuwenhoek* 81:257-261
- Skuja H (1957) Taxonomische und biologische Studien über das Phytoplankton schwedischer Binnengewässer. *Nova Acta Reg Soc Sci Upsala Ser IV*(16):1-404
- Smoot LM, Franke DD, McGillivray G, Actis LA (2002) Genomic analysis of the F3031 brazilian purpuric fever clone of *Haemophilus influenzae* biogroup aegyptius by PCR-based subtractive hybridization. *Infect Immun* 70:2694-2699
- Stachelin LA, Fuller RC, Drews G (1978) Visualisation of the supramolecular architecture of chlorosomes (chlorobium vesicles) in freeze-fractured cells of *Chloroflexus aurantiacus*. *Arch Microbiol* 119:269-277
- Steinert M, Hentschel U, Hacker J (2000) Symbiosis and pathogenesis: evolution of the microbe-host interaction. *Naturwissenschaften* 87:1-11
- Straus D, Ausubel FM (1990) Genomic subtraction for cloning DNA corresponding to deletion mutations. *Proc Natl Acad Sci USA* 87:1889-1893
- Tuschak C, Glaeser J, Overmann J (1999) Specific detection of green sulfur bacteria by in situ hybridization with a fluorescently labeled oligonucleotide probe. *Arch Microbiol* 171:265-272
- van Gemerden H, Mas J (1995) Ecology of phototrophic sulfur bacteria. In: Blankenship RE, Madigan MT, Bauer CE (eds) Anoxygenic photosynthetic bacteria. Kluwer Academic Publishers, Dordrecht, The Netherlands, pp 49-85
- Vendeville A, Winzer K, Heurlier K, Tang CM, Hardie KR (2005) Making “sense” of metabolism: autoinducer-2, LuxS and pathogenic bacteria. *Nature Rev Microbiol* 3:383-396
- Waters CM, Bassler BL (2005) Quorum sensing: cell-to-cell communication in bacteria. *Annu Rev Cell Dev* 21:319-346
- Welch RA (1995) Phylogenetic analyses of the RTX toxin family. In: Roth JA, Bolin CA, Brogden KA, Minion FC, Wannemuehler MJ (eds) Virulence mechanisms of bacterial pathogens 2nd ed. ASM press, Washington DC, pp 195-206



# ***Chlorobium chlorochromatii* sp. nov., a symbiotic green sulfur bacterium isolated from the phototrophic consortium "*Chlorochromatium aggregatum*"**

Kajetan Vogl, Jens Glaeser, Kristina R. Pfannes, Gerhard Wanner and Jörg Overmann

**Keywords:** Chlorobiaceae • *Chlorobium* • symbiosis • phototrophic consortia • carotenoids • "*Chlorochromatium aggregatum*"

**Abbreviations:** *BChl* bacteriochlorophyll, *BPhe* bacteriopheophytin, *C. Chlorochromatium*, *Cba. Chlorobaculum*, *Chl.*, *Chlorobium*, *DGGE* denaturing gradient gel electrophoresis, [*E*, *E*] *BChlc<sub>F</sub>* 8,12-diethyl Bchl<sub>c</sub> esterified with farnesol (analogously: [*M*] methyl, [*Pr*] propyl [*I*] isobutyl)

Kajetan Vogl • Jens Glaeser • Kristina R. Pfannes • Jörg Overmann (✉)  
Bereich Mikrobiologie, Department Biologie I, Ludwig-Maximilians-Universität München,  
Maria-Ward-Str. 1a, D-80638 München, Germany. Tel: ++49-89-2180-6123. Fax: ++49-89-  
2180-6125. Email: j.overmann@lrz.uni-muenchen.de

Gerhard Wanner  
Bereich Botanik, Department Biologie I, Ludwig-Maximilians-Universität München,  
Menzinger Str.67, D-80638 München, Germany.

Jens Glaeser  
Justus-Liebig-Universität Gießen, Institut für Mikro- und Molekularbiologie,  
35392 Gießen, Germany.

## Abstract

A symbiotic green sulfur bacterium, strain CaD, was isolated from an enrichment culture of the phototrophic consortium "*Chlorochromatium aggregatum*". The capability of the epibiont to grow in pure culture indicates that it is not obligately symbiotic. Cells are Gram-negative, nonmotile, rod-shaped and contain chlorosomes. Strain CaD is obligately anaerobic and photolithoautotrophic, using sulfide as electron donor. Acetate and peptone are photoassimilated in the presence of sulfide and hydrogencarbonate. Photosynthetic pigments are bacteriochlorophylls *a* and *c*, and  $\gamma$ -carotene and OH- $\gamma$ -carotene glucoside laurate as dominant carotenoids. In cells from pure cultures, chlorosomes are equally distributed along the inner face of the cytoplasmic membrane. In contrast, the distribution of the chlorosomes in symbiotic epibiont cells is uneven, with chlorosomes being entirely absent at the site of attachment to the central bacterium. Symbiotic epibiont cells display a conspicuous additional layered structure at the attachment site. The G+C content of genomic DNA of strain CaD is 46.7 mol%. On the basis of 16S rRNA sequence comparison, the strain is distantly related to *Chlorobium* species within the green sulfur bacteria phylum ( $\leq 94.6\%$  sequence homology). The novel isolate is therefore described as a novel species within the genus *Chlorobium*, *Chlorobium chlorochromatii*.

## Introduction

Green sulfur bacteria (*Chlorobiaceae*) are anoxygenic and obligately photoautotrophic bacteria. They occur in the chemocline of stratified lakes where light reaches sulfide-containing water layers (van Gemerden and Mas 1995). Within the bacterial radiation, all known green sulfur bacteria form a distinct phylum, which comprises also several environmental 16S rRNA gene clones (Overmann 2001a). Green and brown pigmented *Chlorobiaceae* species are known. The brown species contain bacteriochlorophyll (BChl) *e* and, with one known exception (Glaeser *et al.* 2002), the carotenoids isorenieratene and  $\beta$ -isorenieratene as the major light-harvesting pigments. Green-colored species contain bacteriochlorophyll *c* or *d* and chlorobactene and OH-chlorobactene as the dominant carotenoids (Imhoff 1995). In addition, BChl *a* is present in minor amounts in all green sulfur bacteria. The light-harvesting pigments are located in antenna structures called chlorosomes (Cohen-Bazire *et al.* 1964, Staehelin *et al.* 1978), which are 70-180 nm long and 30-60 nm wide ovoid bodies and are attached to the cytoplasmic face of the cellular membrane.

Particular green sulfur bacteria exist in a highly structured association with chemotrophic *Betaproteobacteria*. Most of these so-called phototrophic consortia consist of a motile, colorless, rod-shaped bacterium surrounded by 13-69 green sulfur bacteria (the epibionts) (Fröstl and Overmann 2000, Overmann 2001b, Overmann and Schubert 2002). Phototrophic consortia are meanwhile known for one century (Buder 1914, Lauterborn 1906). They occur in numerous stratified lakes worldwide (Glaeser and Overmann 2004, Overmann *et al.* 1998) where they can amount to two-thirds of the total bacterial biomass in the chemocline (Gasol *et al.* 1995). Phototrophic consortia are therefore likely to play a significant role in the biochemical cycles of stratified aquatic ecosystems. Fluorescence *in situ* hybridisation has revealed that up to 88% of all green sulfur bacteria in stratified lakes can be associated with phototrophic consortia (Glaeser and Overmann 2003a), indicating a considerable selective advantage of the symbiosis for the green sulfur bacterial partner.

None of the epibiont 16S rRNA gene sequences has been detected in free-living green sulfur bacteria so far (Glaeser and Overmann 2004), suggesting that the green sulfur bacterial epibionts are specifically adapted to life in the associated state. Nevertheless, based on stable carbon discrimination ( $\delta^{13}\text{C}$ ) values of specific lipid biomarkers, epibionts of phototrophic consortia grow photoautotrophically *in situ* like their free-living counterparts and do not seem to utilize organic carbon compounds supplied by the central bacterium (Glaeser and Overmann 2003a). However, several lines of evidence indicate that a rapid signal transfer occurs between

the epibionts and the central bacterium (Fröstl and Overmann 1998, Glaeser and Overmann 2003b) and that cell division occurs in a tightly coordinated fashion (Overmann *et al.* 1998). In order to resolve the molecular basis of the interaction in phototrophic consortia, the biochemistry and physiology of both types of bacteria need to be elucidated in more detail. It is therefore necessary to isolate the partner bacteria in pure culture.

Almost 50 years ago, the isolation of a green sulfur bacterium from a natural population of the phototrophic consortium "*Chlorochromatium aggregatum*" was claimed (Mechsner 1957). Unfortunately the strain was lost before detailed physiological studies could be made. Here, we report the isolation in pure culture of the epibiont from "*C. aggregatum*" using improved cultivation techniques. We demonstrate that the strain reveals distinct differences to all validly described species of green sulfur bacteria. Consequently, the strain is described as a novel species.

## Materials and Methods

### Source of organisms and cultivation

For isolation of the epibiont, a laboratory enrichment culture of "*Chlorochromatium aggregatum*" (Fröstl and Overmann 1998) was employed. The enrichment originated from lake Dagow (Brandenburg, Germany), a small eutrophic freshwater lake 100 km north of Berlin (Overmann *et al.* 1998). The defined mineral medium K3 was used for the maintenance of "*C. aggregatum*" enrichments and for the isolation of the epibiont. The medium contained per liter of double distilled water:  $\text{KH}_2\text{PO}_4$ , 0.25g;  $\text{NH}_4\text{Cl}$ , 0.05g;  $\text{MgCl}_2 \cdot 6\text{H}_2\text{O}$ , 0.05g;  $\text{CaCl}_2 \cdot 2\text{H}_2\text{O}$ , 0.05 g; and  $\text{NaHCO}_3$ , 1.5 g. After autoclaving, the medium was cooled to room temperature under an atmosphere of  $\text{CO}_2$  (10 kPa, 30 min) and then kept under  $\text{N}_2/\text{CO}_2$  (7 kPa/7 kPa).  $\text{NaHCO}_3$  was autoclaved separately and added to the medium after cooling.  $\text{Na}_2\text{S}$  was used as reducing agent and as electron donor for anoxygenic photosynthesis at a final concentration of 0.5 mM. The pH was adjusted to 7.5 by addition of KOH solution. Finally, sterile lipoic acid solution (0.25 ml of a 100 mM stock solution, Bast 2001), 1 ml seven vitamin solution (Pfennig 1978), and 1 ml trace element solution SL10 (Widdel *et al.* 1983) were added per liter of medium. Before inoculation with "*C. aggregatum*", 2-oxoglutarate was added to a final concentration of 0.5 mM from a freshly prepared and sterile filtered stock solution. In order to maintain a growing enrichment, cultures were supplemented with 0.5 mM of 2-oxoglutarate every second day.

*Chlorobium limicola* DSMZ 245<sup>T</sup> was grown under standard conditions in sulfide-containing media supplemented with 3 mM acetate (Overmann and Pfennig 1989).

*Chlorobaculum tepidum* ATCC 49652<sup>T</sup> was grown at 46°C and a light intensity of 1000  $\mu\text{mol}\cdot\text{m}^{-2}\cdot\text{s}^{-1}$  of tungsten lamp bulbs in modified CP-medium (Frigaard and Bryant 2001).

### Isolation of the epibiont

In order to generate a highly enriched inoculum for the subsequent isolation of the epibiont, phototrophic consortia were first concentrated exploiting their chemotactic behavior. Chemotaxis experiments were set up essentially as described earlier (Fröstl and Overmann 2000, Glaeser and Overmann 2003b). Flat microscopic glass chambers (area 20 x 20 mm; height 3 mm) were custom-made from a microscopic slide, using coverslips as spacers and as the top lid. Three sides were sealed with paraffin and the chambers filled with the "*C. aggregatum*" enrichment culture. Rectangular capillaries (length, 50 mm; inner diameter, 0.1 x 1.0 mm; capacity 5  $\mu\text{l}$ ; Vitro Dynamics, Rockaway, NJ, USA) were filled with K3 medium supplemented with 1 mM sulfide. The capillaries were sealed with plasticine at one end and then inserted with the open end into the chemotaxis chamber. Afterwards, the chamber was completely sealed with paraffin and incubated for 2 hours at 15°C in dim light. The chemotactic enrichment of consortia was monitored microscopically in dark field. Capillaries containing accumulated consortia were withdrawn, their surface cleaned with 70% (v/v) ethanol and the first 5 mm from their open end were clipped off in order to separate contaminating bacteria. The remaining volume of the capillaries was used to inoculate fresh K3 medium.

Pure cultures were obtained by repeated deep agar dilution series (Pfennig 1978). To maintain highly reducing conditions throughout, 200  $\mu\text{M}$  dithionite was added to the K3 medium immediately before preparation of the dilution series. A variety of carbon substrates were tested for stimulation of the growth of the epibiont. 2-oxoglutarate, pyruvate, propionate or acetate were added in separate trials to a final concentration of 1 mM. Fermented rumen extract and fermented yeast extract were tested as growth factors. Rumen fluid is a well-established source of growth factors (volatile fatty acids, vitamins and hemin) and known to stimulate growth of various anaerobes like *Bacteroides*, *Eubacterium*, *Ruminococcus*, *Selenomonas* and *Treponema* species (Caldwell and Bryant 1966). For the preparation of fermented rumen extract, fresh rumen fluid was incubated for 4 days in the dark at 32°C, the liquid was clarified by centrifugation (20000 x g for 30 min at 4°C), the supernatant filtered in sterilized glass bottles (Millipore polycarbonate filters; pore size, 0.1  $\mu\text{m}$ ) and stored at -20°C until usage. For production of fermented yeast extract, 20 ml of swamp sediment was mixed with 8 g yeast extract, 80 ml tap water was added and the mixture incubated for 3 days at 25°C. The supernatant was clarified and

sterile filtered as described above. Both growth factor solutions were used at a final concentration of 0.002% (v/v).

After incubation for 6 weeks in the light, macroscopically visible green-colored colonies had appeared in some of the agar tubes. Individual colonies were withdrawn from the agar with sterile Pasteur pipettes and resuspended in 5 ml of K3 medium containing glass beads. The colonies were broken up by shaking and 0.5 ml aliquots of the resulting cell suspension were used for immediate inoculation of a second series of deep agar tubes.

### **Confirmation of the isolation and phylogenetic characterization of the epibiont**

In order to confirm the origin of the epibiont, the 16S rRNA gene sequence of the isolate was compared to that of the epibiont present in intact consortia. Individual "*Chlorochromatium aggregatum*" consortia were mechanically separated from the laboratory enrichment using a micromanipulator connected to an inverted microscope (Fröstl and Overmann 2000). Ten consortia were collected in a PCR tube, and directly subjected to PCR amplification. In parallel, the 16S rRNA gene sequence of the isolate was amplified from a cell pellet of the pure culture. Bacterial sequences of *Chlorobiaceae* were selectively amplified by employing oligonucleotide primers GC 357f and GSB 840r and specific PCR conditions (Overmann *et al.* 1999) in a GeneAmp PCR system 9700 (Applied Biosystems, Weiterstadt, Germany). The generated DNA fragments were then separated and compared by PCR-DGGE fingerprinting using a 6% (w/v) polyacrylamide DGGE gel containing a linear gradient of 35% to 70% denaturing agents which was run at 200 V for 12 hours (Overmann *et al.* 1999). After staining with ethidium bromide, DNA bands were cut from the DGGE gel, recovered by electroelution, reamplified, and fragments with identical melting behaviour were sequenced to confirm sequence identity (Overmann *et al.* 1999).

### **Growth experiments**

Pure cultures of the epibiont were grown in standard SL10 medium for green sulfur bacteria (Overmann and Pfennig 1989) supplemented with 3 mM Na-acetate and with the pH adjusted to 7.2. Cultures of the epibiont were maintained at 25°C in continuous light ( $50 \mu\text{mol quanta}\cdot\text{m}^{-2}\cdot\text{s}^{-1}$ , Osram tungsten lamp, 60 W). Light intensities were determined with a Li Cor LI-189 quantum meter equipped with a LI-200 SA pyranometer sensor (wavelength range, 380 – 1100 nm; Li Cor, Lincoln, Neb., USA). Optimum conditions for growth of the epibiont were determined with pure cultures incubated in 22 ml screw cap tubes. Growth was followed by measuring optical density at 750 nm (Bausch & Lomb Spectronic 20 photometer).

At this wavelength and in media containing acetate, the formation of extracellular sulfur globules did not interfere with OD measurements.

Photoassimilation of organic carbon substrates was tested for 110 different compounds (the complete list is available upon request). In addition, the utilization of  $\text{Fe}^{2+}$  chelated by different agents was tested in growth experiments. For the preparation of  $\text{Fe}^{2+}$ -complexes, chelating agents (0.1 mM) were dissolved under anoxic conditions in an anaerobic chamber and an equimolar amount of  $\text{FeCl}_2$  was added. Afterwards, the solutions were filtered (Millipore polycarbonate filters; pore size, 0.1  $\mu\text{m}$ ).

### Pigment analyses

Absorption spectra were monitored in a Lambda 25 UV/VIS spectrophotometer (Perkin Elmer, Rodgau-Jügesheim, Germany). Spectra of whole cells were determined during exponential growth using cells resuspended in 60% (w/v) sucrose solution. For HPLC analyses, bacterial cells were harvested by centrifugation (15 min at  $9770 \times g$  and  $4^\circ\text{C}$ ) using Pyrex glass centrifuge tubes and the pellets extracted in the dark in HPLC grade acetone/methanol (7/2, v/v) for 30 min at  $4^\circ\text{C}$  in a sonification bath and then at  $4^\circ\text{C}$  over night. The extract was clarified by centrifugation and the supernatant transferred to a brown glass tube and dried in a stream of nitrogen gas. The pigments were redissolved in methanol/acetonitrile (80/15, v/v) and 0.1 volume of 1 M aqueous ammonium acetate solution was added as an ion pairing agent 10 min before injection into an HPLC system (Dionex, Munich, Germany). The composition of pigment extracts was analyzed by the method B of Airs *et al.* (2001). Pigments were separated using a multospher 120 RP18 (4.6  $\times$  250 mm, 5  $\mu\text{m}$  mesh) HPLC column (CS- Chromatography, Langerwehe, Germany), starting with 0.01 M ammonium acetate / methanol / acetonitrile (5/80/15, v/v/v) as the mobile phase for 5 min. Subsequently, the composition of the solvent was changed linearly to 0.01 M ammonium acetate / methanol / acetonitrile / ethyl acetate (1/32/15/52, v/v/v/v) over 76 min. Analyses were performed at a flux rate of  $0.7 \text{ ml}\cdot\text{min}^{-1}$  and at  $20^\circ\text{C}$ . Pigment absorption spectra were recorded between 270 and 800 nm using a diode array spectrophotometer (PDA-1000, Dionex). For identification of individual carotenoids, extracts *Chlorobium tepidum* ATCC 49652<sup>T</sup> with a known composition (Frigaard *et al.* 2004) were analyzed in parallel. For quantification of the carotenoids, the following absorption coefficients were used (in  $\text{l}\cdot\text{g}^{-1}\cdot\text{cm}^{-1}$ ): for chlorobactene and  $\gamma$ -carotene, 265 at a wavelength of 490 nm; for OH- $\gamma$ -carotene glucoside laurate, 158 at 490 nm (Frigaard *et al.* 2004); for unidentified carotenoids, 250 at 490 nm (Züllig 1985).

### Cell surface hydrophobicity

The cell-surface hydrophobicity of the epibiont was determined in a quantitative assay with *n*-hexadecane (Rosenberg *et al.* 1980). The OD<sub>650</sub> of an epibiont culture was measured and 3 ml subsamples were transferred into screw cap test tubes containing 0.5 ml of *n*-hexadecane. The tubes were flushed with nitrogen for 3 minutes, incubated for 10 minutes, and then homogenized on a vortex mixer for 2 minutes. After phase separation the lower aqueous phase was carefully removed with a Pasteur pipette and its OD<sub>650</sub> determined again. The hydrophobicity index was calculated from the OD of the original cell suspension (OD<sub>650</sub>) and the OD after the treatment (OD<sub>650'</sub>) according to:  $H [\%] = 100 \cdot (OD_{650} - OD_{650}') / OD_{650}$

### Electron microscopy

Cells were fixed immediately with 2.5% glutardialdehyde in 75 mM sodium cacodylate, 2 mM MgCl<sub>2</sub>, pH7.0, for 1 h at room temperature. After several rinses in fixative buffer, a post-fixation step followed for 1 h with 1% osmium tetroxide in fixative buffer at room temperature. After two washing steps in distilled water, the cells were stained *en bloc* with 1% uranyl acetate in 20% acetone for 30 min. Dehydration was performed with a graded acetone series. Samples were then infiltrated and embedded in Spurr's low-viscosity resin (Spurr 1969). After polymerisation, ultrathin sections (50 and 70 nm) were cut with a diamond knife and mounted on uncoated copper grids. The sections were post-stained with aqueous lead citrate (100 mM, pH 13.0). All micrographs were taken with an EM 912 electron microscope (Zeiss, Oberkochen, Germany) equipped with an integrated OMEGA energy filter operated in the zero loss mode.

### Sequencing and phylogenetic analysis

Sequences were obtained employing the Big Dye<sup>TM</sup> Terminator Cycle Sequencing Kit (Applied Biosystems) and the ABIPrism<sup>TM</sup> 310 genetic Analyzer (Applied Biosystems GmbH). The almost complete 16S rRNA gene sequence of the pure culture of the epibiont was obtained as outlined before for other pure cultures (Gich *et al.* 2005).

Phylogenetic analysis of 16S rRNA gene sequences was performed using the ARB phylogeny package (Ludwig *et al.* 1998). The program Fast Aligner V1.03 was employed for alignment of all 16S rRNA gene sequences of green sulfur bacteria as available through the National Center for Biotechnology Information website (Altschul *et al.* 1997). The sequence of *Chloroherpeton thalassium* ATCC 35110<sup>T</sup> was chosen as the outgroup, since it has been shown to branch at the root of all known *Chlorobiaceae* (Overmann 2001a). The alignment was manually corrected based on secondary structure information for *Chlorobium vibrioforme* ATCC

6030, and a phylogenetic tree was constructed from all sequences longer than 1300 bp, using the maximum likelihood program Fast DNA\_ML. Distance matrices were calculated employing the algorithm of Kimura (Kimura 1980) by using the Phylip Distance Matrix program, version 3.6a3 within the ARB phylogeny package.

The accession number of the almost full-length 16S rRNA gene sequence of the epibiont is AJ578461.

#### **Determination of the mol% G + C content**

The mol% guanidine plus cytosine of genomic DNA was determined according to Mesbah *et al.* (1989). DNA was hydrolyzed with P1 nuclease, the nucleotides dephosphorylated with bovine alkaline phosphatase, and the resulting deoxyribonucleosides were analyzed by HPLC. These analyses were performed by the DSMZ (Braunschweig, Germany).

## Results and Discussion

### Isolation of the epibiont of "*Chlorochromatium aggregatum*"

The enrichment of "*C. aggregatum*" originating from Lake Dagow (Fröstl and Overmann 1998) was used for the isolation of the epibiont. In these enrichments,  $10^5$  to  $10^6$  consortia were present per ml. Similar to all other consortia investigated to date (Glaeser and Overmann 2004), "*C. aggregatum*" harbors only one single phylotype of green sulfur bacteria. This phylotype could be detected after separation of consortia by micromanipulation, amplification of 16S rRNA gene fragments of green sulfur bacteria by group-specific PCR and separation of the amplicates by DGGE (Fig. 1). Since a cultivation of consortia separated by micromanipulation never yielded growing cultures, the enrichments had to be used in subsequent cultivation attempts.

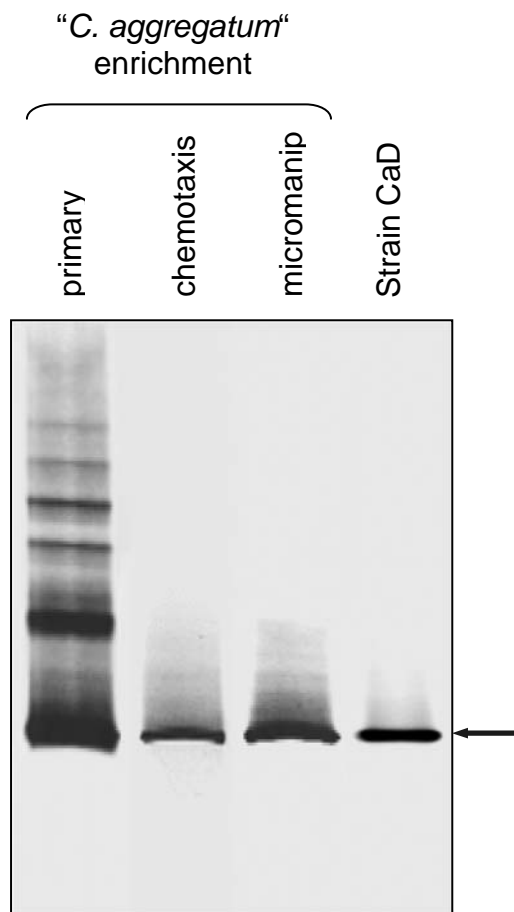


**Figure 1.** DGGE fingerprints of green sulfur bacteria from the primary enrichment (*primary*), from chemotactically enriched "*Chlorochromatium aggregatum*" (*chemotaxis*), from "*C. aggregatum*" mechanically separated by micromanipulation (*micromanip.*) as compared to the isolated epibiont CaD. *Arrow* indicates melting position of the 16S rRNA gene fragment of the epibiont as confirmed by sequence comparison.

However, analysis of the enrichment by PCR-DGGE revealed the presence of several different phylotypes of green sulfur bacteria (Fig. 1). Since all known free-living green sulfur

bacteria are immotile, the chemotaxis of "*C. aggregatum*" consortia towards hydrogen sulfide (Kanzler *et al.* 2005) was exploited in the present work to separate live consortia from accompanying green sulfur bacteria. Individual capillaries containing  $10^2$ - $10^3$  "*C. aggregatum*" consortia were used for subsequent inoculation of liquid K3 medium. After growth of these secondary enrichments, group-specific DGGE fingerprinting confirmed that only one single 16S rRNA gene sequence type of green sulfur bacteria was left. The melting behavior of this fragment was identical to that amplified from mechanically separated "*C. aggregatum*" (Fig. 1, arrow).

In the secondary enrichments, the green sulfur bacteria were also observed as single cells. This observation for the first time indicated that the epibiont was capable of growing in a non-associated state. Therefore, deep agar dilution series were employed to isolate the epibiont in pure culture. Because the numbers of contaminating colorless bacteria exceeded those of free epibionts, differential centrifugation (650 x g, 5 min) was used to enrich the epibiont cells prior to dilution in deep agar media. The pellets thus generated contained mainly epibionts and phototrophic consortia and were directly transferred to liquefied agar media supplemented with various organic carbon sources and growth factors. After incubation for at least 4 weeks, small green colonies appeared in deep agar series, which had been supplemented with 200  $\mu$ M dithionite and fermented rumen extract. None of the other additives promoted growth of the epibiont in the agar media. The dependence on highly reducing conditions for cultivation in deep agar media is not a unique property of strain CaD, but was also described to be essential for the isolation of two free living green sulfur bacteria, *Chl.* (formerly *Pelodictyon*) *phaeoclathratiforme* DSMZ 5477<sup>T</sup> (Overmann and Pfennig 1989) and a low-light-adapted *Chlorobium* (strain MN1) from the Black Sea (Overmann *et al.* 1992).

Colonies from the highest dilutions were picked, resuspended in K3 medium, and used immediately for a subsequent passage through deep agar media. After growing in the second deep agar series, colonies were isolated from the highest dilutions and inoculated into liquid media. Similar to the agar media, green sulfur bacteria in the small picked colonies could divide exclusively in the presence of dithionite and fermented rumen extract. One of the resulting strains (CaD) was chosen for subsequent characterization. Its 16S rRNA gene fingerprint was identical to those of epibionts from consortia, which had been isolated by micromanipulation (Fig. 1, arrow). Sequencing of these fingerprints yielded identical nucleotide sequences, confirming that the generated culture indeed contained the epibiont of "*C. aggregatum*" (compare Fig. 4). Purity of the culture was checked by microscopic analysis. PCR/DGGE-

fingerprinting of eubacterial 16S rRNA genes present in the culture of strain CaD yielded only one band (data not shown).

### **Morphology and cell surface hydrophobicity**

Individual cells of the isolated epibiont were  $2.7 (\pm 0.6) \mu\text{m}$  long and  $0.5 (\pm 0.1) \mu\text{m}$  wide nonmotile rods. Some cells occurred in short chains (Fig. 2A). Cells were Gram variable upon staining (Bartholomew 1962). Similarly, the KOH test (Gregersen 1978) resulted in ambiguous results. Electron micrographs of thin sections revealed that epibiont cells exhibit a typical Gram negative cell wall structure in which the outer and cytoplasmic membranes were clearly distinguishable (Fig. 2C). Electron microscopy also demonstrated the presence of chlorosomes (Fig. 2B), which represent the typical light harvesting structures of green sulfur bacteria (Cohen-Bazire and Sistrom 1966, Olson 1980). In pure cultures, chlorosomes were equally distributed over the inner face of the cytoplasmic membrane. In contrast, gaps devoid of chlorosomes were observed in epibiont cells associated with intact consortia (Fig. 2D). These gaps existed exclusively at the sites of cell-cell-contact to the central bacterium and featured an additional layered structure, which was never observed in epibiont cells of pure cultures (Fig. 2D, arrows). Intracellular sorting of chlorosomes and specific structures at the cell-cell-contact thus are specific for the symbiotic state. Based on our previous work, several lines of evidence indicate that a specific signal exchange occurs between the epibionts and the central bacterium in intact phototrophic consortia. Firstly, cell division of epibionts and the central bacterium proceed in a highly coordinated fashion (Overmann *et al.* 1998). Secondly, phototrophic consortia exhibit a scotophobic response in which epibionts function as light sensors whereas the central bacterium confers motility to the entire cell aggregate (Fröstl and Overmann 1998). Thirdly, incorporation of 2-oxoglutarate of intact consortia most likely is mediated by the central bacterium, but occurs only in the presence of light and sulfide, which are utilized by the epibionts (Glaeser and Overmann 2003b). Our present data now indicate that signal exchange between the bacterial partners in phototrophic consortia also causes an asymmetric distribution of chlorosomes and hence conspicuous changes in the cellular morphology of the epibiont.

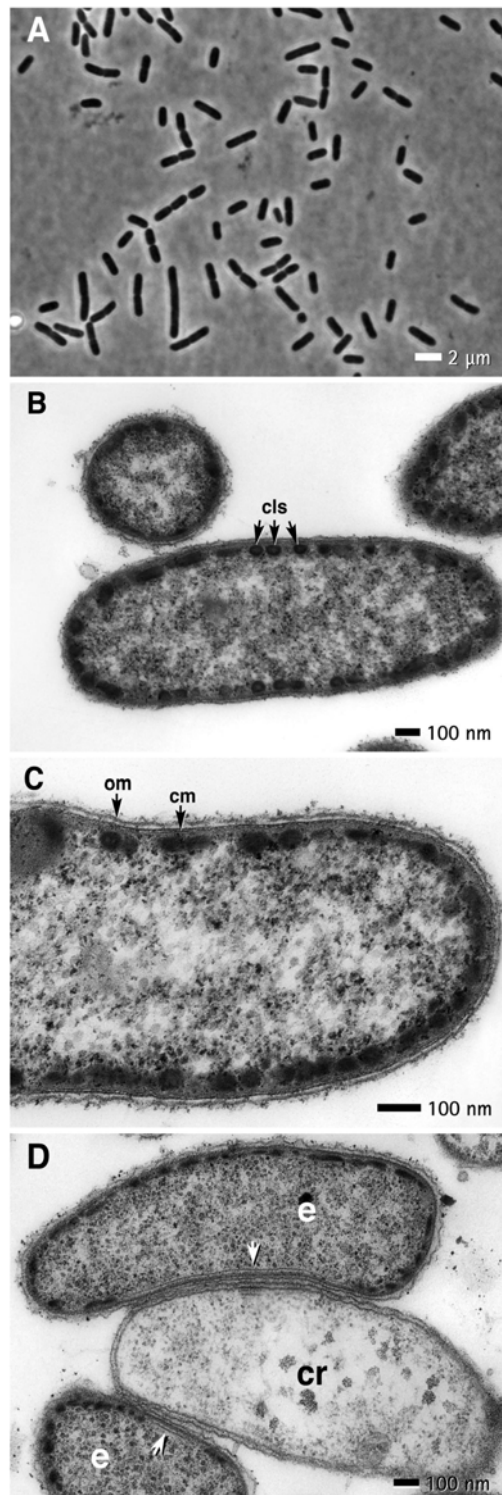


**Figure 2.** **A.** Phase-contrast micrograph of cells of a pure culture of strain CaD. **B.** Transmission electron micrograph of ultrathin sections of cell in a pure culture of strain CaD. Note the presences of chlorosomes (*arrows*). **C.** Detail of one epibiont cell in pure culture. The outer and cytoplasmic membranes are visible. **D.** Transmission electron micrograph of two epibiont cells associated to a central rod in an intact consortium. The attachment sites (*arrows*) are characterized by laminar layers and the absence of chlorosomes. *Cls*, chlorosomes, *cm*, cytoplasmic membrane, *cr*, central rod, *e*, epibiont, *om*, outer membrane.

The hydrophobicity index of free epibiont cells was 8.6%. Formation of aggregates due to cell-to-cell adhesion in the purple sulfur bacterium *Amoebobacter purpureus* (Overmann and Pfennig 1992), interactions between bacteria and phagocytes (Cunningham *et al.* 1975), and adhesion to substrates (Bryant *et al.* 1983) or surfaces (Marshall *et al.* 1971, Fletcher and Floodgate 1973) are partially mediated by hydrophobic interactions. Aggregating *Amb. purpureus* cells exhibit a hydrophobicity index of 96% (Overmann and Pfennig 1992). By comparison, the low hydrophobicity index of the epibiont cells indicates that they, at least under the conditions tested in pure culture, do not form a sufficiently hydrophobic cell surface, which would enable the formation of consortia based on hydrophobic interactions alone.

### Photosynthetic pigments

Densely grown cultures exhibited a green to olive green color. The absorption spectrum of whole cells showed maxima at 748 and 453 nm. Cell extracts in acetone revealed major peaks at 662 and 433 nm. Both results indicated the presence of bacteriochlorophyll *c* (Fig. 3).

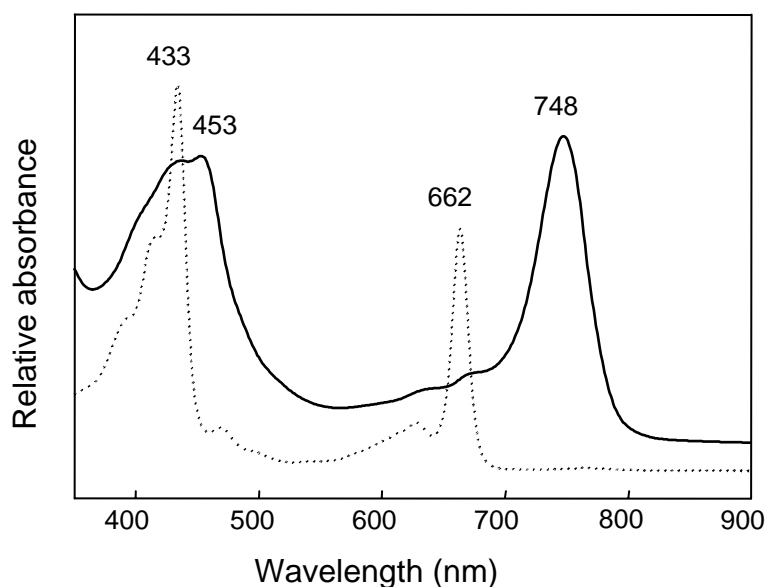


**Figure 3.** Absorption spectra of whole cells (—) and of acetone extract (••••) of strain CaD.

Four different bacteriochlorophyll *c* homologs esterified with farnesol, [E, M] BChl<sub>CF</sub>, [E, E] BChl<sub>CF</sub>, [Pr, E] BChl<sub>CF</sub>, and [I, E] BChl<sub>CF</sub> were detected by HPLC analyses. Similar to *Cba. tepidum* ATCC 49652<sup>T</sup> and *Chl. limicola* DSMZ 245<sup>T</sup> (Borrego *et al.* 1999), [E, E] BChl<sub>CF</sub> and [Pr, E] BChl<sub>CF</sub> represented the dominant bacteriochlorophyll *c* homologs in strain CaD. In contrast, the elution profile monitored at 470 nm revealed a distinct carotenoid composition of epibiont strain CaD. A total of 12 different carotenoids could be distinguished. As compared to data from the literature (Frigaard *et al.* 2004) and to the corresponding elution profile of *Cba.*

*tepidum* determined in parallel, two carotenoids had retention times and absorption spectra similar to *trans*- and *cis*-chlorobactene. Two other compounds were identified as OH- $\gamma$ -carotene glucoside laurate and  $\gamma$ -carotene. Based on this tentative assignment, OH- $\gamma$ -carotene glucoside laurate represents the major carotenoid in strain CaD, amounting to 24% of the total carotenoid content. The tentatively identified chlorobactene isomers together represents 13% of the total carotenoid content, and  $\gamma$ -carotene amounted to 11%, respectively. In contrast, *Cba. tepidum* contained chlorobactene as the dominant carotenoid which amounted to 61% of all carotenoids. By comparison, OH- $\gamma$ -carotene glucoside laurate constituted only 7% and  $\gamma$ -carotene only 4% of all carotenoids in *Cba. tepidum*. Our values are comparable to those reported by Takaishi *et al.* (1997) and Frigaard *et al.* (2004) for the same strain. *Chl. limicola* DSMZ 245<sup>T</sup> resembled *Cba. tepidum* in that chlorobactene amounted to 54%, OH- $\gamma$ -carotene glucoside laurate represented 10% and  $\gamma$ -carotene 6% of all carotenoids. By comparison to the strains previously investigated, strain CaD thus contains a significantly higher amount of highly hydrophobic carotenoids, which also comprise six unidentified compounds. Two of these unidentified compounds so far have only been detected in the epibiont. Particular features are the low concentrations of chlorobactene and the absence of its derivatives OH-chlorobactene glucoside, OH-chlorobactene, OH-chlorobactene glucoside laurate and 1',2'-dihydrochlorobactene. The distinct carotenoid composition of strain CaD indicates that the biosynthetic pathways of carotenoid biosynthesis differ from those found in other green sulfur bacteria.

### Physiological properties

Photolithoautotrophic growth of the epibiont occurred only under strictly anoxic conditions with hydrogen sulfide as electron donor. Thiosulfate and elemental sulfur were not utilized. Also Fe<sup>2+</sup> added in different types of complexes (deferoxamine-Fe or diethylenetriaminepentaacetic acid-Fe) was not used as electron donor.

In the presence of hydrogen sulfide and hydrogencarbonate, only acetate and peptone were photoassimilated. 108 of the substrates tested were not used, including (concentrations in mM) L-(+)-alanine (5), L-(+)-arginine (5), benzoate (2), butyrate (2.5), caproate (0.5; 5), caprylate (0.5; 5), casaminoacids (0.05%), citrate (2), crotonate (0.5; 5), formate (2.5), fructose (5), fumarate (5), glucose (5), L-(+)-glycine (5), glyoxylate (5), L-(+)-lysine (5), malate (5), ornithine (5), 2-oxobutyrate (5), 2-oxoglutarate (= 2-oxoglutarate) (5), 2-oxohexanoic acid (5), 2-oxoisocaproate (5), 2-oxooctanoic acid (5), 2-oxovalerate (5), L-(+)-proline (5), propionate (5), pyruvate (5), L-(+)-serine (5), succinate (10), tartrate (2), oxaloacetate (5), L-(+)-threonine (5),

valerate (0.5; 5), L-(+)-valine (5) (the full list is available upon request). In addition, no growth stimulation occurred with molecular hydrogen provided as a H<sub>2</sub>:N<sub>2</sub> mixture of 20:80 (v/v).

2-oxoglutarate is known to be indispensable for the cultivation of "*Chlorochromatium aggregatum*" in enrichment culture (Fröstl and Overmann 1998). Based on microautoradiography after incubation with radioactively labelled 2-oxoglutarate, this substrate is incorporated by intact consortia (Glaeser and Overmann 2003b). Based on our present results, 2-oxoglutarate is not utilized by the isolated epibiont, however. It is therefore concluded that the uptake of 2-oxoglutarate observed for "*C. aggregatum*" is mediated by the central bacterium.

The limited range (two) of organic substrates utilized for photomixotrophic growth is commensurate with the very limited physiological flexibility of other *Chlorobiaceae*. In contrast to the present results, the use of thiosulfate and atypical substrates like glycerol and malate was reported for a culture obtained from "*C. aggregatum*" five decades ago (Mechsner 1957). It therefore appears possible that the earlier cultivation attempts did not yield the epibiont, but another type of green sulfur bacteria.

The epibiont was capable of nitrogen fixation and required only vitamin B<sub>12</sub> for growth. With sulfide as electron donor, growth became light saturated above light intensities of 10 μmol quanta·m<sup>-2</sup>·s<sup>-1</sup>. A maximum growth rate of 0.04 h<sup>-1</sup> (doubling time, 17.3 h) was obtained under light-saturated conditions. The epibiont had an optimal growth temperature of 25°C and showed no growth at temperatures ≥40°C. Optimum pH was 7.0 to pH 7.3 and no growth occurred at pH values lower than pH 6.4. In comparison with free-living species of green sulfur bacteria, which mostly exhibit a pH optimum of 6.8 (Overmann 2001a), the pH optimum of growth of the epibiont thus is slightly shifted towards the alkaline range. This may reflect an adaptation to the close association of the epibiont with the central rod in phototrophic consortia. At salinities between 0.4% and 0.7%, the epibiont showed comparable growth rates. A pronounced lag phase of up to 114 hours was observed for cultures growing at salinities between 0.5% and 0.7%. Growth rates declined rapidly at higher salt concentrations. No growth occurred above a salinity of 0.8%.

### **Phylogeny and GC-content of the epibiont**

The newly isolated bacterium is Gram negative, rod shaped and nonmotile. It grows only under strict anaerobic conditions and is obligately phototrophic. The photosynthetic pigment bacteriochlorophyll *c* and chlorosomes are present. Based on its morphological and physiological properties, strain CaD represents a member of the green sulfur bacteria (Overmann 2001a). So far, only a 540 bp-fragment of the 16S rRNA gene had been sequenced and analyzed

phylogenetically (Fröstl and Overmann 2000, Glaeser and Overmann 2004). The phylogenetic analysis of the full-length 16S rRNA gene obtained in this study confirmed this identification, placing the new isolate in the phylum green sulfur bacteria. Strain CaD is related to green sulfur bacteria of group 2 and 3 (group designations according to Imhoff 2003) (Fig. 4). Since all green sulfur bacteria of these groups belong to the genus *Chlorobium*, strain CaD is classified as a member of this genus. However, no close relationship was found to any strain cultured so far; the highest sequence similarity (94.6%) was found to the 16S rRNA gene sequence of *Chlorobium phaeobacteroides* III (Tab. 1).

The G+C content of the epibiont was 46.7 mol%. This DNA base composition is the lowest value known for the genus *Chlorobium* (*Chlorobium clathratiforme* DSM 5477, 47.9 mol%) and it is one of the lowest among green sulfur bacteria as a whole (*Chloroherpeton* spp.: mol%: 45.0 - 48.2) (Overmann 2001a).

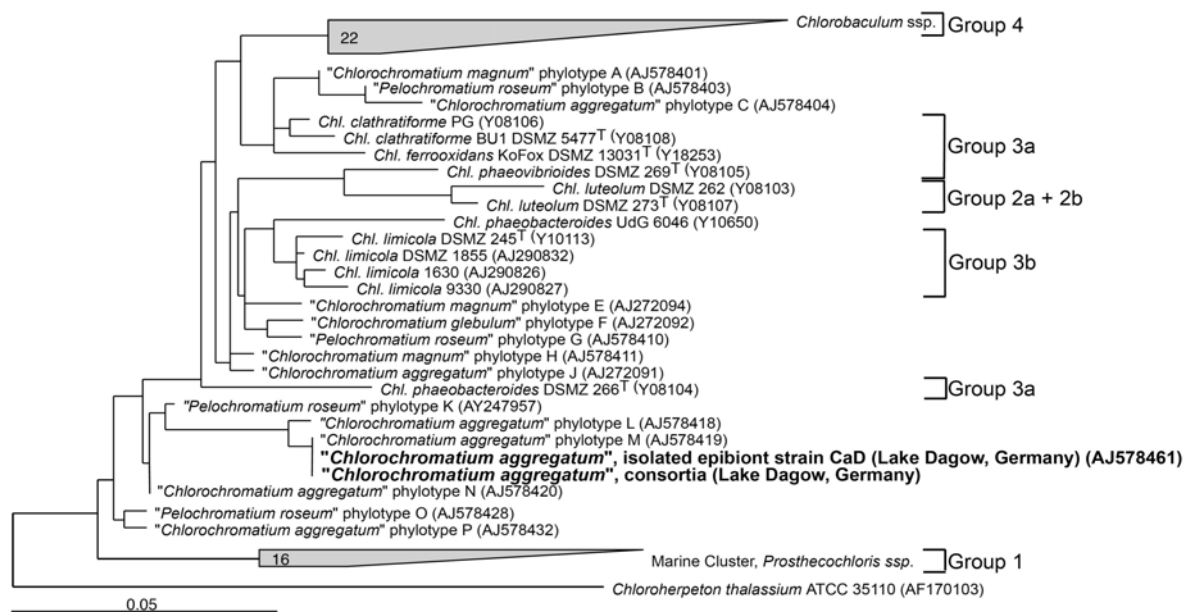


**Figure 4.** Phylogenetic affiliation of strain CaD. The 16S rRNA gene sequence of picked "*Chlorochromatium aggregatum*" consortia and of the isolate CaD were identical and are indicated in **bold type**. Numbers in polygons give number of phylotypes in the corresponding clusters. Groups of Chlorobiaceae are given according to Imhoff (2003). Bar = 0.05 fixed point mutation per nucleotide position.

**Table 1.** Evolutionary distances between strain CaD and its closest cultured relatives. Values represent percentage of dissimilarity of the 16S rRNA gene sequences corrected for multiple base changes by the method of Kimura (1980)

	1	2	3	4	5	6	7	8	9	10	11	12
1 Strain CaD	-											
2 <i>Chl. phaeobacteroides</i> III	5.4	-										
3 <i>Chl. phaeovibrioides</i> DSMZ 261	5.5	3.3	-									
4 <i>Chl. limicola</i> DSMZ 1855	5.5	0.0	3.3	-								
5 <i>Chl. limicola</i> 1630	5.5	0.1	3.4	0.1	-							
6 <i>Chl. ferrooxidans</i> DSMZ 13031 <sup>T</sup>	5.6	4.4	3.5	4.3	4.4	-						
7 <i>Chl. phaeobacteroides</i> Glu	5.6	0.0	3.3	0.0	0.1	4.4	-					
8 <i>Chl. phaeovibrioides</i> DSMZ 269 <sup>T</sup>	5.6	3.5	0.0	3.3	3.4	3.6	3.5	-				
9 <i>Chl. phaeovibrioides</i> DSMZ 265	5.6	3.5	0.3	3.5	3.6	3.8	3.5	0.3	-			
10 <i>Chl. limicola</i> 9330	5.7	0.2	3.6	0.2	0.3	4.5	0.2	3.6	3.8	-		
11 <i>Chl. limicola</i> DSMZ 245 <sup>T</sup>	5.7	0.2	3.4	0.1	0.2	4.6	0.3	3.6	3.6	0.2	-	
12 <i>Chl. phaeobacteroides</i> DSMZ 266 <sup>T</sup>	5.9	3.9	3.9	3.6	3.7	4.1	4.2	3.9	4.3	3.7	3.9	-

The alleged isolation of a green sulfur bacterium from consortia was described almost 50 years ago (Mechsner 1957). However, the strain was lost before being characterized in detail. Whereas the present study did not reveal conspicuous differences with respect to physiology, strain CaD is clearly unique based on the cellular distribution of chlorosomes, the architecture of the cell-cell-adhesion site and the carotenoid composition. Based on these as well as the phylogenetic differences to validly described species of green sulfur bacteria, we propose a new species of the genus *Chlorobium*, *Chlorobium chlorochromatii* with strain CaD as the type strain. *Chlorobium* strain CaD is the first epibiont of phototrophic consortia, which is available in pure culture.

### Description of *Chlorobium chlorochromatii* sp. nov.

*Chlorobium chlorochromatii* sp. nov. chlo.ro'chro.ma'ti.i. Gr. adj. *chloros*, green, yellowish green; Gr. n. *chromatium* color, paint. M.L. gen. n. *chlorochromatii* of, originating from "*Chlorochromatium*".

In laboratory pure culture individual cells are rod-shaped. Cells are 2.7 ( $\pm$  0.6)  $\mu\text{m}$  long and 0.5 ( $\pm$  0.1)  $\mu\text{m}$  wide, nonmotile and Gram negative. In free-living cells, chlorosomes are equally distributed over the inner face of the entire cell. In contrast, cells associated with intact consortia "*Chlorochromatium aggregatum*" lack chlorosomes at the site of attachment to the central chemotrophic bacterium but instead possess additional layered structures at this site. Contains bacteriochlorophyll *c*. The major carotenoids are  $\gamma$ -carotene and its derivatives, mostly OH- $\gamma$ -carotene glucoside laurate.

Strictly anaerobic and phototrophic. Growth occurs exclusively under anoxic and highly reducing conditions in the light. Electron donor sulfide. Thiosulfate, sulfur flower and molecular hydrogen not utilized. In the presence of sulfide and carbon dioxide, acetate and peptone are photoassimilated. Optimum pH for growth 7.0-7.3. Optimum temperature 25°C. Saturating light intensity 10  $\mu\text{mol quanta}\cdot\text{m}^{-2}\cdot\text{s}^{-1}$  (daylight fluorescent tubes). NaCl is not required for growth. Growth is inhibited at a salinity of  $\geq$  0.8%. Vitamin B<sub>12</sub> required for growth.

Habitat: Isolated from anoxic sulfide containing water of stratified lakes. In nature, the epibiont is so far only found in association with non-cultured *Betaproteobacterium* forming the phototrophic consortium "*Chlorochromatium aggregatum*".

DNA base ratio: 46.7 mol% G+C.

### Acknowledgements

We thank Dr. Karin Schubert for support during the HPLC analysis. Silvia Dobler is gratefully acknowledged for skilful technical assistance. This work was supported by a grant of the Deutsche Forschungsgemeinschaft to J. Overmann (grant no. Ov 20/10-1).

## References

- Airs RL, Atkinson JE Keely BJ (2001) Development and application of a high resolution liquid chromatographic method for the analysis of complex pigment distributions. *J Chromatogr A* 917:167-177
- Altschul SF, Madden TL, Schäffer AA, Zhang J, Miller W, Lipmann DJ (1997) Gapped BLAST and PSI-BLAST: a new generation of protein database search programs. *Nucleic Acids Res* 25:3389-3402
- Bartholomew JW (1962) Variables influencing results and precise definition of steps in Gram staining as a means of standardizing the results obtained. *Stain Technol* 37:139-155
- Bast E (2001) *Mikrobiologische Methoden*. 2<sup>nd</sup> ed. 429 pp.
- Borrego CM, Gerola PD, Miller M, Cox RP (1999) Light intensity effects on pigment composition and organisation in the green sulfur bacterium *Chlorobium tepidum*. *Photosynth Res* 59:159-166
- Bryant RD, Costerton JW, Laishely EJ (1983) The role of *Thiobacillus albertis* glycocalyx in the adhesion of cells to elemental sulfur. *Can J Microbiol* 30:81-90
- Buder J (1914) *Chloronium mirabile*. *Berichte deutsche botanische Gesellschaft* 31:80-97
- Caldwell DR, Bryant MP (1966) Medium without rumen fluid for nonselective enumeration and isolation of rumen bacteria. *Appl Microbiol* 14 794-801
- Cohen-Bazire G, Pfennig N, Kunizawa R (1964) The fine structure of green bacteria. *J Cell Biol* 22:207-225
- Cohen-Bazire G, Sistrom WR (1966) The prokaryotic photosynthetic apparatus. In: Veron LP, Seeley GR (eds) *The chlorophylls*. Academic press, New York, pp 290-298
- Cunningham RK, Soderstrom TO, Gillman CF, van Oss CJ (1975) Phagocytosis as a surface phenomenon. V. Contact angles and phagocytosis of rough and smooth strains of *Salmonella typhimurium*, and the influence of specific antiserum. *Immunol Commun* 4:429-442.
- Fletcher M, Floodgate (1973) An electron-microscopic demonstration of an acidic polysaccharide involved in the adhesion of a marine bacterium to solid surfaces. *J Gen Microbiol* 74:325-334
- Frigaard NU, Bryant DA (2001) Chromosomal gene inactivation in the green sulfur bacterium *Chlorobium tepidum* by natural transformation. *App Environ Microbiol* 67:2538-2544
- Frigaard NU, Maresca JA, Yunker CE, Jones AD, Bryant DA (2004) Genetic manipulation of carotenoid biosynthesis in the green sulfur bacterium *Chlorobium tepidum*. *J Bacteriol* 186:5210-5220
- Fröstl J, Overmann J (1998) Physiology and tactic response of "*Chlorochromatium aggregatum*". *Arch Microbiol* 169:129-135
- Fröstl J, Overmann J (2000) Phylogenetic affiliation of the bacteria that constitute phototrophic consortia. *Arch Microbiol* 174:50-58
- Gasol JM, Jürgens K, Massana R, Calderón-Paz JI, Pedrós-Alió C (1995) Mass development of *Daphnia pulex* in a sulphide-rich pond (Lake Cisó). *Arch Hydrobiol* 132:279-296

- Gich F, Schubert K, Bruns A, Hoffelner H, Overmann J (2005) Specific detection, isolation and characterization of selected, previously uncultured members of freshwater bacterioplankton. *Appl. Environ. Microbiol.* 71: 5908-5919
- Glaeser J, Bañeras L, Rütters H, Overmann J (2002) Novel bacteriochlorophyll *e* structures and species-specific variability of pigment composition in green sulfur bacteria. *Arch Microbiol* 177:475-485
- Glaeser J, Overmann J (2003a) Characterization and *in situ* carbon metabolism of phototrophic consortia. *Appl Environ Microbiol* 69:3739-3750
- Glaeser J, Overmann J (2003b) The significance of organic carbon compounds for *in situ* metabolism and chemotaxis of phototrophic consortia. *Environ Microbiol* 5:1053-1063
- Glaeser J, Overmann J (2004) Biogeography, evolution, and diversity of epibionts in phototrophic consortia. *Appl Environ Microbiol* 70:4821-4830
- Gregersen T (1978) Rapid method for distinction of Gram-negative from Gram-positive bacteria. *Eur J Appl Microbiol Biotechnol* 5:123-127
- Imhoff JF (1995) Taxonomy and physiology of phototrophic purple bacteria and green sulfur bacteria. In: Blankenship RE, Madigan MT Bauer CE (eds) *Anoxygenic photosynthetic bacteria*. Kluwer Academic Publishers, Dordrecht, The Netherlands, pp 1-15
- Imhoff JF (2003) Phylogenetic taxonomy of the family *Chlorobiaceae* on the basis of 16S rRNA and *fmo* (Fenna-Matthews-Olsen protein) gene sequence. *Int J System Evol Microbiol* 53:941-951
- Kanzler B, Pfannes KR, Vogl K, Overmann J (2005) Molecular characterization of the non-photosynthetic partner bacterium in the consortium "*Chlorochromatium aggregatum*". *Appl Environ Microbiol* 71: 7434-7441
- Kimura M (1980) A simple method for estimating evolutionary rates of base substitutions through comparative studies of nucleotide sequences. *J Mol Evol* 16:111-112
- Lauterborn R (1906) Zur Kenntnis der sapropelischen Flora. *Allg Bot Z* 12:196-197
- Ludwig W, Strunk O, Klugbauer S, Klugbauer N, Weizenegger J, Neumair J, Bachleitner M, Schleifer KH (1998) Bacterial phylogeny based on comparative sequence analysis. *Electrophoresis* 19:554-568
- Marshall KC, Stout R, Mitchell R (1971) Mechanism of the initial events in the sorption of marine bacteria to surfaces. *J Gen Microbiol* 68:337-348
- Mechsner K (1957) Physiologische und morphologische Untersuchungen an Chlorobacterien. *Arch Mikrobiol* 26:32-51
- Mesbah M, Premachandran U, Whitman W (1989) Precise measurement of the G+C content of deoxyribonucleic acid by high performance liquid chromatography. *Int J Syst Bact* 39:159-167
- Olson JM (1980) Chlorophyll organization in green photosynthetic bacteria. *Biochim Biophys Acta* 594:33-51
- Overmann J (2001a) Green sulfur bacteria. In: Boone DR, Castenholz RW, Garrity GM (eds) *Bergey's Manual of Systematic Bacteriology* 2nd ed. Springer, New York, pp 601-605
- Overmann J (2001b) Phototrophic consortia. A tight cooperation between non-related eubacteria. In: Seckbach J (ed) *Symbiosis. Mechanisms and model systems*. Kluwer, Dordrecht, pp. 239-255

- Overmann J, Coolen MJL, and Tuschak C (1999) Specific detection of different phylogenetic groups of chemocline bacteria based on PCR and denaturing gradient gel electrophoresis of 16S rRNA gene fragments. *Arch Microbiol* 172:83-94
- Overmann J, Cypionka H, Pfennig N (1992) An extremely low-light-adapted phototrophic sulfur bacterium from the Black Sea. *Limnol Oceanogr* 32:150-155
- Overmann J, Pfennig N (1989) *Pelodictyon phaeoclathratiforme* sp. nov., a new brown-colored member of the *Chlorobiaceae* forming net-like colonies. *Arch Microbiol* 152:401-406
- Overmann J, Pfennig N (1992) Buoyancy regulation and aggregate formation in *Amoebobacter purpureus* from Mahoney Lake. *FEMS Microbiol Ecol* 10:67-79
- Overmann J, Schubert K (2002) Phototrophic consortia: model systems for symbiotic interrelations between prokaryotes. *Arch Microbiol* 177:201-208
- Overmann J, Tuschak C, Fröstl J, Sass H (1998) The ecological niche of the consortium "*Pelochromatium roseum*". *Arch Microbiol* 169:120-128
- Pfennig N (1978) *Rhodocyclus purpureus* gen. nov. and spec. nov., a ring-shaped, vitamin B<sub>12</sub>-requiring member of the family *Rhodospirillaceae*. *Int J Syst Bacteriol* 28:283-288
- Rosenberg M, Gutnick D, Rosenberg E (1980) Adherence of bacteria to hydrocarbons: a simple method for measuring cell-surface hydrophobicity. *FEMS Microbiol Lett* 9:29-33
- Spurr AR (1969) A low-viscosity epoxy resin embedding medium for electron microscopy. *J Ultrastruct Res* 26:31-43
- Staehelin LA, Fuller RC, Drews G (1978) Visualisation of the supramolecular architecture of chlorosomes (chlorobium vesicles) in freeze-fractured cells of *Chloroflexus aurantiacus*. *Arch Microbiol* 119:269-277
- Takaichi S, Wang ZY, Umetsu M, Nozawa T, Shimada K, Madigan MT (1997) New carotenoids from the thermophilic green sulfur bacterium *Chlorobium tepidum*: 1',2'-dihydro- $\gamma$ -carotene, 1',2'-dihydrochlorobactene, and OH-chlorobactene glucoside ester, and the carotenoid composition of different strains. *Arch Microbiol* 168:270-276
- van Gemerden H, Mas J (1995) Ecology of phototrophic sulfur bacteria. In: Blankenship RE, Madigan MT, Bauer CE (eds) *Anoxygenic photosynthetic bacteria*. Kluwer Academic Publishers, Dordrecht, The Netherlands, pp 49-85
- Widdel F, Kohring GW, Mayer F (1983) Studies on dissimilatory sulfate-reducing bacteria that decompose fatty acids. III. Characterization of the filamentous gliding *Desulfonema limicola* gen. nov., sp. nov., and *Desulfonema magnum* sp. nov. *Arch Microbiol* 134:286-293.
- Züllig H (1985) Pigmente phototropher Bakterien in Seesedimenten und ihre Bedeutung für die Seeforschung. *Schweiz Z Hydrol* 47:87-126

# Identification and analysis of four candidate symbiosis genes from "*Chlorochromatium aggregatum*", a highly developed bacterial symbiosis

Kajetan Vogl, Martina Dreßen, Roland Wenter, Martina Schlickerrieder and Jörg Overmann\*

Bereich Mikrobiologie, Department Biologie I, Ludwig-Maximilians-Universität München,  
Maria-Ward-Str. 1a, D-80638 München, Germany.

**Keywords:** Cell-cell-interaction, *Chlorobium*, "*Chlorochromatium aggregatum*", bacterial interactions, phototrophic consortia, RTX toxin, symbiosis, symbiosis genes

\*Corresponding author. Tel: ++49-89-2180-6123. Fax: ++49-89-2180-6125. Email: [j.overmann@lrz.uni-muenchen.de](mailto:j.overmann@lrz.uni-muenchen.de)

## Summary

The consortium "*Chlorochromatium aggregatum*" represents the most highly developed interaction between prokaryotes known to date. Four putative symbiosis genes of the epibiont were recovered by suppression subtractive hybridisation and bioinformatics approaches. These genes are transcribed constitutively and do not occur in the free-living relatives. The hemagglutinin-like putative gene products of ORFs Cag0614 and Cag0616 are unusually large and contain repetitive regions and RGD tripeptides. Cag0616 harbors two  $\beta\gamma$ -crystallin Greek key motifs. Cag1920 codes for a putative hemolysin-type protein whereas the gene product of Cag1919 is a putative RTX-like protein. Based on detailed analyses of Cag1919, the C-terminal amino acid sequence comprises six repetitions of the motif GGXGXD predicted to form a  $\text{Ca}^{2+}$ -binding beta roll. Intact "*Chlorochromatium aggregatum*" consortia disaggregated upon the addition of EGTA or pyrophosphate, but stayed intact in the presence of various lectine-binding sugars or proteolytic enzymes.  $^{45}\text{Ca}^{2+}$ - autoradiography detected four calcium-binding proteins in the membrane fraction of the epibiont which were considerably smaller in size than predicted from the size of Cag1919. The RTX-type C-terminus coded by Cag1919 exhibited a significant similarity to RTX modules of various proteobacterial proteins, suggesting that this putative symbiosis gene has been acquired via horizontal gene transfer from a proteobacterium.

## Introduction

To date, functional studies of microbial symbioses have focussed on the associations of bacteria with eukaryotes (Overmann and Schubert, 2002; Overmann, 2006). Meanwhile, an increasing number of spatially close associations which consist exclusively of prokaryotes have been discovered (Overmann, 2001a). Such associations occur in habitats like dental plaque, the digestive tract, deep sea sediments or in upflow anaerobic sludge bed reactors for wastewater treatment, and catalyze key metabolic processes. So far, however, only the interspecific syntrophic associations involved in methanogenic degradation are understood in sufficient detail (Schink, 1998, 2002).

Phototrophic consortia are highly structured associations between green sulphur bacteria and a chemotrophic bacterium and mostly consist of one motile, colourless betaproteobacterium surrounded by up to 69 green sulphur bacterial epibionts (Fröstl and Overmann, 2000; Overmann, 2001b; Overmann and Schubert, 2002). Phototrophic consortia were discovered a century ago (Lauterborn, 1906) and typically occur in the chemocline of stratified lakes (Overmann *et al.*, 1998; Glaeser and Overmann, 2004) where they can amount to two-thirds of the total bacterial biomass (Gasol *et al.*, 1995). 19 different types of phototrophic consortia have been described (Glaeser and Overmann, 2004). Several independent experimental findings indicate that a rapid signal transfer occurs between the epibionts and the central bacterium. This signal exchange seems to be involved in the coordination of cell division between the partners (Overmann *et al.*, 1998), the scotophobic accumulation of consortia in the light (Fröstl and Overmann, 1998; Glaeser and Overmann, 2003) and the control of carbon uptake of the central bacterium by the epibiont (Glaeser and Overmann, 2003). Phototrophic consortia thus represent the most highly developed interspecific association of bacteria which are recognized so far and serve as a valuable model system to study the molecular basis of cell-cell interactions between different prokaryotes.

Phototrophic consortia can be maintained intact in laboratory cultures (Fröstl and Overmann, 1998). Recently, the epibiont of the phototrophic consortium "*Chlorochromatium aggregatum*", *Chlorobium chlorochromatii* strain CaD, could be isolated in pure culture. Extensive physiological analyses of this strain did not reveal conspicuous differences to free-living green sulphur bacteria (Vogl *et al.*, 2006). Although *Chl. chlorochromatii* is capable of growing in pure culture and hence is not obligately symbiotic, none of the epibionts of the 19 known types of phototrophic consortia has ever been detected in a free-living state in the natural habitat (Glaeser and Overmann, 2004). The epibionts therefore seem to be specifically adapted to life in

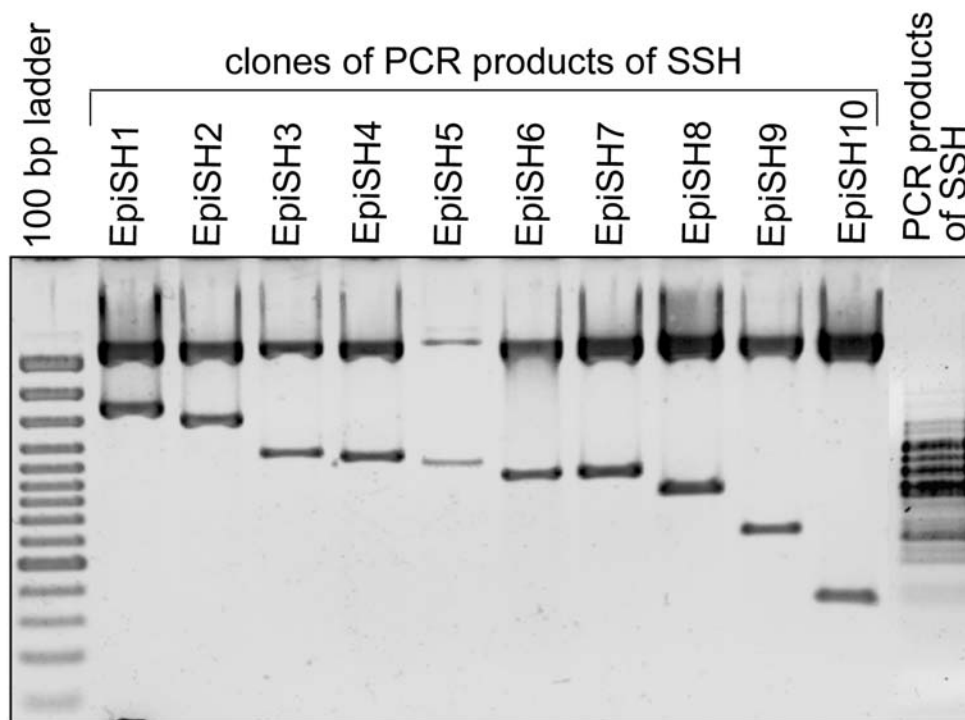
the symbiotic state, but the molecular basis of this adaptation is entirely unknown.

The goal of the present work was to identify symbiosis-specific genes of *Chl. chlorochromatii*. Several candidate genes were detected. At least one of these genes is likely to be involved in a specific Ca<sup>2+</sup>-dependent cell-cell-adhesion of the symbiotic association.

## Results

### Identification and localization of putative symbiosis genes

Suppression subtractive hybridisation (SSH) of genomic DNA of *Chlorobium chlorochromatii* CaD against that of 16 free-living green sulphur bacteria yielded amplification products of 10 different size classes (Suppl.Fig. 1).



**Suppl. Figure 1.** Fragments cloned from the PCR products of the suppression subtractive hybridisation. The ten different size classes are depicted. PCR products are shown on the right for comparison. A negative image of an ethidium bromide-stained gel is shown. The size of the inserts surpasses that of the respective PCR products due to the presence of short vector fragments at both ends.

Representatives of each size class were sequenced. Sequences of clones EpiSH1 and EpiSH8 were found in two size classes but represented the same sequence type. This was also the case for clones EpiSH6 and EpiSH7. Six of the remaining 8 different sequence types (clones EpiSH2, EpiSH3, EpiSH5, EpiSH6, EpiSH9, EpiSH10) coded for enzymes of the central nucleic acid metabolism, amino acid and protein metabolism, or bacteriochlorophyll biosynthesis. Corresponding genes are also present in genomes of other green sulphur bacteria (Table 1).

**Table 1.** Results of BLAST searches of amino acid sequences deduced from SSH clone sequences (for size classes of clone types see Suppl.Fig. 1)

SSH clone/ ORF <sup>1</sup>	DNA insert/ ORF (bp)	Accession no. protein	BLAST X hits	Expected value	Similarity of amino acid sequences
EpiSH2/ Cag1814	1438/ 1623	ZP_ 00590656.1	Light-independent protochlorophyllide reductase, B subunit, BchB [ <i>Chlorobium clathratiforme</i> DSMZ 5477 <sup>T</sup> ]	3e-85	Identities = 161/242(66%) Positives = 183/242(75%)
EpiSH3/ Cag1237	1126/ 1011	ZP_ 00589080.1	Arginine kinase, ArgK [ <i>Chlorobium clathratiforme</i> DSMZ 5477 <sup>T</sup> ]	4e-50	Identities = 99/145 (68%), Positives = 119/145(82%)
<b>EpiSH4/ Cag0616</b>	<b>1038/ 61941</b>	<b>ZP_ 00606097.1</b>	<b>Hemagglutinin</b> [ <i>Magnetococcus</i> sp. MC- 1]	<b>7e-06</b>	<b>Identities = 77/351 (21%), Positives = 135/351(38%)</b>
EpiSH5/ Cag1990	963/864	ZP_ 00512181.1	2,3,4,5-tetrahydropyridine- 2,6-dicarboxylate N- succinyltransferase, DapD [ <i>Chlorobium limicola</i> DSMZ 245 <sup>T</sup> ]	2e-54	Identities = 104/126(82%) Positives = 119/126 (94%)
Cag1991	963/174 9	ZP_ 00512179.1	Serine Peptidase of S41A family, C-terminal protease [ <i>Chlorobium limicola</i> DSMZ 245 <sup>T</sup> ]	2e-24	Identities = 65/158 (41%), Positives = 95/158 (60%)
EpiSH6/ Cag0375	877/189 6	ZP_ 00589495.1	ABC transporter [ <i>Chlorobium clathratiforme</i> DSMZ 5477 <sup>T</sup> ]	8e-141	Identities = 249/292(85%), Positives = 269/292(92%)
<b>EpiSH8/ Cag1920</b>	<b>753/ 11505</b>	<b>ZP_ 00660950.1</b>	<b>Hemolysin-type calcium- binding region:Glycosyl hydrolase, BNR repeat; Hemagglutinin</b> [ <i>Prosthecochloris vibrioformis</i> DSMZ 265]	<b>3e-14</b>	<b>Identities = 62/178 (34%), Positives = 92/178 (51%)</b>
EpiSH9/ Cag0763	521/338 4	ZP_ 00590336.1	Exodeoxyribonuclease V, $\gamma$ -subunit, RecC [ <i>Chlorobium clathratiforme</i> DSMZ 5477 <sup>T</sup> ]	3e-54	Identities = 107/167(64%), Positives = 130/167(77%)
EpiSH10 /Cag0941	238/126 9	ZP_ 00590490.1	Zn-metalloprotease Peptidase M48, Ste24p [ <i>Chlorobium clathratiforme</i> DSMZ 5477 <sup>T</sup> ]	5e-25	Identities = 50/78 (64%), Positives = 68/78 (87%)

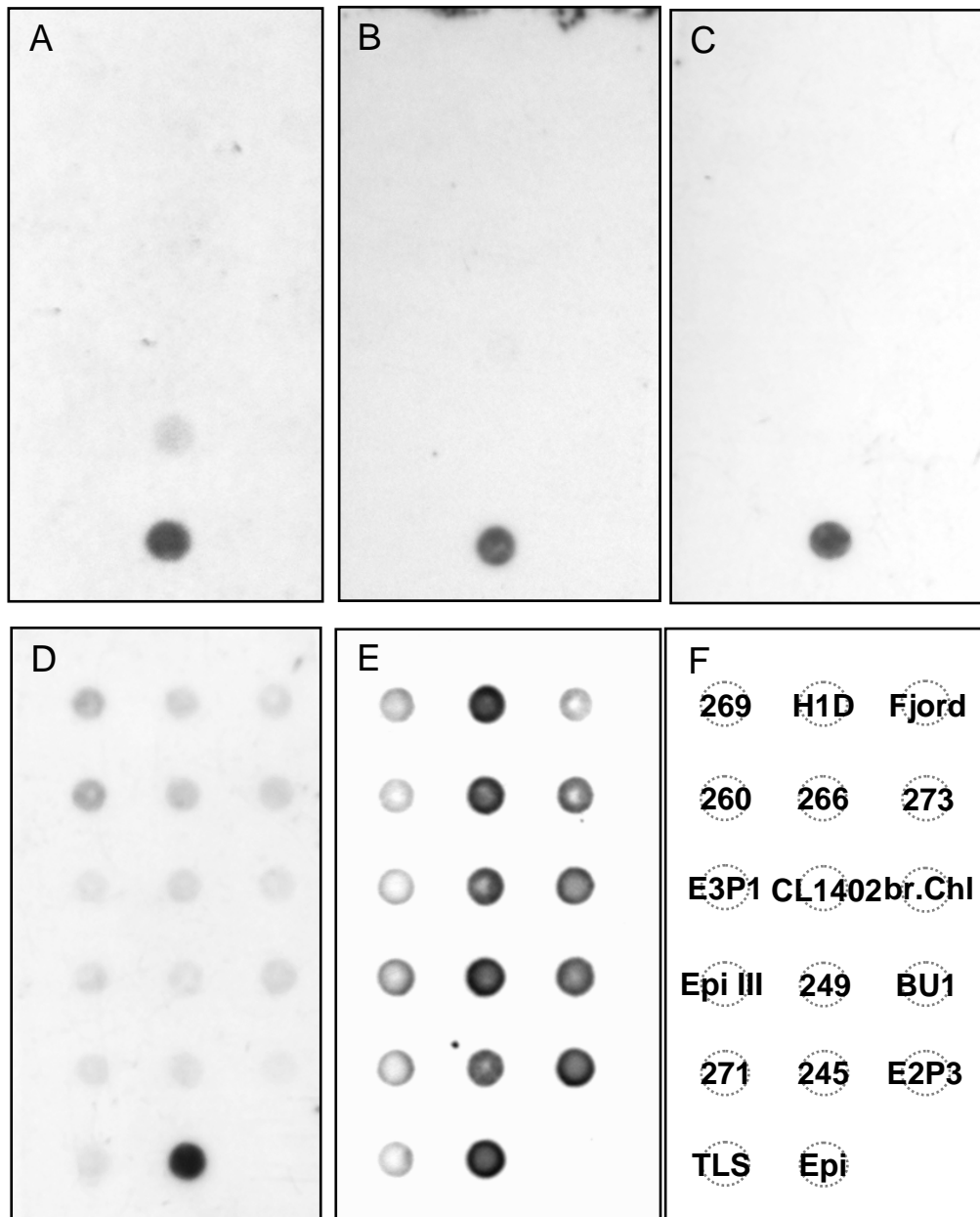
<b>Cag0614</b>	<b>-/110418</b>	<b>YP_866103.1</b>	<b>Hemolysin-type calcium-binding region</b> [ <i>Magnetococcus</i> sp. MC-1]	<b>1e-102</b>	<b>Identities = 338/1124 (30%), Positives = 563/1124 (50%)</b>
<b>Cag1919</b>	<b>-/4581</b>	<b>YP_345893.1</b>	<b>Glycosyl hydrolase, BNR repeat</b> [ <i>Pseudomonas fluorescens</i> PfO-1]	<b>5e-111</b>	<b>Identities = 410/1286 (31%), Positives = 575/1286(44%)</b>
		<b>ZP_00660950.1</b>	<b>Hemolysin-type calcium-binding region:Glycosyl hydrolase, BNR repeat; Hemagglutinin</b> [ <i>Prosthecochloris vibriiformis</i> DSMZ 265]	<b>2e-68</b>	<b>Identities = 394/1396 (28%), Positives = 598/1396(42%)</b>

<sup>1</sup>putative symbiosis genes are indicated in bold; Cag0614 and Cag1919 were identified by bioinformatic methods

In contrast, the sequences of the two clones EpiSH4, EpiSH8 were previously unknown for green sulphur bacteria or exhibited only a low similarity to the available sequences (Table 1). The corresponding ORFs in the genome sequence of *Chl. chlorochromatii* CaD were Cag0616 and Cag1920, respectively. As annotated, ORF Cag0616 would code for an extremely large putative protein of 20,646 amino acids (aa) exhibiting low similarity to a hemagglutinin of *Magnetococcus* sp. MC-1. ORF Cag1920 codes for a 3,834 aa long protein which shows little similarity to a BNR glycosyl hydrolase with a hemolysin-type calcium binding region (Table 1). Subsequent genome analyses revealed the presence of additional unusual sequences in the neighbourhood of ORFs Cag0616 and Cag1920. Cag0614 shows considerable sequence similarity to downstream ORF 0616 and would code for an even longer (36,805 aa) gene product (Table 1). Upstream of Cag1920, ORF Cag1919 codes for a protein of 1,526 aa which exhibits low similarity to a glycosyl hydrolase with bacterial neuraminidase repeat (BNR) and a hemolysin-type calcium binding region.

### **Candidate symbiosis genes are absent in other free-living green sulphur bacteria**

Corresponding to the results of our SSH analysis, no close homologues (identities  $\geq 35\%$ ) of Cag 0614, 0616, 1919 and 1920 could be detected in the 8 available genome sequences of free-living green sulphur bacteria. To investigate the distribution of the candidate symbiosis genes in a larger number of free-living green sulphur bacteria, specific probes targeting ORFs Cag0616, 1919 and 1920 were generated and used in dot blot hybridisations against genomic DNA of 16 phylogenetically diverse green sulphur bacterial strains as well as the epibiont *Chl. chlorochromatii*. The candidate symbiosis genes could not be detected in the free-living strains (Suppl.Fig. 2).



**Suppl. Figure 2.** Dot Blot hybridisations of genomic DNA from 17 different green sulphur bacteria with probes targeting putative symbiosis genes of *Chlorobium chlorochromatii* CaD. **A.** Hybridization with a probe against ORF Cag1919. **B.** Probe targeting clone EpiSH4 (ORF Cag0616). **C.** Probe targeting clone EpiSH8 (ORF Cag1920). **D.** Probe targeting clone EpiSH6 (ABC transporter, compare Table 1). **E.** Probe targeting the 16S rRNA gene of *Chl. chlorochromatii*. **F.** Blotting scheme of the samples. Strain designations: 269, *Chl. phaeovibrioides* DSMZ 269<sup>T</sup>; H1D, *Chlorobium* strain H1D; Fjord, *Chlorobium* strain Fjord; 260, *Ptc. vibrioformis* DSMZ 260<sup>T</sup>; 266, *Chl. phaeobacteroides* DSMZ 266<sup>T</sup>; 273, *Chl. luteolum* DSMZ 273<sup>T</sup>; E3P1, *Chl. limicola* E3P1; CL 1402, *Chl. phaeobacteroides* CL 1402; br. Chl, *Chl. phaeobacteroides* br.Chl.; DagIII, *Chl. phaeobacteroides* DagIII; 249, *Cba. thiosulfatiphilum* DSMZ 249<sup>T</sup>; BU1, *Chl. clathratiforme* DSMZ 5477<sup>T</sup> (BU1); 271, *Ptc. aestuarii* DSMZ 271<sup>T</sup>; 245, *Chl. limicola* DSMZ 245<sup>T</sup>; E2P3, *Chl. phaeobacteroides* E2P3; TLS, *Cba. tepidum* ATCC 49652<sup>T</sup> (TLS); Epi, *Chl. chlorochromatii* CaD (epibiont).

Only a faint hybridization signal was detected for *Chl. limicola* DSMZ 245<sup>T</sup> with the probe against Cag 1919, however, the corresponding sequence was absent from the genome of this strain. For comparison, we also generated and tested a probe targeting the gene for a putative ABC transporter (clone EpiSH6) of *Chl. chlorochromatii*. Weak hybridisation signals were obtained for all other 16 tested strains (Suppl.Fig. 2D), which indicates the presence of similar gene sequences in free-living green sulphur bacteria and corroborates the higher similarity of the EpiSH6 sequence to that of other green sulphur bacteria which had been detected by the bioinformatic approach (Table 1). As a second control, dot blot hybridisation with a 16S rRNA gene probe specific for *Chl. chlorochromatii* was conducted and yielded much stronger hybridisation signals (Suppl.Fig. 2E) which is commensurate with the high similarity of the 16S rRNA sequences of > 90% among the green sulphur bacteria (Overmann and Tuschak, 1997). The above results substantiate the unique occurrence of candidate symbiosis genes in *Chl. chlorochromatii* CaD.

### **Transcription of putative symbiosis genes in the symbiotic and nonsymbiotic state**

Initially, a series of Northern blot analyses was conducted to determine the lengths of the transcripts of Cag1919 and 1920 (Cag0614 and 0616 being too long for this type of analyses). No signals could be detected with the specific probes, indicating a low abundance of the transcripts. Therefore, a RT-PCR approach was employed to assess the transcription of the three putative symbiosis genes. Two different primer sets were employed to study transcripts of Cag1919 (Suppl. Tab.1). Because of the unusual size of ORF Cag1920 and, particularly, of the alleged ORF Cag0616, three different primer sets were constructed which amplified three different regions of each of the two ORFs. The different primer sets targeted regions 695 - 868, 4650 - 4798 and 9881 - 10057 in ORF Cag1920 and regions 2436 - 2556, 27378 - 27546 and 53556 - 53697 in ORF Cag0616 (Suppl. Table 1). Highly specific PCR conditions were established by using RNA extracts of all 16 nonsymbiotic green sulphur bacterial strains as negative controls. As controls for the contamination with genomic DNA, direct amplification trials of the RNA extracts without prior reverse transcription were included in each PCR and amplifications with a primer set targeting the *sigA* gene were performed. The latter method permits a detection of traces of DNA at a significantly higher sensitivity than the PCR targeting 16S rRNA genes.

487 bp-long cDNA fragments of Cag1919 were obtained from the consortium "*Chlorochromatium aggregatum*" as well as from pure cultures of *Chl. chlorochromatii* (Fig.

1A). Employing primers binding to the 5'- and 3'-ends of Cag1919 in a long-range RT-PCR analysis, transcripts of the entire ORF Cag1919 could be detected (Fig. 1B). Also constitutively transcribed were the central part of Cag1920 as well as the 5' end and central parts of Cag0616 (data not shown). However, transcripts of the 5' and 3'-regions of Cag 1920 and of the 3'-region of Cag 0616 could not be detected.

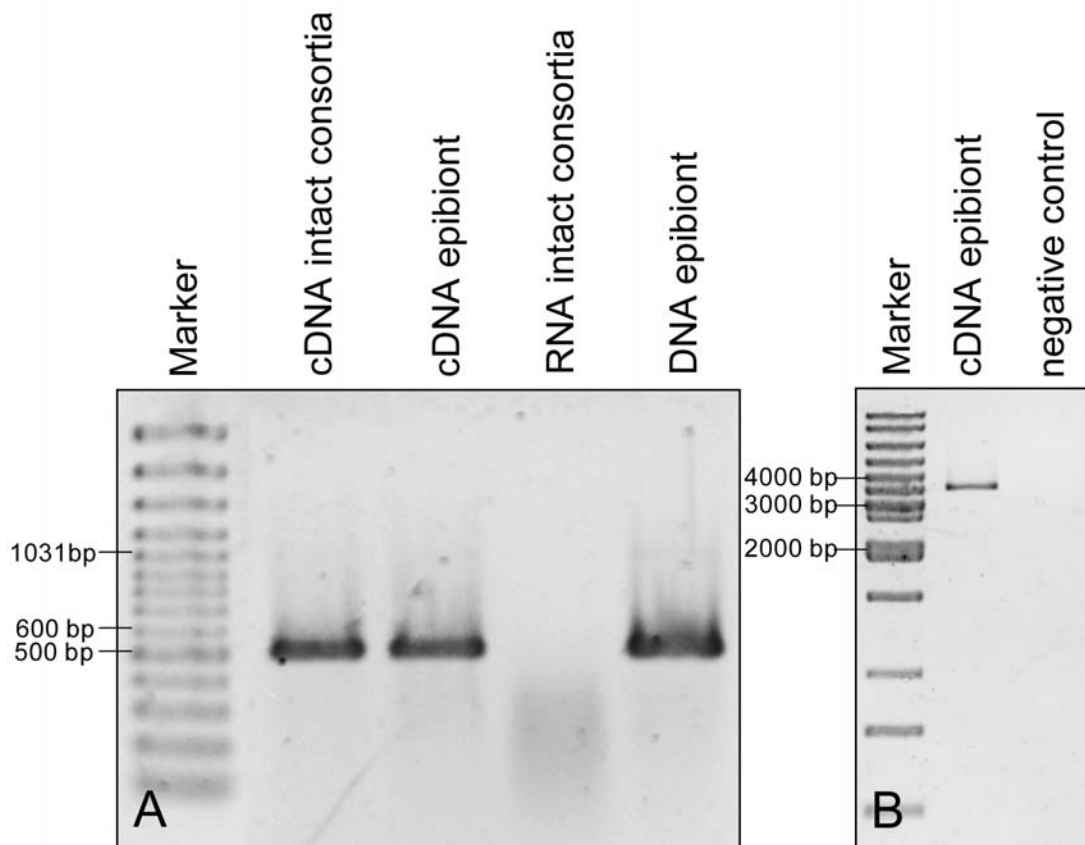


**Figure 1.** Detection of transcripts of ORF Cag1919. **A.** Detection of transcripts of ORF Cag1919 in pure cultures of *Chlorobium chlorochromatii* and in intact "*Chlorochromatium aggregatum*" consortia. A 487 bp-long PCR product was generated with the primer pair RTX 3797f and RTX 4266r (see Supplementary Table 1). RNA extracts from "*Chlorochromatium aggregatum*" without reverse transcription served as a negative control, and genomic DNA from *Chlorobium chlorochromatii* as a positive control. **B.** Transcript of the almost complete ORF Cag1919 detected in *Chlorobium chlorochromatii* cultures employing the primer pair RTX502f and RTX 4284r. A PCR without addition of the reverse transcriptase was used as a negative control.

### Sequence analysis and modelling of the gene products

Subsequent bioinformatic analyses focussed on the detection of functional modules in Cag0614, 0616, 1919 and 1920. Motif Scan and Inter Pro Scan detected a hemagglutinin repeat and

crystallins beta and gamma Greek key motifs in Cag0616 (Fig. 2). The two consecutive Greek key motifs contained all characteristic elements, namely the conserved sequence (Y/F/W) $X_6GX_{28-34}S$  (Ranjini *et al.*, 2001), two putative  $Ca^{2+}$  binding sites and the presence of three or four beta strands, respectively (Fig. 2B). Outside of the Greek key motifs, the putative gene product of Cag0616 harbours three RGD tripeptide motifs known from filamentous hemagglutinin (Relman *et al.*, 1989) plus four different types of repeats (R1'-R4'; Fig. 2A). The first repeat (1194 – 3328) consists of three 711 aa-long sequences, the following three repeat regions span positions 13913 - 14391, 14974 - 16863 and 18374 – 20129 and consist of sequences with lengths of 236, 933 and 877 aa, respectively.

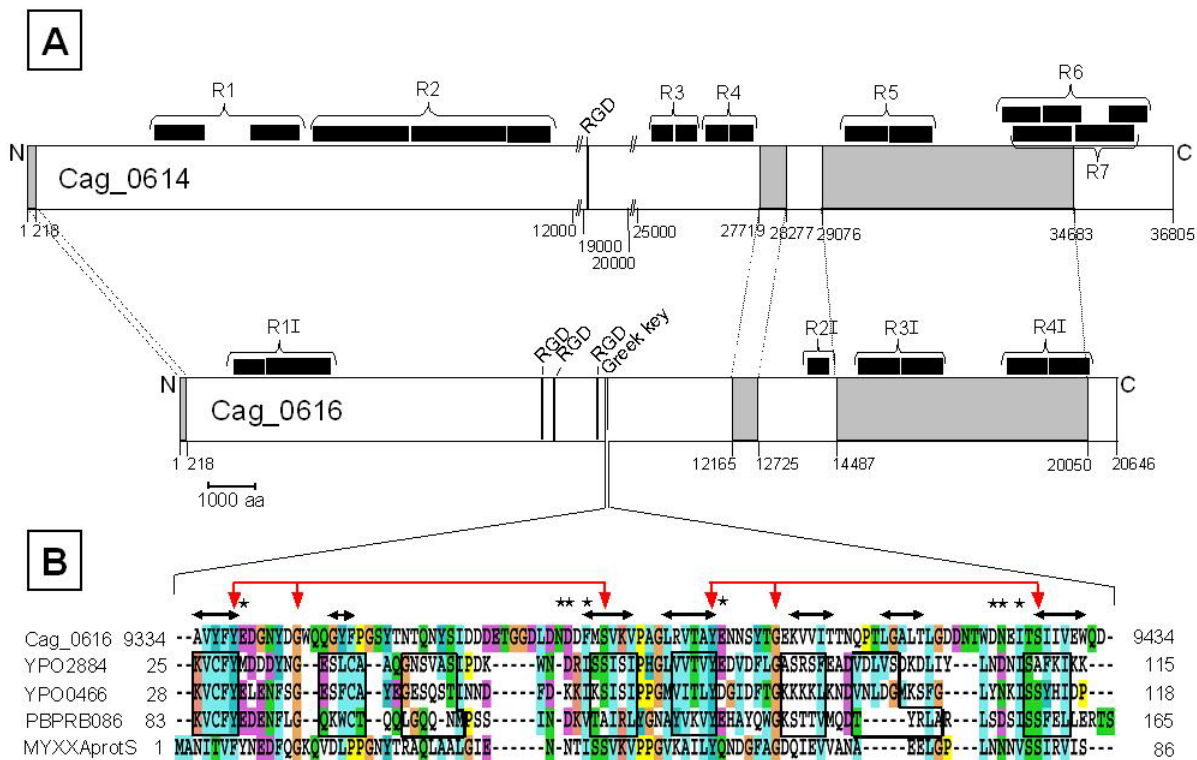


**Figure 2.** **A.** Bioinformatic analysis of putative gene products of ORFs Cag0614 and Cag0616. Areas of high sequence similarity between the two products are shaded in grey, black bars denote sequence repeats within each product. In addition, the positions of RGD motifs (one in Cag0614, three in Cag0616) and of the greek key motifs (in Cag0616) are indicated. **B.** Alignment of the 100 aa-sequence of Cag0616 containing the two greek key motifs (Y/F/W) $X_6GX_{28-34}S$  (red arrows) with sequences of the hypothetical proteins YPO2884 and YPO0466 of *Yersinia pestis* CO92, PBPRB0866 of *Photobacterium profundum* SS9 and the development-specific protein S of *Myxococcus xanthus* FB. Putative calcium-binding sites (Rajini *et al.*, 2001) are indicated by asterisks.  $\beta$ -strands predicted for Cag0616 are denoted as double-headed arrows and for comparison are boxed for the *Y. pestis* and *P. profundum* proteins according to Jobby and Sharma (2005). Bar represents 1000 amino acids.

Three sequence regions of Cag0616 were found to be almost identical to Cag0614 (Fig. 2A). These regions spanned amino acid positions 1 - 218, 12165 - 12725 and 14487 - 20050 in Cag0616 and positions 1 - 218, 27719 - 29076 and 34683 - 36805 in Cag0614. In contrast to Cag0616, the amino acid sequence of Cag0614 contains only one RGD tripeptide but harbours seven different repeat regions. Repeat regions 1 (2813-3924; 4897-5909), 3 (25316-26279), 4 (26549-27579), 5 (29577-31505), and 7 (33134-36000) each consisted of two individual repeats with lengths of 1102 aa, 479 aa, 507 aa, 957 aa and 1348 aa. Repeat 2 contains two complete 2072 aa repeats and one incomplete 952 aa fragment. Repeat 6 comprises three 862 aa repeats (Fig. 2A). Amino acid identities between repeats R5 (Cag0614) and R3' (Cag0616), and between R6 (Cag0614) and R4' (Cag0616) were 83 and 79%, respectively. A Greek key motif was not detected in the putative gene product of Cag0614.

Employing the ScanProsite software yielded no hit for ORF Cag1920. With the Motif Scan and Inter Pro Scan software, however, a bacterial neuraminase repeat (BNR)/Asp box repeat and an inosine-5'-monophosphate (IMP) dehydrogenase/GMP reductase domain was found to match the query sequence.

Within the putative gene product encoded by Cag1919, a distinct C-terminal hemolysin-type calcium-binding region was identified. Hemolysin-type calcium-binding modules are characterized by multiple repeats of the nine residue sequence GGXGXDXLX which include a GGXGXD consensus sequence. The three-dimensional structure of such a  $\text{Ca}^{2+}$ -binding motif was already reported for the alkaline protease of *Pseudomonas aeruginosa* and features a parallel beta roll structure in which the  $\text{Ca}^{2+}$  ions are bound at the turns between the two strands (Fig. 3A). Within the turns, the  $\text{Ca}^{2+}$  ions are directly coordinated by the aspartic acid residues of the repeat sequence GGXGXD (Baumann *et al.*, 1993) (Fig. 3A,C). Additional binding sites have been deduced from the crystal structure (Baumann *et al.*, 1993) (Fig. 3A,C). Accordingly, modelling of the Cag1919 gene product yielded a C-terminal beta roll structure (Fig. 3B). Six repeats of the consensus sequence GGXGXD were identified within a 100 amino acid-long region, and included an additional motif not found in *Pseudomonas aeruginosa* (Fig. 3C, marked by a brown bar). The entire C-terminal region aligned well with  $\text{Ca}^{2+}$ -binding domains of different proteobacterial proteins, which strongly supports the presence of a parallel beta roll structure in the gene product of Cag1919 (Fig. 3C). No secretion signals known for RTX-toxins such as a C-terminal hydrophobic region flanked by glutamic acid or aspartic acid (Economou *et al.*, 1990) or the conserved sequence (E/D) $\text{X}_{11}$ DX<sub>3-5</sub>(E/D)  $\text{X}_{14}$ E (Sebo and Ladant, 1993) were found in Cag1919. Analyses using the SignalP (Bendtsen *et al.*, 2004) and Predisi software (Hiller *et al.*, 2004) also did not indicate the presence of other secretion signals and a homolog to

the pore-forming region of the adenylate cyclase (CyaA) of *Bordetella pertussis* (Bauche *et al.*, 2006) could not be detected. A hydropathicity plot according to Kyte and Doolittle employing the ProtScale (Gasteiger *et al.*, 2005) software confirmed the absence of transmembrane helices. In contrast to Cag1919, no matching templates were found during the automated modelling of putative gene products of Cag 0614, 0616 and 1920.

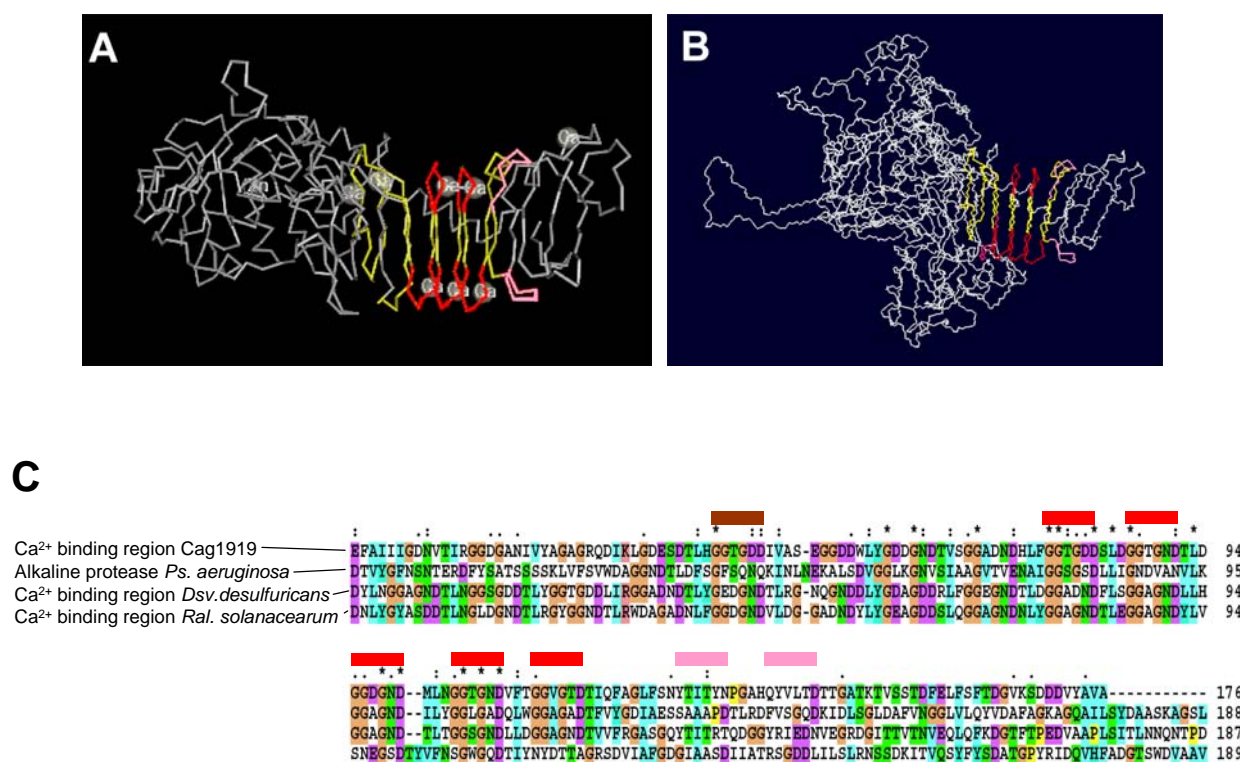


**Figure 3.** **A.** Three-dimensional structure of the alkaline protease of *Pseudomonas aeruginosa* (Baumann *et al.*, 1993) as available through the structure database of NCBI (Chen *et al.*, 2003) under accession number 1KAP. The structure was displayed with the Cn3D application of the NCBI Entrez retrieval service (<http://www.ncbi.nlm.nih.gov/Structure/CN3D/cn3d.shtml>). **B.** Three-dimensional model of the gene product of ORF Cag1919 which at the C-terminus exhibits close similarity to the alkaline protease of *Pseudomonas aeruginosa*. In A. and B., the parallel beta roll is marked in yellow, amino acid residues involved in Ca<sup>2+</sup> binding are marked in red and pink. **C.** Alignment of the sequences of parallel beta roll motives present in proteins from different proteobacteria. Amino acid residues of the RTX-motif shown to be involved in Ca<sup>2+</sup> binding in alkaline protease are marked by red bars, Ca<sup>2+</sup>-binding regions inferred from the crystal structure are denoted by pink bars. An additional Ca<sup>2+</sup> binding motif which is only found in the putative product of Cag1919 is indicated by a brown bar. Besides the most closely related sequences of *Dsv. desulfuricans* G20 and *Ral. solanacearum* GMI 1000 (see Fig. 4), the well characterised alkaline protease of *Ps. aeruginosa* are included in the alignment.

The phylogenetic analysis of the amino acid sequence coded by Cag1919 revealed that the most closely related RTX toxin  $\text{Ca}^{2+}$ -binding region is present in the deltaproteobacterium *Desulfovibrio desulfuricans* G20 (Fig. 4). Also, most of the other related proteins are RTX toxins and proteins with a hemolysin-type calcium-binding region and include autotransporter adhesins of *Pseudomonas fluorescens* PfO-1 and *Vibrio vulnificus* YJ016, an iron-regulated protein FrpC from *Vibrio fischeri* ES114, a cable pili-associated 22kDa adhesin AdhA from *Burkholderia cepacia* and a Fat protein of *Synechocystis* sp. PCC6803. A common feature of these proteins is their involvement in adhesion. The Fat protein and the iron-regulated protein FrpC have the ability to bind calcium like RTX toxins and proteins with a hemolysin-type calcium binding region. All related proteins occur in proteobacteria with the exception of the Fat protein of the cyanobacterium *Synechocystis* sp. PCC 6803, which represents the most distantly related amino acid sequence (Fig. 4).

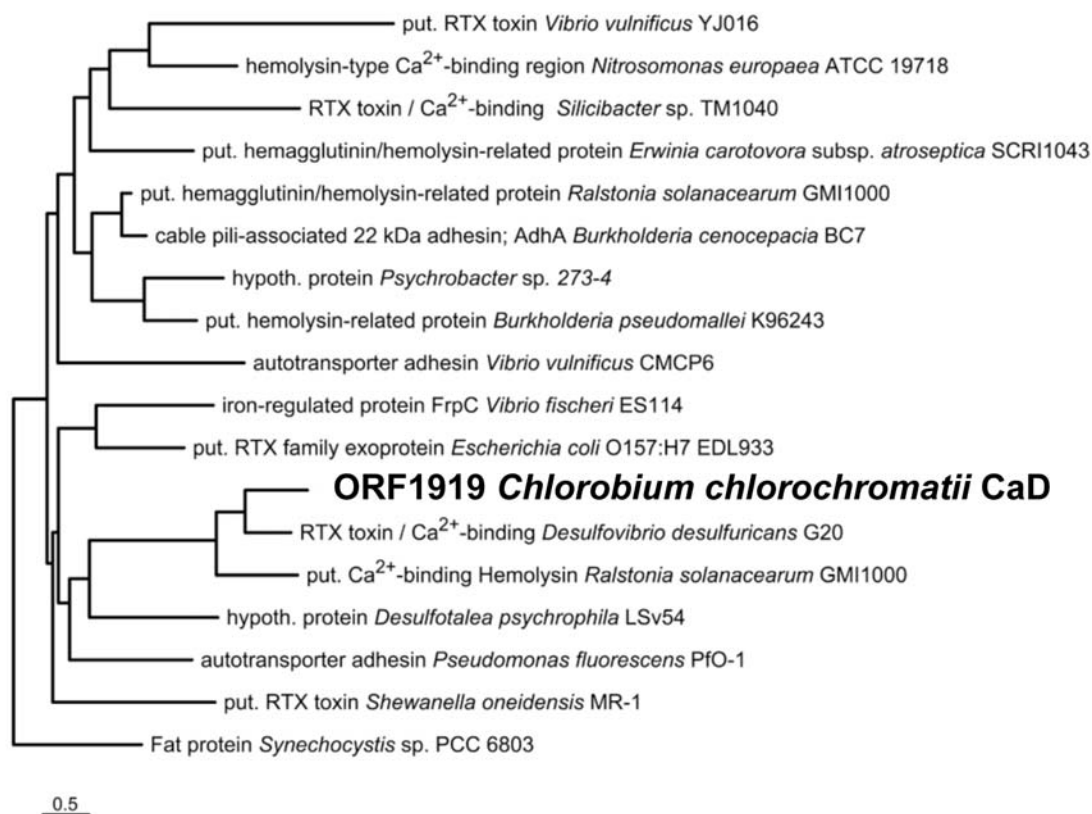


**Figure 4.** Phylogenetic analysis of the RTX-module of the C-terminal amino acid sequence of Cag1919. The analysis is based on an alignment of the sequences of other bacteria to the 176 amino acid-long protein sequence of RTX-type motif of *Chl. chlorochromatii* (compare Fig. 3C). The bar refers to 0.5 substitutions per 100 amino acid sites.

### Detection of Ca<sup>2+</sup>-binding proteins and role of Ca<sup>2+</sup> in cell-cell-adhesion

Ca<sup>2+</sup>-binding proteins in *Chlorobium chlorochromatii* were studied by <sup>45</sup>Ca<sup>2+</sup>-autoradiography. Within the membrane fraction of the isolated epibiont, three individual protein bands with a molecular mass of about 22, 25 and 29 kD could be detected (Fig. 5, filled arrowheads). In the membrane fraction of the consortium "*C. aggregatum*", four radioactive bands (Fig. 5, hollow arrowheads) could be detected and matched proteins with an estimated molecular mass of 22, 25, 29 and 34 kD. No Ca<sup>2+</sup>-binding proteins were observed in the cytoplasmic fraction of the isolated epibiont *Chl. chlorochromatii* and the consortium "*C. aggregatum*" (Fig 5). Ca<sup>2+</sup>-binding proteins were also missing in both, the cytoplasmic and membrane fractions of *Cba. tepidum* (Fig 5). As a positive control, the purified adenylate cyclase from *Bordetella pertussis* which contains a beta roll motif could also be detected by this method (data not shown). It is highly unlikely that the <sup>45</sup>Ca<sup>2+</sup>-binding bands contained outer membrane lipopolysaccharides since (1) the majority of lipids were extracted in the acetone precipitation step during protein preparation and (2) no signals could be obtained when purified LPS of *Escherichia coli* B or *Serratia marcescens* (Sigma L-6136) were run on the SDS gels (data not shown).

The role of Ca<sup>2+</sup> in the phototrophic consortium "*Chlorochromatium aggregatum*" was investigated by studying the effects of different chemicals on aggregate stability and motility of the consortia. The impact of the redox potential was assessed with reducing agents (ascorbate, L-cysteine, sodium sulphite), and the contribution of lectins to the adhesion by adding a suite of sugars and sugar derivatives (D-(+)-mannose, L-rhamnose, D-galactose, glucose, fucose, arabinose, N-acetylglucosamine, glucuronic acid, galacturonic acid, methyl glucoside, methyl mannoside). Also, a variety of ionic and nonionic detergents (SDS, Tween20, Tween80, Triton X-100) and denaturing agents (urea, formamid) was applied. Finally, the testing scheme comprised several hydrolytic enzymes (hyaluronidase, β-glucuronidase, proteinase K, pepsin, trypsin, chymotrypsin, lysozyme) and complexing agents (EDTA, EGTA, pyrophosphate, citrate, tartrate).

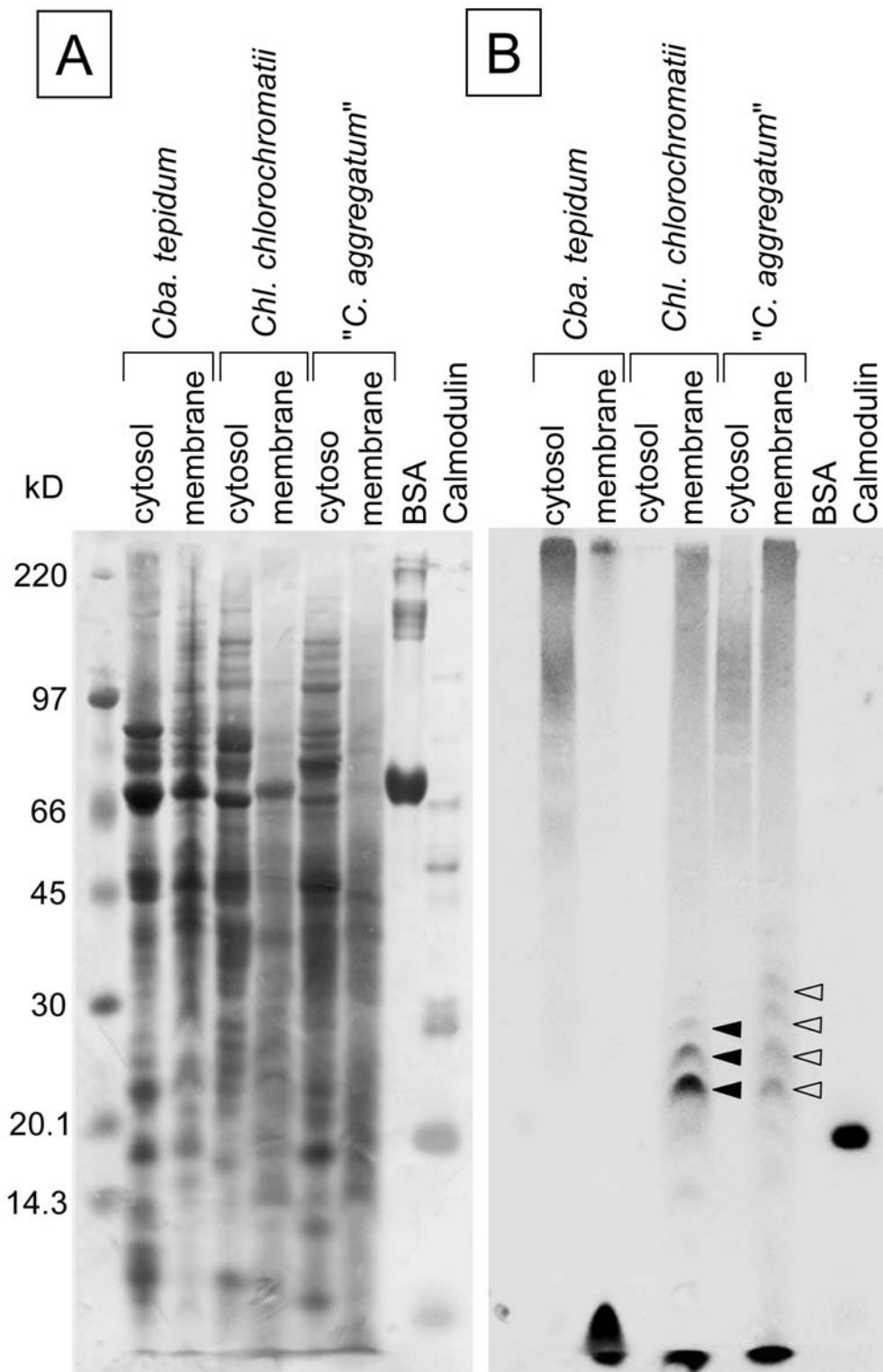


**Figure 5.**  $\text{Ca}^{2+}$  binding assay for cytoplasmic and cell wall proteins from *Cba. tepidum*, *Chl. chlorochromatii* and "*Chlorochromatium aggregatum*". Calmodulin served as positive and BSA as negative control. Proteins were separated by SDS-PAGE, electrotransferred to a polyvinylidene difluoride membrane and incubated with  $^{45}\text{Ca}$ . **A.** PVDF membrane stained with amido black. **B.** Autoradiograph. Solid arrowheads denote membrane proteins of *Chl. chlorochromatii*, hollow arrowheads membrane proteins of the consortium "*C. aggregatum*" binding  $^{45}\text{Ca}^{2+}$ .

Of all compounds, only  $\text{Ca}^{2+}$ -complexing agents (EGTA, EDTA, pyrophosphate) and the strong detergents SDS and TritonX-100 exerted a significant effect on cell-cell-binding in "*C. aggregatum*" (Fig. 6). The extent of disaggregation by EGTA, EDTA and pyrophosphate was dependent on the concentration applied. While more than 70% of the consortia remained intact after 10 min of exposure to 2 mM concentrations of these agents, almost all consortia disaggregated in the presence of 20 mM EGTA over this time period. Disaggregation by pyrophosphate was slower compared to that by EDTA and EGTA (Fig. 6). While ascorbate and sulphite at concentrations of 20 mM inhibited the motility of the consortia, they did not affect cell-cell-binding, however. None of the sugar compounds or the denaturing agents exerted any effect (shown for arabinose in Fig. 6). Similarly, no effect was observed for Tween 20 and Tween 80, whereas the stronger detergents SDS and TritonX-100 led to complete immotility and a partial but significant disaggregation of the consortia. Of the hydrolytic enzymes, lysozyme, hyaluronidase,  $\beta$ -glucuronidase, trypsin and chymotrypsin affected motility, but not cell-cell-binding of the consortia (Fig. 6).

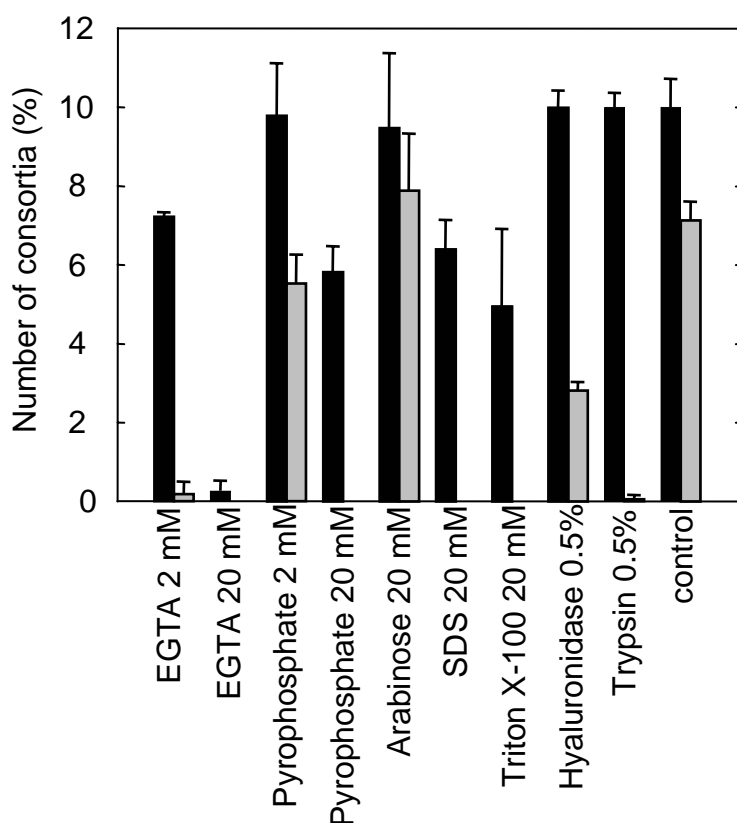


**Figure 6.** Percentage of intact (■) and motile (▒) "*Chlorochromatium aggregatum*" consortia remaining after 10 min of incubation in the presence of different chemical agents (final concentrations are given). Vertical bars indicate one standard deviation.

## Discussion

### Occurrence and transcription of candidate symbiosis genes in *Chl. chlorochromatii*

The adaptation of bacteria to their particular ecological niches has been traced back to genomic differences in either single genes or gene clusters, or to the differential expression of common genes (Perna *et al.*, 2001; Reid *et al.*, 2003; Jones *et al.*, 2006). A well-studied case is the evolution of high- and low-light adapted lineages of the marine genus *Prochlorococcus* leading to hundreds of lineage-specific genes (Rocap *et al.*, 2003). 16S rRNA gene sequence similarities between lineages with different adaptation are below 98 % (Moore *et al.*, 1998). At a similarity value of 96%, the epibiont *Chl. chlorochromatii* CaD of the consortium "*Chlorochromatium aggregatum*" is phylogenetically even more distant to its free-living relatives (Glaeser and Overmann, 2004). Therefore, niche-specific genes were expected to occur in the genome of *Chl. chlorochromatii* CaD.

So far, identification of niche-specific genes in other bacterial groups has mostly been performed by comparing two or three bacterial genomes (Perna *et al.*, 2001; Jones *et al.*, 2003; Reid *et al.*, 2003; van Ham *et al.*, 2003). In order to reliably identify putative symbiosis-specific genes in the epibiont genome, our suppression subtractive hybridisation (SSH) included 16 free-living strains of green sulphur bacteria of different physiology (Overmann, 2001b) which appeared promising since the members of this group are phylogenetically rather closely related (Overmann and Tuschak, 1997). Our results demonstrate that such a mixture of genomic DNA from a larger number of related bacterial strains can be employed as driver to recover genes which are unique to a single tester strain. The unique nature of the putative symbiosis-specific ORFs Cag0614, 0616, 1919 and 1920 were fully confirmed by subsequent *in silico* analyses of the eight available genome sequences of green sulphur bacteria. Apart from the putative symbiosis genes, SSH retrieved several gene fragments with similarity to functional genes of free-living green sulphur bacteria. This result is explained by the fact that functional genes of green sulphur bacteria exhibit a larger sequence divergence than the 16S rRNA genes (Figueras *et al.*, 2002), as exemplified by the weak dot blot hybridisation of the ABC transporter in Fig. 2D. If sufficiently different, such functional genes will not be depleted during SSH.

Interestingly, the transcription of the putative symbiosis genes does not seem to be regulated by the symbiotic interaction with the *Betaproteobacterium* since our highly specific RT-PCR approach detected transcripts of ORF Cag0616, Cag1919 and Cag1920 in pure (i.e. nonsymbiotic) cultures of the epibiont *Chl. chlorochromatii* as well as in intact "*Chlorochromatium aggregatum*" consortia. Therefore, either the regulation is

posttranscriptional or expression of the ORFs is not regulated at all. It is likely that the expression of the ORFs is not regulated since proteins detected by autoradiography were present in *Chl. chlorochromatii* as well as in "*Chlorochromatium aggregatum*". Epibionts seem to be specifically adapted to the life in association with the central bacterium and have never been detected in the free-living state in nature (Glaeser and Overmann, 2004). Therefore, a regulation mechanism for the expression of the three potential symbiosis genes may actually be dispensable.

### **Cag0614, Cag0616 and Cag1920**

ORFs Cag0614 and 0616 show similarity to a putative hemagglutinin and contained numerous internal repeats. The high sequence similarity and similar structure of Cag0614 and Cag0616 suggests that these two ORFs arose through a gene duplication event. Contiguous repeats of several hundred amino acids are known for other hemagglutinin-like proteins (Ward *et al.*, 1998). In addition, Cag0616 codes three arginyl-glycyl-aspartic acid tripeptides, and one Greek key motif. The RGD motif occurs in proteins (e.g., fibronectin) of the extracellular matrix of mammalian cells, in toxins of plant pathogenic fungi or in surface proteins of certain animal viruses, and mediates adhesion of cell surface receptors (Ruoslahti and Pierschbacher, 1986; Isberg and Tran Van Nhieu, 1994; Tan *et al.*, 2001; Senchou *et al.*, 2004). In prokaryotes, the RGD motif is present in the integrin-binding proteins of pathogens like *Bordetella pertussis* that attach to mammalian cells (Isberg and Tran Van Nhieu, 1994; Kajava *et al.*, 2001). Based on their frequent involvement in host-pathogen-interactions, the three RGD tripeptides detected in ORF Cag0616 may participate in the cell-cell-binding of phototrophic consortia.

The Greek key motif is composed of four antiparallel beta strands and occurs as duplicate motif in vertebrate proteins of the  $\beta\gamma$ -crystallin superfamily. In bacteria, the motif was found in the spore coat protein S of *Myxococcus xanthus*, a metalloprotease inhibitor of *Streptomyces* and an extracellular protein of *Yersinia pestis* (Wistow, 1990; Rajini *et al.*, 2001; Jobby and Sharma, 2005). These bacterial proteins have been assumed to participate in the response to stress conditions. Among the Green Sulphur Bacteria, Cag0616 occurs only in the symbiotic *Chl. chlorochromatii*, which indicates that the  $\beta\gamma$ -crystallin-type gene product is involved in the symbiotic interaction. Duplicate Greek key motifs have been shown to bind two calcium ions (Rajini *et al.*, 2001). Similarly, the gene product of Cag0616 may be stabilised by binding of  $\text{Ca}^{2+}$  ions.

Since the protein sequence with the closest similarity to Cag0616 was a putative hemagglutinin, we searched for additional properties of the putative gene product of Cag0616. The filamentous hemagglutinin adhesin (coded by *fhaB*) of *Bordetella pertussis* contains a binding site for sulphated glycolipids and a carbohydrate recognition domain besides its two RGD motifs (Kajava *et al.*, 2001). Adhesion mediated through the lectine-like activity can be partially blocked by galactose (Isberg and Tran Van Nhieu, 1994). In contrast, our disaggregation studies did not yield any evidence for the participation of lectines in the cell-cell-interaction in "*C. aggregatum*".

Spanning 110,418 and 61,938 bp, respectively, the Cag0614 and Cag0616 are amongst the largest open reading frames known to date. Open reading frames of similar size have only been found in the cyanobacterium *Synechococcus* sp. RS9917 (RS9917\_01402; 84,534 bp). Since known hemagglutinins, like the products of the 10774 bp-long *fhaB* of *B. pertussis* (Domenighini *et al.*, 1990) or of the 12,500 and 14,800 bp-long *lspA1* and *lspA2* of *Haemophilus ducreyi* (Ward *et al.*, 1998) have been shown to be post-translational processed, only parts of ORFs Cag0614 and 0616 may actually be expressed in the epibiont of phototrophic consortia.

The analysis of ORF 1920 revealed the presence of a bacterial neuraminase repeat (BNR)/Asp box repeat which has been found in more than nine non-homologous protein families, including bacterial ribonucleases, sulphite oxidases, reelin, netrins, some lipoprotein receptors and a variety of glycosyl hydrolases. So far, few experimental data are available concerning the general functions of Asp boxes (Copley *et al.*, 2001).

### **Cag1919**

Cag 1919 seems not to be secreted employing one of the mechanisms known for the RTX-type toxins like, e.g. adenylate cyclase of *Bordetella pertussis* (Bauche *et al.*, 2006). Similarly, pore formation by the N-terminal hydrophobic domain like in the adenylate cyclase is highly unlikely since no transmembrane helices were detected in the Cag1919 gene product. The C-terminal hemolysin-type  $\text{Ca}^{2+}$ -binding region coded by Cag1919 contains several RTX repeats and is highly similar to the RTX-region in alkaline protease of *Pseudomonas aeruginosa*. RTX toxins are typically found in Gram-negative pathogenic bacteria and are characterised by repetitive nonapeptide motifs, which include a GGXGXD consensus (Welch, 1995). The RTX module is necessary for binding to the target cell and without loss of this function can be separated from the other, lytic (as in the *Pasteurella* leukotoxin; Cruz *et al.*, 1990) or catalytic domains (as in adenylate cyclase of *Bordetella pertussis*; El-Azami-El-Idrissi *et al.*, 2003). The binding of RTX

toxins of pathogenic bacteria to the target cell involves  $\text{Ca}^{2+}$  ions (Ludwig *et al.*, 1988; Knapp *et al.*, 2003) which are bound at the GGXGXDXLX repeats with low affinity (Rose *et al.*, 1995; Lilie *et al.*, 2000). Our sequence comparisons and 3D-modeling strongly indicates that the Cag1919 gene product forms a C-terminal beta roll which represents a bona fide  $\text{Ca}^{2+}$  binding structure. Based on the results of our disaggregation studies, it appears feasible that the RTX domain encoded by Cag1919 of *Chl. chlorochromatii* is involved in the cell-cell-adhesion between the partner bacteria of phototrophic consortia.

In Gram-negative bacteria,  $\text{Ca}^{2+}$  is also bound within the outer membrane bridging negatively charged phosphate groups of the lipopolysaccharides (LPS). Removal of divalent cations with chelating agents like EDTA can strip a fraction of the LPS from the cell surface and thereby destabilize the outer membrane (Jia *et al.*, 2004). Although it cannot be completely excluded that this effect contributes towards the disaggregation of phototrophic consortia, the presence of several  $^{45}\text{Ca}^{2+}$ -binding membrane proteins in the epibiont was clearly demonstrated.

RT-PCR analyses of Cag1919 revealed that this ORF is transcribed over its entire length. The corresponding protein is expected to have a molecular mass of 155 kD, but was not detected by  $^{45}\text{Ca}^{2+}$  autoradiography on SDS gels. This may be due to a low abundance of the Cag1919 protein since the detection limit of the autoradiography method is 2  $\mu\text{g}$  of calcium binding protein corresponding to 3% of the membrane protein (Maruyama *et al.*, 1984). More likely, posttranslational processing and/or limited proteolysis of the Cag1919 gene product would result in the observed pattern of protein bands based on the following reasoning. For the adenylate cyclase toxin CyaA of *Bordetella pertussis* it has been shown that the RTX domain is protected against trypsin proteolysis due to its particular structure (Bauche *et al.*, 2006). The smallest  $^{45}\text{Ca}^{2+}$  binding protein detected in the membrane fraction of *Chl. chlorochromatii* had a molecular weight of 22 kD which is exactly the expected size of the RTX domain of Cag1919 (amino acid positions 1319 – 1526; cf. Fig. 3C). The fact that the smallest protein band yielded the most prominent signal in the membrane fraction of *Chl. chlorochromatii* provides additional evidence for a high stability of this particular protein fragment. Furthermore, posttranslational processing of RTX-type proteins of other Gram-negative bacteria has been demonstrated (Osicka *et al.*, 2004)

### **Origin of symbiosis genes of the epibiont**

Obligately intracellular bacterial symbionts and pathogens are characterized by a reductive evolution of their genome (Cole *et al.*, 2001; van Ham *et al.*, 2003). In contrast, the genome size

of epibiont *Chl. chlorochromatii* CaD (2.57 Mb) falls well within the size range of all sequenced green sulphur bacterial genomes (1.97 – 4.44 Mb; [http://genome.jgi-psf.org/mic\\_home.html](http://genome.jgi-psf.org/mic_home.html)), which is commensurate with the capacity of the epibiont to grow also independently in the free-living state. *Vice versa*, an *in silico* subtractive hybridization analysis of the available genome sequences of green sulphur bacteria identified 188 additional ORFs to be unique for *Chl. chlorochromatii* CaD (data not shown), most of them coding for hypothetical proteins without any homology to sequences in free-living green sulphur bacteria. This number is considerably lower than the numbers of niche-specific genes in high-light-adapted (364 ORFs) and low-light-adapted *Prochlorococcus* strains (923 ORFs) (Rocap *et al.*, 2003) and indicates that the adaptation to the symbiosis in phototrophic consortia does not require a large number of additional genes.

Most remarkably, the four putative symbiosis genes identified in the present study showed similarity to different types of virulence factors of typical bacterial pathogens. Genes underlying the adaptation of different evolutionary lineages are either differentially retained from the common ancestor, acquired through gene duplication and divergent evolution, or laterally transferred to an individual lineage from distantly related prokaryotes (Rocap *et al.*, 2003). The four symbiosis-specific ORFs of *Chl. chlorochromatii* lack some of the properties thought to be characteristic for horizontally transmitted genes (Lawrence and Roth, 1996; Lawrence and Ochman, 1998; Jones *et al.*, 2003;), like (i) neighbouring tRNA genes which have been used to localize insertion events, (ii) a different G+C content (symbiosis genes: 42% - 46% GC, *Chl. chlorochromatii* genome average: 44.3 mol% GC), or (iii) a codon usage which differs from that of the entire genome (data not shown).

While the putative gene products of ORFs Cag0614, 0616 and 1920 were only very distantly related to known proteins and could not be phylogenetically analysed further, the pronounced similarity of the RTX-like protein coded by Cag1919 to other amino acid sequences permitted a detailed phylogenetic analysis. The closest relatives are Ca<sup>2+</sup>-binding proteins from  $\gamma$ - and  $\delta$ -proteobacteria, indicating that *Chl. chlorochromatii* acquired at least the RTX-module from proteobacteria via a horizontal gene transfer event. This is further corroborated by the presence of a transposases (Cag1918) in close proximity to Cag1919 and 1920 which also suggests that both ORFs were laterally transferred during the same event.

In conclusion, the different lines of experimental evidence gathered in the present study provide the first indication that genetic modules known from proteobacterial pathogens of eukaryotes have been laterally transferred to nonrelated bacteria and are employed in symbiotic interactions between prokaryotes

## Experimental Procedures

### Bacterial strains

Cultures of green sulphur bacteria were grown in standard SL10 medium (Overmann and Pfennig, 1989) supplemented with 3 mM acetate. For *Chlorobium chlorochromatii* the pH was set to 7.2. It was adjusted to 6.8 in media for *Chlorobium* strains H1D and 'Fjord', *Chl. phaeobacteroides* DSMZ 266<sup>T</sup>, *Chl. limicola* E3P1, *Chl. phaeobacteroides* CL 1402, *Chl. phaeobacteroides* brChl, *Chl. phaeobacteroides* DagIII, *Chlorobaculum thiosulfatophilum* DSMZ 249<sup>T</sup>, *Chl. clathratiforme* DSMZ 5477<sup>T</sup>, *Chl. limicola* DSMZ 245<sup>T</sup> and *Chl. phaeobacteroides* E2P3. *Chl. phaeovibrioides* DSMZ 269<sup>T</sup>, *Chl. luteolum* DSMZ 273<sup>T</sup>, *Prosthecochloris vibrioformis* DSMZ 260<sup>T</sup> and *Ptc. aestuarii* DSMZ 271<sup>T</sup> were grown at pH 6.8, 2% (w/v) NaCl and 0.3% (w/v) MgCl<sub>2</sub>·6H<sub>2</sub>O. Cultures were incubated at 25°C at 50 μmol quanta·m<sup>-2</sup>·s<sup>-1</sup> of continuous illumination (tungsten lamp bulb; Osram 60 W). Light intensity was determined with a Li Cor LI-189 quantum meter equipped with a LI-200 SA pyranometer sensor (Li Cor, Lincoln, Neb., USA). *Chlorobaculum tepidum* ATCC 49652<sup>T</sup> was grown in CL medium (Frigaard and Bryant, 2001), at 46°C and 1000 μmol quanta·m<sup>-2</sup>·s<sup>-1</sup>. The consortium "*Chlorochromatium aggregatum*" was grown in K4 medium (Kanzler *et al.*, 2005) in 10 l glass flasks at 15°C and 20 μmol quanta·m<sup>-2</sup>·s<sup>-1</sup>. Under these conditions, "*Chlorochromatium aggregatum*" forms an almost pure biofilm on the inner surface of the vessel which can be harvested separately (Pfannes *et al.*, 2007).

### Retrieval of putative symbiosis genes by subtractive hybridisation

Genomic DNA was prepared with the DNeasyTissue Kit (Qiagen, Hilden, Germany) according to a modified protocol. Twice the amount of proteinase K was added to the samples and cell lysis was performed at 55°C for 4 h. After elution, the DNA was diluted in 2 mM Tris (pH 7.0), purified by ultrafiltration in Centricon Ultracel YM-50 Ultrafiltration units (Millipore, Schwalbach, Germany) and quantified by fluorescent dye binding with PicoGreen (MoBiTec, Göttingen, Germany).

Suppression subtractive hybridisation (Diatchenko *et al.*, 1996; Gurskaya *et al.*, 1996) was carried out employing the CLONTECH PCR-Select<sup>TM</sup> Bacterial Genome Subtraction Kit (BD Biosciences Clontech, Heidelberg, Germany). As tester DNA, 2 μg of *Chl. chlorochromatii* strain CaD was used. As driver, 2 μg of DNA each of the 16 free-living green sulphur bacteria (cf the section 'Bacterial strains') were employed. The tester DNA was split into two samples and the DNA of each sample was ligated to one specific set adaptors. Then, 1 μl of each sample

was hybridised separately with 2 µl of each driver DNA at 63°C for 1.5 h. Both hybridisation reactions were combined, 1 µl of driver DNA was added and the mixture was hybridised again at 63°C for 16 h. The resulting second hybridisation mixture was then diluted to a total volume of 200 µl and amplified in two consecutive steps in a GeneAmp PCR System 9700 (Applied Biosystems, Weiterstadt, Germany) employing the BD Advantage™ 2PCR Enzyme System (BD Biosciences Clontech) with primers complementary to the adaptor sequences. The first PCR comprised a 2 min incubation at 72°C to extend the adaptors, then an initial denaturation (95°C, 0.5 min), followed by 30 cycles with denaturation at 94°C for 0.5 min, annealing at 66°C for 0.5 min and primer extension at 72°C for 1.5 min. The second PCR comprised an initial denaturation step at 95°C for 1 min, followed by 15 thermal cycles with denaturation at 94°C for 0.5 min, primer annealing at 68°C for 0.5 min, elongation at 72°C for 1.5 min and a final extension at 72°C for 10 min.

PCR products were ligated into vector pCR®2.1-TOPO and cloned through chemical transformation using the TOPO TA cloning kit (version R; Invitrogen, Carlsbad, CA). Plasmids were extracted with a QIAprep spin miniprep (Qiagen), and the presence of inserts was verified by digestion with *EcoRI* (MBI Fermentas, St. Leon-Rot, Germany). Nucleotide sequence data were obtained with a ABI Prism 310 genetic analyser (Applied Biosystems), employing the AmpliTaq FS Big Dye Terminator cycle sequencing kit and M13 forward and M13 reverse primers.

### **Sequence analysis and modelling of three-dimensional structures**

The genome sequence of *Chl. chlorochromatii* was recently determined by the Joint-Genome Institute (Department of Energy, USA; <http://img.jgi.doe.gov/cgi-bin/pub/main.cgi>) and annotation of the data is in progress (D. Bryant and J. Overmann, unpublished data). Based on this genome sequence, the open reading frames (ORFs) corresponding to the gene fragments recovered by subtractive hybridisation could be identified. Similarities to known sequences were assessed by BLAST searches (Altschul *et al.*, 1997) using the BLAST X algorithmus. Subsequent analyses were conducted with the InterProScan (Zdobnow and Apweiler, 2001), ScanProsite (Gattiker *et al.*, 2002) and Motif Scan (Falquet *et al.*, 2002) software packages. Conserved sequence motifs were identified with 3of5 complex pattern search (Seiler *et al.*, 2006), the secondary structure was analysed with PredictProtein (Rost *et al.*, 2004) and repeats within the protein were identified with the REPRO (George and Heringa, 2000) software. Secretion signals were searched with SignalP 3.0. (Bendtsen *et al.*, 2004) and PrediSi (Hiller *et*

*al.*, 2004) software. Hydropathicity plots were obtained with the ProtScale software (Gasteiger *et al.*, 2005).

For sequence comparisons and phylogenetic analyses, related protein sequences were recovered from the Genbank database (Benson *et al.*, 2002) and aligned with Clustal X version 1.8 (Thompson *et al.*, 1997). Phylogenetic trees were calculated with the PROTML program of the Phylogeny Inference Package (PHYLIP Version 3.6.3) (Felsenstein, 2002), employing the maximum likelihood algorithm and the Dayhoff PAM probability model.

In order to recover the appropriate modelling template for ORF Cag 1919, the protein sequence was submitted to the Ex-PDB database (<http://swissmodel.expasy.org/>) and a SWISS-Model BLAST search was performed. The modelling template and the query sequence were aligned with Clustal X version 1.8. Using the SWISS-MODEL interface in the alignment mode, the alignment was submitted to the SWISS-Model Expert Protein Analysis System (ExPASy) web server (Peitsch, 1995, Schwede *et al.*, 2003). After return, the model was displayed with the DeepView-Swiss-PdbViewer (Guex and Peitsch, 1997).

### **Dot blot hybridisation**

Probes for the detection of the putative symbiosis genes were generated from the plasmids carrying the respective inserts as obtained by subtractive hybridisation. Probes were randomly PCR labelled with digoxigenin (DIG)-11-dUTP (PCR DIG probe synthesis kit; Roche, Mannheim, Germany), employing the nested primers from CLONTECH PCR-Select<sup>TM</sup> Bacterial Genome Subtraction Kit in a step-down PCR. After an initial 5 min denaturing step at 95°C, 10 cycles were conducted which comprised melting at 94°C for 0.5 min, annealing at 60°C for 0.75 min and extension at 72°C for 1 min, and were followed by 25 cycles with the annealing temperature changed to 55°C. Final extension proceeded at 72°C for 10 min. The probe targeting the ORF Cag 1919 was generated with the same PCR program using the primers RTX 3797f and 4266r (Suppl. Table 1) but setting the annealing temperatures to 70°C and 65°C respectively.

For blotting, 10 ng of genomic DNA of each green sulphur bacterium was denatured for 10 min at 95°C and vacuum blotted onto positively charged nylon membrane (Hybond N+; Amersham, Freiburg, Germany). The membrane was baked at 120°C for 30 min and prehybridised in 10 ml of DIG Easy Hyb buffer (Roche) at 40°C for 1 h. Hybridisation was carried out for 16 h at 40°C in 10 ml Easy Hyb buffer after adding the denatured probe. After hybridisation, the blot was washed twice for 15 min at room temperature in 2x SSC (1x SSC is 150 mM NaCl plus 15 mM sodium citrate [pH 7.0]) containing 0.1 % SDS, followed by three

stringent washing steps (twice in 1x SSC plus 0.1% SDS, once in 0.5x SSC plus 0.1 % SDS; each at 40°C). The hybridisation signal was detected with the DIG luminescence detection kit (Roche) and X-ray film (WICO Rex+; Linhardt Röntgenbedarf, Munich, Germany) according to the instructions of the manufacturer.

### **RNA extraction and RT-PCR**

RNA was extracted from *Chl. chlorochromatii* and "*Chlorochromatium aggregatum*" using the RNeasy Mini Kit (Qiagen). After eluting the RNA from the purification columns, the eluates were treated twice with 20 units of RNase-free DNase I (10 U/μl; Roche; overnight at room temperature) in DNase I buffer (10 mM HEPES, 2.5 mM MgCl<sub>2</sub>, 0.1 mM CaCl<sub>2</sub> [pH 7.5] incubated with 0.1 % diethylpyrocarbonate overnight and autoclaved). Eluates were subsequently purified with RNeasy columns (Qiagen) according to the instructions of the manufacturer. RNA concentrations were determined spectrophotometrically at 260 nm. As a highly sensitive test for contamination with genomic DNA, a step-down PCR with a primer set targeting the *sigA* gene (Suppl. Table 1) was performed using 1 μM of the RNA preparation.

Reverse transcription was performed in 20 μl with SuperScript<sup>TM</sup> III Reverse Transcriptase (Invitrogen) using 800 ng RNA and 183 ng random hexamer primer as recommended by the supplier. The generated cDNA was then amplified with custom designed gene-specific primers at optimized PCR conditions (Suppl. Table 1). Fifty ng of genomic DNA of *Chl. chlorochromatii* served as positive control and 800 ng of total RNA without reverse transcription of *Chl. chlorochromatii* as negative PCR control. Full length transcripts of ORF Cag 1919 were detected by reverse transcription in 20 μl employing LongRange Reverse Transcriptase (Qiagen), 700 ng RNA and 183 ng random hexamer primer. cDNA was then treated with 2U RNase H (Roche Diagnostics GmbH, Mannheim, Germany) to remove RNA-cDNA-Hybrids. A long range PCR amplification with custom designed gene-specific primers RTX 502f and RTX 4284r (Supplementary Table 1) followed. A reaction mix without addition of the reverse transcriptase served as a negative control.

**Supplementary Table 1.** Gene specific oligonucleotides used for PCR amplification

Target gene	Oligonucleotide sequence (5' to 3')*	Annealing temperature (°C)	Components of PCR reaction
<i>RTX toxin-like protein</i> <i>ORF Cag 1919</i>			
RTX502f RTX4284r	ACGTTACCGTTGACCTGC CACATCGTTACCCGTACC	40x63°C	1x PCR buffer (Qiagen) 1xQ-solution 2 mM MgCl <sub>2</sub> 0.3 mM of each dNTP 5U of Taq DNA polymerase (Qiagen)
RTX3797f RTX4266r	ATCAACGCCAGACCAAGC CACATCGTTACCCGTACC	10x70°C, 30x65°C	1x PCR buffer (GeneAmp) 2 mM MgCl <sub>2</sub>  0.2 mM of each dNTP  1.25U of AmpliTaq Gold
<i>ORF Cag1920</i>			
RTX695f RTX868r	CGTTGGCGTATCCTTCAGT GGAGTAGGGGCATAATCAAA	10x72°C, 30x67°C	
RTX4650f RTX4798r	AATGGTATGCCGGCGGTATG AGTTACGGTACCGGTTGGCT TATC	10x72°C, 30x67°C plus 5 % acetamide	
RTX9881f RTX10057r	GAAGTGGCGATTAACAGG GCATAAGCATCCGGTACAAT	10x74°C, 30x69°C	
<i>Putative adhesion protein</i> <i>ORF Cag 0616</i>			
Adh2436f Adh2556r	ACACATGGCAGTTCCTTCA TAGCAATTGCCCGCGTATCT	10x72°C, 30x67°C	
Adh27378f Adh27546r	TGGTAGTGGCACGGGTGAG TCCAGCGGTCATTTTCTCA	10x68°C, 30x63°C	
Adh53556f Adh53697r	AGGCGATGCAGAGATTA TGGCTTCAAGTCTCAGG	10x70°C, 30x65°C	
<b>Sigma factor A</b>			
GSB-SigA-F4 GSB-SigA-R1	ATTGTGCG(AC)(CT)T(GT)CC AT(AT)GG(CT)ATGGA(CT)AA TCCGCT	10x61°C, 30x56°C	1x PCR buffer (GeneAmp) 3.5 mM MgCl <sub>2</sub> 0.2 mM of each dNTP 1.25U of AmpliTaq Gold

\*all primers were used at a final concentration of 1µM

### **Kinetics of disaggregation**

The disaggregation of phototrophic consortia upon exposure to different chemical agents was observed in a microscopic chamber. The chamber consisted of a microscopic slide (26 x 76 mm) and a micro cover slip (24 x 60 mm) spaced apart by 0.1 mm. After sealing the chamber with paraffin at three sides, it was filled with an enrichment culture of "*Chlorochromatium aggregatum*" to which different test compounds had been added from anoxic stock solutions. The fourth edge of the chamber was subsequently sealed and the effect of the substances on cell-cell-adhesion in consortia and on their motility was examined by phase contrast microscopy.

### **Detection of Calcium-binding proteins**

Cells were harvested at 10,000 x g for 30 min, resuspended in 10 mM Tris buffer pH 7.5 containing 1 mM phenylmethanesulfonyl fluoride (PMSF), and broken by three subsequent passages through a French press cell at 16,000 lb in<sup>-2</sup>. The homogenate was clarified by centrifugation at 20,000 x g for 30 min at 4°C. The membrane fraction was pelleted by centrifugation at 200,000 x g for 1 h and then solubilised with 2% SDS. The extract was centrifuged again at 200,000 x g for 1 h and proteins in the supernatants were precipitated by adding 9 volumes of acetone and incubation at 0°C for 16 h. After collecting membrane proteins by centrifugation at 20,000 x g for 30 min, the pellets were washed once with acetone and resuspended in 10 mM Tris buffer pH 7.5 containing 1 mM PMSF and 1% SDS. Protein concentrations were estimated using the BCA Protein Assay Reagent (Pierce Biotechnology, Rockford, IL, USA) (Smith *et al.*, 1985). 75 µg of each protein fraction, 15 µg of BSA, 15 µg calmodulin (Sigma-Aldrich, Taufkirchen, Germany) and 20 µg of protein marker (high-range rainbow molecular weight marker; Amersham, Buckinghamshire, England) were separated by Tricine-SDS polyacrylamide gel electrophoresis in 8% acrylamide gels (Schägger and von Jagow, 1987). To determine their Ca<sup>2+</sup>-binding ability, the proteins were blotted onto a Porablot PVDF membrane (Macherey–Nagel, Düren, Germany). The detection of the calcium binding proteins by <sup>45</sup>Ca autoradiography was performed according to the method of Maruyama *et al.* (1984) with an extended incubation time of 30 min.

## **Acknowledgements**

We thank Barbara Pfitzner for laboratory assistance. Lutz Eichacker and Veronika Reisinger are gratefully acknowledged for providing lab space for radioactivity work and for helpful discussions. We are indebted to Peter Sebo for providing purified adenylate cyclase. The genomes of nine green sulphur bacteria were sequenced by the Joint Genome Institute (JGI, Department of Energy). We thank Donald Bryant for helpful discussions during genome sequence analysis. This work was supported by a grant of the Deutsche Forschungsgemeinschaft to J. Overmann (grant no. Ov20/10-1 and 10-2).

## References

- Altschul, S.F., Madden, T.L., Schäffer, A.A., Zhang, J., Miller, W., and Lipmann, D.J. (1997) Gapped BLAST and PSI-BLAST: a new generation of protein database search programs. *Nucleic Acids Res* **25**:3389-3402
- Bauche, C., Chenal, A., Knapp, O., Bodenreider, C., Benz, R., Chaffotte, A., and Ladant, D. (2006) Structural and functional characterization of an essential RTX subdomain of *Bordetella pertussis* adenylate cyclase toxin. *J Biol Chem* **281**:16914-16926
- Baumann, U., Wu, S., Flaherty, K.M., and McKay, D.B. (1993) Three-dimensional structure of the alkaline protease of *Pseudomonas aeruginosa*: a two-domain protein with a calcium binding parallel beta roll motif. *EMBO J* **12**:3357-3364
- Bendtsen, J.D., Nielsen, H., von Heijne, G., and Brunak, S. (2004) Improved prediction of signal peptides: SignalP 3.0. *J Mol Biol* **340**: 783-795
- Benson, D.A., Karsch-Mizrachi, I., Lipmann, D.J., Ostell, J., Rapp, B.A., and Wheeler, D.L. (2002) Gen Bank. *Nucleic Acids Res* **30**:17-20
- Chen, J., Anderson, J.B., DeWeese-Scott, C., Fedorova, N.D., Geer, L.Y., He, S., Hurwitz, D.I., Jackson, J.D., Jacobs, A.R., Lanczycki, C.J., Liebert, C.A., Liu, C., Madej, T., Marchler-Bauer, A., Marchler, G.H., Mazumder, R., Nikolskaya, A.N., Rao, B.S., Panchenko, A.R., Shoemaker, B.A., Simonyan, V., Song, J.S., Thiessen, P.A., Vasudevan, S., Wang, Y., Yamashita, R.A., Yin, J.J., and Bryant, S.H. (2003) MMDB: Entrez's 3D-structure database. *Nucleic Acids Res* **31**: 474-477
- Cole, S.T., Eiglmeier, K., Parkhill, J., James, K.D., Thomson, N.R. et al. (2001) Massive gene decay in the leprosy bacillus. *Nature* **409**: 1007-1011
- Copley, R.R., Russell, R.B., and Ponting, C.P. (2001) Sialidase-like Asp-boxes: sequence-similar structures within different protein folds. *Protein Science* **10**: 285-292
- Cruz, W.T., Young, R., Chang, Y.F., and Struck, D.K. (1990) Deletion analysis resolves cell-binding and lytic domains of the *Pasteurella* leukotoxin. *Mol Microbiol* **4**:1933-1939
- Diatchenko, L., Lau, Y.F.C., Campell, A.P., Chenchik, A., Moqadam, F., Huang, B., Lukyanov, S., Lukyanov, K., Gurskaya, N., Sverdlov, E.D., and Siebert, P.D. (1996) Suppression subtractive hybridization: a method for generating differentially regulated or tissue-specific cDNA probes and libraries. *Proc Natl Acad Sci USA* **93**: 6025-6030
- Domenighini, M., Relman, D., Capiou, C., Falkow, S., Prugnola, A., Scarlato, V., and Rappuoli, R. (1990) Genetic characterization of *Bordetella pertussis* filamentous haemagglutinin: a protein processed from an unusually large precursor. *Mol Microbiol* **4**: 787-800
- Economou, A., Hamilton, W.D.O., Johnston, A.W.B., and Dowie J.A. (1990) The *Rhizobium* nodulation gene *nodO* encodes a Ca<sup>2+</sup>-binding protein that is exported without N-terminal cleavage and is homologous to haemolysin and related proteins. *EMBO J* **9**: 349-354
- El-Azami-El-Idrissi, M., Bauches, C., Loucka, J., Osicka, R., Sebo, P., Ladant, D., and Leclerc, C. (2003) Interaction of *Bordetella pertussis* adenylate cyclase with CD11b/CD18. *J Biol Chem* **278**: 38514-38521
- Falquet, L., Pagni, M., Bucher, P., Hulo, N., Sigrist, C.J., Hofmann, K., and Bairoch, A. (2002) The PROSITE database, its status in 2002. *Nucleic Acids Res* **30**: 235-238

- Felsenstein, J. (2002) PHYLIP, Phylogeny Inference Package, Version 3.6(alpha3). Retrieved from <http://evolution.genetics.washington.edu/phylip.html>, Department of Genome Sciences, University of Washington, Seattle, Washington
- Figueras, J.B., Cox, R.P., Højrup, P., Permentier, H.P., and Miller, M. (2002) Phylogeny of the PscB reaction center protein from green sulfur bacteria. *Photosynthesis Res* **71**: 155-164
- Frigaard, N.U., and Bryant, D.A. (2001) Chromosomal gene inactivation in the green sulfur bacterium *Chlorobium tepidum* by natural transformation. *Appl Environ Microbiol* **67**: 2538-2544
- Fröstl, J., and Overmann, J. (1998) Physiology and tactic response of "*Chlorochromatium aggregatum*". *Arch Microbiol* **169**:129-135
- Fröstl, J., and Overmann, J. (2000) Phylogenetic affiliation of the bacteria that constitute phototrophic consortia. *Arch Microbiol* **174**:50-58
- Gasol, J.M., Jürgens, K., Massana, R., Calderón-Paz, J.I., and Pedrós-Alió, C. (1995) Mass development of *Daphnia pulex* in a sulphide-rich pond (Lake Cisó). *Arch Hydrobiol* **132**: 279-296
- Gasteiger, E., Hoogland, C., Gattiker, A., Duvaud, S., Wilkins, M.R., Appel, R.D., and Bairoch, A. (2005) Protein Identification and Analysis Tools on the ExPASy Server. In: Walker, J.M. (ed): The Proteomics Protocols Handbook. Humana Press p. 571-607
- Gattiker, A., Gasteiger, E., and Bairoch, A. (2002) ScanProsite: a reference implementation of a PROSITE scanning tool. *Applied Bioinformatics* **1**:107-108
- George, R. A., and Heringa, J. (2000) The REPRO server: finding protein internal sequence repeats through the web. *Trends Biochem Sci* **25**: 515-517
- Glaeser, J., and Overmann, J. (2003) The significance of organic carbon compounds for *in situ* metabolism and chemotaxis of phototrophic consortia. *Environ Microbiol* **5**:1053-1063
- Glaeser, J., and Overmann, J. (2004) Biogeography, evolution, and diversity of epibionts in phototrophic consortia. *Appl Environ Microbiol* **70**: 4821-4830
- Guex, N., and Peitsch, M.C. (1997) SWISS-MODEL and the Swiss-PdbViewer: An environment for comparative protein modelling. *Electrophoresis* **18**: 2714-2723
- Gurskaya, N.G., Diatchenko, L., Chenchik, A., Siebert, P.D., Khaspekov, G.L., Lukyanov, K.A., Vagner, L.L., Ermolaeva, O.D., Lukyanov, S.A., and Sverdlov, E.D. (1996) Equalizing cDNA subtraction based on selective suppression of polymerase chain reaction: cloning of Jurkat cell transcripts induced by phytohemagglutinin and phorbol 12-myristal 13-acetate. *Anal Biochem* **240**: 90-97
- Hiller, K., Grote, A., Scheer, M., Münch, R., and Jahn, D. (2004) PrediSi: prediction of signal peptides and their cleavage positions. *Nucleic Acids Res* **32**: W375-W379
- Isberg, R.R., and Tran Van Nhieu, G. (1994) Binding and internalization of microorganisms by integrin receptors. *Trends Microbiol* **2**: 10-14
- Jia, W., Zoeiby, A.E., Petruzzello, T.N., Jayabalasingham, B., Seyedirashti, S., and Bishop, R.E. (2004) Lipid trafficking controls endotoxin acylation in outer membranes of *Escherichia coli*. *J Biol Chem* **279**: 44966-44975
- Jobby, M.K., and Sharma, Y. (2005) Calcium-binding crystallins from *Yersinia pestis*. *J Biol Chem* **280**: 1209-1216

- Jones, H., Ostrowski, M., and Scanlan, D.J. (2006) A suppression subtractive hybridization approach reveals niche-specific genes that may be involved in predator avoidance in marine *Synechococcus* isolates. *Appl Environ Microbiol* **72**: 2730-2737
- Kajava, A.V., Cheng, N., Cleaver, R., Kessel, M., Simon, M.N., Willery, E., Jacob-Dubuisson, F., Loch, C., and Steven, A.C. (2001) Beta-helix model for the filamentous haemagglutinin adhesin of *Bordetella pertussis* and related bacterial secretory proteins. *Mol Microbiol* **42**: 279-292
- Kanzler, B.E.M., Pfannes, K.R., Vogl, K., and Overmann, J. (2005) Molecular characterization of the nonphotosynthetic partner bacterium in the consortium "*Chlorochromatium aggregatum*". *Appl Environ Microbiol* **71**: 7434-7441
- Knapp, O., Maier, E., Polleichtner, G., Masin, J., Sebo, P., and Benz, R. (2003) Channel formation in model membranes by the adenylate cyclase toxin of *Bordetella pertussis*: Effect of calcium. *Biochemistry* **42**: 8077-8084
- Lauterborn, R. (1906) Zur Kenntnis der sapropelischen Flora. *Allg Bot Z* **12**: 196-197
- Lawrence, J. G., and Ochman, H. (1998) Molecular archaeology of the *Escherichia coli* genome. *Proc Natl Acad Sci USA* **95**: 9413-9417
- Lawrence, J.G., and Roth, J.R. (1996) Selfish operons: horizontal transfer may drive the evolution of gene clusters. *Genetics* **143**: 1843-1860
- Lilie, H., Haehnel, W., Rudolph, R., and Baumann, U. (2000) Folding of a synthetic parallel beta-roll protein. *FEBS Lett* **470**: 173-177
- Ludwig, A., Jarchau, T., Benz, R., and Goebel, W. (1988) The repeat domain of *Escherichia coli* haemolysin (Hyl A) is responsible for its Ca<sup>2+</sup>-dependent binding to erythrocytes. *Mol Gen Genet* **214**: 553-561
- Maruyama, K., Mikawa, T., and Ebashi, S. (1984) Detection of calcium binding proteins by <sup>45</sup>Ca autoradiography on nitrocellulose membrane after sodium dodecyl sulfate gel electrophoresis. *J Biochem* **95**: 511-519
- Moore, L.R., Rocap, G., and Chisholm, S.W. (1998) Physiology and molecular phylogeny of coexisting *Prochlorococcus* ecotypes. *Nature* **393**: 464-467
- Osicka, R., Prochazkova, K., Sulc, M., Linhartova, I., Havlicek, V., and Sebo, P. (2004) A novel "clip-and-link" activity of repeat in toxin (RTX) proteins from gram-negative pathogens. *J Biol Chem* **279**: 24944-24956
- Overmann, J. (2001a) Phototrophic consortia: A tight cooperation between non-related eubacteria. In: Seckbach, J. (ed.) *Symbiosis: Mechanisms and Model systems*. Kluwer Academic Publishers, Dordrecht, The Netherlands, p. 239-255
- Overmann, J. (2001b) Green sulfur bacteria. In: *Bergey's Manual of Systematic Bacteriology 2nd ed.* Boone, D.R., Castenholz, R.W., and Garrity, G.M. (eds) Springer, New York, pp. 601-605
- Overmann, J. (2006) (ed.) *Molecular basis of symbiosis. Progress in molecular and subcellular biology*. Vol. 41. Springer, Berlin, Heidelberg, New York, 310 p.
- Overmann, J., and Pfennig, N. (1989) *Pelodictyon phaeoclathratiforme* sp. nov., a new brown-colored member of the *Chlorobiaceae* forming net-like colonies. *Arch Microbiol* **152**: 401-406

- Overmann, J., and Schubert, K. (2002) Phototrophic consortia: model systems for symbiotic interrelations between prokaryotes. *Arch Microbiol* **177**: 201-208
- Overmann, J., and Tuschak, C. (1997) Phylogeny and molecular fingerprinting of green sulfur bacteria. *Arch Microbiol* **167**: 302-309
- Overmann, J., Tuschak, C., Fröstl, J., and Sass, H. (1998) The ecological niche of the consortium "*Pelochromatium roseum*". *Arch Microbiol* **169**: 120-128
- Peitsch, M.C. (1995) Protein modeling by E-mail. *Bio/Technology* **13**: 658-660
- Perna, N.T., Plunkett, G., Burland, V., Mau, B., Glasner, J.D. et al. (2001) Genome sequence of enterohaemorrhagic *Escherichia coli* O157:H7. *Nature* **409**: 529-533
- Pfannes, K.R., Vogl, K., and Overmann, J. (2007) Heterotrophic symbionts of phototrophic consortia: members of a novel diverse cluster of *Betaproteobacteria* characterized by a tandem *rrn* operon structure. *Environ Microbiol* **9**:2782-94.
- Rajini, B., Shridas, P., Sundari, C.S., Muralidhar, D., Chandani, S., Thomas, F., and Sharma, Y. (2001) Calcium binding properties of  $\gamma$ -crystallin. *J Biol Chem* **276**: 38464-38471
- Reid, T.D., Peterson, S.N., Tourasse, N., Baillie, L.W., Paulsen, I.T., et al. (2003) The genome sequence of *Bacillus anthracis* Ames and comparison to closely related bacteria. *Nature* **423**: 81-86
- Relman, D.A., Domenighini, M., Tuomanan, E., Rappuoli, R., and Falkow, S. (1989) Filamentous hemagglutinin of *Bordetella pertussis*: Nucleotide sequence and crucial role in adherence. *Proc Natl Acad Sci USA* **86**: 2637-2641
- Rocap, G., Larimer, F.W., Lamerdin, J., Malfatti, S. Chain, P. et al. (2003) Genome divergence in two *Prochlorococcus* ecotypes reflects oceanic niche differentiation. *Nature* **424**: 1042-1046
- Rose, T., Sebo, P., Bellalou, J., and Ladant, D. (1995) Interaction of calcium with *Bordetella pertussis* adenylate cyclase toxin. Characterization of multiple calcium-binding sites and calcium-induced conformational changes. *J Biol Chem* **270**: 26370-26376
- Rost, B., Yachdav, G., and Liu, L. (2004) The PredictProtein Server. *Nucleic Acids Research* **32**:W321-W326
- Ruoshlati, E., and Pierschbacher, M.D. (1986) Arg-Gly-Asp: a versatile cell recognition signal. *Cell* **44**: 517-518
- Schägger, H., and von Jagow, G. (1987) Tricine-sodium dodecyl sulfate-polyacrylamide gel electrophoresis for the separation of proteins in the range from 1 to 100 kDa. *Anal Biochem* **166**:368-379
- Schink, B. (1998) Energetics of syntrophic cooperation in methanogenic degradation. *Microbiol Mol Biol Rev* **61**: 262-280
- Schink, B. (2002) Synergistic interactions in the microbial world. *Antonie van Leeuwenhoek* **81**: 257-261
- Schwede, T., Kopp, J., Guex, N., and Peitsch, M.C. (2003) SWISS-MODEL: an automated protein homology-modeling server. *Nucleic Acids Res* **31**: 3381-3385
- Sebo, P., and Ladant, D. (1993) Pepeat sequences in the *Bordetella pertussis* adenylate cyclase toxin can be recognized as alternative carboxy-proximal secretion signals by the *Escherichia coli*  $\alpha$ -haemolysin translocator. *Mol Microbiol* **9**: 999-1009

- Seiler, M., Mehrle, A., Poustka, A., and Wiemann, S. (2006) The 3of5 web application for complex and comprehensive pattern matching in protein sequences. *BMC Bioinformatics* **7**:144
- Senchou, V., Weide, R., Carrasco, A., Bouyssou, H., Pont-Lezica, R., Govers, F., and Canut, H. (2004) High affinity recognition of a *Phytophthora* protein by *Arabidopsis* via an RGD motif. *Cell Mol Life Sci* **61**: 502-509
- Smith, P.K., Krohn, R.I., Hermanson, G.T., Mallia, A.K., Gartner, F.H., Provenzano, M.D., Fujimoto, E.K., Goeke, N.M., Olsen, B.J., and Klenk, D.C. (1985) Measurement of protein using bicinchoninic acid. *Anal Biochem* **150**: 76-85
- Tan, B.-H., Nason, E., Staeuber, N., Jiang, W., Monastyrskaya, K., and Roy, P. (2001) RGD tripeptide of bluetongue virus VP7 protein is responsible for core attachment to *Culicoides* cells. *J. Virol.* **75**: 3937-3947
- Thompson, J.D., Gibson, T.J., Plewniak, F., Jeanmougin, F., and Higgins, D.G. (1997) The ClustalX windows interface: flexible strategies for multiple sequence alignment aided by quality analysis tools. *Nucleic Acids Res* **24**: 4876-4882
- van Ham, R.C.H.J., Kamerbeek, J., Palacios, C., Rausell, C., Abascal, F. *et al.* (2003) Reductive genome evolution in *Buchnera aphidicola*. *Proc Natl Acad Sci* **100**: 581-586
- Vogl, K., Glaeser, J., Pfannes, K.R., Wanner, G., and Overmann, J. (2006) *Chlorobium chlorochromatii* sp. nov., a symbiotic green sulfur bacterium isolated from the phototrophic consortium "*Chlorochromatium aggregatum*". *Arch Microbiol* **185**: 363-372
- Ward, C.K., Lumbley, S.R., Latimer, J.L., Cope, L.D., and Hansen, E.J. (1998) *Haemophilus ducreyi* secretes a filamentous hemagglutinin-like protein. *J Bacteriol* **180**: 6013-6022
- Welch, R.A. (1995) Phylogenetic analyses of the RTX toxin family. In *Virulence mechanisms of bacterial pathogens 2nd ed.* Roth, J.A., Bolin, C.A., Brogden, K.A., Minion, F.C., and Wannemuehler, M.J. (eds) ASM press, Washington DC, pp. 195-206
- Wistow, G. (1990) Evolution of a protein superfamily: relationship between vertebrate lens crystallins and microorganism dormancy proteins. *J Mol Evol* **30**: 140-145
- Zdobnov, E.M., and Apweiler, R. (2001) "InterProScan – an integration platform for the signature-recognition methods in InterPro". *Bioinformatics* **17**: 847-848



# Ultrastructural characterization of the prokaryotic symbiosis in "*Chlorochromatium aggregatum*"

Gerhard Wanner<sup>1,\*</sup>, Kajetan Vogl<sup>2</sup>, Jörg Overmann<sup>2</sup>

<sup>1</sup> Department Biology I, Electron microscopy, Ludwig-Maximilians-Universität München  
Menzingerstr. 67, D-80638 München, Germany

<sup>2</sup> Department Biology I, Section Microbiology, Ludwig-Maximilians-Universität München  
Maria-Ward-Str. 1a, D-80638 München, Germany

Running title: Ultrastructure of "*Chlorochromatium aggregatum*"

**Keywords:** Cell-cell-interaction, *Chlorobium*, "*Chlorochromatium aggregatum*", electron microscopy, phototrophic consortia, symbiosis, ultrastructure

---

\* Corresponding author. Ph: +49 -89-17861-237 Fax: +49 -89-17861-248, e-mail: wanner@lrz.uni-muenchen.de

## Abstract

The phototrophic consortium "*Chlorochromatium aggregatum*" currently represents the most highly developed interspecific association of bacteria and consists of green sulfur bacteria, so-called epibionts, surrounding a central, motile, chemotrophic bacterium. In order to identify subcellular structures characteristic for this symbiosis, consortia were studied by a combination of high resolution analytical SEM, TEM, 3D reconstruction and image analysis. Cohesion of the cells in consortia is based on electron-dense hair-like filaments which interconnect the epibionts and, to a lower extent, epibionts with the central bacterium. In addition, numerous periplasmic tubules extend from the outer membrane of the central bacterium and are in direct contact to the epibionts, thereby forming a common periplasmic space which is likely to be involved in the exchange of substances between the partners. In each epibiont cell, the attachment site to the central bacterium is characterized by absence of chlorosomes and an additional, 17 nm-thick layer (epibiont contact layer, ECL) attached to the inner side of the cytoplasmic membrane. The ECL is only occasionally observed in pure cultures of the epibiont, where it occurs in about 10-20% of the free-living cells. A striking feature of the central bacterium is the presence of one or two hexagonally packed flat crystals (central bacterium crystal, CBC) per cell. The CBC reaches 1  $\mu\text{m}$  in length, is 35 nm thick and consists of a bilayers of subunits with a spacing of 9 nm. An investigation by serial sectioning revealed that the CBC is formed through the accumulation of subunits at the inner side of the cytoplasmic membrane, initially as a monolayer (central bacterium membrane layer; CML) and subsequently developing to a bilayer, which in its final stage can be oriented freely within the cytoplasm. A detailed 3D model for consortia as derived from the combined analytical data is presented.

## Introduction

During the course of evolution, prokaryotes have entered into numerous symbiotic relationships. Until now, mostly symbioses between bacteria and eukaryotes have been investigated (see 23 for review). These studies have revealed different ways in which prokaryotic cells have morphologically adapted to the symbiosis with eukaryotes. Morphological changes have been especially well documented for cyanobacteria. Cyanobacteria of the genus *Nostoc* that occur intracellularly in the fungus *Geosiphon* and the angiosperm *Gunnera* or extracellularly in Bryophytes, the water fern *Azolla* and cycads are characterized by an increase in heterocyst frequency, an increased cell size and more rounded cell shape, the appearance of shorter filaments or even single cells, a reduction in the thickness of the sheath and cell wall, and, in some cases, altered thylacoid arrangements (28). During root nodule formation in clover, *Rhizobium leguminosarum* cells differentiate to bacteroids by enlargement and distortion, loss of the capability of cell division and formation of polyhydroxybutyrate granules (18). In *Azoarcus* sp. BH72, the betaproteobacterial endophyte of kallar grass, low oxygen concentrations induce the formation of diazosomes, stacks of intracytoplasmic membranes in which the iron protein of nitrogenase is highly enriched (29).

However, various types of highly structured associations, so-called consortia, exist between different prokaryotes (19, 23). Typically, these consortia consist of two different types prokaryotes which maintain a permanent cell-to-cell contact. In contrast to the interactions of prokaryotes with eukaryotes, no specific morphological adaptations have been reported for symbiotic prokaryotic consortia (13).

Phototrophic consortia consist of a motile, colorless, rod-shaped central bacterium which is surrounded by up to 69 green sulfur bacteria cells, the epibionts (5, 20, 23). Phototrophic consortia occur in numerous stratified lakes worldwide (10, 24) where they can amount up to two-thirds of the total bacterial biomass in the chemocline (7). Based on 16S rRNA gene sequence analysis of natural populations of green sulfur bacteria, the epibionts do not occur as free-living cells (10), suggesting that they are specifically adapted to life in the association. The central bacterium belongs to the *Comamonadaceae* within the Betaproteobacteria (14, 26). As indicated by microautoradiography using labeled carbon substrates, the central bacterium is capable of assimilating 2-oxoglutarate (9).

Several independent experimental findings indicate that a rapid signal transfer occurs between the epibionts and the central bacterium in phototrophic consortia. Firstly, cell division of both central bacterium and epibionts is highly coordinated (24). Secondly, intact consortia

exhibit a scotophobic response and accumulate at wavelengths of light which correspond to the absorption maxima of the bacteriochlorophylls present in the immotile green sulfur bacterial epibionts (4) while only the central bacterium is flagellated and confers motility to the consortium (8). Thirdly, the incorporation of 2-oxoglutarate by the central bacterium occurs only in the presence of light and sulfide used by the epibiont (9).

In the present study, detailed ultrastructural investigations combining high resolution analytical scanning electron microscopy (SEM), transmission electron microscopy (TEM), 3D reconstruction and image analysis were conducted with the aim to elucidate the structural basis for the close cell-cell-interaction in phototrophic consortia. By comparison of intact consortia with epibiont cells in the recently established pure cultures (33), symbiosis-specific subcellular structures could be identified, serving as the basis for an ultrastructural model of phototrophic consortia.

## Materials and Methods

**Bacterial strains and growth conditions.** *Chlorobium chlorochromatii* was grown in standard SL10 medium for green sulfur bacteria (22) supplemented with 3 mM acetate and adjusted to pH 7.2. Cultures were incubated at 25°C with continuous illumination by a tungsten lamp (Osram, 60 W) at a light intensity of 50  $\mu\text{mol quanta}\cdot\text{m}^{-2}\cdot\text{s}^{-1}$  as determined with a Li Cor LI-189 quantum meter equipped with a LI-200 SA pyranometer sensor (Li Cor, Lincoln, Neb., USA). The consortium "*Chlorochromatium aggregatum*" was grown in K4 medium (14) in 10 l glass vessels at 15°C under continuous illumination of 20  $\mu\text{mol quanta}\cdot\text{m}^{-2}\cdot\text{s}^{-1}$ . Under these conditions, "*Chlorochromatium aggregatum*" forms an almost pure biofilm on the inner surface of the vessel (26). The biofilm was scraped off the glass wall and used in the subsequent ultrastructural investigations.

**Cell fractionation and isolation of chlorosomes.** Cells were harvested by centrifugation at 10,000 x g for 30 min, then resuspended in 10 mM Tris buffer pH 7.5 and broken by three passages through a French press cell at 110 MPa. Unbroken cells and cell debris were removed from the homogenate by centrifugation at 2000 x g for 5 min; the supernatant was centrifuged again at 3000 x g for 5 min and the pellet was finally resuspended in 10 mM Tris. The resulting supernatants and resuspended pellets were used for ultrastructural analysis.

**Electron microscopy.** Immediately after collection, cells were fixed with 2.5% glutardialdehyde in fixative buffer (75 mM sodium cacodylate, 2 mM  $\text{MgCl}_2$ , pH 7.0), for 1 h at room temperature. Afterwards, samples were rinsed several times in fixative buffer and post-fixed at

room temperature for 1 h with 1% osmium tetroxide in fixative buffer. After two washing steps in distilled water, the cells were stained *en bloc* for 30 min with 1% uranyl acetate in 20% acetone. Dehydration was performed with a graded acetone series. Samples were then infiltrated and embedded in Spurr's low-viscosity resin.

For high pressure freezing, cellulose capillary tubes were filled by capillary forces with concentrated cell suspensions and the cells immobilized by high-pressure freezing (Leica EMPACT2) as described previously (27, 30). Freeze-substitution was performed in ethanol with 0.25% glutaraldehyde, 1% formaldehyde and 0.5% uranyl acetate, including 5% water (2, 35). After embedding the samples in Epon, ultrathin sections were cut with a diamond knife and mounted onto uncoated copper grids. The sections were post-stained with aqueous lead citrate (100 mM, pH 13.0).

For negative staining, a drop of the sample of an appropriate dilution was placed on a 400 mesh carbon-coated copper grid, freshly hydrophilized by glow discharge. After incubation for 2 min, the drop was quickly removed with a pasteur pipette, the grid was air dried and then stained with 2% uranyl acetate and 0.01% glucose.

Transmission electron micrographs were taken with an EM 912 electron microscope (Zeiss, Oberkochen, Germany) equipped with an integrated OMEGA energy filter operated at 80 kV in the zero loss mode. Fast Fourier transformation of digital images (1024 x 1024 pixel, taken with a CCD camera; Proscan GmbH, Germering, Germany) was performed employing the analySIS<sup>®</sup> software 3.0. Auto-correlation of image details was performed with DigitalMicrograph 3.4 (Gatan, Pleasanton CA, USA) as follows. After Fourier transformation of the real image, the resulting image was multiplied by its complex conjugate and the inverse Fourier transformation was calculated. Finally, the resulting image was normalized to a maximum value of 1. Cross-correlation was performed with DigitalMicrograph (Gatan) of real data in the following way: Fourier transformation was applied to each of the two source images; the Fourier transform of the first image was multiplied by the complex conjugate of the Fourier transform of the resulting image; the inverse Fourier transform of the resulting image was calculated (Gatan). Electron energy loss specific imaging (ESI) of the phosphorus distribution was performed with the 3 windows method (analySIS<sup>®</sup> software 3.0;  $E = 110.0$  eV,  $121.0$  eV and  $153.0$  eV).

For scanning electron microscopy (SEM), drops of the sample were placed onto a glass slide, covered with a cover slip and rapidly frozen with liquid nitrogen. The cover slip was removed with a razor blade and the glass slide was immediately fixed with 2.5% glutaraldehyde in 75 mM cacodylate buffer (pH 7.0), postfixated with 1% osmium tetroxide in fixative buffer, dehydrated in a graded series of acetone solutions and critical-point dried after transfer to liquid

CO<sub>2</sub>. Specimens were mounted on stubs, coated with 3 nm platinum using a magnetron sputter coater, and examined with a Hitachi S-4100 field emission scanning electron microscope operated at 5 kV.

## Results

The dimensions of "*Chlorochromatium aggregatum*" were determined by scanning electron microscopy of cryopreparations of consortia on glass slides (Fig. 1A). Individual consortia were  $5.2 \pm 1.0 \mu\text{m}$  long and  $2.5 \pm 0.2 \mu\text{m}$  wide. On average, each consortium harbored  $16 \pm 3$  epibionts (Table 1).

**Table 1.** Dimensions for "*Chlorochromatium aggregatum*", pure culture *Chlorobium chlorochromatii* and their respective chlorosomes

Object	Length ( $\mu\text{m}$ )	Width ( $\mu\text{m}$ )	Surface ( $\mu\text{m}^2$ )	Volume ( $\mu\text{m}^3$ )
" <i>Chlorochromatium aggregatum</i> "	$5.2 \pm 1.0$	$2.5 \pm 0.2$	40.8	21.4
Epibiont (in symbiotic state)	$2.05 \pm 0.5$	$0.7 \pm 0.1$	4.80	0.79
<i>Chlorobium chlorochromatii</i>	$1.2 \pm 0.6$	$0.6 \pm 0.05$	2.30	0.29
Central bacterium	$2.9 \pm 0.6$	n.d.	4.5 - 7.5	0.7 - 1.5*
	Length ( $\mu\text{m}$ )	Width ( $\mu\text{m}$ )	Cross section ( $\mu\text{m}^2$ )	Volume ( $\mu\text{m}^3$ )
Chlorosomes of " <i>Chlorochromatium aggregatum</i> "	$0.139 \pm 0.041$	$0.053 \pm 0.010$	0.023	0.00027
Chlorosomes of <i>Chlorobium chlorochromatii</i>	$0.133 \pm 0.040$	$0.060 \pm 0.011$	0.025	0.00032

\*Length to width ratio was determined for several consortia; the mean value was used for volume estimation.

n.d. = not determined

**Ultrastructure of the epibiont cells.** In the symbiotic state, the rod-shaped epibionts are  $2.05 \mu\text{m}$  long and  $0.7 \mu\text{m}$  wide (Fig. 1A, Table 1). Their cell volume amounted to  $0.7 \mu\text{m}^3$  and their surface to  $4.5 \mu\text{m}^2$ . Division stages were regularly observed. Interestingly, cell division of the epibionts proceeded in an asymmetric fashion (Fig. 1D). Ultrathin sections revealed a typical Gram-negative architecture of the 25 nm-thick bacterial envelope, which consisted of a 6-7 nm thick outer membrane, an electron dense peptidoglycan layer measuring 3-4 nm and a cytoplasmic membrane with a thickness of 6-7 nm (Fig. 1B). Tangential sections demonstrated that the inner surface of the cytoplasmic membrane of epibiont cells is covered by chlorosomes

which do not exhibit a particular orientation (Fig. 1E). In order to determine their dimensions in a reliable fashion, chlorosomes were isolated from "*C. aggregatum*" cultures and negatively stained (Fig. 1F) which yielded mean values for chlorosome length and width of 139 and 53 nm, respectively. These data are comparable with those of chlorosomes from free-living epibiont cells (133 x 60 nm; Table 1).

At low magnification, epibionts in intact consortia exhibited a rough surface structure and bulb-shaped protrusions (Fig. 1A). Analysis of thin sections indicated that the outer membrane frequently undulates with distances from 10-35 nm to the peptidoglycan layer which results in local changes of the periplasmic space (Fig. 1C). Within intact phototrophic "*C. aggregatum*" consortia, neighboring epibionts are interconnected by thin filaments (Fig. 1G). To exclude artificial changes of the periplasmic space during conventional fixation, consortia were cryofixed by high-pressure freezing and freeze substituted. In these specimens 150 nm-long electron dense hair-like filaments could be discerned which covered the entire surface. Furthermore, the variability of the periplasmic space was even more pronounced (Fig. 1H). The hair-like filaments also interconnect epibiont cells with the central bacterium (Fig. 1J). A characteristic feature of the epibionts were 50-200 nm large, bulb-shaped protuberances which occurred at a frequency of up to 20 per epibiont cell (Fig. 1A, G). These protuberances were also observed in pure cultures (Fig. 1K) where the abundance of these protrusions was negatively correlated with growth rate. Exponentially growing cells were almost free of protuberances, whereas during the transition from late exponential to stationary phase the number of protuberances on cells increased. TEM of ultrathin sections demonstrated, that these protuberances are contiguous with the outer membrane and represent a rather localized enlargement of the periplasmic space (Fig. 1K).

The cytoplasm of symbiotic as well as the free-living epibionts contained one to three globules of a rather low electron density which resembled plant and fungal lipid bodies and were typically attached or closely positioned to the cytoplasmic membrane (Fig. 1L). The diameter of these ultrastructures varied between 100 and 250 nm. Multiple parallel membrane-like layers were detected in the periphery of the globules, frequently exhibiting a myelin-like pattern with a periodicity of 3.5 nm as determined by fast Fourier transformation (FFT) (Fig. 1M). In addition, osmiophilic globules with diameters of up to 170 nm were frequently observed in the cytoplasm of epibionts (Fig. 2B, F). Energy filtering (ESI) of ultrathin sections (20-30 nm) of cells fixed only with glutaraldehyde revealed a high content of phosphorus within these globules, which can therefore be classified as polyphosphate.

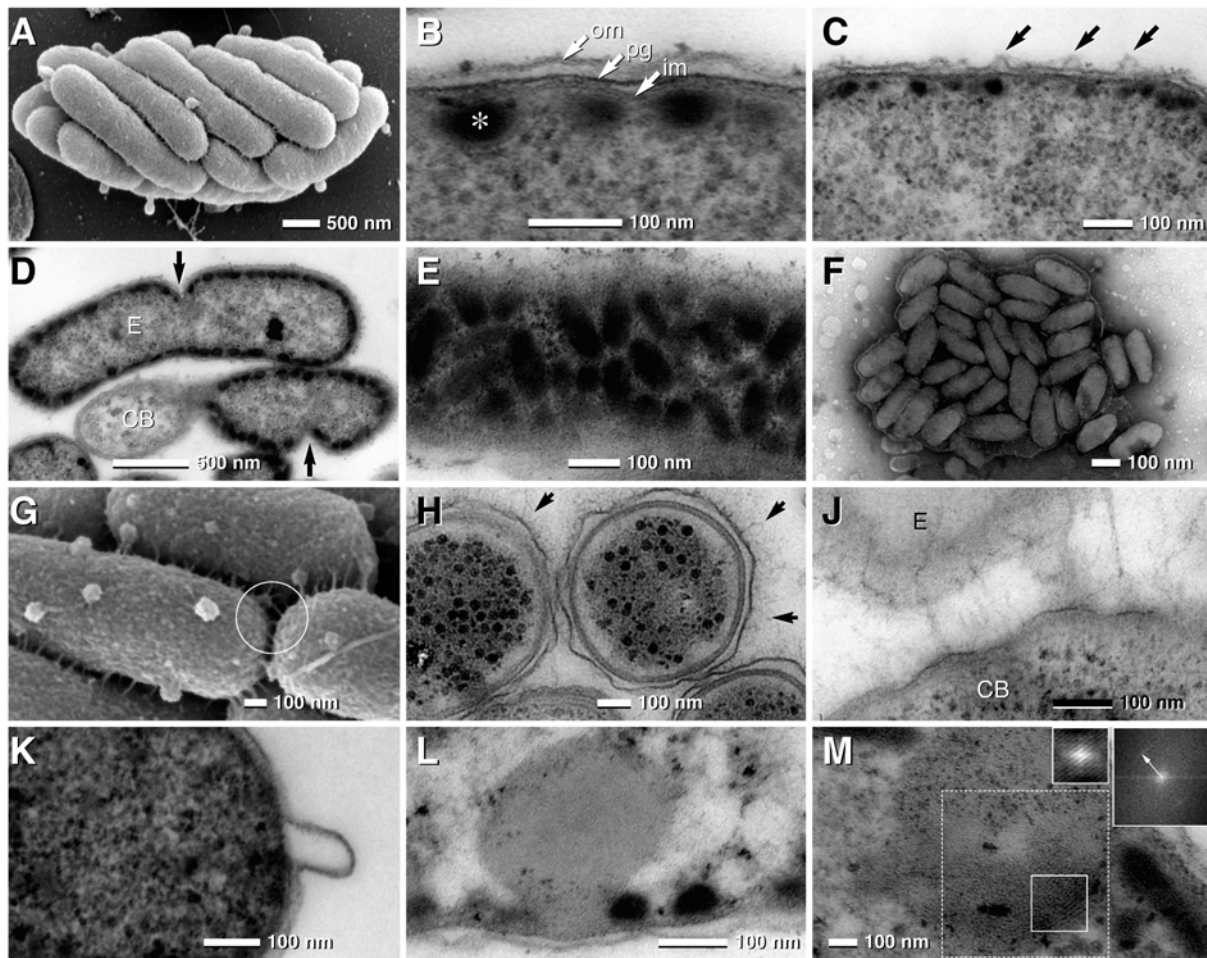


**Figure 1.** Scanning (SEM) and transmission electron micrographs (TEM) of *Chlorochromatium aggregatum* and epibionts, *Chlorobium chlorochromatii* in symbiotic state and pure culture. **A** SEM of "*Chlorochromatium aggregatum*" showing their epibionts tightly packed; the cells exhibit a rough surface and bulb shaped protrusions. **B**, **C** TEM detail of the epibiont cell with typical gram-negative envelope (**B**; om = outer membrane; pg = peptidoglycan; im = inner membrane) and chlorosomes attached to the cytoplasmic membrane (**B**; asterisk). Typically the outer membrane is undulating, leading to local changes of the periplasmic space (**C**; arrows). **D** TEM of epibionts (**E**) – attached to a central bacterium (**CB**) – revealing asymmetric cell division (**D**; arrows). **E**, **F** TEM of chlorosomes of the epibiont *in situ* (**E**) and after isolation and negative staining (**F**). The chlorosomes are rather freely orientated, covering 50-60% of the cytoplasmic membrane (**E**). Both, length and width of the chlorosomes vary in a wide range (**E**; **F**). **G** SEM of the cell surface of epibionts which appears rough and exhibits numerous thin filaments interconnecting neighboring cells (**G**; circle); bulbshaped protrusions are typically observed. **H**, **J** TEM of consortia after cryo fixation by high-pressure freezing showing with high contrast the long carbohydrate chains of LPS (arrows) and the undulating outer membrane (the chlorosomes appear electron translucent due to extraction during freeze substitution) of the epibionts (**H**). Carbohydrate chains of LPS connecting the epibiont (**E**) with the central bacterium (**CB**) (**J**). **K** TEM of an epibiont bulbshaped protrusions which is formed from the outer membrane by local enlargement of the periplasmic space. **L** TEM of a lipid-body-like globule attached to the cytoplasmic membrane. **M** Lipid-body-like globule of pure culture of *Chl. chlorochromatii* exhibiting a myelin-like structure which is enhanced after auto-correlation (small insert) with a spacing of 3.5 nm, determined by FFT (insert upper right; arrow indicates the first order reflex) of dotted area.

**Differences between symbiotic and free-living epibiont cells.** Chlorosomes showed similar dimensions in symbiotic and free-living epibiont cells. Tangential sections revealed, however, that chlorosomes covered the inner face of the cytoplasmic membrane area at a density of 78 chlorosomes per  $\mu\text{m}^2$  (corresponding to 53% of the area; Fig. 1E), whereas the density was reduced in free-living epibiont cells to a value of 53 chlorosomes per  $\mu\text{m}^2$  cytoplasmic membrane (38% of area). When also accounting for the larger cell volume of epibionts in the symbiotic state (Table 1), the absolute number of chlorosomes per cell was 374 in the symbionts, but only 121 in the free-living cells. Due to its limited area, the chlorosome-free contact site in symbiotic cells (see below) did not affect this estimate significantly.

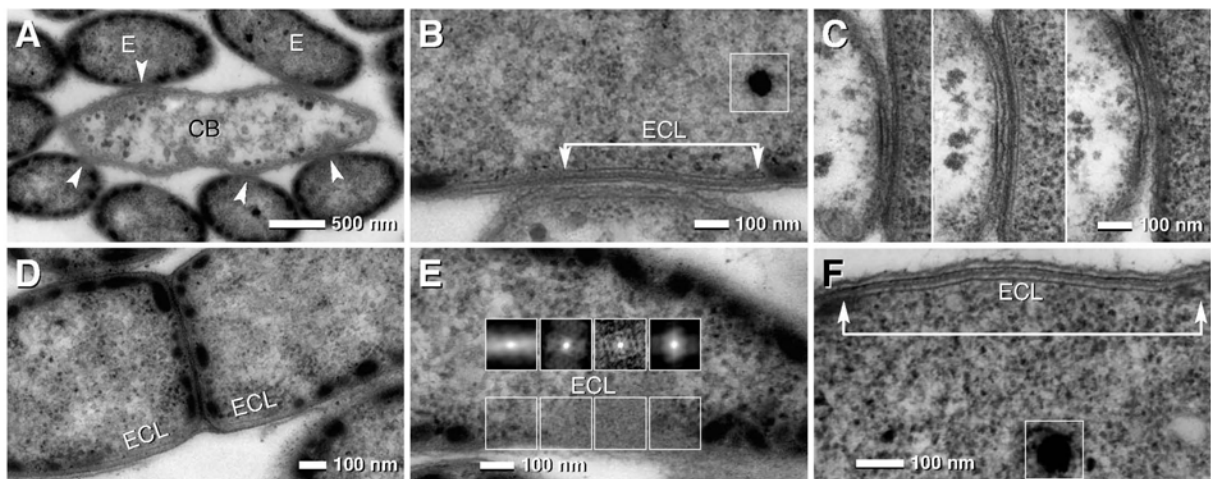


**Figure 2.** Transmission electron micrographs (TEM) of consortia and epibionts in symbiotic state and pure culture.

**A** TEM of a longitudinal ultrathin section of a consortium with central bacterium (CB) with shape of an elongated ellipse (with beginning cell division) and several attached epibionts (E); at the site of attachment the cytoplasmic membrane of the epibionts is free of chlorosomes (arrowheads). **B, C** Area of attachment of the epibiont cell and the central bacterium (epibiont contact layer; ECL) which is characterized by a laminar layer (arrow bar) and the absence of chlorosomes; osmiophilic globule (square) represents polyphosphate (B). The ECL is rather narrow and therefore only visible on one to three consecutive sections (C). **D** ECL of epibiont which is split during cell division. **E** Auto-correlation of oblique section of an ECL revealing a pattern of regularly arranged particles (inserts); at transition zones from ECL to cytoplasm, the pattern disappears (upper inserts, outer left and right). **F** TEM of an ECL of *Chl. chlorochromatii* in pure culture; although the ECL are present only in approx 20% of the cells, their architecture is identical to those formed in symbiosis; osmiophilic globule (square) represents polyphosphate.

The most conspicuous morphological feature of symbiotic epibionts cells is the absence of chlorosomes at the contact site to the central bacterium (Figs. 2A-D). Higher magnification revealed that this epibiont contact layer (ECL) is 17 nm-thick and consists of two parallel 4.5 nm-wide electron dense layers which are separated by a 8 nm-wide less electron dense zone (Fig. 2B). Reconstruction of serial sections demonstrated that each symbiotic epibiont cell contains

one ECL and that the ECL has an ellipsoid shape about 100 nm wide and up to 800 nm long. Thus the ECL occupies 1-2% of the total area of the cytoplasmic membrane. During cell division, the ECL is distributed to both daughter cells (Fig. 2D). Auto-correlation of the ECL in tangential sections revealed a pattern of regularly arranged particles which disappeared in the transition zones from ECL to cytoplasm (Fig. 2E). Electron microscopy of consortia after high pressure freezing and freeze substitution confirmed the presence of ECL in the epibionts. The ECL also occurred in free-living epibionts from pure cultures (Fig. 2F) but was detected only in 10-20% of the cells.

**Ultrastructure of the central bacterium.** The shape of the central bacterium of "*Chlorochromatium aggregatum*" is a prolate ellipsoid with a length of 2.9  $\mu\text{m}$  and a maximum width of 0.7  $\mu\text{m}$  (Fig. 3A; Table 1). Depending on the state of division, the cell surface of the central bacterium ranges between 4.5 and 9  $\mu\text{m}^2$  and the cell volume between 0.7  $\mu\text{m}^3$  and 1.5  $\mu\text{m}^3$ . SEM showed a rough surface of the central bacterium (Fig. 3A, B), which according to ultrathin sections can be attributed to undulation of the outer membrane (Fig. 3C). The cell envelope was 25 to 30 nm thick and had a typical Gram-negative architecture consisting of a 7 nm-thick outer membrane, an electron dense peptidoglycan layer of 3 nm thickness and a 7 nm-thick cytoplasmic membrane (Fig. 3C).

Two types of protrusions are typical for the cell envelope of the central bacteria: i) small papillae, approx. 10-20 nm in length and regularly occurring at a distance of about 25 nm from each other, formed by protuberances of the outer membrane and local changes of the periplasmic space (Fig. 3D) and ii) numerous periplasmic tubules (= PT) formed by the outer membrane which are in linear contact to the epibionts (Fig. 3E). High-pressure freezing and freeze substitution confirms the undulations of outer membranes (Fig 3J). Although PT are best observed at the poles of the central bacterium where the distance to the epibionts reaches a maximum of approx. 200 nm (Fig. 3E, F) they are distributed over the entire cell surface with distances in the range of 50-100 nm. The mean diameter of the PT as calculated from their cross sections was 25 nm, which, after subtracting the thickness of the outer membrane (7 nm) leaves 11 nm for the free tubular space. Occasionally, small membrane vesicles were observed at the end of the PT (Fig. 3G, H).

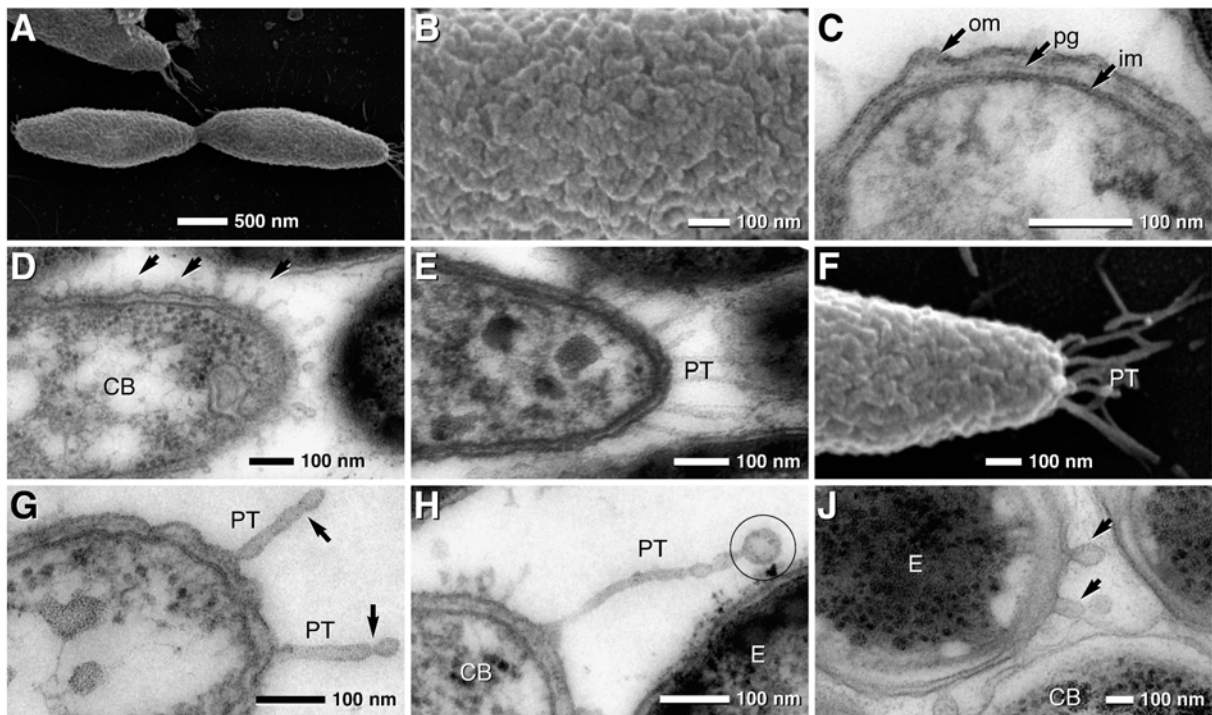


**Figure 3.** Scanning (SEM) and transmission electron micrographs (TEM) of the central bacterium of "*C. aggregatum*".

**A** SEM of a central bacterium of "*C. aggregatum*". Cell division is achieved by medial constriction. **B** SEM of the cell surface of the central bacterium which appears rough due to undulations. **C** TEM detail of the central bacterium cell with typical gram-negative envelope (om = outer membrane; pg = peptidoglycan; im = inner membrane). **D** TEM of the central bacterium showing small papillae with different degree of elongation, formed by undulating outer membrane (**D**, arrows). **E**, **F** TEM of 150 nm section (**E**) and SEM of isolated central bacterium (**F**; detail of **A**) of periplasmic tubules (PT) formed by the outer membrane which were in contact to the epibionts (**F**). **G**, **H** PT without contact to epibionts typically show constrictions (**G**, arrows) and vesiculation (**H**, circle). **J** TEM of cryo-fixed and cryo-substituted specimen proving the occurrence of papillae and bulbshaped protrusions (arrows)

The most conspicuous ultrastructure within cells of the central bacterium was the presence of 35 nm-thick and up to 1  $\mu\text{m}$ -long zipper-like crystalline structures. These structures were either located parallel to the cytoplasmic membrane (Fig. 4A) or occurred freely oriented within the cytoplasm. Based on serial sections of entire "*C. aggregatum*" consortia, each central bacterium on average contained 1.5 central bacterium crystals (CBCs), with numbers ranging between 1 and 3 per cell. At higher magnification, CBCs were observed to consist of two parallel layers of subunits. Subunits were oriented either in an orthogonal or slightly oblique manner with regard to the axis of the CBC (Fig. 4B, C). Employing Fast Fourier transformation (FFT) the diameter of the subunits was determined to be 9 nm (Figs. 4D-F). Within the CBC, the relative orientation of the subunits changed by up to 20° over 100 nm (Fig. 4D). Tangential sections of the CBC were obtained by serial sectioning and revealed a hexagonal pattern of subunits with the typical spacing of 9 nm (Fig. 4F, G). As for the other ultrastructural details present in phototrophic

consortia, the architecture of the CBC was confirmed using consortia treated by high-pressure freezing and freeze substitution. Although the contrast of the CBC in these latter preparations was very low, subsequent auto-correlation of CBC yielded a pattern similar to conventionally fixed specimens (Fig. 4H, J).

Estimating from serial sections and volume considerations, the CBC are an almost negligible fraction of about 0.015% of the consortia biofilm biomass. CBC can be enriched by fractionating centrifugation of crude extract from French-pressed biofilm. Due to their high specific density they co-sediment with cellular fragments. In TEM, they are recognized after negative staining by their characteristic size and shape and a paracrystalline arrangement of subunits (Fig. 4K-M). The sheets are typically folded, forming locally double or multiple layers. This “overlay” impedes analysis of the subunit pattern by formation of superimposed pattern. Only part of CBC is accessible to FFT, resulting in a diffuse Debye-Scherrer-ring corresponding to a distance of 9 nm spacing (Fig. 4L). At favorable regions of the CBC, auto-correlation exhibits an arrangement of subunits similar to CBC *in situ* in tangential ultrathin sections (compare Fig. 4M with 4G).

Frequently underlying a CBC, additional membranous structures were observed at the inner face and parallel to the cytoplasmic membrane (Fig. 5A-C). These additional central bacterium membrane layers (CMLs) were 30-35 nm thick and 50-150 nm long and at higher magnification resembled the CBC at least in some of the preparations. Due to the small size, FFT analysis of the CML is not possible. Furthermore, the curvature of the CML in cross sections impeded auto-correlation. However, auto-correlation of oblique or tangential sections revealed locally restricted regular patterns (Fig 5D, E) with the same periodicity as detected in the CBC (Fig. 5D). The presence of CML was confirmed by high pressure freezing and freeze substitution (see Fig. 4H).

Typical for all central bacteria is the presence of 2-3 complex membranous whirls (= MW) that are compact aggregates of tubules in continuity with the cytoplasmic membrane (Fig. 5F). 3D reconstruction from serial section reveals that the size of the MW is variable in the range of 150 to 400 nm (Fig. 5G). Reconstruction from serial sections reveals that there is a significant contact or even continuity between the MW and the CBC (Fig. 5H). Auto-correlation of transition areas (between the MW and the CBC) shows the regular arrangement of subunits as typical for the CBC (Fig. 5J; compare with Figs 4G).

Osmiophilic globules, of varying diameters (up to 100 nm) are frequently observed in the cytoplasm of central bacteria (Fig. 4A). 3D reconstruction from serial section reveals that a central bacterium has 0-3 osmiophilic globules.

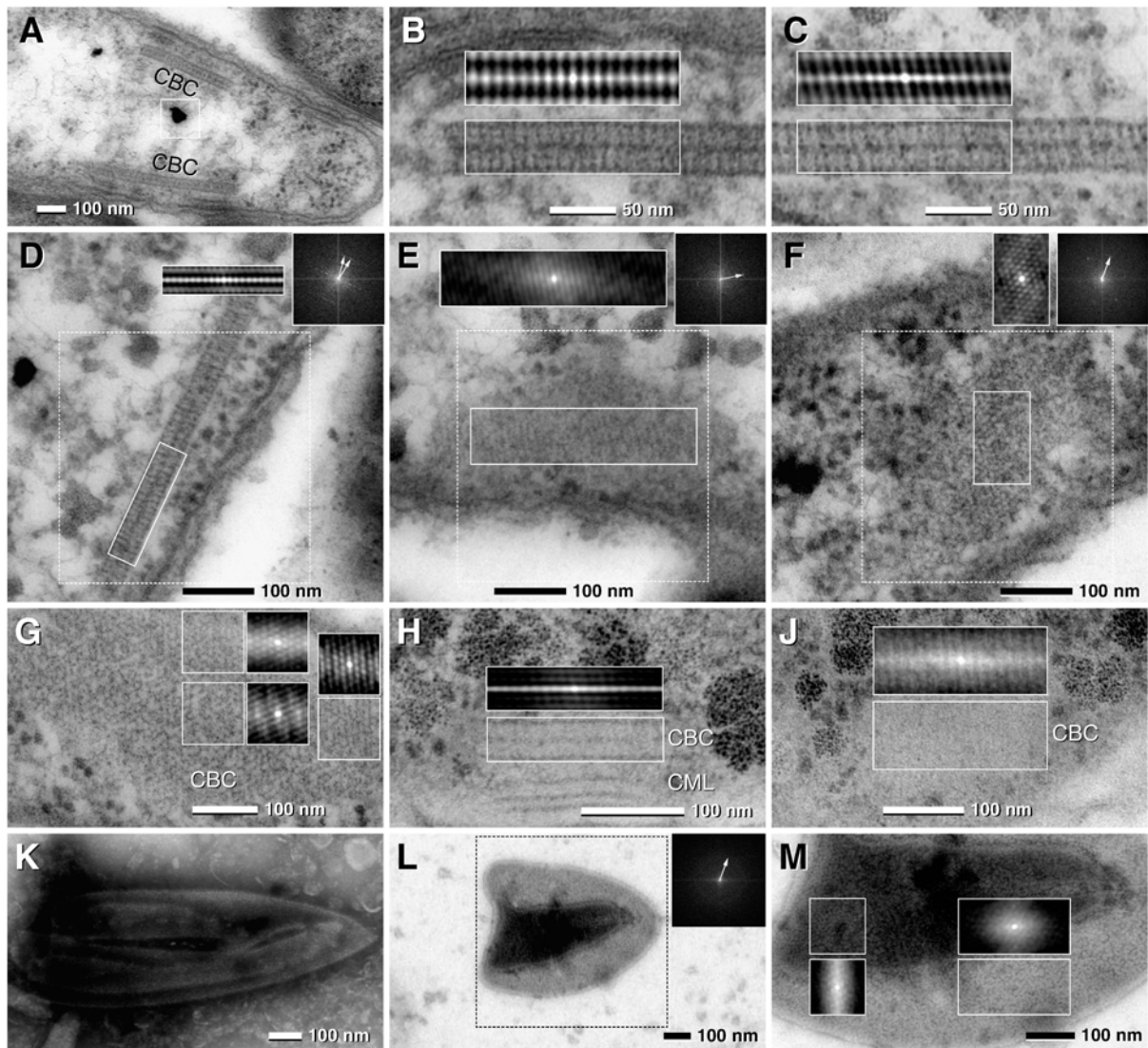


**Figure 4.** Transmission electron micrographs of ultrathin sections the central bacterium of "*C. aggregatum*" revealing paracrystalline structures (central bacterium crystal, CBC). FFTs of dotted areas are presented as inserts (upper right; arrows indicate first order reflexes); auto-correlation is presented in the same size as the analyzed area.

**A** Longitudinal section of central bacterium with two cross sectioned CBC located parallel to the cytoplasmic membrane; (square: osmiophilic granules). **B, C** Detail of CBC showing a paracrystalline zipper-like organization in cross sections; two less electron dense layers are bordered and separated by electron dense layers. Auto-correlation of CBC reveals different orientation of the subunits: vertical (B) or oblique to the axis (C). **D-G** Comparison of FFT and auto-correlation of CBC (D = cross section; E = oblique section; F = tangential section) showing spacing and orientation of subunits which are 9 nm in diameter as calculated from FFT. Dependent on the section plane and the planity of the CBC, transitional patterns between hexagonal and parallel segments are visible (G; compare with E). **H, J** CBC after high pressure freezing and freeze substitution also show a paracrystalline zipper-like organization when cross sectioned; a CML is present attached to the cytoplasmic membrane (H). Oblique sectioned CBC shows a pattern of parallel striations with a spacing of 9 nm (J). **K-M** Negative staining of the isolated CBC. Isolated CBC are frequently observed as double or multiple layers (K). FFT shows a Debye-Scherrer-ring corresponding to a distance of 9 nm (L) indicating a lower degree of subunit orientation of the CBC compared to *in situ*; auto-correlation shows local patterns of subunit orientation similar to CBC *in situ* in a tangential ultrathin section (M; for comparison see G).

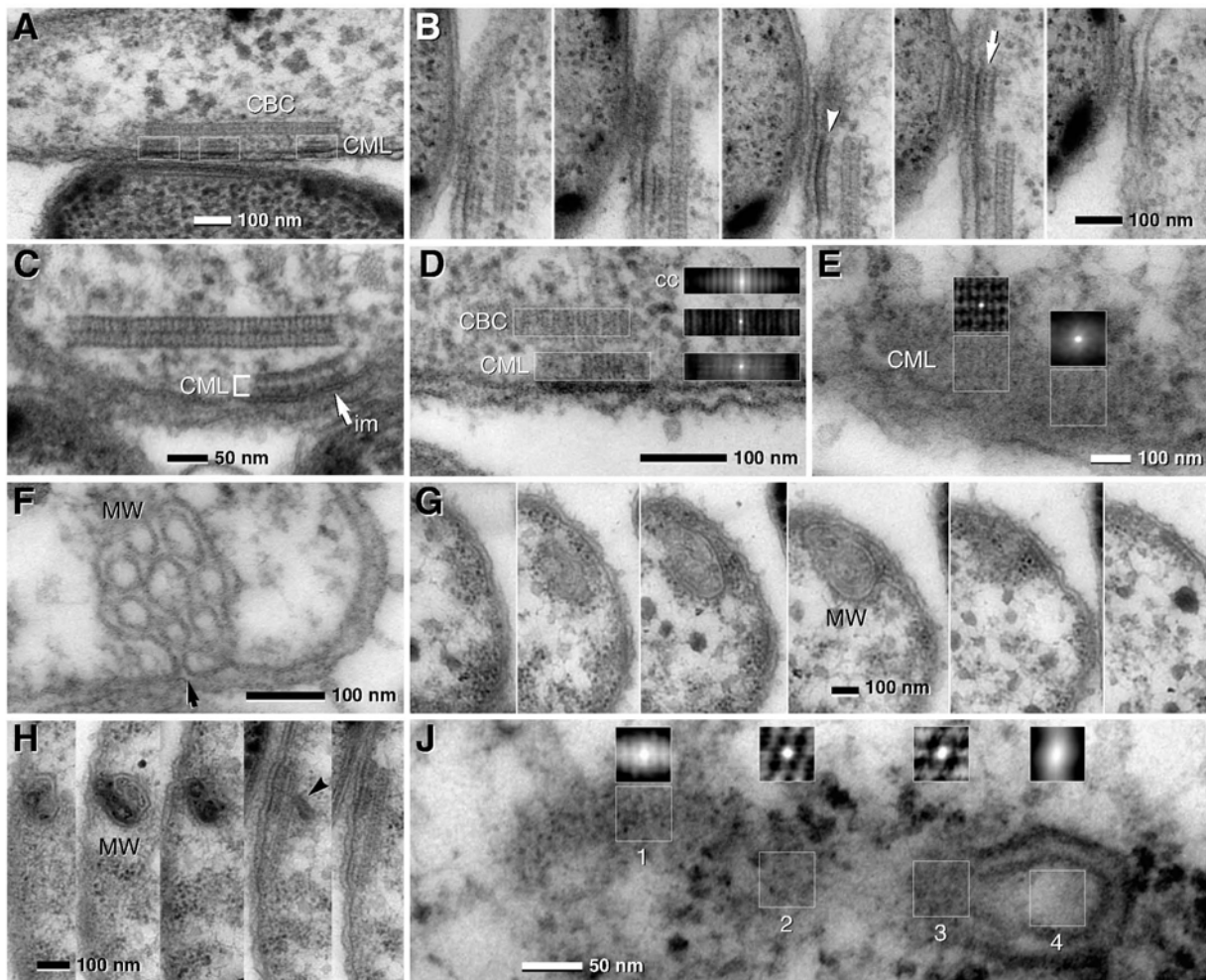


**Figure 5.** Transmission electron micrographs of ultrathin sections the central bacterium of "*C. aggregatum*" revealing the central bacterium membrane layer (CML) and membranous whirls (MW).

**A-E** Cross sections of the CML, a characteristic layer attached strictly parallel to the cytoplasmic membrane of the central bacterium. Serial sections show that the CML is only visible in two to three consecutive sections (**B**) proving that it is locally restricted (**A**, frames; **B**). The CML are found with different thicknesses, suggesting the composition of a monolayer (**B**; arrowhead) or bilayer (**B**; arrow). The electron density of the outer leaflet of the cytoplasmic membrane is higher at the site of attachment of the CML (**C**; arrow). Auto-correlation of oblique (**D**) and tangential (**E**) sectioned CML shows that the degree of order of substructures changes within short distances (**D** and **E**); cross-correlation (**cc**) of CML and CBC confirms that the patterns are similar (**D**). **F-H** Details of the central bacterium showing membranous whirls (MW) which are formed by invaginations of the cytoplasmic membrane (**F**; arrow). Serial sections prove that the MW are in contact with the cytoplasmic membrane (**G**, **H**) and frequently with the CBC (**H**; arrowhead). **J** Auto-correlation of different areas of a section through a CBC in contact with a MW: oblique section of the CBC is characterized by striations (1), tangential sections by hexagonal patterns (2, 3); no significant pattern is visible at the area of the MW (4).

In order to determine whether the ultrastructural features detected in laboratory grown "*Chlorochromatium aggregatum*" also occur under natural conditions, a natural population of the phototrophic consortia "*Pelochromatium roseum*" and "*Chlorochromatium aggregatum*" was obtained from Lake Dagow (26) and their ultrastructure investigated by electron microscopy. This revealed that all consortia in the samples shared the structural features described in the preceding sections for laboratory cultures of "*Chlorochromatium aggregatum*".

## Discussion

The fact that *Chl. chlorochromatii* grows in pure culture demonstrates that this epibiont is not obligatorily symbiotic. Despite this capability, neither *Chl. chlorochromatii* nor any other epibiont of the known 19 types of phototrophic consortia has ever been detected in a free-living state in natural bacterial communities (10), indicating that epibionts of phototrophic consortia are specifically adapted to life in the symbiotic state. So far it was not known whether this adaptation to a symbiosis in phototrophic consortia involves specific morphological characteristics of the cells, like adhesion structures or specific organelles. In the course of the present study, different ultrastructures of the epibionts and the central bacterium were discovered (Fig. 6A).

**Symbiosis-specific ultrastructure of the epibiont in "*Chlorochromatium aggregatum*".** SEM and TEM micrographs revealed up to 150 nm-long hair-like filaments which covered the surface of the epibionts and formed an interconnecting network between the cells of "*C. aggregatum*". These filaments occur exclusively on epibionts, suggesting that the interconnected epibionts form an elastic cage which encloses the central bacterium. This conclusion is also supported by the observation that the epibionts stay associated with the central bacterium when consortia are subjected to shearing forces (by squeezing consortia on a glass slide with a cover slip, or by vacuum filtration of consortia through membrane filters) (23).

Recent disaggregation experiments with the consortium "*C. aggregatum*" (34) demonstrated that cell-cell-aggregation is not susceptible to proteolysis with proteinase K, pepsin, trypsin, chymotrypsin, or to treatment with lysozyme, hyaluronidase,  $\beta$ -glucuronidase, indicating that typical extracellular capsule polysaccharides or easily degradable proteins are not involved in the cell-cell-binding. Extracellular appendages resembling the filaments seen on the epibiont surface have been identified as long carbohydrate chains of lipopolysaccharides (12, 15) and may therefore be also involved in the adhesion in phototrophic consortia.

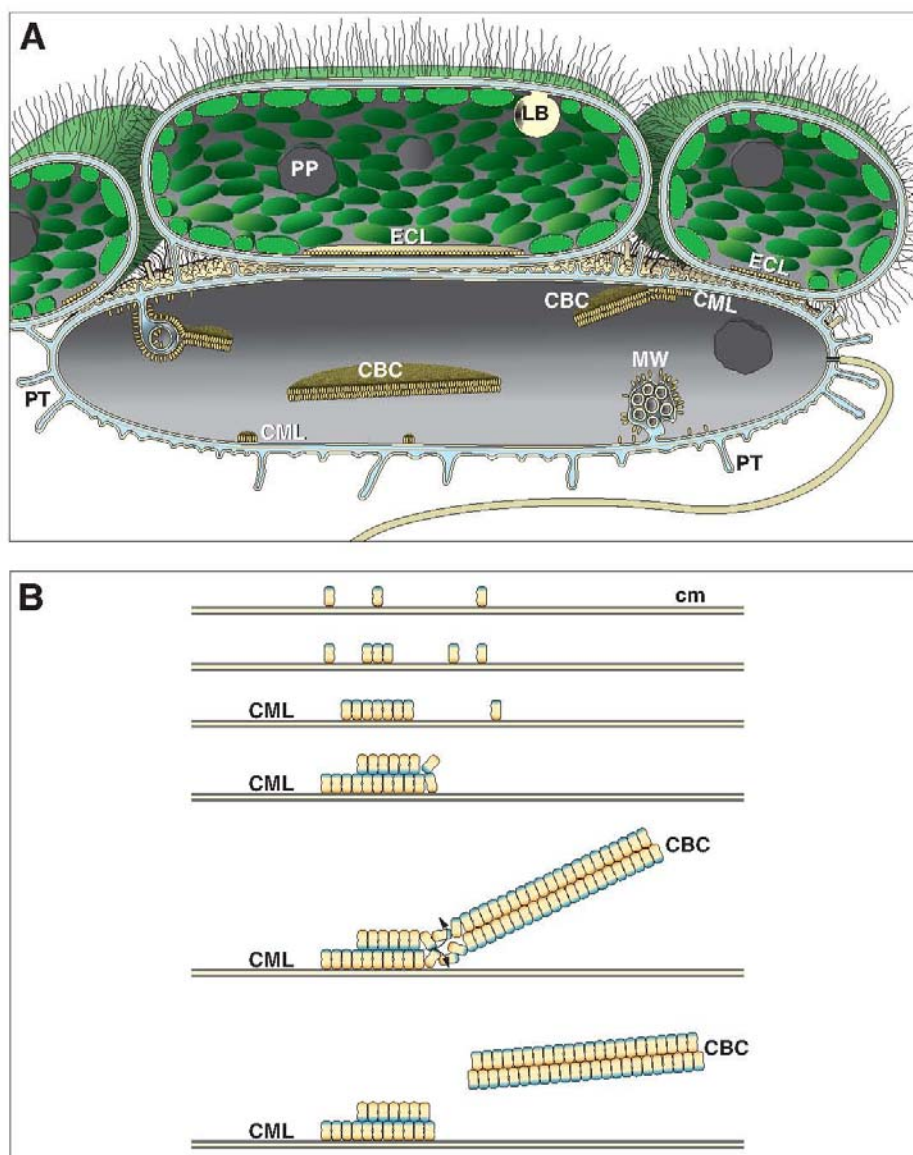


**Figure 6.** **A** Schematic representation according to 3D-reconstruction data of "*Chlorochromatium aggregatum*" summarizes the results of this study. Epibionts are connected by long hair-like carbohydrate chains of lipopolysaccharides. The epibionts harbor lipid bodies (LB) with a myelin-like pattern which are attached to the cytoplasmic membrane and polyphosphate globules (PP). The attachment site of the epibiont is characterized by the absence of chlorosomes and single contact layer (epibiont contact layer, ECL). Striking features of the flagellated central bacterium are i) periplasmic tubules (PT) which can be in direct contact to the epibionts, forming a common periplasmic space; ii) complex invaginations (membranous whorls, MW) of the cytoplasmic membrane; iii) subunits arranged in small monolayers or bilayers directly associated with the cytoplasmic membrane (central bacterium membrane layer, CML); iv) paracrystalline structures (central bacterium crystals, CBC) which are formed on the inner side of the cytoplasmic membrane (or membranous invaginations) by the accumulation of subunits. Globular structures occur in the cytoplasm of the central bacterium. **B** Schematic representation of the putative formation of central bacterium membrane layer (CML) and central bacterium crystals (CBC). Subunits with a hydrophilic (blue) and a hydrophobic (yellow) poles are associated to the cytoplasmic membrane (cm). As subunits accumulate, first a monolayer, then a bilayer develops. When a critical bilayer size is reached, a transitional stage from CML to CBC occurs: the subunits dissociate from the cytoplasmic membrane and "flip", re-orientating to a stable paracrystalline state with their hydrophobic poles facing the bilayer interior and hydrophilic poles facing the cytoplasm.

The protuberances seen at the surface of epibionts of intact consortia also appeared at the cell surface of pure cultures of *Chl. chlorochromatii* when entering the stationary phase. The presence of protuberances on symbiotic epibiont cells indicates that their growth rate is strongly limited within phototrophic consortia. In fact, phototrophic consortia in the enrichment cultures exhibit a generation time which is twice as long as that of *Chl. chlorochromatii* growing under optimal conditions in pure culture (4, 33). It is likely that the physiological activity of the central bacterium is one factor controlling the growth rate of the epibiont.

Underlying a typical outer membrane, peptidoglycan layer and cytoplasmic membrane at the contact site, the epibiont contact layer clearly differs in ultrastructure from typical biomembranes. Auto-correlation of cross sections did not reveal a characteristic pattern, whereas oblique sections showed that the ECL is composed of regularly arranged elements, possibly globular proteins. Within "*C. aggregatum*" the ECL was invariably observed in all epibiont cells and always at the site of contact between the epibiont and the central bacterium, indicating that the ECL is an ultrastructure which is essential for symbiosis. In contrast, ECL-like structures were observed only in a small fraction of the cells from pure cultures, suggesting that biosynthesis of this ultrastructure in epibionts is subject to regulation and induced in the symbiotic state.

**Interior substructures of the central bacterium in "*Chlorochromatium aggregatum*".** The central bacterium crystalline structure was found in varying number and orientation. Since they were primarily cytoplasmic structures, their direct involvement in cell-cell adhesion is unlikely. The three dimensional organisation of the CBC can be well reconstructed, mainly due to its large size and characteristic pattern in cross sections. Using FFT and auto-correlation, it was determined that the CBC is composed of two symmetrical layers of rather large subunits arranged in a regular hexagonal pattern at a spacing of 9 nm. Neighboring subunits are highly ordered, however, the orientation of the subunit axis ranges from 90° to 70° over larger distances. The crystalline structure of the CBC as well as the size of subunits suggest that the CBC is of a proteinaceous nature. Interestingly, the CBC structurally resembles the chemotaxis receptor Tsr of *Escherichia coli* (16, 36, 37, 38). In fact, overproduction of Tsr in *E. coli* resulted in internal membrane networks composed of stacks and tubular structures (16) which resemble the membranous whirls discovered in the central bacterium of "*C. aggregatum*".

When comparing CBC *in situ* with isolated CBC, there are discrepancies in their appearance. Isolated CBC are not flat bilayers or fragments thereof, but rather are folded multilayers (Fig. 4K). Although a regular pattern of subunits is assumed at first glance, auto-correlation shows

that only distinct areas show a pattern for CBC (Fig. 4M). This explains why FFT analysis often fails or results in Debye-Scherrer-rings corresponding to a distance of 9 nm (Fig. 4L) instead of hexagonally arranged first order peaks (Fig. 4F): the areas of regular arrangement of subunits are too small. Double CBC (4-layers) were not observed in the cytoplasm, as deduced from serial sections.

In addition to the CBC, the CML, the layer parallel to the plasma side of the cytoplasmic membrane, is characteristic for the central bacterium. The ultrastructure of these CMLs ranged from single 17 nm-lamina to double laminae with a thickness of 30-35 nm which resembled typical CBC. The electron dense line in the axis of symmetry was absent in most CML, however. The different morphologies of the CML appear to be a transition from single to double laminated structures. Accordingly, CMLs may represent early stages of the CBC. Based on the combined information gathered during the present investigation, the following working hypothesis appears plausible for the formation of CML and CBC (Fig. 6B). We assume that subunits with hydrophilic and hydrophobic poles are associated to the inner side of the cytoplasmic membrane with the hydrophobic poles oriented toward it. As subunits accumulate, a monolayer develops. Further association of subunits causes the formation of a bilayer, representing a metastable state due to the orientation of hydrophobic poles of one layer to the cytoplasm. When a critical bilayer size is reached, a transitional stage from CML to CBC occurs. The subunits dissociate from the cytoplasmic membrane and flip, re-orientating with their hydrophobic poles facing the bilayer interior and hydrophilic poles facing the cytoplasm. So far, however, possible connections between CML and the CBC could not be investigated due to resolution limits of ultrathin sections.

**Implications of ultrastructural features.** Although knowledge on the physiology of the central Betaproteobacterium so far is still rather limited, experimental data indicate that it incorporates external 2-oxoglutarate (9). Theoretically, the tight arrangement of cells in phototrophic consortia as observed in TEM and SEM micrographs could lead to a diffusion limitation and hence a physiological isolation of the central bacterium. However, TEM analyses, including the cryo-fixed and cryo-substituted preparations, revealed that considerable intercellular space exists between the cells. Based on volumetric calculations, the central bacterium only occupies 25% of the volume available. Together with the gaps left by the epibiont cells forming the cortex of the consortia, this extracellular space likely prevents diffusion limitation of "*C. aggregatum*".

A conspicuous feature of the intercellular space between the epibionts and the central bacterium are the periplasmic tubules which extend from the outer membrane of the central

bacterium towards the cell surface of the epibionts. Together with the numerous papillae, these outer membrane structures results in a surface enlargement of 300% compared to a smooth membrane, as calculated from TEM tangential sections and SEM micrographs. Based on the close association between the periplasmic tubules and the outer membrane of the epibionts, the two partner bacteria may actually share a common periplasmic space.

Whereas the dimensions of chlorosomes in the epibiont of "*C. aggregatum*" are comparable to those of *Chlorobaculum tepidum* or *Chlorobium* sp. MN1 (3, 6) the cellular chlorosome content of free-living epibionts was 121 chlorosomes·cell<sup>-1</sup> and thus lower than the values reported for *Cba. tepidum* (200-250 chlorosomes·cell<sup>-1</sup>; 3). However, the chlorosomes content of symbiotic epibionts within the consortia surpassed these values and reached 374 chlorosomes·cell<sup>-1</sup>. Since free-living epibionts had a smaller cell volume than *Cba. tepidum*, the coverage of the inner face of the cytoplasmic membrane was comparable in the two (53 chlorosomes/μm<sup>2</sup> in *Chl. chlorochromatii*, 51 chlorosomes/μm<sup>2</sup> in *Cba. tepidum*) when grown under saturating light intensities. Symbiotic epibiont cells grown at limiting light intensities reached a coverage of 78 chlorosomes/μm<sup>2</sup>. Based on these values, the epibiont does not represent one of the extremely low-light adapted members of the green sulfur bacteria (6, 17, 21) which is consistent with the observation that growth of pure epibiont cultures becomes light-saturated only at >10 μmol·m<sup>-2</sup>·s<sup>-1</sup> (33) in contrast to low-light-adapted relatives which grow light-saturated above 1 μmol·m<sup>-2</sup>·s<sup>-1</sup> (17, 21). Although phototrophic consortia inhabit low-light environments (24), their limited adaptation to the *in situ* light intensities does not necessarily represent a disadvantage based on the following reasoning. Green sulfur bacteria are known to excrete considerable amounts of photosynthetically fixed organic carbon which has recently also been confirmed for the epibiont (25) and it has been suggested that the epibiont supplies the central bacterium with these organic carbon excretion products (9). Although the rate of anoxygenic photosynthesis per cell decreases under light-limiting conditions, the surrounding epibionts together may still be able to maintain a considerable rate of carbon supply for the single central bacterium in phototrophic consortia. The disadvantage of carbon assimilation under limited light conditions is compensated by the acquired motility, enabled by the flagellated central bacterium, to ensure a habitat with favorable conditions, i.e. presence of sufficient sulfides, light and absence of oxygen.

The CBC detected in the current study represents one of the most conspicuous ultrastructural elements of phototrophic consortia. An exhaustive search of the literature revealed that there is a variety of striking internal structures in several other, non-related bacteria. Microtubule-like structures have been documented for numerous Gram-negative and Gram-positive bacteria (1),

but they clearly differ in fine structure from the CBC detected in phototrophic consortia. For the sulfur-oxidizing Epsilonproteobacterium "*Arcobacter sulfidicus*" discrete, 27–33 nm thick structures underlying the cytoplasmic membrane at the cell pole were described. Although they look similar to CBC at lower magnification, they consist – in contrast to phototrophic consortia – of 4 - 5 membrane lamellae with a thickness of 7.5 nm each (32). Electron dense membrane-like elements were observed in the thermophilic *Persephonella marina*, a member of the Aquificales (11). Some of these structures exhibited a bilayered substructure, thereby resembling the CBC in phototrophic consortia. Most notably, however, ultrastructural elements which exhibit a conspicuous similarity to the CBC have recently been documented for multicellular magnetotactic bacteria (31). These "striated structures" are identical to the CBC with respect to dimensions and shape. Although not explicitly described, in TEM micrographs published in Silva et al. (31) a structure which resembles CML can also be recognized. The occurrence of structures similar to CBC and CML in nonrelated bacteria forming multicellular associations suggests that these structures are involved in prokaryotic cell-cell-interactions.

Our study has identified several ultrastructural elements of epibionts as well as central bacteria. Some of these structures appear to be highly specific for phototrophic consortia and hence are likely to be involved in either the cell-cell-aggregation or in the physiological interaction in this most highly developed symbiosis between prokaryotes.

## Acknowledgements

We wish to thank Prof. Reinhard Rachel and Andreas Klingel for high-pressure freezing and freeze substitution of consortia and valuable discussions. Silvia Dobler is gratefully acknowledged for skilful technical assistance, Dr. Elizabeth Schroeder-Reiter for carefully reading the manuscript and Dr. H.-P. Grossart and Kristina Pfannes for providing samples from Lake Dagow. This work was supported in part by a grant of the Deutsche Forschungsgemeinschaft to J. Overmann (grants no. Ov 20/10-1 and 10-2).

## References

1. **Bermudes, D., G. Hinkle and L. Margulis.** 1994. Do prokaryotes contain microtubules? *Microbiol. Rev.* **58**: 387-400
2. **Burghardt, T., D.J. Näther, B. Junglas, H. Huber, and R. Rachel.** 2007. The dominating outer membrane protein of the hyperthermophilic Archaeum *Ignicoccus hospitalis*: a novel pore-forming complex. *Mol. Microbiol.* **63**:166-176
3. **Frigaard, N.-U., A.G.M. Chew, H. Li, J.A. Maresca and D.A. Bryant.** 2003. *Chlorobium tepidum*: insights into the structure, physiology, and metabolism of a green sulfur bacterium derived from the complete genome sequence. *Photosynth. Res.* **78**: 93-117
4. **Fröstl, J., and J. Overmann.** 1998. Physiology and tactic response of "*Chlorochromatium aggregatum*". *Arch. Microbiol.* **169**:129-135
5. **Fröstl, J., and J. Overmann.** 2000. Phylogenetic affiliation of the bacteria that constitute phototrophic consortia. *Arch. Microbiol.* **174**:50-58
6. **Fuhrmann S., J. Overmann, N. Pfennig and U. Fischer.** 1993. Influence of vitamin B<sub>12</sub> and light on the formation of chlorosomes in green- and brown-colored *Chlorobium* species. *Arch. Microbiol.* **160**: 193-198
7. **Gasol, J.M., K. Jürgens , R. Massana, J.I. Calderón-Paz, and C. Pedrós-Alió.** 1995. Mass development of *Daphnia pulex* in a sulphide-rich pond (Lake Cisó). *Arch. Hydrobiol.* **132**:279-296
8. **Glaeser, J., and J. Overmann.** 2003a. Characterization and *in situ* carbon metabolism of phototrophic consortia. *Appl. Environ. Microbiol.* **69**:3739-3750
9. **Glaeser, J., and J. Overmann.** 2003b. The significance of organic carbon compounds for *in situ* metabolism and chemotaxis of phototrophic consortia. *Environ. Microbiol.* **5**:1053-1063
10. **Glaeser, J., and J. Overmann.** 2004. Biogeography, evolution, and diversity of epibionts in phototrophic consortia. *Appl. Environ. Microbiol.* **70**:4821-4830
11. **Götz, D., A. Banta, T.J. Beveridge, A.I. Rushdi, B.R.T. Simoneit and A.-L. Reysenbach.** 2002. *Persephonella marina* gen. nov. and *Persephonella guaymasensis* sp. nov., two novel, thermophilic hydrogen-oxidizing microaerophiles from deep-sea hydrothermal vents. *Int. J. Syst. Evol. Microbiol.* **52**: 1349-1359

12. **Graham, L. L., and T. J. Beveridge.** 1990. Evaluation of freeze-substitution and conventional embedding protocols for routine electron microscopic processing of eubacteria. *J. Bacteriol.* **172**:2141-2149
13. **Huber, H., M. J. Hohn, R. Rachel, T. Fuchs, V. C. Wimmer, and K. O. Stetter.** 2002. A new phylum of Archaea represented by a nanosized hyperthermophilic symbiont. *Nature* **417**: 63-67
14. **Kanzler, B., K. R. Pfannes, K. Vogl, and J. Overmann** 2005. Molecular characterization of the non-photosynthetic partner bacterium in the consortium "*Chlorochromatium aggregatum*". *Appl. Environ. Microbiol.* **71**: 7434-7441
15. **Lam, J.S., L. L. Graham, J. Lightfoot, T. Dasgupta, T. J. Beveridge.** 1992. Ultrastructural examination of the lipopolysaccharides of *Pseudomonas aeruginosa* strains and their isogenic rough mutants by freeze-substitution. *J. Bacteriol.* **174**:7159-7167
16. **Lefman, J., P. Zhang, T. Hirai, R. M. Weis, J. Juliani, D. Bliss, M. Kessel, E. Bos, P. J. Peters, and S. Subramaniam.** 2004. Three-dimensional electron microscopic imaging of membrane invaginations in *Escherichia coli* overproducing the chemotaxis receptor Tsr. *J. Bacteriol.* **186**:5052-5061
17. **Manske, A.K., J. Glaeser, M.M.M. Kuypers and J. Overmann.** 2005. Physiology and phylogeny of green sulfur bacteria forming a monospecific phototrophic assemblage at 100 m depth in the Black Sea. *Appl. Environ. Microbiol.* **71**: 8049-8060
18. **Oke, V., and S. R. Long.** 1999. Bacteroid formation in the *Rhizobium*-legume symbiosis. *Curr. Op. Microbiol.* **2**: 641-646
19. **Overmann, J.** 2001a. Green sulfur bacteria, p. 601-605 *In* D. R. Boone, R. W. Castenholz, and G. M. Garrity (ed) *Bergey's Manual of Systematic Bacteriology* 2nd ed., Springer, New York, NY.
20. **Overmann, J.** 2001b. Phototrophic consortia. A tight cooperation between non-related eubacteria, p. 239-255 *In* J. Seckbach (ed) *Symbiosis. Mechanisms and model systems.* Kluwer, Dordrecht.
21. **Overmann J., H. Cypionka and N. Pfennig.** 1992. An extremely low-light-adapted phototrophic sulfur bacterium from the Black Sea. *Limnol. Oceanogr.* **37**: 150-155
22. **Overmann, J., and N. Pfennig.** 1989. *Pelodictyon phaeoclathratiforme* sp. nov., a new brown-colored member of the *Chlorobiaceae* forming net-like colonies. *Arch. Microbiol.* **152**:401-406
23. **Overmann, J., and K. Schubert.** 2002. Phototrophic consortia: model systems for symbiotic interrelations between prokaryotes. *Arch. Microbiol.* **177**:201-208

24. **Overmann, J., C. Tuschak, J. Fröstl, and H. Sass.** 1998 The ecological niche of the consortium "*Pelochromatium roseum*". Arch. Microbiol. **169**:120-128
25. **Pfannes, K.** 2007. Characterization of the symbiotic bacterial partners in phototrophic consortia. Ph.D. Dissertation, Universität München, 180 p.
26. **Pfannes, K. R., K. Vogl, and J. Overmann.** 2007. Heterotrophic symbionts of phototrophic consortia: members of a novel diverse cluster of *Betaproteobacteria* characterised by a tandem *rrn* operon structure. Environ. Microbiol. **9**:2782-2794
27. **Rachel, R., I. Wyschkony, S. Riehl, and H. Huber.** 2002. The ultrastructure of Ignicoccus: evidence for a novel outer membrane and for intracellular vesicle budding in an archaeon. Archaea **1**:9-18.
28. **Rai, A. N., E. Söderbäck, and B. Bergman.** 2000. Cyanobacterium-plant symbiosis. New Phytol. **147**:449-481
29. **Reinhold-Hurek, B., and T. Hurek.** 1998. Life in grasses: diazotrophic endophytes. Trends Microbiol. **6**:139-144
30. **Rieger, G., K. Müller, R. Hermann, K. O. Stetter, and R. Rachel.** 1997. Cultivation of hyperthermophilic archaea in capillary tubes resulting in improved preservation of fine structures. Arch. Microbiol. **168**:373-379
31. **Silva, K. T., F. Abreu, F. P. Almeida, C. Neumann Keim, M. Farina, and U. Lins.** 2007. Flagellar apparatus of south-seeking many-celled magnetotactic prokaryotes. Microsc. Res. Tech. **70**:10-17
32. **Taylor, C.D. and C.O. Wirsen.** 1997. Microbiology and ecology of filamentous sulfur formation. Science **277**: 1483-1485
33. **Vogl, K., J. Glaeser, K. R. Pfannes, G. Wanner, and J. Overmann.** 2006. *Chlorobium chlorochromatii* sp. nov., a symbiotic green sulfur bacterium isolated from the phototrophic consortium "*Chlorochromatium aggregatum*". Arch. Microbiol. **185**:363-372
34. **Vogl, K., M. Dreßen, R. Wenter, M. Schlickerrieder and J. Overmann.** 2007. Identification and analysis of candidate symbiosis genes from "*Chlorochromatium aggregatum*", a highly developed bacterial symbiosis. Mol. Microbiol. (submitted)
35. **Walther, P., and A. Ziegler.** 2002. Freeze-substitution of high-pressure frozen samples: the visibility of biological membranes is improved when the substitution medium contains water. J. Microsc. **208**:3-10.
36. **Weis, R. M., T. Hirai, A. Chalah, M. Kessel, P. J. Peters, and S. Subramaniam.** 2003. Electron microscopic analysis of membrane assemblies formed by the bacterial chemotaxis receptor Tsr. J. Bacteriol. **185**:3636-3643

37. **Zhang, P., E. Bos, J. Heymann, H. Gnaegi, M. Kessel, P. J. Peters, and S. Subramaniam.** 2004. Direct visualization of receptor arrays in frozen-hydrated sections and plunge-frozen specimens of *E. coli* engineered to overproduce the chemotaxis receptor Tsr. *J. Microsc.* **216**:76-83
38. **Zhang, P., C. M. Khursigara, L. M. Hartnell, and S. Subramaniam.** 2007. Direct visualization of *Escherichia coli* chemotaxis receptor arrays using cryo-electron microscopy. *Proc. Natl. Acad. Sci. USA* **104**:3777-3781

# **Molecular characterization of the non-photosynthetic partner bacterium in the consortium “*Chlorochromatium aggregatum*”**

Birgit Kanzler<sup>1</sup>, Kristina R. Pfannes<sup>1</sup>, Kajetan Vogl<sup>1</sup> and Jörg Overmann<sup>1,\*</sup>

---

<sup>1</sup> Bereich Mikrobiologie, Ludwig-Maximilians-Universität München, Maria-Ward-Str. 1a, D-80638 München, Germany

\* corresponding author. e-mail: [j.overmann@lrz.uni-muenchen.de](mailto:j.overmann@lrz.uni-muenchen.de). Tel.: +49-89-2180-6123, FAX: +49-89-2180-6125

## Abstract

Phototrophic consortia represent valuable model systems for the study of signal transduction and coevolution between different bacteria. The phototrophic consortium "*Chlorochromatium aggregatum*" consists of a colorless central rod-shaped bacterium surrounded by about 20 green-colored epibionts. Whereas the epibiont was identified as a member of the green sulfur bacteria, and recently isolated and characterized in pure culture, the central colorless bacterium has been identified as a  $\beta$ -*Proteobacterium* but so far could not be characterized further. In the present study, "*C. aggregatum*" was enriched chemotactically and the 16S rRNA gene sequence of the central bacterium was elucidated. Based on the sequence information, fluorescence *in situ* hybridization (FISH) probes targeting four different regions of the 16S rRNA were designed and shown to hybridize exclusively to cells of the central bacterium. Phylogenetic analyses of the 1437 bp-long sequence revealed that the central bacterium of "*C. aggregatum*" represents a so far isolated phylogenetic lineage related to *Rhodoferrax* spp., *Polaromonas vacuolata* and *Variovorax paradoxus* within the family *Comamonadaceae*. The majority of relatives are not-yet-cultured and were found in low-temperature aquatic environments, or aquatic environments containing xenobiotica or hydrocarbons. In CsCl-bisbenzimidazole equilibrium density gradients, genomic DNA of the central bacterium of "*Chlorochromatium aggregatum*" formed a distinct band, which could be detected by Quantitative PCR using specific primers. Using this method, the mol% G+C content of the central bacterium was determined to be 55.6%.

## Introduction

During the course of evolution, prokaryotes have entered into numerous symbiotic relationships. So far, mostly the symbioses between bacteria and eukaryotes have been investigated (Overmann and Schubert 2002). On the contrary, interactions between different prokaryotes have received much less attention, such that only the syntrophic associations of anaerobic chemotrophic bacteria with archaea are understood in sufficient detail (Schink 1991). Microscopic studies have revealed, however, that morphologically highly structured associations of different prokaryotes exist in natural habitats (Overmann 2001a, Overmann and Schubert 2002). In these so-called consortia, prokaryotes maintain a permanent cell-to-cell contact; hence their mutual interdependence may be obligatory.

Of the consortia known, only two phototrophic consortia have been cultivated in the laboratory (Fröstl and Overmann 1998, Glaeser *et al.* 2002). Phototrophic consortia consist of a colorless central rod-shaped bacterium surrounded by 13-69 green- or brown-colored epibionts (Overmann 2001a), and typically occur in the chemocline of many stratified lakes (Caldwell and Tiedje 1974, Croome and Tyler 1984, Gasol *et al.* 1995, Glaeser and Overmann 2003a, Glaeser and Overmann 2004) where they may constitute up to 66% of the total bacterial biomass (Gasol *et al.* 1995).

Several lines of evidence indicate that a direct communication exists between the two different types of bacteria in phototrophic consortia (Fröstl and Overmann 1998, Glaeser and Overmann 2003b). Intact consortia accumulate scotophobically in the light, at wavelengths, which correspond to the absorption maxima of the bacteriochlorophylls present in the epibionts (Fröstl and Overmann 1998). Epibiont cells are nonflagellated, however, whereas the central bacterium is motile by means of a single polar flagellum (Glaeser and Overmann 2003a, Overmann *et al.* 1998). Consequently, the scotophobic response must involve signal exchange between the epibionts and the central bacterium. As a second observation, intact phototrophic consortia take up 2-oxoglutarate, most likely mediated by the central bacterium. This uptake is strictly dependent on the presence of sulfide and light, both utilized by the epibionts (Glaeser and Overmann 2003b). Accordingly, the physiological state of the epibiont cells appears to control the 2-oxoglutarate uptake by the central bacterium. Phototrophic consortia thus represent valuable model systems for the study of signal transduction and coevolution between different bacteria.

Using 16S rRNA-based methods, the epibionts of phototrophic consortia have been identified as green sulfur bacteria (Fröstl and Overmann 2000, Tuschak *et al.* 1999). In the associated state, epibionts grow photoautotrophically like their free-living green sulfur bacterial relatives (Glaeser and Overmann 2003a). Recently, the epibiont of the phototrophic consortium “*Chlorochromatium aggregatum*” could be isolated in pure culture and its physiology characterized in detail (Vogl *et al.* 2006). Also, the genome sequence of the epibiont has just been completed ([http://genome.jgi-psf.org/finished\\_microbes/chlag/chlag.download.html](http://genome.jgi-psf.org/finished_microbes/chlag/chlag.download.html)). In contrast, only very little is known of the central bacterium. By fluorescence *in situ* hybridization (FISH), it could be identified as a member of the  $\beta$ -subclass of the *Proteobacteria* (Fröstl and Overmann 2000). However, its precise phylogenetic position could not be determined because of the notoriously low cell numbers of central bacteria which are present in the available “*C. aggregatum*” cultures.

## Material and Methods

### Source of organisms

Enrichment cultures of “*Chlorochromatium aggregatum*” were established previously from a sediment sample of the eutrophic Lake Dagow (100 km north of Berlin) (Fröstl and Overmann 1998). “*C. aggregatum*” consists of a colorless central rod and approximately 20 green-pigmented epibionts. A recently isolated pure culture of the epibiont strain CaD of „*C. aggregatum*” (Vogl *et al.* 2006), and cultures of *Rhodocyclus tenuis* DSMZ 109<sup>T</sup>, *Ralstonia eutropha* DSMZ 428, *Chlorobium phaeobacteroides* DSMZ 266<sup>T</sup> and *Clostridium acetobutylicum* DSMZ 792 were used for reference.

### Media and growth conditions

„*C. aggregatum*” was grown in K4-medium of the following composition (components in grams per liter): KH<sub>2</sub>PO<sub>4</sub>, 0.25; NH<sub>4</sub>Cl, 0.05; MgCl<sub>2</sub> · 6 H<sub>2</sub>O, 0.05; CaCl<sub>2</sub> · 2 H<sub>2</sub>O, 0.05; HEPES, 2.38; NaHCO<sub>3</sub>, 0.84. After autoclaving, the medium was cooled under an N<sub>2</sub>/CO<sub>2</sub> atmosphere, and sterile sulfide solution (Na<sub>2</sub>S · 9 H<sub>2</sub>O, 0.12 g in 20 ml), 1 ml of a seven-vitamin solution (Pfennig 1978), 1 ml trace element solution SL10 (Widdel *et al.* 1983), and 0.25 ml lipoic acid solution (100 mg·l<sup>-1</sup>) were added. The pH was adjusted to 7.4 and the medium dispensed into air-tight, screw-capped bottles. Prior to inoculation with 5% (v/v) of an enrichment culture of „*C. aggregatum*”, the medium was supplemented with 0.05% (v/v) of trace element solution SL12B (Overmann *et al.* 1992) and 0.5 mM 2-oxoglutarate (final concentrations).

Cultures were incubated at 15°C and at 20  $\mu\text{mol quanta m}^{-2} \text{ s}^{-1}$  of a daylight fluorescent tube (Lumilux de Lux, 18W, Osram, Munich, Germany). Light intensities were monitored using a LiCor LI-250 lightmeter equipped with the pyranometer sensor PY38153 (Walz, Effeltrich, Germany). During exponential growth, cultures received 0.5 mM neutral sulfide solution (Siefert and Pfennig 1984) and 0.5 mM 2-oxoglutarate every two days.

### **Enrichment by chemotaxis**

For subsequent molecular analyses, „*C. aggregatum*” was enriched exploiting the chemotactic behaviour of the intact consortia. The original method (Fröstl and Overmann 1998) was modified. All manipulations were carried out in an anaerobic chamber under an atmosphere of 95% N<sub>2</sub> and 5% H<sub>2</sub>. 100 ml Meplats bottles with twelve bore holes (Fröstl and Overmann 1998) were filled with 20 ml of a densely grown culture of „*C. aggregatum*” containing  $2.6 \cdot 10^5$  consortia per ml. Sulfide solution (1 mM) was prepared in sterile filtered (0.1  $\mu\text{m}$  pore Durapore membrane filters; Millipore, Eschborn, Germany) culture supernatant. Flat rectangular capillaries (length 50 mm; inside diameter 0.1 x 1.0 mm or 0.1 x 2.0 mm; Vitrocom, New Jersey, USA) or round capillaries (volume 5  $\mu\text{l}$ , 10  $\mu\text{l}$ , 20  $\mu\text{l}$  and 100  $\mu\text{l}$ ; Servoprax, Wesel, Germany; Brand, Wertheim, Germany; or Assistent, Sondheim/Röhn, Germany) were filled by capillary action with the sulfide solution and sealed at one end with plasticine (Münchner Künstler Plastilin, Munich, Germany). Capillaries were then inserted through the holes in the Meplats bottle until their open end reached the culture liquid, and fixed with plasticine. Incubations proceeded overnight at 15°C and an ambient light intensity of 20  $\mu\text{mol quanta m}^{-2} \text{ s}^{-1}$ . Afterwards, the content of the capillaries was transferred into 100  $\mu\text{l}$  of sterile double-distilled water and centrifuged for 15 min at 13,000 rpm. The cell pellet was resuspended in 10  $\mu\text{l}$  of double-distilled water and stored at -20°C.

### **PCR**

Chemotaxis enrichments were lysed by five consecutive freeze-thaw cycles (each cycle consisting of a 3 min-incubation each at 100°C and at -20°C). One  $\mu\text{l}$  of the cell lysate was used for amplification. Amplification reactions for pure cultures received 50 ng of genomic DNA. Standard PCR conditions (Overmann *et al.* 1999) were performed with a DNA thermal cycler (GeneAmp PCR-system 2400, Applied Biosystems, Forster City, USA) and PCR-products were analyzed by standard agarose gel electrophoresis.

For amplifications with primers GC341f or 341f and 907r (Muyzer *et al.* 1995), the cycling conditions described previously were employed (Overmann and Tuschak 1997). For the specific amplification of betaproteobacterial sequences, primers Beta680f (Overmann *et al.* 1999) and an improved version of primer 13R (Aakra *et al.* 1999) (5'-TCGCCAAGGCATCCA-CC-3', *E. coli* position 23-39 of the 23S rRNA) were used. The step down PCR program comprised 10 cycles with denaturation at 94°C for 30 s, primer annealing at 61°C for 1 min, and elongation at 72°C for 3 min, followed by 25 cycles with the annealing temperature changed to 56°C. Two primers CRa641f (5'-ACTGCAGATGCTAGAGTA-3') and CRa641r (5'-CGTACTCTAGCATC-TGCAGT-3) were designed in the present study and are specific for the 16S rRNA gene sequence of the central bacterium of "*C. aggregatum*". The specific primers were combined either with GC341f, or with universal primers 8f or 1492r (Lane 1991). For amplification with primer pair 8f / CRa641r, the optimized step down program comprised 10 cycles with denaturation at 94°C for 30 s, primer annealing at 70°C for 30 s, and elongation at 72°C for 2 min, followed by 20 cycles with the annealing temperature changed to 65°C. Cycling conditions for primer pair GC341f / CRa641r were: 10 cycles with denaturation at 94°C for 30 s, primer annealing at 58°C for 45 s, and elongation at 72°C for 1 min, followed by 30 cycles with the annealing temperature changed to 53°C. For amplification with the primer pair CRa641f / 1492r, the annealing temperature was set to 60°C for 30 s during the first 10 cycles, and to 55°C for the subsequent 25 cycles. In this case, elongation proceeded for 1 min at 72°C.

### Quantitative PCR

The relative amount of genomic DNA of the central bacterium from „*C. aggregatum*” in CsCl-bisbenzimidazole density gradients was determined by quantitative PCR (iQ<sup>TM</sup> iCycler, BIO-RAD, München, Germany) employing the primer pair 341f / CRa641r and the SYBR Green Supermix (BIO-RAD) for the detection of double-stranded PCR products. Each reaction received 4 ng of template DNA. For standardization of the values, tenfold dilutions of genomic DNA from the „*C. aggregatum*” culture (concentration range 4 pg to 400 ng) were measured in parallel. Cycling conditions included 5 min of denaturation (95°C), 45 s of annealing (67°C, 40 cycles) and 1 min of elongation (72°C). All measurements were done in quadruplicate and negative controls were included throughout. The relative enrichment factor for genomic DNA of the central bacterium was derived from a comparison of the Ct values determined directly for the enrichment culture and the Ct values determined for DNA fractions from the CsCl-gradients.

### **Denaturing gradient gel electrophoresis (DGGE)**

16S rRNA gene fragments amplified were separated by DGGE (Muyzer *et al.* 1993, Muyzer *et al.* 1995), conducted in the Ingeny phorU2 system (Ingeny International BV, Goes, The Netherlands) for 15 min at 200 V, then 12 h at 180 V at a constant temperature of 60°C. After staining with SYBRGold (MoBiTec, Göttingen, Germany) the DNA bands were visualized on a UV-transilluminator and DNA fragments of interest were excised with a sterile scalpel. Gel pieces were incubated for 1 h at 65°C in 20 µl of 2 mM Tris/HCl (pH 8.0), the eluted DNA reamplified, and the amplification products purified for sequencing using the QiaQuick PCR purification kit (Qiagen GmbH, Hilden, Germany). Gel images were captured with a digital camera (Spot RT color; Diagnostic Instruments Inc., USA) and processed with the Spot RT version 3.1 software.

### **Cloning**

PCR-products were cloned through chemical transformation with the TOPO TA Cloning-Kit (version P; Invitrogen, Carlsbad, California, USA). Plasmids were extracted with the QIAprep Spin Miniprep-Kit (Invitrogen) and the presence of inserts verified by digestion with *EcoRI*, *PvuI*, *HaeIII* (MBI Fermentas, St. Leon-Rot, Germany).

### **Sequencing**

Sequencing was performed by the dideoxynucleotide method (Sanger *et al.* 1977) using the AmpliTaq FS BigDyeTerminator Cycle Sequencing Kit according to the protocol of the manufacturer and the ABI Prism 310 Genetic Analyzer (Applied Biosystems, Weiterstadt, Germany). Additionally to the primers described above, oligonucleotides 926f, 1055f and 1055r (Amann *et al.* 1995, Lane 1991) were employed in the sequencing reactions. The computer program Lasergene (Seqman II, DNASTAR Inc., Madison, Wisconsin, USA) was used for sequence editing.

### **Phylogenetic analyses**

16S rRNA sequences were analyzed using the software packages ARB (Ludwig *et al.* 2004) and PHYLIP (Phylogeny Inference Package, version 357c; Felsenstein 1989). Sequences of the 50 phylogenetically closest relatives of the central bacterium were retrieved from the GenBank database employing BLAST 2.0.4. (Altschul *et al.* 1997) and imported into the ARB database. The Fast Aligner V1.03 tool was used for automatic sequence alignment. The latter was checked

and manually corrected based on secondary structure information, yielding an alignment of 1542 informative nucleotide positions.

Phylogenetic trees were constructed using the Maximum Likelihood and Maximum Parsimony algorithms within the ARB package and the Neighbour Joining and distance-based methods (DNADIST plus FITCH) as implemented in the PHYLIP software package. To identify variable branching points, the phylogenetic trees generated were compared pairwise employing the COMPARE TOPOLOGY function of the ARB program. In addition, reproducibility of the branching pattern of the Maximum Likelihood tree was tested by bootstrap analysis, generating a set of 100 resamplings. Those branches which were observed to vary between the four methods and which had low bootstrap support were collapsed with deeper branching points to yield multifurcations, using the ARB software (W. Ludwig, pers. communication).

### **Fluorescence *in situ* hybridization (FISH)**

In order to verify the 16S rRNA gene sequence determined for the central rod of „*C. aggregatum*”, specific FISH-probes were created with the DESIGN PROBES function of the ARB software package. The accessibility of the target sites was checked based on data available for *Escherichia coli* (Fuchs *et al.* 1998). For probes targeting sites with limited accessibility, corresponding helper oligonucleotides (Fuchs *et al.* 2000) were designed. Overall, four specific probes and 8 helper oligonucleotides were used (Table 1). Fluorescence *in situ* hybridization was carried out on black polycarbonate filters resulting in disintegration of the phototrophic consortia, thereby exposing the central rod (Tuschak *et al.* 1999). Twenty ng each of the Cy3-labeled probe and the corresponding helper oligonucleotides at the appropriate hybridization stringency were used (Table 1). Hybridization stringency was tested and optimized by varying the formamide concentrations between 5 and 35%. After counterstaining with 4',6-diamidino-2-phenylindole (DAPI), hybridizations were analyzed by epifluorescence microscopy.

### **CsCl – bisbenzimidazole density gradient centrifugation**

The mol% G+C content of the central bacterium was determined in cesium chloride-bisbenzimidazole equilibrium density gradients (Bostock-Smith and Searle. 1999, Holben and Harris 1995, Holben *et al.* 2004, Nüsslein and Tiedje 1998, Vinograd and Hearst 1962), using a modified protocol. Ten µl of bisbenzimidazole stock solution (Hoechst # 33258; 25 µg·µl<sup>-1</sup>) were added to 10 ml of CsCl-TE (1.3g CsCl · ml<sup>-1</sup> in TrisHCl/EDTA 10 mM/1 mM). The mixture was transferred to a 16 x 76 mm ultracentrifuge Quick-Seal tube (# 342413; Beckman Coulter, USA), overlaid with 1 ml of DNA extract containing 150 µg DNA from a consortia culture, the

headspace completely filled with paraffin oil, balanced and sealed. Centrifugation proceeded at  $232.000 \times g$  for 48 h at 15°C in a fixed-angle rotor (70.1 Ti, Beckman Coulter, USA). DNA bands were visualized under UV at 365 nm and 100  $\mu$ l fractions were collected from below via a 21-G needle connected to silicon tubing, employing a peristaltic pump.

Subsequently, the refractive index of each fraction was determined. Bisbenzimidazole and CsCl were removed using three repeated extractions in CsCl-saturated isopropanol, followed by two wash steps with Tris-HCl in Centricon-50 ultrafiltration units (Millipore, Eschborn, Germany). The DNA content of all purified fractions was determined fluorimetrically using PicoGreen (Molecular Probes, Eugene, Oregon, USA). For standardization, genomic DNA of bacterial strains with known GC content (*Clostridium acetobutylicum*, mol% G+C = 30.9; *Chlorobium phaeobacteroides*, mol% G+C = 49.0; *Ralstonia eutropha*, mol% G+C = 64.4) was separated in the same gradient and a standard curve established correlating the known GC contents to the refractive index.

### **Accession numbers**

The almost full-length 16S rRNA gene sequence of the central bacterium of "*C. aggregatum*" has been deposited in the EMBL database under accession number DQ009030. Partial sequences of the accompanying bacteria are deposited under numbers DQ009027–DQ009029 and DQ009031–DQ009034.

**Table 1.** Fluorescently labeled probes, helper oligonucleotides and hybridization conditions employed for FISH

Probe/helper <sup>a</sup>	sequence	T (°C)	formamide(%)
CR-207	5'- CGC GCG AGG CCC TCT -3'	48	20
CR-207-H1	5'- CAG GTC CCC CGC TTT CAT -3'		
CR-207-H2	5'- CTG ATA TCA GCC GCT CCA AT -3'		
CR-442	5'- AAG GCT GTT TCG CTC CGT -3'	45	20
CR-641	5'- TAC TCT AGC ATC TGC AGT -3'	45	20
CR-641-H1	5'- CAC AAA TGC AAT TCC CAG -3'		
CR-641-H2	5'- GTT GAG CCC GGG GAT -3'		
CR-641-H3	5'- TTC ACA TCC GTC TTA CAG -3'		
CR-641-H4	5'- CAT CCC CCT CTG CCG -3'		
CR-1282	5'- CGA CTG ACT TTA TGG -3'	45	5
CR-1282-H1	5'- GGT TGG CTC CCT CTC -3'		
CR-1282-H2	5'- CTG CGA TCC GGA CTA -3'		
Cont-645	5'- TGC CAT ACT CTA GCC TTC -3'	45	20
Cont-645-H1	5'- CAG TCA CAA GCG CAG TT -3'		
Cont-645-H2	5'- CCC AAG TTG AGC CCG -3'		
Cont-645-H3	5'- GGG ATT TCA CGC CTG -3'		
Cont-645-H4	5'- AAT TCC ACC CCC CTC -3'		
Cont-995	5'- CTT CAG GCT CCT GGA CAT -3'	45	20
Cont-995-H1	5'- GTC AAG GGT AGG TAA GGT TTT-3'		
Cont-995-H2	5'- TCG GGC ACA CCC AAA TCT-3'		
Cont-995-H3	5'- CCT GTG TTC CAG TTC CCT T-3'		

<sup>a</sup> Numbers indicate 5'-end according to *E.coli* numbering. Suffix "CR" denotes probes specific for the central rod-shaped bacterium of "*C. aggregatum*", "Cont" for probes specific for free-living  $\beta$ -*Proteobacteria*. Helper oligonucleotides are denoted by the suffix "H".

## Results and Discussion

### Improved chemotactic enrichment of intact phototrophic consortia

Based on DAPI counting of standard enrichment cultures of "*Chlorochromatium aggregatum*", cells of the central bacterium reach  $\leq (0.071 \pm 0.003)\%$  of total cell counts. At such low frequencies, 16S rRNA gene sequences cannot be detected by PCR/DGGE (Muyzer *et al.* 1993, Straub *et al.* 1998). Therefore, the chemotaxis of "*C. aggregatum*" towards sulfide (Fröstl and Overmann 1998) was exploited as a rapid means to selectively enrich intact consortia. In small flat rectangular capillaries (0.1 mm x 1.0 mm), "*C. aggregatum*" accumulated within the first 3 mm from the capillary opening. However, these enrichments also contained a high number of motile chemotrophic bacteria, which still amounted to 85% of all cells (similar to the accumulation depicted in Fig. 1B). Experiments with round capillaries of different sizes and volumes did not yield suitable enrichments. In flat capillaries with a larger width (0.1 mm x 2.0 mm), however, "*C. aggregatum*" accumulated in two distinct zones. In addition to the primary enrichment detected near the capillary opening, a second zone of accumulation formed in the center of the capillary, at a distance approximately 1 cm from the primary accumulation. Direct phase contrast microscopy of the capillaries revealed that much less accompanying bacteria were present in this secondary accumulation (Fig. 1A) than in the accumulation near the capillary end (Fig. 1B).

In order to gather sufficient material for subsequent molecular analyses, chemotactic enrichments from 48 flat rectangular capillaries were collected by breaking off the capillaries in the center (Fig. 1A), and blowing out their contents into an eppendorf vial using sterile filtered air. Then, the cells were concentrated by centrifugation to a final titer of  $10^7$  consortia  $\text{ml}^{-1}$ .

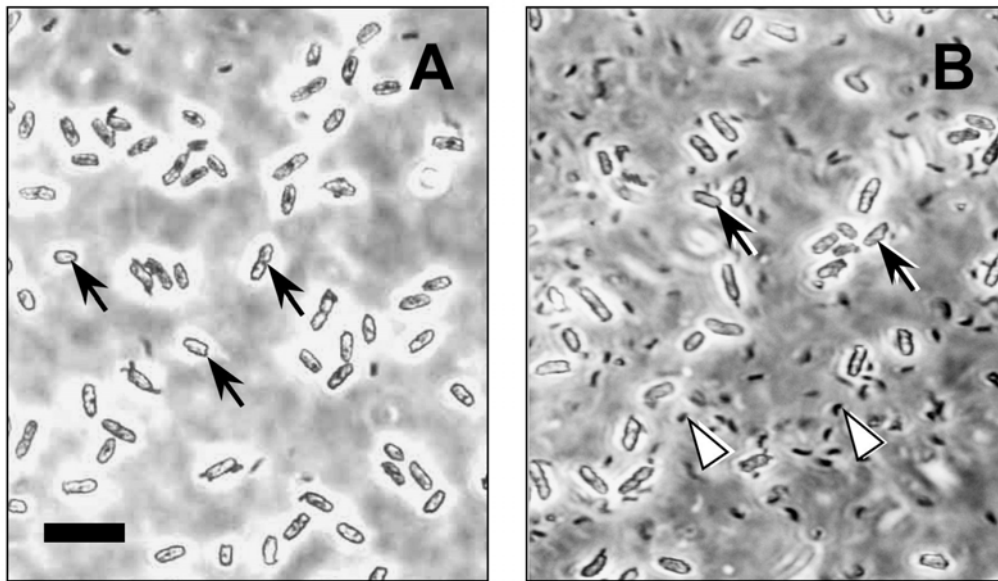


**Figure 1.** **A.** Phase contrast photomicrograph of the accumulation of "*Chlorochromatium aggregatum*" (black arrows) formed in the center of the 0.1 x 2 mm rectangular capillary. **B.** Photomicrograph of the bacteria accumulated at the opening of the capillary. Besides phototrophic consortia (black arrows), numerous motile contaminants (white arrow heads) are present in this accumulation. Bar = 20  $\mu$ m

#### **Analysis of the 16S rRNA gene sequence of the central bacterium of "*C. aggregatum*"**

In a first step, partial 16S rRNA genes were amplified from the chemotactic enrichment of "*Chlorochromatium aggregatum*" using primers GC341f and 907r. Subsequent separation by denaturing gradient gel electrophoresis revealed the presence of 7 different DNA fragments among the amplification products (Fig. 2, bands *a* through *g*). All bands were excised, reamplified and sequenced. In parallel, a 1400 bp-long DNA fragment was amplified with the betaproteobacterial primer pair Beta680f/13R, and was also sequenced.

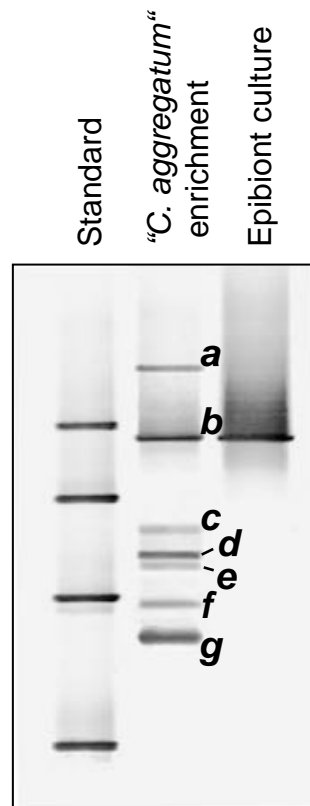


**Figure 2.** Separation by DGGE of 16S rRNA gene fragments amplified with primers GC341f and 907r from the chemotaxis enrichment of "*Chlorochromatium aggregatum*" and from a pure culture of the epibiont of "*Chlorochromatium aggregatum*". Italic letters denote DNA bands, which were excised and sequenced. A negative image of an SYBRGold-stained gel is shown.

Band *b* could be identified as the 16S rRNA gene fragment of the epibiont (Fig. 2), which was confirmed by sequence comparison. Of the remaining sequences, three (*c*, *d* and *e*) were affiliated with the *Betaproteobacteria*, two (*f* and *g*) with the  $\delta$ -*Proteobacteria*, and one (*a*) with the  $\epsilon$ -*Proteobacteria*. In previous FISH-analyses of the "*C. aggregatum*" enrichment culture, the central bacterium could be identified as a member of the *Betaproteobacteria* (Fröstl and Overmann 2000). In order to investigate whether the 16S rRNA sequence of the central bacterium was present among sequences *c* – *e*, specific oligonucleotide probes were constructed for each of the sequences and used to analyze the central bacterium by FISH. The sequence of the long DNA fragment amplified with the betaproteobacterial primer pair matched sequence type *c* and was therefore used to construct a specific probe (Cont-995) for this sequence type.

Probes Cont-995 and Cont-645, targeting sequence type *c* and type *d*, respectively, hybridized only to free-living bacteria but not to the central bacterium of "*C. aggregatum*", and hence must originate from accompanying bacteria present in the enrichment. In contrast, probes

CR-442 and CR-641, targeting sequence type *e*, hybridized exclusively to the central bacterium (Fig. 3A-D).

**Table 2.** Phylogenetic affiliation of partial 16S rRNA gene sequences from DGGE fingerprints (compare Figs. 3 and 6)

Melting type	Closest relative	(Sub)Phylum	Accession number	Similarity (%)
<i>a</i>	<i>Sulfurospirillum arsenophilum</i> MIT-13	$\epsilon$ -Proteobacteria	U85964	97.8
<i>b</i>	<i>Chlorobium chlorochromatii</i> CaD*	Chlorobi	AJ578461	100.0
<i>c</i>	<i>Azonexus fungiphilus</i> MFC-EB24	$\beta$ -Proteobacteria	AJ630292	99.0
<i>d</i>	<i>Quadricoccus australiensis</i> Ben177	$\beta$ -Proteobacteria	AY007722	98.5
<i>e</i>	<i>Rhodoferax ferrireducens</i> DSMZ15236 <sup>T</sup>	$\beta$ -Proteobacteria	AF435948	94.8
<i>f</i>	<i>Desulfovibrio aerotolerans</i> DvO5	$\delta$ -Proteobacteria	AY746987	98.9
<i>g</i>	<i>Desulfovibrio aerotolerans</i> DvO5	$\delta$ -Proteobacteria	AY746987	97.2
<i>h</i>	<i>Cellulomonas terrae</i> DB5	Actinobacteria	AY884570	97.1

\* = epibiont of "*Chlorochromatium aggregatum*"

Subsequently, the missing sequence stretches at the beginning and the end of the 16S rRNA gene of the central bacterium were amplified. To this end, PCR primers identical (CRa641r) or complementary (CRa641f, see Materials and Methods section) to the specific probe CR-641 were combined with primers 8f and 1492r, respectively. Genomic DNA of the two *Betaproteobacteria* *Rhodocyclus tenuis* DSMZ 109<sup>T</sup> and *Ralstonia eutropha* DSMZ 428 was employed to establish highly specific PCR conditions. Sequencing of the resulting amplification products yielded a 650 bp-long sequence from the 5'-end, and a 850 bp-long sequence from the 3'-end of the 16S rRNA gene. Both sequences showed 100% identity in the overlapping regions to the central fragment (sequence *e*) obtained by PCR-DGGE.

Finally, the origin of the two 16S rRNA gene sequences was verified by FISH. Two probes were designed for the terminal sequence regions (CR-207 and CR-1282; Table 1) and were found to hybridize exclusively to cells of the central bacterium of "*Chlorochromatium aggregatum*" (Fig. 3E,F). Assembling all three 16S rRNA gene sequence fragments of the central bacterium yielded an almost complete 16S rRNA gene sequence of a total length of 1437 bp.

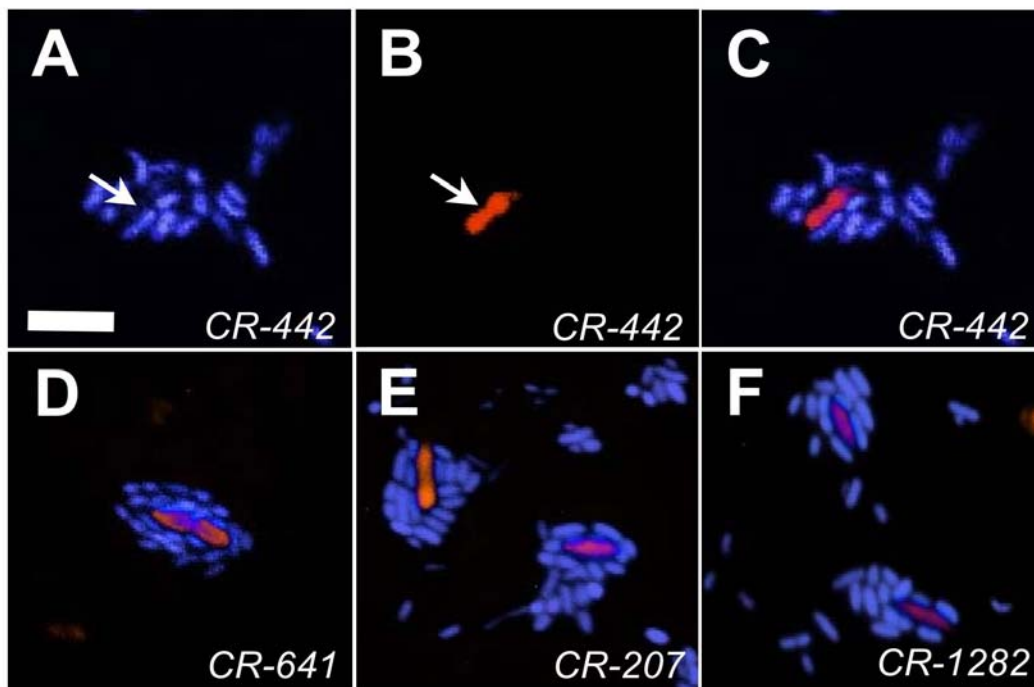


**Figure 3.** Specific detection of the central bacterium of "*Chlorochromatium aggregatum*" by FISH with four different oligonucleotide probes (compare Table 1). All bacterial cells were stained with DAPI. **A.** FISH with probe CR-442, DAPI fluorescence. Arrow indicates location of the central bacterium. **B.** Same field of view as in A., but showing Cy3 fluorescence. **C.** Overlay of A. and B. **D.** Overlay of DAPI fluorescence and Cy3-fluorescence after FISH using probe CR-641. **E.** Overlay of DAPI fluorescence and Cy3-fluorescence after FISH using probe CR-207. **F.** Overlay of DAPI fluorescence and Cy3-fluorescence after FISH using probe CR-1282. Bar = 10  $\mu$ m

### Phylogenetic classification of the central rod

Based on 16S rRNA gene sequence comparisons, the phylogenetically closest relatives of the central bacterium are *Rhodoferrax ferrireducens*, *Rfx. antarcticus* and a variety of not-yet-cultured bacteria. Sequence similarity was always lower than 95%, however (the closest cultured relative *Rfx. ferrireducens* DSMZ 15236<sup>T</sup> being 94.77% similar). According to our phylogenetic analyses (Fig. 4), the central rod of "*C. aggregatum*" represents a so far isolated phylogenetic lineage, and clusters with the genera *Rhodoferrax* and *Polaromonas* within the family *Comamonadaceae* (Beta I – subgroup; Glöckner *et al.* 2000). The majority of relatives are not-yet-cultured and were found in low-temperature aquatic environments, or aquatic environments containing pollutants like monochlorobenzene and tetrachloroethene, or hydrocarbons (Fig. 4) (Alfreider *et al.* 2002, Brinkmeyer *et al.* 2003, Finneran *et al.* 2003, Hiraishi *et al.* 2001, Jung *et al.* 2004, Watanabe *et al.* 2000).

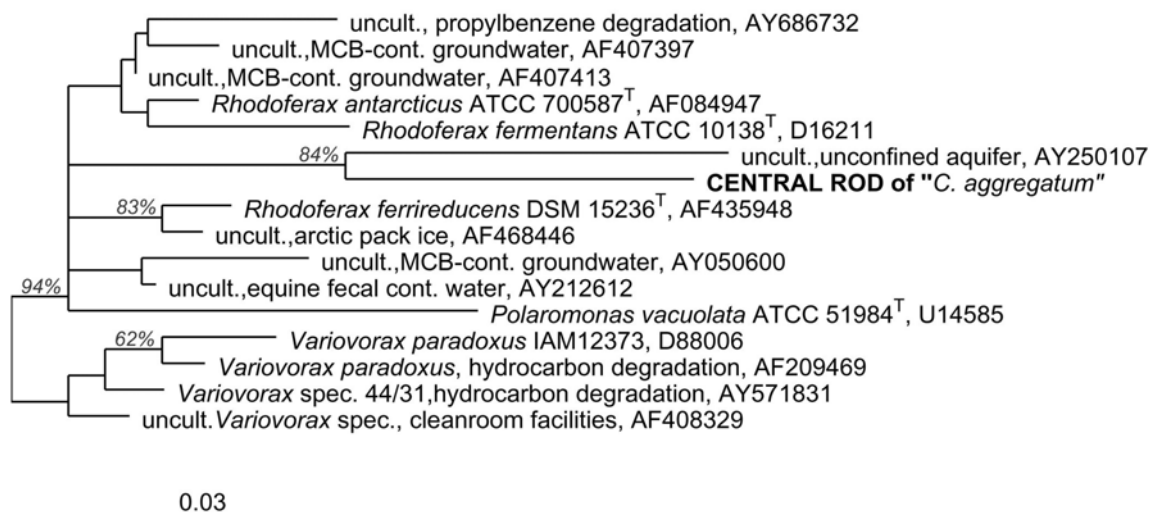


**Figure 4.** Phylogenetic affiliation of the central bacterium of "*Chlorochromatium aggregatum*". The consensus tree was constructed in ARB, based on Maximum Likelihood, Maximum Parsimony, Neighbor Joining and distance-based phylogenetic analyses (see Materials and Methods section). Percentages at nodes indicate bootstrap values out of 100 bootstrap resamplings as determined for the Maximum Likelihood tree. Only values above 50% are shown. Uncult., uncultured bacteria detected as environmental clones. Bar indicates 3% fixed point mutations per nucleotide base.

### GC-content and enrichment of genomic DNA of the central bacterium

CsCl-bisbenzimidazole equilibrium density centrifugation was used to determine the mol% G+C content of the central bacterium and to establish a large-scale purification method for its genomic DNA. Due to the inherently small volumes, which can be generated in the chemotaxis enrichments, the DNA had to be extracted directly from conventional laboratory cultures of "*C. aggregatum*" in this case.

Density gradient centrifugation separated the genomic DNA into four distinct bands as visualized by UV illumination (bands 1 through 4, Fig. 5A). Since the fluorescence of the DNA-bisbenzimidazole complex is proportional to the amount of bisbenzimidazole bound and thus decreases with mol% G+C content (Holben and Harris 1995), genomic DNA with a high mol% G+C content is barely detectable. The gradient was separated into 54 fractions and the DNA content of each fraction was determined by PicoGreen dye binding (Fig. 5B, filled circles). This second method confirmed the presence of band 4 and demonstrated its high DNA content, whereas band 2 was barely detectable with PicoGreen. Each fraction was PCR amplified with eubacterial primers, the products separated by DGGE and sequenced. Five major phylotypes could be distinguished (melting position *a*, *b*, *d*, *g*, *h*; Fig. 5C). With one exception (sequence type *h*), these sequences could be assigned to those identified in the chemotaxis enrichment. The genomic DNA of the epibiont of "*C. aggregatum*" (type *b*) accumulated in the center of the gradient, corresponding to the GC content of 46.7 mol% as recently determined (Vogl *et al.*

2006). Band 1 of the CsCl gradient was formed mainly by genomic DNA from the accompanying *Sulfospirillum arsenophilum* (sequence type *a*). According to our analysis, band 2 contained a mixture of genomic DNA from *Ssp. arsenophilum*, the epibiont and a relative of *Desulfovibrio aerotolerans* (sequence types *a*, *b*, and *g*). In band 3, predominantly *Desulfovibrio aerotolerans* was detected, whereas band 4 also contained DNA from an actinobacterium related to *Cellulomonas terrae* (sequence type *h*).

The genomic DNA of the central bacterium of "*C. aggregatum*" in the density gradients did not reach a concentration sufficient for the detection with eubacterial primers. However, amplification with the specific primer pair GC341f / CRA641r yielded amplification products for several fractions of the gradient. DGGE analysis revealed the presence of only one melting type (Fig. 5D) and sequencing confirmed that it was indeed identical to that of the central bacterium of "*C. aggregatum*". The specific amplification protocol was therefore used to quantify the enrichment factor for genomic DNA of the central bacterium in the CsCl-gradient by Quantitative PCR (Fig. 5B, diamonds). Compared to the original enrichment culture of "*C. aggregatum*", genomic DNA of the central bacterium was enriched 150-fold in fractions 27 – 29. At an enrichment factor of 150x and a frequency of 0.07% in the original culture, the genomic DNA of the central bacterium therefore amounted to approximately 10% of the total DNA in these fractions. Despite this relatively high frequency, the 16S rRNA gene sequence of the central bacterium could not be detected in the complex bacterial communities by PCR-DGGE with eubacterial primers. Our result is in line with data from another study, in which a detection limit of 9% was determined (Straub *et al.* 1998).

The distinct banding of the genomic DNA of the central bacterium of "*Chlorochromatium aggregatum*" in CsCl density gradients was used to estimate its GC content, using the median of the refractive indices of all ten fractions with enrichment factors  $\geq 50$  (Fig. 5B). This yielded a mol% G+C content of the central bacterium of "*C. aggregatum*" of 55.6%, which is commensurate with the values determined for other *Comamonadaceae*, spanning a range between 52 and 70% (Hiraishi *et al.* 1991, Irgens *et al.* 1996, Jung *et al.* 2004, Willems *et al.* 1991). Whereas the most closely related *Rhodoferrax* species have a GC-content of 59.8-61.5%, values of *Polaromonas vacuolata* strains are between 52 and 57 mol% and those of *Variovorax paradoxus* strains range between 67 and 69 mol%.

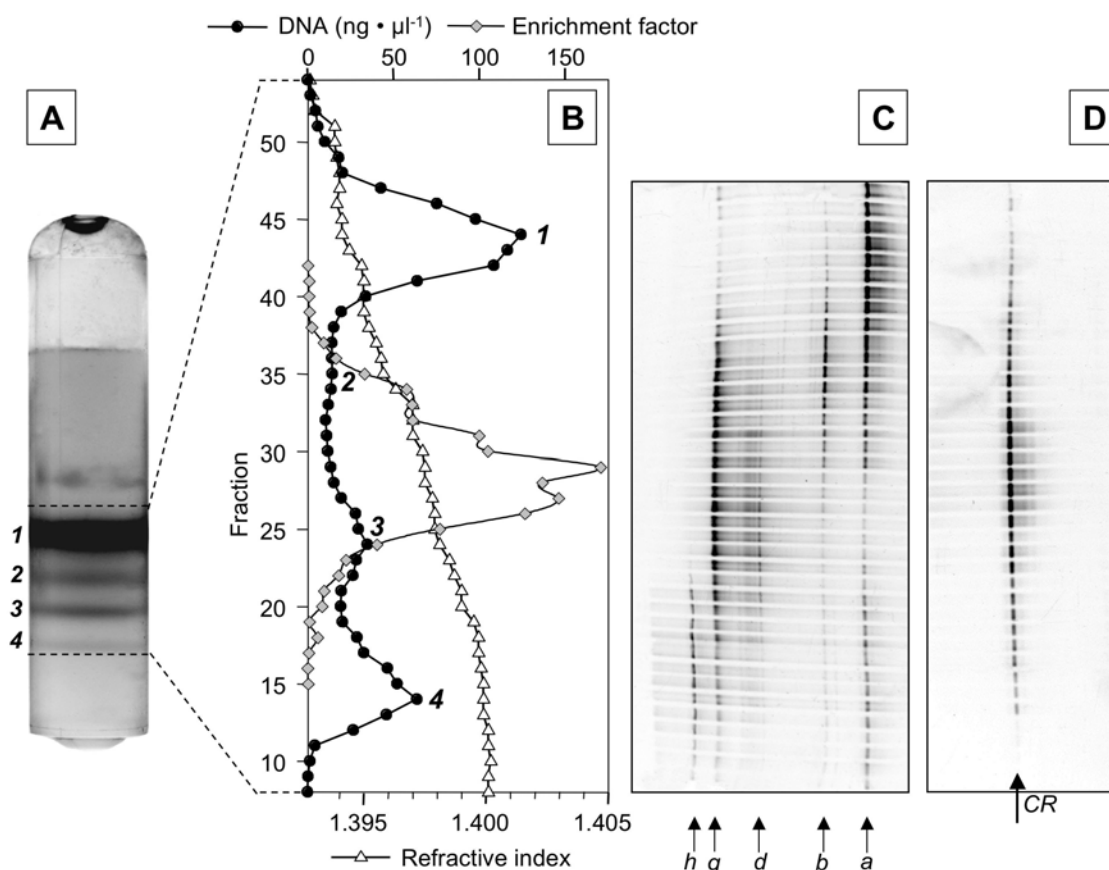


**Figure 5.** A. Separation of genomic DNA of different bacteria present in the enrichment culture of "*Chlorochromatium aggregatum*" using CsCl-bisbenzimidazole gradient density centrifugation. A negative image of DNA bands visualized by fluorescence under UV illumination is shown. B. DNA concentration (●), refractive index (Δ), and enrichment factor of the genomic DNA from the central bacterium (◆) along the CsCl-gradient. DNA concentrations are presented as moving averages (n = 3). Numbering 1 to 4 refers to the respective bands in A. C. DGGE fingerprinting of 16S rRNA gene fragments amplified from the different fractions using eubacterial primers GC341f and 907r. Melting types a to h represent DNA fragments from accompanying bacteria. D. DGGE fingerprinting of 16S rRNA gene fragments of the central bacterium amplified with primers GC341f and the specific primer CR641r. CR, melting position of the DNA fragment of the central bacterium.

### Relevance for future studies

For future enrichment and isolation attempts of the central bacterium of "*Chlorochromatium aggregatum*", it is important to resolve stimulating effects of accompanying bacteria in the enrichment culture. Interestingly, one bacterium which reacted chemotactically towards sulfide was identified as *Sulfurospirillum arsenophilum*. A similar bacterium has been detected as an essential partner in coculture with the green sulfur bacterium *Chlorobium ferrooxidans*, where it is thought to provide the green sulfur bacterium with an essential growth factor (Heising *et al.* 1999). It therefore appears possible that the accompanying bacteria fulfil similar functions in the "*Chlorochromatium aggregatum*" enrichment culture. Also, sulfur cycling between the

*Sulfurospirillum* and consortia may occur in the enrichment cultures, since the phylogenetically related sulfur-reducing *Sulfurospirillum deleyianum* DSMZ 6946<sup>T</sup> is known to grow syntrophically by sulfur cycling with green sulfur bacteria (Wolfe and Pfennig 1977). Another interesting finding is the presence of the  $\beta$ -*Proteobacterium Azonexus fungiphilus*, which is known to require 2-oxoglutarate for growth (Reinhold-Hurek and Hurek 2000), which may explain the failure to eliminate this bacterium from the enrichment cultures.

So far, only very little is known of the physiology of the central rod-shaped bacterium of phototrophic consortia. Due to the large phylogenetic distance to other known bacteria, however, physiological properties cannot be inferred from its phylogenetic position. Phototrophic consortia exhibit a chemotactic response towards 2-oxoglutarate (Fröstl and Overmann 1998, Glaeser and Overmann 2004), which is taken up by the cells (Glaeser and Overmann 2003b). Recently, the epibiont of "*C. aggregatum*" could be isolated in pure culture and was found to be incapable of using 2-oxoglutarate (Vogl *et al.* 2006). Taken together, these findings suggest that 2-oxoglutarate is utilized by the central bacterium. The specific oligonucleotide probes developed in the present work now allow to perform enrichment experiments with different substrates and to selectively and sensitively screen for the growth of the central bacterium alone. One question central to the understanding of the bacterial association in phototrophic consortia is whether the association is an obligatory one. The specific oligonucleotide probes now available permit to track the central bacterium in its natural habitat in order to determine whether it occurs in the free-living state. Finally, the CsCl-bisbenzimidazole density gradient centrifugation is suitable for the separation of genomic DNA of the central bacterium from DNA of some of the accompanying bacteria and therefore is relevant for subsequent genome sequencing efforts.

### **Acknowledgements**

We thank Martina Müller for initial help with the specific PCR amplifications. This work was supported by the *Deutsche Forschungsgemeinschaft* (grant Ov20/10-1).

## References

- Aakra A, Utaker JB, Nes IF** (1999) RFLP of rRNA genes and sequencing of the 16S-23S rDNA intergenic spacer region of ammonia oxidizing bacteria: a phylogenetic approach. *Int J Syst Bacteriol* **49**:123-130
- Alfreider A, Vogt C, Babel W** (2002) Microbial diversity in an *in situ* reactor system treating monochlorobenzene contaminated groundwater as revealed by ribosomal DNA analysis. *Syst Appl Microbiol* **25**:232-240
- Altschul SF, Madden TL, Schäffer AA, Zhang J, Zhang Z, Miller W, Lipman DJ** (1997) Gapped BLAST and PSI-BLAST: a new generation of protein database search programs. *Nucleic Acids Res* **25**:3389-3402
- Amann RI, Ludwig W, Schleifer K-H** (1995) Phylogenetic identification and *in situ* detection of individual microbial cells without cultivation. *Microbiol Rev* **59**:143-169
- Bostock-Smith CL, Searle MS** (1999) DNA minor groove recognition by *bis*-benzimidazole analogues of Hoechst 33258: insights into structure DNA affinity relationships assessed by fluorescence titration measurements. *Nucleic Acids Res.* **27**:1619-1624
- Brinkmeyer R, Knittel K, Jürgens J, Weyland H, Amann R, Helmke E** (2003) Diversity and structure of bacterial communities in arctic versus antarctic pack ice. *Appl Environ Microbiol* **69**:6610-6619
- Caldwell DE, Tiedje JM** (1974) A morphological study of anaerobic bacteria from the hypolimnia of two Michigan lakes. *Can J Microbiol* **21**:362-376
- Croome RL, Tyler PA** (1984) Enrichment and nutritional studies on "*Chlorochromatium aggregatum*" in two meromictic lakes in Tasmania. *J Gen Microbiol* **130**:2717-2723
- Felsenstein J** (1989) PHYLIP – phylogenetic interference package (version 3.2). *Cladistics* **5**:164-166
- Finneran KT, Johnsen CV, Loveley DR** (2003) *Rhodoferrax ferrireducens* sp. nov., a psychrotolerant, facultatively anaerobic bacterium that oxidizes acetate with the reduction of Fe (III). *Int J Syst Evol Microbiol* **53**: 669-673
- Fröstl JM, Overmann J** (1998) Physiology and tactic response of the phototrophic consortium "*Chlorochromatium aggregatum*". *Arch Microbiol* **169**:129-135
- Fröstl JM, Overmann J** (2000) Phylogenetic affiliation of the bacteria that constitute phototrophic consortia. *Arch Microbiol* **174**:50-58
- Fuchs BM, Wallner G, Beisker W, Schwippl I, Ludwig W, Amann R** (1998). Flow cytometric analysis of the *in situ* accessibility of *Escherichia coli* 16S rRNA for fluorescently labeled oligonucleotide probes. *Appl Environ Microbiol* **64**:4973-4982

- Fuchs BM, Glöckner FO, Wulf J, Amann R** (2000) Unlabeled helper oligonucleotides increase the *in situ* accessibility to 16S rRNA of fluorescently labeled oligonucleotide probes. *Appl Environ Microbiol* **66**:3606-3607
- Gasol JM, Jürgens K, Massana R, Celaderón-Paz JA, Pedrós-Alió C** (1995) Mass development of *Daphnia pulex* in a sulfide-rich pond (Lake Ciso). *Arch Microbiol* **132**:279-296
- Glaeser J, Baneras L, Rütters H, Overmann J** (2002) Novel bacteriochlorophyll *e* structures and species-specific variability of pigment composition in green sulfur bacteria. *Arch Microbiol* **177**:475-485
- Glaeser J, Overmann J** (2003a) Characterization and *in situ* carbon metabolism of phototrophic consortia. *Appl Environ Microbiol* **69**:3739-3750
- Glaeser J, Overmann J** (2003b) The significance of organic carbon compounds for *in situ* metabolism and chemotaxis of phototrophic consortia. *Environ Microbiol* **5**:1053-1063
- Glaeser J, Overmann J** (2004) Biogeography, evolution, and diversity of epibionts in phototrophic consortia. *Appl Environ Microbiol* **70**:4821-4830
- Glöckner FO, Zaichikov E, Belkova N, Denissova L, Pernthaler J, Pernthaler A, Amann R** (2000) Comparative 16S rRNA analysis of lake bacterioplankton reveals globally distributed phylogenetic clusters including an abundant group of actinobacteria. *Appl Environ Microbiol* **66**:5053-5065
- Heising S, Richter L, Ludwig W, Schink B** (1999) *Chlorobium ferrooxidans* sp. nov., a phototrophic green sulfur bacterium that oxidizes ferrous iron in coculture with a “*Geospirillum*” sp. strain. *Arch Microbiol* **172**:116-124
- Hiraishi A, Hoshino Y, Satoh T** (1991) *Rhodofera fermentans* gen. nov., sp. nov., a phototrophic purple nonsulfur bacterium previously referred to as the “*Rhodocyclus gelatinosus*-like” group. *Arch Microbiol* **155**:330-336
- Holben WE, Harris D** (1995) DNA-based monitoring of total bacterial community structure in environmental samples. *Mol Ecol* **4**:627-631
- Holben WE, Feris KP, Kettunen A, Apajalahti JHA** (2004) GC-fractionation enhances microbial community diversity assessment and detection of minority populations of bacteria by denaturing gradient gel electrophoresis. *Appl Environ Microbiol* **70**:2263-2270
- Irgens RL, Gosink JJ, Staley JT** (1996) *Polaromonas vacuolata* gen. nov., sp. nov., a psychrophilic, marine, gas vacuolate bacterium from Antarctica. *Int J Syst Bacteriol* **46**:822-826
- Jung DO, Achenbach LA, Karr EA, Takaichi S, Madigan MT** (2004) A gas vesiculate planktonic strain of the purple non-sulfur bacterium *Rhodofera antarcticus* isolated from Lake Fryxell, Dry Valleys, Antarctica. *Arch Microbiol* **182**:236-243

- Lane DJ** (1991) 16S/23S rRNA sequencing. In: Stackebrandt, E., and M. Goodfellow (eds.) *Nucleic acid techniques in bacterial systematics*. Wiley, Chichester. pp. 115-175
- Ludwig W, Strunk O, Westram R, Richter L, Meier H, Yadhukumar A, Buchner A, Lai T, Steppi S, Jobb G, Förster W, Brettske I, Gerber S, Ginhart AW, Gross O, Grumann S, Hermann S, Jost R, König A, Liss T, Lüßmann R, May M, Nonhoff B, Reichel B, Strehlow R, Stamatakis A, Stuckmann N, Vilbig A, Lenke M, Ludwig T, Bode A, Schleifer K-H** (2004) ARB: a software environment for sequence data. *Nucleic Acids Res* **32**:1363-1371
- Muyzer G, De Waal EC, Uitterlinden AG** (1993) Profiling of complex microbial populations by denaturing gradient gel electrophoresis of polymerase chain reaction-amplified genes coding for 16S rRNA. *Appl Environ Microbiol* **59**:695-700
- Muyzer G, Hottenträger S, Teske A, Waver C** (1995) Denaturing gradient gel electrophoresis of PCR-amplified 16S rDNA – a new molecular approach to analyse the genetic diversity of mixed microbial communities. In: Akkermans, A.D.L., J.D. van Elsas, F.J de Bruijn (eds). *Molecular microbial ecology manual*, 2<sup>nd</sup> edn., Kluwer, Dordrecht, pp 3.4.4.1.-3.4.4.22
- Nüsslein K, Tiedje JM** (1998) Characterization of the dominant and rare members of a young Hawaiian soil bacterial community with small-subunit ribosomal DNA amplified from DNA fractionated on the basis of its guanine and cytosine composition. *Appl Environ Microbiol* **64**:1283-1289
- Overmann J** (2001a) Green sulfur bacteria. In: Garrity GM (ed.) *Bergey's manual of systematic bacteriology*, Vol 1. Williams and Wilkins, Baltimore, pp. 601-623
- Overmann J** (2001b) Phototrophic consortia: A tight cooperation between non-related eubacteria. In: Seckbach J (ed.) *Symbiosis*, Kluwer, Dordrecht, Boston, London. pp. 289-255
- Overmann J, Coolen MJL, Tuschak C** (1999) Specific detection of different phylogenetic groups of chemocline bacteria based on PCR and denaturing gradient gel electrophoresis of 16S rRNA gene fragments. *Arch Microbiol* **172**:83-94
- Overmann J, Fischer U, Pfennig N** (1992) A new purple sulfur bacterium from saline littoral sediments, *Thiorhodovibrio winogradskyi* gen. nov. and sp. nov. *Arch Microbiol* **157**:329-335
- Overmann J, Schubert K** (2002) Phototrophic consortia: model systems for symbiotic interrelations between prokaryotes. *Arch. Microbiol.* **177**:201-208
- Overmann J, Tuschak C** (1997) Phylogeny and molecular fingerprinting of green sulfur bacteria. *Arch Microbiol* **167**:302-309
- Overmann J, Tuschak C, Fröstl JM** (1998) The ecological niche of the consortium “*Pelochromatium roseum*”. *Arch Microbiol* **169**:120-128

- Pfennig N** (1978) *Rhodocyclus purpureus* gen. nov., a ring-shaped, vitamin B<sub>12</sub>-requiring member of the family *Rhodospirillaceae*. *Int J Syst Bact* **28**:283-288
- Reinhold-Hurek B, Hurek T** (2000) Reassessment of the taxonomic structure of the diazotrophic genus *Azoarcus sensu lato* and description of three new genera and new species, *Azovibrio restrictus* gen. nov., sp. nov., *Azospira oryzae* gen. nov., sp. nov. and *Azonexus fungiphilus* gen. nov., sp. nov. *Int J Syst Evol Microbiol* **50**:649-659
- Sanger F, Air GM, Barrell BG, Brown NL, Coulson AR, Fiddes CA, Hutchison CA, Slocombe PM, Smith M** (1977) Nucleotide sequence of bacteriophage phi X174 DNA. *Nature* **265**:687-695
- Schink B** (1991) Syntrophism among prokaryotes. In: Balows A, Trüper HG, Dworkin M, Harder W, Schleifer K-H (eds.): *The Prokaryotes*. 2nd edition. Springer Verlag, New York, Berlin, Heidelberg. pp. 276-299
- Siefert E, Pfennig N** (1984) Convenient method to prepare neutral sulfide solution for cultivation of phototrophic sulfur bacteria. *Arch Microbiol* **139**:100-101
- Straub KL, Buchholz-Cleven BEE** (1998) Enumeration and detection of anaerobic ferrous iron-oxidizing, nitrate-reducing bacteria from diverse European sediments. *Appl Environ Microbiol* **64**:4846-4856
- Tuschak C, Glaeser J, Overmann J** (1999) Specific detection of green sulfur bacteria by *in situ* hybridization with a fluorescently labeled oligonucleotide probe. *Arch Microbiol* **171**:265-272
- Vinograd J, Hearst JE** (1962) Equilibrium sedimentation of macromolecules and viruses in a density gradient. *Fortschr. Chem Org Naturst* **20**:373-422
- Vogl K, Glaeser J, Pfannes KR, Wanner G, Overmann J** (2006) *Chlorobium chlorochromatii* sp. nov., a symbiotic green sulfur bacterium isolated from the phototrophic consortium "*Chlorochromatium aggregatum*". *Arch Microbiol* **185**:363-372
- Watanabe K, Kodama W, Syutsupo K, Harayama S** (2000) Molecular characterization of bacterial populations in petroleum-contaminated groundwater discharged from underground crude oil storage cavities. *Appl Environ Microbiol* **66**:4803-4809
- Widdel F, Kohring GW, Mayer F** (1983) Studies on dissimilatory sulfate-reducing bacteria that decompose fatty acids. III. Characterization of the filamentous gliding *Desulfonema limicola* gen. nov., sp. nov., and *Desulfonema magnum* sp. nov. *Arch Microbiol* **134**:286-294
- Willems A, DeLey J, Gillis M, Kersters K** (1991) *Comamonadaceae*, a new family encompassing the *Acidovorans* rRNA complex, including *Variovorax paradoxus* gen. nov., comb. nov., for *Alcaligenes paradoxus* (Davis 1969). *Int J Syst Bacteriol* **41**:445-450
- Wolfe RS, Pfennig N** (1977) Reduction of sulfur by *Spirillum* 5175 and syntrophism with *Chlorobium*. *Appl Environ Microbiol* **33**:427-433



# **Heterotrophic symbionts of phototrophic consortia: members of a novel diverse cluster of *Betaproteobacteria* characterised by a tandem *rrn* operon structure**

Kristina R. Pfannes, Kajetan Vogl and Jörg Overmann\*

Bereich Mikrobiologie, Department Biologie I, Ludwig-Maximilians-Universität München,  
Maria-Ward-Str. 1a, D-80638 München, Germany.

**Keywords:** "*Chlorochromatium aggregatum*", microbial diversity, microdiversity,  
phototrophic consortia, *rrn* operon, 16S rRNA, symbiosis, tandem *rrn* operon

**Running head:** *Betaproteobacteria* with a tandem *rrn* operon structure

\*Corresponding author. Tel: +49-89-2180-6123, Fax: +49-89-2180-6125.

Email: [j.overmann@lrz.uni-muenchen.de](mailto:j.overmann@lrz.uni-muenchen.de)

## Summary

Phototrophic consortia represent the most highly developed type of interspecific association of bacteria and consist of green sulfur bacterial epibionts attached around a central colourless rod-shaped bacterium. Based on 16S rRNA gene sequencing, the central bacterium of the consortium "*Chlorochromatium aggregatum*" was recently shown to represent a novel and phylogenetically isolated lineage of the *Comamonadaceae* within the  $\beta$ -subgroup of the *Proteobacteria*. To date, 19 types of phototrophic consortia are distinguished based on the different 16S rRNA gene sequences of their epibionts, but the diversity and phylogenetic relationships of the heterotrophic partner bacteria are still unknown. We developed an approach based on the specific *rrn* (ribosomal RNA) operon structure of the central bacterium of "*C. aggregatum*" to recover 16S rRNA gene sequences of other central bacteria and their close relatives from natural consortia populations. Genomic DNA of the central bacterium of "*C. aggregatum*" was first enriched several hundred fold by employing a selective method for growth of consortia in a monolayer biofilm followed by a purification of the genome of the central bacterium by cesium chloride-bisbenzimidazole equilibrium density gradient centrifugation. A combination of inverse PCR, cloning and sequencing revealed that two *rrn* operons of the central bacterium are arranged in a tandem fashion and are separated by an unusually short intergenic region of 195 base pairs. This rare gene order was exploited to screen various natural microbial communities by PCR. We discovered a diverse and previously unknown subgroup of *Betaproteobacteria* in the chemoclines of freshwater lakes. This group was absent in other freshwater and soil samples. All the 16S rRNA gene sequences recovered are related to that of the central bacterium of "*C. aggregatum*". Fluorescence *in situ* hybridization indicated that two of these sequences originated from central bacteria of different phototrophic consortia, which, however, were only distantly related to the central bacterium of "*C. aggregatum*". Based on a detailed phylogenetic analysis, these central bacterial symbionts of phototrophic consortia have a polyphyletic origin.

## Introduction

Phototrophic consortia were first described one century ago (Lauterborn, 1906) and subsequently have been detected in many freshwater lakes worldwide (Caldwell and Tiedje, 1974; Croome and Tyler, 1984; Gorlenko 1988; Overmann and Tilzer, 1989; Gasol *et al.*, 1995; Overmann *et al.*, 1998; Glaeser and Overmann, 2004). Phototrophic consortia represent symbiotic associations between a colourless chemotrophic central bacterium surrounded by a fixed number of green sulfur bacteria, so-called epibionts (Pfennig, 1980). The epibionts represent unique phylotypes among green sulfur bacteria and so far have only been observed in the associated state (Fröstl and Overmann, 2000; Glaeser and Overmann, 2004).

Recently, the epibiont of the phototrophic consortium "*Chlorochromatium aggregatum*" could be isolated in pure culture, which allowed the detailed investigation of its physiological and molecular properties (Vogl *et al.*, 2006) and the sequencing of its genome ([http://genome.jgi-psf.org/draft\\_microbes/chlag/chlag.home.html](http://genome.jgi-psf.org/draft_microbes/chlag/chlag.home.html)). A combination of micromanipulation and 16S rRNA gene analyses of natural populations of phototrophic consortia uncovered an unexpected large phylogenetic diversity among the green sulfur bacterial epibionts (Glaeser and Overmann, 2004). As a result, 19 different types of phototrophic consortia are recognized to date. A detailed phylogenetic analysis revealed that epibionts are not monophyletic, indicating that the ability to form symbiotic associations either arose independently from different ancestors, or was present in a common ancestor prior to the radiation of the green sulfur bacteria and the transition to the free-living state in the independent lineages (Glaeser and Overmann, 2004).

In contrast to the epibionts, very little is known of the phylogeny and molecular biology of the central bacterium. This has to be attributed to the fact that this bacterium could not be cultured separately from its epibionts and that it usually represents less than 0.1% of all cells in typical enrichment cultures (Kanzler *et al.*, 2005). The central bacterium is colourless and is assumed to grow chemoheterotrophically. Based on indirect evidence obtained by microautoradiography, it is capable of assimilating 2-oxoglutarate (Glaeser and Overmann, 2003). Fluorescence *in situ* hybridization (FISH) with group-specific oligonucleotides demonstrated that the central bacteria of different consortia belong to the  $\beta$ -subgroup of the *Proteobacteria* (Fröstl and Overmann, 2000). Recently, the 16S rRNA gene of the central bacterium of "*C. aggregatum*" was sequenced (Kanzler *et al.*, 2005). Sequence analysis confirmed its affiliation with the *Betaproteobacteria* and revealed that it represents an isolated phylogenetic lineage within the family *Comamonadaceae*. So far, nothing is known of the

diversity of central bacteria in the different consortia. It is therefore still unknown whether different types of heterotrophic partner bacteria exist in phototrophic consortia and, if the latter is the case, whether the different heterotrophic partners are phylogenetically closely related.

Since central bacteria of phototrophic consortia constitute only a minor fraction of the cells in natural bacterial communities, highly specific molecular methods are required to selectively retrieve their 16S rRNA gene sequences. In search for flanking DNA sequences which would allow the specific amplification of the 16S rRNA genes of the central bacteria, a method for large-scale enrichment and purification of genomic DNA of the central bacterium of "*C. aggregatum*" was established and applied to analyse the structure of its rRNA operons and the genome organisation in its vicinity. Our study of the genome of the central bacterium of "*C. aggregatum*" revealed a tandem operon organisation, which so far has been observed only rarely among prokaryotes. The sequence obtained from the central bacterium of "*C. aggregatum*" is unique due to the extremely small size of the intergenic region between both *rrn* operons. Exploiting this unusual operon structure in a culture-independent PCR approach enabled us to detect a highly diverse and novel subgroup of aquatic *Betaproteobacteria*, and to recover and analyse two novel phylotypes of central bacteria of phototrophic consortia.

## Results and Discussion

### Isolation and purification of genomic DNA of the central bacterium of "*C. aggregatum*"

In the enrichment cultures of "*C. aggregatum*" grown under standard laboratory conditions, the cells of the central bacterium are accompanied by a larger number of free epibionts and additional chemotrophic bacteria and thus typically amount to only  $\leq 0.1\%$  of all cells present (Kanzler *et al.*, 2005) (Fig. 1A). Previously, the chemotactic behaviour of intact consortia towards sulfide has been used to enrich them for subsequent PCR amplifications (Kanzler *et al.*, 2005). However, these chemotaxis enrichments yielded numbers of consortia far too small for the preparation of genomic DNA of the central bacterium.

In the present study, we established a method to selectively grow large numbers of intact consortia in a biofilm on the walls of large (10 l) culture flasks. At homogenous illumination, consortia first grew in the suspended state until reaching an optical density (OD<sub>650</sub>) of 1.0, after which they accumulated at the wall of the culture bottles due to the severe self-shading in the culture liquid and the resulting scotophobic response of the consortia (Fig. 1B). Within four weeks of cultivation, a dense monolayer biofilm had formed which consisted mostly of "*C. aggregatum*" (Fig. 1C). After extraction, the genomic DNA of the central bacterium was separated from that of the epibiont by the previously established CsCl-bisbenzimidazole equilibrium density centrifugation (Kanzler *et al.*, 2005). The overall efficiency of enrichment of the combined method was compared to that of the chemotaxis method or the density gradient centrifugation method alone, by employing denaturing gradient gel electrophoresis (DGGE) fingerprinting of 16S rRNA gene fragments (Fig. 2). Our new combined approach is clearly superior to all previously used techniques and allows an enrichment of genomic DNA from the central bacterium by several hundred fold as estimated from the corresponding band intensities in Fig. 2.

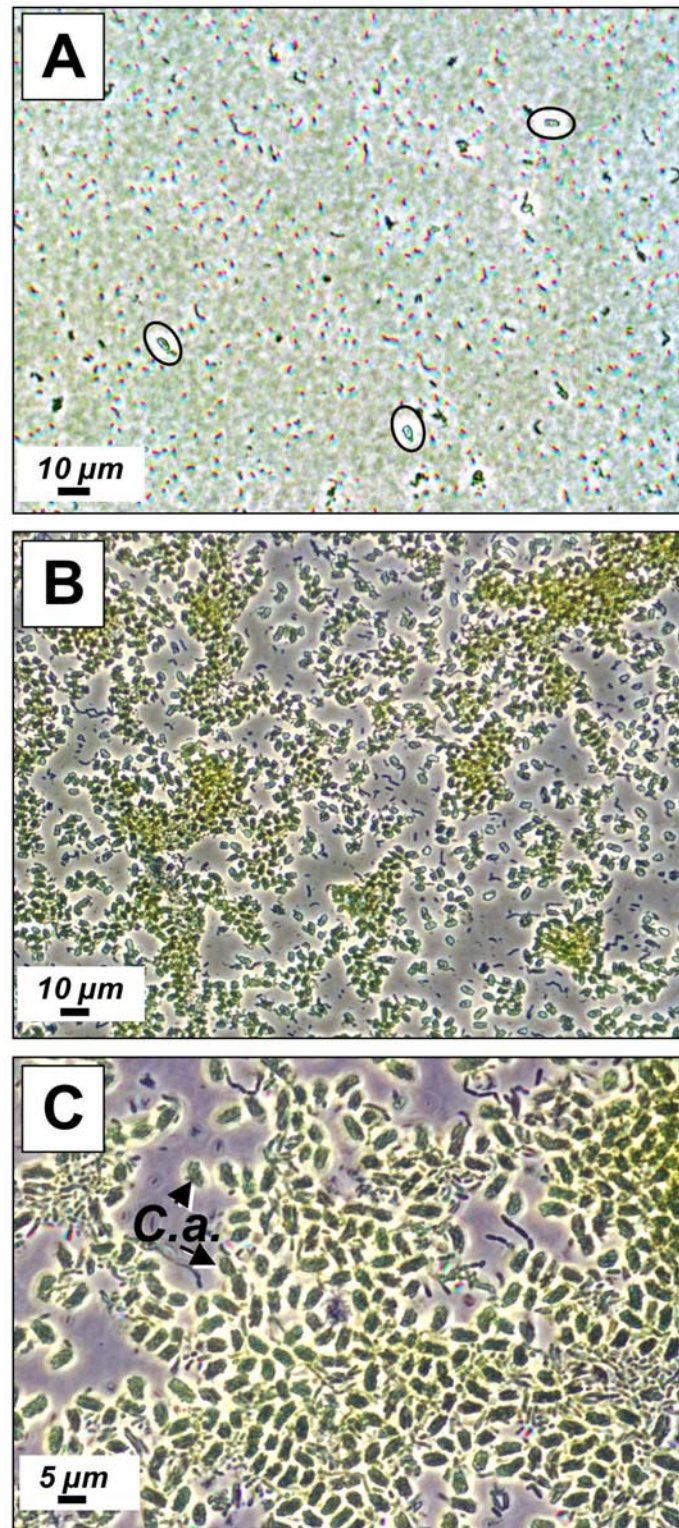


**Figure 1.** **A.** Phase contrast micrograph of a typical enrichment culture of "*Chlorochromatium aggregatum*". Intact consortia are denoted by circles. **B.** Accumulation of "*C. aggregatum*" forming a monolayer biofilm at the wall of 10 l bottles after 4 weeks of incubation under light-limited conditions. **C.** Biofilm at higher magnification. The number of consortia is greatly increased relative to the number of accompanying free-living bacteria. *C.a.*, intact "*C. aggregatum*" consortia.

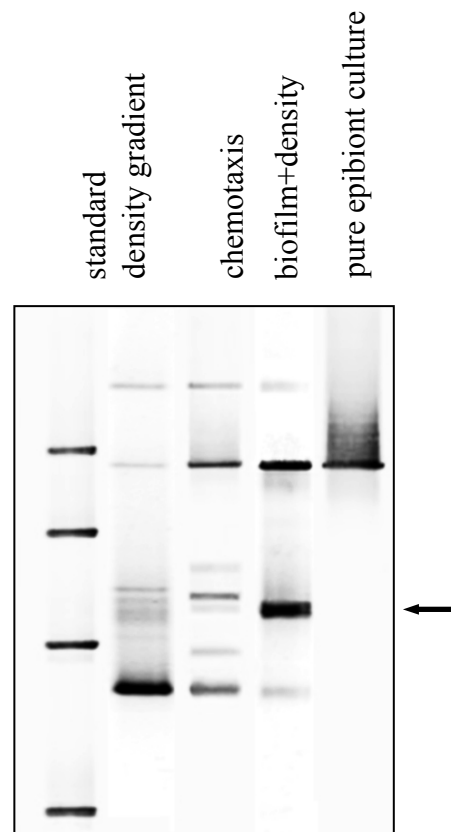


**Figure 2.** Different methods for the enrichment and purification of genomic DNA of the central bacterium of "*C. aggregatum*", as analysed by DGGE-fingerprinting of 16S rDNA gene fragments after amplification with primers GC341f and 907r. Enrichments were conducted by CsCl-bisbenzimidazole density gradient centrifugation alone, by chemotaxis, and by growth of intact consortia in biofilms followed by CsCl-bisbenzimidazole density gradient centrifugation (see text). The arrow indicates the specific melting position of the fragment from the central bacterium of "*C. aggregatum*". The fingerprint of a pure culture of the epibiont *Chlorobium chlorochromatii* CaD is shown for comparison (rightmost lane).

### Organisation of *rrn* operons in the central bacterium of "*C. aggregatum*"

The purified genomic DNA of the central bacterium of "*C. aggregatum*" was used to analyse the regions flanking its known 16S rRNA gene sequence. Inverse PCR amplification of the region located upstream of the 5'-end of the 16S rRNA gene yielded a 489 bp-long DNA fragment. As expected, the 3'-end of the amplified fragment represented the first 204 bp of the previously determined 16S rRNA (*rrs*) gene of the central bacterium (Kanzler *et al.*, 2005). However, sequence analysis of the upstream portion of the fragment revealed that the first 90 bp were part of a 5S rRNA (*rrf*) gene which was separated from the downstream *rrs* gene by a short 195 bp spacer sequence (Fig. 3). The spacer sequence did not contain start or stop codons and did not show homology to any open reading frame in the GenBank database. In order to assess whether the *rrs* gene of the central bacterium is followed by a 23S rRNA gene (*rrl*) as in the vast majority

of known bacterial *rrn* operons, the corresponding region was amplified with primers CR-1282f and  $\beta$ -23S-1027r (Supplementary table 1) and sequenced. Based on this analysis, the *rrs* gene of the central bacterium is 1533 bp long and is followed by a 662 bp-long internal transcribed spacer (ITS)1 region and the *rrl* gene (Fig. 3). The ITS1 region was found to contain two tRNA genes, tRNA<sup>Ile</sup> and tRNA<sup>Ala</sup>. The presence of tRNA genes within the ITS1 spacer regions is a common, yet not universal, feature of rRNA operons (Krawiec and Riley, 1990).

The canonical *rrn*-operon of *Bacteria* consists of genes coding structural 16S rRNA (*rrs*), 23S rRNA (*rrl*) and 5S rRNA (*rrf*) in the order *rrs* - ITS1 - *rrl* - ITS2 - *rrf* (Krawiec and Riley, 1990; Srivastava and Schlessinger, 1990). Within the operon, the rRNA genes are separated by internal transcribed spacers which usually contain the genes for one or two tRNAs. Our results suggested a tandem organisation of two *rrn* operons (*rrnA* and *rrnB*; Fig. 3) separated by only 195 bp.

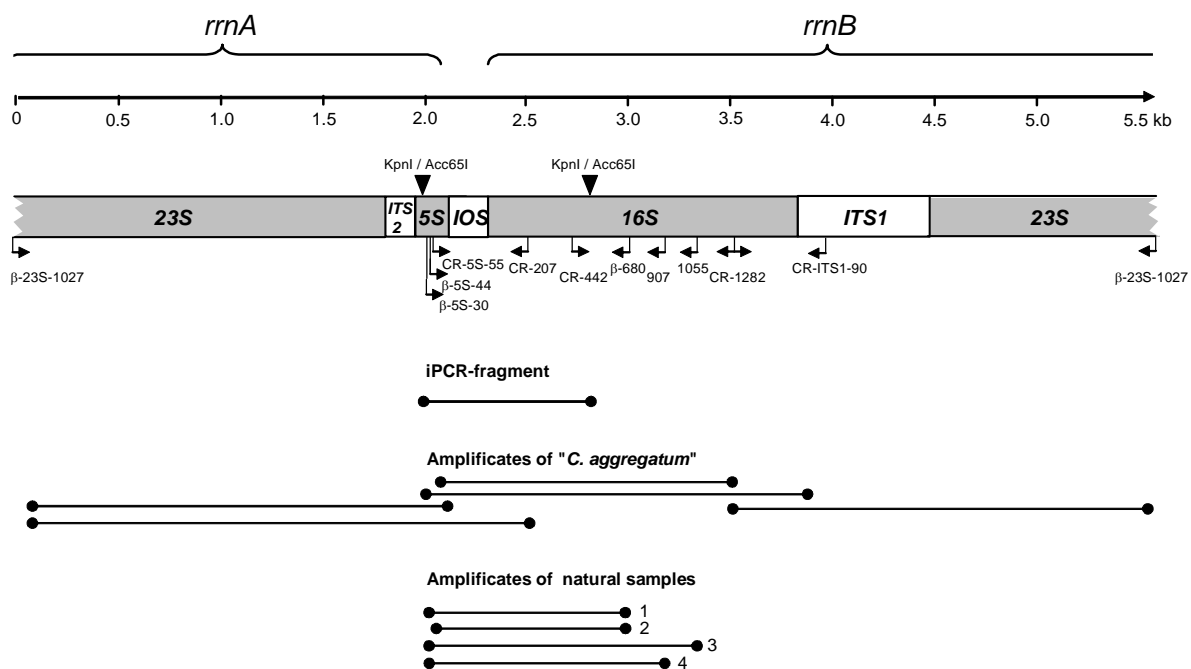


**Figure 3.** Gene order and lengths of ribosomal RNA genes in the central bacterium of "*C. aggregatum*". The KpnI / Acc65I restriction sites for the generation of the iPCR fragment are indicated. Binding sites of the primers (compare Supplementary table 1) used for overlapping amplification and sequencing of the central bacterium of "*C. aggregatum*" and for the retrieval of *rrn* sequences from natural communities are indicated.

This unusually close tandem arrangement of two *rrn* operons was confirmed by several independent tests. First, the inverse PCR was repeated with an isoschizomeric enzyme (Acc65I). After cloning and sequencing of the respective PCR product, the sequence completely matched

the previous amplicon. Second, a fragment spanning *rrfA*, the interoperon sequence and the beginning of the *rrsB* gene could be amplified using a primer targeting the novel 5S rRNA gene sequence of the central bacterium (CR-5S-55f) and a reverse primer specific for its 16S rRNA gene (CR-1282r) (amplification products indicated in Fig. 3). Third, the region between the *rrlA* and the *rrsB* genes could be amplified with the primer pair  $\beta$ -23S-1027f and CR-207r (Fig. 3). Sequencing of all amplicates obtained yielded an identical sequence of the 195 bp-long intergenic region.

All of the above results are in line with the gene order *rrlA* - *rrfA* - *rrsB*. The overall sequence information obtained in the present study spans a total of 5,460 bp of the tandem *rrn* operon of the central bacterium of "*C. aggregatum*" (Fig. 3). The *rrlA* gene is separated by a 93 bp ITS2 from the 116 bp long *rrfA* gene. So far, there are no reports of the presence of any tRNA gene in the ITS2 of any bacterium (Chen *et al.*, 2000). Correspondingly, no tRNA-like structures were identified within the ITS2. The 195 bp-long interoperon spacer (IOS) is followed by a 1,533 bp long *rrs*. An ITS1 of 662 bp and a *rml* gene follow. The available information indicates a canonical order *rrs* - ITS1 - *rml* - ITS2 - *rrf* in the central bacterium of "*C. aggregatum*" as in most other bacteria investigated (Srivastava and Schlessinger, 1990). Comparison of the sequences of the more than 30 clones obtained from the central bacterium of "*C. aggregatum*" during this part of our study showed no sequence ambiguity. We therefore conclude that the sequence divergence of the *rrn* operons in this bacterium must be very small. Similarly to the central bacterium, the genome of the phylogenetically closely related *Rhodoferrax ferrireducens* DSMZ15236<sup>T</sup> harbours *rrnA* and *rrnB* operons with identical sequences (National Center for Biotechnology Information (NCBI) Microbial Genome database; <http://www.ncbi.nlm.nih.gov/genomes/MICROBES/Complete.html>) which are, however, separated by a 350 bp-long intergenic region (Table 1)

Because of the unusual organisation of the *rrn* operon in the central bacterium of "*C. aggregatum*", all available rRNA operon sequences of the NCBI Microbial Genome database for eubacterial genomes (404 entries; as of January, 2007) were systematically examined for a tandem organisation of their *rrn* operons. This revealed that only 24 (5.9%) of the sequenced genomes harbour complete *rrn* operons in a tandem arrangement and with an interoperon spacer of  $\leq 1000$  bp (Table 1). Tandem *rrn* operons were found in the two Gram-positive phyla *Actinobacteria* and *Firmicutes* and in 4 classes of the phylum *Proteobacteria*, but occurred most frequently among the *Firmicutes* (10.5% of all genomes) and the *Gammaproteobacteria* (10% of all genomes) (Table 1).

**Table 1.** Overview about all sequenced bacteria with tandem *rrn* operons separated by an interoperon spacer (IOS) < 1,000 bp

Phylum/Class and Strain <sup>a</sup>	IOS (bp) <sup>b</sup>	Total number of <i>rrn</i> operons
<b>Actinobacteria</b> (1 of 36 genomes)		
<i>Bifidobacterium longum</i> NCC2705	868	4
<b>Firmicutes</b> (10 of 95 genomes)		
<i>Bacillus subtilis</i> subsp. <i>subtilis</i> str. 190	190	10
<i>Clostridium acetobutylicum</i> ATCC 824 <sup>T</sup>	354, 354, 354, 354	11
<i>Clostridium tetani</i> E88	350	6
<i>Lactobacillus johnsonii</i> NCC 533	381	6
<i>Lactobacillus gasserii</i> ATCC 33323 <sup>T</sup>	409	6
<i>Lactobacillus sakei</i> subsp. <i>sakei</i> 23K	497	7
<i>Staphylococcus aureus</i> subsp. <i>aureus</i> COL	212	6
<i>Staphylococcus aureus</i> subsp. <i>aureus</i> MW2	212	6
<i>Staphylococcus epidermidis</i> RP62A	229	6
<i>Staphylococcus saprophyticus</i> subsp. <i>saprophyticus</i> ATCC 15305 <sup>T</sup>	296	6
<b>α-Proteobacteria</b> (1 of 54 genomes)		
<i>Novosphingobium aromaticivorans</i> DSMZ 12444 <sup>T</sup>	533, 533	3
<b>β-Proteobacteria</b> (1 of 31 genomes)		
<i>Rhodospirillum rubrum</i> DSMZ 15236 <sup>T</sup>	350	2
<b>γ-Proteobacteria</b> (10 of 100 genomes)		
<i>Colwellia psychrerythraea</i> 34H	593, 546, 539	9
<i>Photobacterium profundum</i> SS9	419, 419, 409, 418, 419	14
<i>Pseudomonas putida</i> KT2440	463	7
<i>Psychrobacter arcticus</i> 273-4 <sup>T</sup>	773	4
<i>Psychrobacter cryohalolentis</i> K5 <sup>T</sup>	758	4
<i>Vibrio cholerae</i> O1 biovar <i>eltor</i> str. N16961	367	8
<i>Vibrio fischeri</i> ES114	404, 404, 405, 404, 404	11
<i>Vibrio parahaemolyticus</i> RIMD 2210633	319	11
<i>Vibrio vulnificus</i> CMCP6	330	8
<i>Vibrio vulnificus</i> YJ016	336	9
<b>δ-Proteobacteria</b> (1 of 14 genomes)		
<i>Pelobacter carbinolicus</i> DSMZ 2380 <sup>T</sup>	390	2

<sup>a</sup> All completely sequenced eubacterial genomes within the NCBI database were considered (404 entries; as of January 01, 2007). Numbers in parenthesis give number of genomes with tandem operons of total number of genome sequences of each phylum or class.

<sup>b</sup> Multiple numbers indicate the presence of different pairs of tandem operons with the exception of *Novosphingobium aromaticivorans* DSMZ 12444<sup>T</sup>. In the latter, the three existing *rrn* operons all occur in close vicinity to each other.

Most notably, of all 31 available genomes of *Betaproteobacteria*, only the closest relative of the central bacterium, *Rhodoferax ferrireducens* DSMZ15236<sup>T</sup>, exhibits a tandem arrangement of *rrn* operons. None of the genomes of all other 16 phyla which are currently represented in the NCBI Microbial Genome database contained closely spaced tandem *rrn* operons.

In conclusion, only few of the known bacterial genome sequences match that of the central bacterium of "*C. aggregatum*" with respect to its *rrn* operon organisation. Within this group, the central bacterium of "*C. aggregatum*" exhibits the shortest interoperon spacer, together with *Bacillus subtilis* subsp. *subtilis* strain 190.

### **Occurrence and phylogenetic diversity of tandem operons in chemocline microbial communities**

The fact that the tandem *rrn* operon structure was found only once among the *Betaproteobacteria* and particularly in the closest relative of the central bacterium of "*C. aggregatum*" suggested that tandem *rrn* operons may represent a specific feature of the chemotrophic symbiont of phototrophic consortia and its relatives. These relatives potentially also include central bacteria of other phototrophic consortia. We therefore developed a PCR-based method to specifically recover fragments of tandem *rrn* operons from complex natural communities known to harbour different types of phototrophic consortia. To this end, two primers ( $\beta$ -5S-30f and  $\beta$ -5S-44f; Supplementary table 1) which target the 5S rDNA gene of all known *Betaproteobacteria* were designed based on an alignment of all available betaproteobacterial *rrf* sequences in the databases. These primers were then combined with two eubacterial 16S primers (907r or 1055r) or the betaproteobacterial primer  $\beta$ -680r. Initially, four different primer combinations ( $\beta$ -5S-30f/ $\beta$ -680r,  $\beta$ -5S-44f/ $\beta$ -680r,  $\beta$ -5S-30f/907r, and  $\beta$ -5S-30f/1055r) were tested, using DNA extracts from the chemocline of one lake (Lake Dagow). This revealed that betaproteobacterial sequences encompassing the *rrnA-rrnB* interoperon region could be recovered reproducibly if the two primer pairs  $\beta$ -5S-30f/907r and  $\beta$ -5S-30f/1055r were employed.

The two primer pairs were subsequently employed to screen eight different aquatic and soil bacterial communities for the presence of *Betaproteobacteria* with tandem rRNA operons. The sampling sites comprised six freshwater lakes (Dagowsee, Lake Cisó, Jones Lake, Silver Lake, Starnberger See, Walchensee), two different soils (Jochberg and Staudach) and one lake sediment (Walchensee). Four of these, Lake Dagow, Lake Cisó, Jones and Silver Lake represent typical oxic-anoxically stratified environments, and are known to harbour different types of

phototrophic consortia (Glaeser and Overmann, 2004). Indeed, amplicons were exclusively obtained from chemocline environments whereas all other samples did not yield any amplification product independently of the primer combination used. In the case of Lake Cisó, amplification products of different lengths (between 1300 and 1500 bp) were obtained.

All amplification products were cloned, the clones subjected to a restriction digest analysis and representative clones of each restriction type were sequenced. This first limited sequence analyses yielded different 16S rRNA gene sequences for several of the individual restriction types, thereby indicating the presence of an unexpected diversity of bacteria with a tandem *rrn* operon structure in the chemocline microbial communities of the four stratified lakes. Clones from Lake Cisó exhibited the largest variation in size due to lengths of interoperon spacers of 333 bp and 466 bp, which is commensurate with the larger length variation observed for the amplification products from this lake. Our first screen yielded the highest number of different sequence types for the chemocline microbial community from Lake Dagow. In order to evaluate the diversity of bacteria with a tandem *rrn* operon structure in more detail, the chemocline of Lake Dagow was sampled again in the year 2006 and a larger clone library of *rrn* sequences after amplification with primer pairs  $\beta$ -5S-30f/907r and  $\beta$ -5S-30f/1055r was analysed. From this sample, 62 different clones yielded correct inserts and nonchimeric sequences. All 62 sequences were found to contain *rrf* and *rrs* genes separated by a short spacer.

The entire set of 16S rRNA gene sequences generated in the present study was subjected to detailed phylogenetic analyses, by employing maximum likelihood, maximum parsimony and distance-based algorithms. A comparison of the topology of the three different phylogenetic trees demonstrated that the branching patterns of many sequences, or groups of sequences, varied considerably between the trees. In addition, these variable branches had a very low bootstrap support independent of the phylogenetic method employed. Because of this uncertainty, a consensus phylogenetic tree (Fig. 4) was calculated employing the majority rule algorithm as implemented in the PHYLIP program package (Felsenstein, 1989). Our analyses unequivocally demonstrated that all 74 individual 16S rRNA gene sequences which had been recovered from the different chemocline bacterial communities in the different years are closely related to each other and form a novel, distinct subcluster within the phylum *Betaproteobacteria* (Fig. 4). This novel subcluster also encompassed the sequence of the central bacterium of "*C. aggregatum*" (Fig. 4). *Rhodoferax ferrireducens* DSMZ 15236<sup>T</sup>, one of the closest cultivated relatives of the novel subcluster is characterized by a tandem *rrn* operon, whereas the genome of the more distantly related *Polaromonas vacuolata* DSMZ 15660<sup>T</sup> contains only a single *rrn* operon (<http://www.ncbi.nlm.nih.gov/genomes/MICROBES/Complete.html>).



**Figure 4.** Phylogenetic analysis of all 16S rRNA gene sequences obtained in the present study for *Betaproteobacteria* exhibiting a tandem *rrn* operon structure, and for their closest relatives. The consensus tree depicted was constructed based on individual maximum likelihood, maximum parsimony and distance-based phylogenetic trees employing the majority rule as implemented in the CONSENSE program of the PHYLIP package (see Material and Methods). Percentages at nodes indicate bootstrap values out of 100 resamplings, as determined for all trees. Bootstrap values for maximum likelihood, maximum parsimony and distance-based trees differed by no more than 1%, therefore means of the three methods are given. Only values above 50% are shown. The phylogenetic position of the central bacteria (CB) of three different phototrophic consortia (including a novel type of "*Chlorochromatium*", see text) are highlighted. Bar indicates 5% fixed point mutations per nucleotide base.

Although information on the genome sequences of other members of this group is so far missing, it appears likely that other cultivated relatives of the novel betaproteobacterial subcluster similarly bear tandem *rrn* operons in their genome. *Rhodoferrax ferrireducens* DSMZ 15236<sup>T</sup> possesses two *rrn* operons with identical nucleotide sequences. Furthermore, a close arrangement of three *rrn* operons was only observed in one single case out of the 404 genomes available in the database (*Novosphingobium aromaticivorans* DSMZ 12444<sup>T</sup>; Table 1).

Among the 62 clones retrieved from the chemocline of Lake Dagow in 2006, 39 clones were found to be unique, whereas one phylotype occurred 12 times, another one 3 times and four phylotypes were found twice among the clone library (Fig. 4). We used rarefaction (Holland, 2003) to elucidate how well our clone library represented the total diversity of chemocline *Betaproteobacteria* harbouring tandem *rrn* operons. This analysis revealed that only a small fraction of the total sequence diversity of this group had been recovered as the rarefaction curve was far from saturation (Fig. 5).

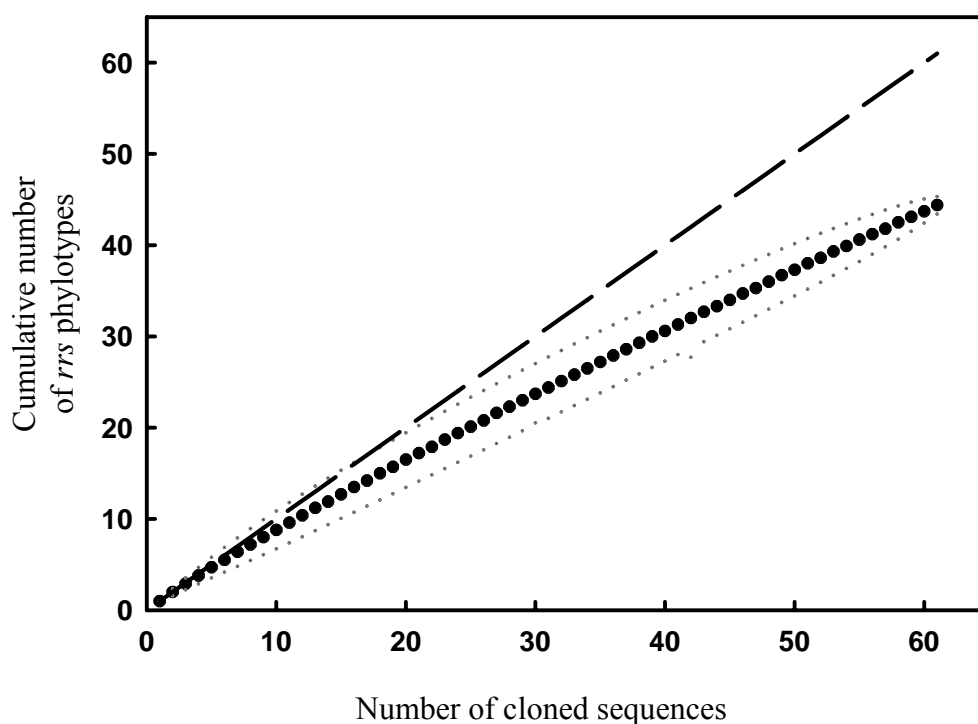


**Figure 5.** Rarefaction curve of 63 *rrs*-sequence types originating from tandem *rrn* operon fragments as cloned from a chemocline water sample of Lake Dagow in the year 2006. Dotted lines represent the upper and the lower 95% confidence intervals. For comparison, the dashed line indicates a rarefaction curve for a set of unique phylotypes.

Clone library depth was analysed further employing the EstimateS software package (Version 8.0.0) (Colwell, 2005). Employing the nonparametric Chao-1 estimator, we calculated the total diversity of *Betaproteobacteria* with tandem *rrn* operon organisation in the chemocline of Lake Dagow to amount to 235 species. Since the Chao-1 richness estimator tends to overestimate species richness in small samples, we also used the ACE estimator, which is based on the frequency of species with 10 or fewer individuals in the sample (Chao *et al.* 1993). Applying the ACE estimator, we arrived at a diversity value of 193 individual sequence types. Due to the particular design of our PCR, which relies on the presence of a *rrf* gene preceding the *rrs* gene, our PCR would retrieve only one out of the two *rrn* sequences from genomes with a tandem arrangement of canonical *rrn* operons. By inference, a major fraction of the sequence diversity discovered in the present work is likely to reflect the diversity of different bacteria rather than microheterogeneity of different *rrn* operons within the same genome. All of the above diversity analyses thus point towards an unexpectedly high diversity of cooccurring phylotypes of the newly discovered betaproteobacterial subcluster.

Whereas considerable microdiversity has been described for ribotype clusters of sulphate-reducing bacteria from salt marshes (Klepac-Ceraj *et al.*, 2004), for coastal bacterioplankton communities (Acinas *et al.*, 2004) and some open-ocean microbial groups (Rappé and Giovannoni, 2003), virtually nothing is known so far of the microdiversity patterns of chemocline microbial communities in lacustrine (Overmann *et al.*, 1999; Bosshard *et al.*, 2000; Casamayor *et al.*, 2000) and marine (Madrid *et al.*, 2001; Sass *et al.*, 2001; Vetriani *et al.*, 2003) habitats. As revealed by our analysis, 45 different and novel phylotypes of *Betaproteobacteria* cooccurred in the same 100 ml water sample and hence in the same chemocline microbial community sampled in the same year. Of the combined dataset, 53 of the phylotypes were closely related and exhibited a sequence divergence of < 3% (Fig. 4), indicating that chemoclines of freshwater lakes may provide a multitude of ecological niches not only for phylogenetically distant and physiologically different groups like sulfate-reducing bacteria, methanogenic archaea, purple and green sulfur bacteria or sulfur oxidizing *Gamma*- or *Epsilonproteobacteria* (Overmann *et al.*, 1999; Vetriani *et al.*, 2003) but also for phylogenetically much closely related groups of aquatic bacteria. It remains to be elucidated whether the considerable microdiversity is limited to the newly discovered subcluster of *Betaproteobacteria* or also occurs among the other phylogenetic groups present in the chemocline.

Comparison of the interoperon spacer sequences of all our clones revealed a much higher sequence variability as compared to that of the 16S rRNA gene sequences. Moreover, the length of IOS regions varied considerably, ranging between 195 bp as in the case of the central

bacterium of "*C. aggregatum*" to 466 bp in clone C1 from Lake Cisó (Fig. 6). The vast majority of interoperon spacers exhibited lengths between 340 and 349 bp.

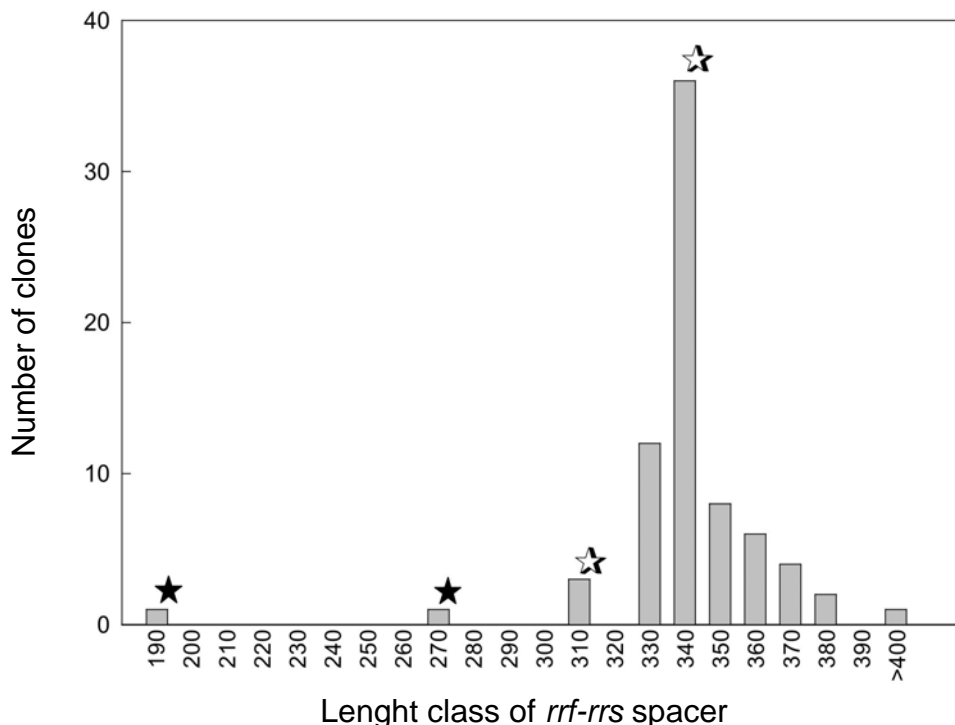


**Figure 6.** Frequency distribution of lengths of all *rrf-rrs* spacer sequences cloned in the present study. The lower boundary of each length class is indicated (i.e., 190 for the length class 190-199). Filled asterisks (★) mark the 195 bp long *rrf-rrs* spacer sequence of the central bacterium of "*C. aggregatum*" and the 276 bp long *rrf-rrs* spacer sequence of the central bacterium of the newly discovered green "*Chlorochromatium*". Hollow asterisks (☆), indicate the length classes of the four clones which potentially originate from the central bacterium of "*Pelochromatium roseum*".

### Identification of novel types of central symbionts of phototrophic consortia by FISH

One goal of the present investigation was to establish a method which permits a more selective retrieval of 16S rRNA gene sequences of the chemotrophic partner bacterium in phototrophic consortia and their phylogenetic relatives, and to subsequently analyse the phylogenetic relatedness of central bacteria originating from different types of phototrophic consortia.

We hypothesised that, if different phylotypes of central bacteria occur in different phototrophic consortia, they may exhibit a tandem arrangement of their *rrn* operons similar to the central bacterium of "*C. aggregatum*". Previous molecular analysis of the phototrophic consortia indigenous to Lake Dagow identified four different types, namely "*Chlorochromatium aggregatum*", "*Chlorochromatium magnum*", "*Pelochromatium roseum*" as well as "*Pelochromatium latum*" (Overmann *et al.*, 1998; Glaeser and Overmann, 2004). By comparison,

the number of sequence types with tandem *rrn* arrangement in this lake was estimated to be two orders of magnitude larger (193 - 235; see preceding section). Of this large diversity, 45 different phylotypes, corresponding to only about 19 - 23% were covered by our clone library, implying that the probability to recover sequences of central bacteria of consortia was rather small.

Most notably, however, the interoperon spacer sequence of the central bacterium of "*C. aggregatum*" was the shortest among all clones of our libraries (195 bp; Fig. 6). We therefore employed fluorescence *in situ* hybridization (FISH) to check whether other clones with unusually short IOS sequences (marked by asterisks in Fig. 6) possibly originated from the central bacteria of other phototrophic consortia. Accordingly, FISH oligonucleotide probes were designed targeting a 16S rRNA sequence of a clone with a 276 bp long IOS sequence (clone 27GS4, Fig. 4; probes 27GS4-208 and 27GS4-454, Supplementary table 2) and two sequences with a 318 bp long IOS sequence (clones D4a and 53GS2, Fig. 4; probe D4a-443, Supplementary table 2). However, the latter probe also detected two closely related sequences (38GS4, 66GS4) which were present in clones with a 347 bp-long IOS sequence. In order to also cover some additional 16S rRNA sequence types representing different phylogenetic affiliations and different lengths (343-375 bp) of the IOS sequence, the five oligonucleotide probes (D1-444, D2a-454, D2b-447, D3-210, D4b-453; Supplementary table 2) were constructed to target the five 16S rRNA sequence types D1, D2a, D2b, D3, D4b (Fig. 4). All probes were then applied to a sample from the chemocline of Lake Dagow obtained in the year 2006.

Six out of the seven FISH probes or probe combinations yielded a positive FISH result (Fig. 7A-F). Only sequence type D4b which had been detected in 1996 could not be found again in the chemocline community of the year 2006. Probes D1-444, D2a-454, D2b-447, D3-210 were observed to bind to long rod-shaped, short rod-shaped or coccal free-living planktonic bacteria (Fig. 7A-D). In contrast, the oligonucleotide probes targeting phylotypes with the shortest IOS sequences (clone 27GS4, clones D4a/53GS2) specifically hybridized to the central rod-shaped bacteria of phototrophic consortia (Fig. 7E,F). The two probes targeting clone 27GS4 hybridised to the central bacterium of a novel type of phototrophic consortium with green epibionts (Fig. 7F). Second, the probe targeting the sequence types D4a/53GS2/38GS4/66GS4 hybridised to the majority of the phototrophic consortia present in the chemocline of Lake Dagow. In Lake Dagow, "*Pelochromatium roseum*" represents the by far dominating type of consortium (Overmann *et al.*, 1998; Glaeser and Overmann, 2004). Therefore, it is concluded that D4a/53GS2/38GS4/66GS4 represent candidate sequences for this brown-coloured phototrophic consortium.

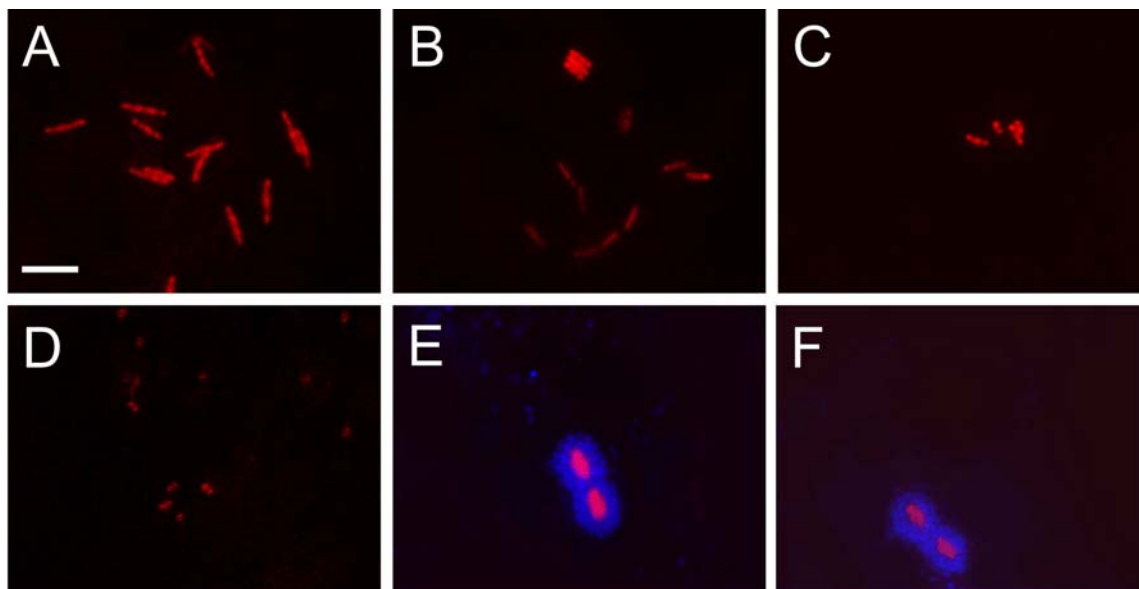


**Figure 7.** A–E. Specific detection of different phylotypes obtained in the DNA sample from Lake Dagow (1996). All probes were labelled with Cy3. A–D. Free-living *Betaproteobacteria* detected with probe DagowD1-444 (A) Dagow2a-454 (B) Dagow2b-447 (C) and Dagow3-210 (D). E. Overlay of DAPI and Cy3 fluorescence image after FISH employing probe Dagow4a-443. F. Overlay of DAPI and Cy3 fluorescence image after FISH employing the two different oligonucleotide probes Dagow27GS4-208 and Dagow27GS4-454. Bar = 10  $\mu$ m

Targeting specifically those environmental clones with a short intergenic spacer sequence of the tandem *rrn* operons thus resulted in the identification of two novel phylotypes of central bacteria in addition to the symbiont of "*Chlorochromatium aggregatum*". Interestingly, our comprehensive phylogenetic analysis demonstrated that the three known phylotypes of central bacteria (highlighted in Fig. 4) do not form a distinct group within the new subcluster of the *Betaproteobacteria*, indicating that these central bacteria of phototrophic consortia have a polyphyletic origin.

## Conclusions

All chemotrophic symbionts of phototrophic consortia identified so far are members of a newly discovered subcluster *Betaproteobacteria* with a tandem *rrn* operon organisation. Our combined phylogenetic analyses as well as the different bootstrap analyses imply that the chemotrophic symbiont of the novel green-coloured "*Chlorochromatium*" is most closely related to that of "*Pelochromatium roseum*". However, both these phylotypes are more closely related to free-living *Betaproteobacteria* like phylotypes D1, D2a, D2b or D3, rather than the central bacterium of "*Chlorochromatium aggregatum*" (Fig. 4). The current phylogeny of the chemotrophic partner bacteria therefore reveals a polyphyletic origin of these bacteria, similar to the phylogeny of their

phototrophic counterparts (Glaeser and Overmann, 2004). This suggests that the ability to form a symbiotic association with green sulfur bacteria either arose independently from different ancestors or, alternatively, may have been present in a common ancestor prior to the radiation of the newly discovered subcluster of *Betaproteobacteria* and a transition to the free-living state in independent lineages.

## Experimental Procedures

### Source of organisms and genomic DNA extraction and enrichment

The enrichment culture of "*Chlorochromatium aggregatum*" was originally obtained from the eutrophic Lake Dagow (Brandenburg, eastern Germany; Fröstl and Overmann, 1998). Cultures were grown in K4 medium (Kanzler *et al.*, 2005) in 10 l glass bottles at 15 °C and under continuous illumination at 20  $\mu\text{mol quanta} \cdot \text{m}^{-2} \cdot \text{s}^{-1}$ . In order to create a homogenous light field, the glass bottles were wrapped in one layer of white paper and illuminated by four 25 W tungsten light bulbs which were placed at regular distances around the bottles. In contrast to the standard enrichment cultures, which frequently contain only a small number of intact "*C. aggregatum*" consortia, a dense monolayer biofilm of "*C. aggregatum*" formed on the walls of the vessels during four weeks of cultivation. This wall coating was harvested for DNA extraction and the supernatant discharged.

DNA was extracted by a standard protocol using CTAB (Ausubel, 1995). Briefly, cell pellets were resuspended in Tris/EDTA buffer containing 0.5% SDS and 100  $\mu\text{g proteinase K} \cdot \text{ml}^{-1}$ . After addition of NaCl and CTAB, the crude DNA was extracted with chloroform/isoamylalcohol, precipitated with isopropanol and finally washed with 70% (v/v) ethanol. Genomic DNA of the central bacterium was subsequently separated from that of accompanying bacteria using the CsCl-bisbenzimidazole equilibrium density centrifugation method established previously (Kanzler *et al.*, 2005). The efficiency of purification was checked against the chemotaxis enrichment method used in earlier investigations (Kanzler *et al.*, 2005) by amplifying the 16S rRNA gene fragments and separating them by denaturing gradient gel electrophoresis (Muyzer *et al.*, 1995). Whereas the chemotaxis enrichment method yields only a faint band of the 16S rRNA gene fragment of the central bacterium of "*C. aggregatum*", this fragment clearly dominated in DNA extracts from the monolayer biofilms after separation by density gradient centrifugation (Fig. 2, arrow).

Environmental genomic DNA was extracted from freshwater and sediment samples collected from Lake Dagow (in July 1996 and September 2006), Jones Lake (September 1998; Michigan,

USA), Silver Lake (September 1998; Wisconsin, USA), Lake Cisó (March 2005; near Girona, NE-Spain), mesotrophic prealpine Lake Starnberger See (March 2004; near Starnberg, S-Germany), oligotrophic alpine Walchensee (March 2004; near Kochel am See, S-Germany), from an alpine soil from Jochberg (February 2002; near Kochel am See, S-Germany) and a forest soil from Staudach (October 2005; near Starnberg, S-Germany). Genomic DNA from *Ralstonia eutropha* DSMZ 428 was used for reference.

### **PCR amplification, cloning of the rRNA operon**

The rRNA operon gene sequence was recovered by a combination of inverse PCR, the construction of specific PCR primers, and their subsequent utilization in PCR. Ten µg of genomic DNA were digested with KpnI (MBI Fermentas, St. Leon-Rot, Germany) overnight and the digest was purified with the QIAquick PCR-purification kit (Qiagen, Hilden, Germany). Within the 16S rRNA gene of the central bacterium, the KpnI restriction site is located at position 482-487 (*E. coli* numbering). Three µg of the resulting DNA fragments were diluted in 1.5 ml of Tris-buffer and circularised with 30 units T4 DNA ligase (MBI Fermentas) at 15 °C for 16 h. The DNA was then purified in a Centricon 100 ultrafiltration unit (Millipore, Eschborn, Germany) and concentrated to a final volume of 100 µl. Of the resulting DNA, 200 ng were applied in an iPCR amplification, which was performed in a GeneAmp 9700DNA thermal cycler (Applied Biosystems, Weiterstadt, Germany) and employing primers CR-442f and CR-207r (Kanzler *et al.*, 2005; Supplementary table 1) and AmpliTaq Gold polymerase (Applied Biosystems). Cycling conditions comprised 30 cycles with a denaturation step at 95 °C for 30 s, annealing at 51°C for 1 min, elongation at 72 °C for 4 min, and a final extension step at 72 °C for 10 min. In order to achieve a higher stringency of the iPCR, acetamide was added to a final concentration of 5% (Tuschak *et al.*, 2005).

Our analysis revealed a previously unknown tandem *rrn* operon structure for the central bacterium of "*Chlorochromatium aggregatum*". Three different approaches were used to confirm this result (compare Fig. 3). First, inverse PCR was repeated with the isoschizomeric enzyme Acc65I (MBI Fermentas) and the sequence of the resulting DNA fragments was compared to that of the first iPCR. Second, primers specifically targeting the novel 5S rRNA gene sequence (CR-5S-55f) were constructed based on the determined sequence (Supplementary table 1). This primer was combined with primer CR-1282r which targets the 16S rRNA gene sequence of the central bacterium (Kanzler *et al.*, 2005) and direct amplification trials were performed with genomic DNA from the central bacterium, using a step down PCR protocol with 40 cycles, which comprised a denaturation step at 95 °C for 30 s, annealing at 60°C (first 10 cycles), then at

55°C (following 30 cycles) for 1 min, elongation at 72 °C for 1 min, and a final extension step at 72 °C for 10 min. Third, a primer pair consisting of the *Betaproteobacteria*-specific primer  $\beta$ -23S-1027f (binding within the 23S rRNA gene; Manz *et al.*, 1992) and of CR-207r (Supplementary table 1) were used in a step down PCR protocol under the above conditions.

For the purpose of recovering the portion downstream of the 16S rRNA gene of the second *rrn* operon which in most bacteria includes the ITS1 and the 23S rRNA gene regions, genomic DNA from the central bacterium of "*C. aggregatum*" was amplified with primer  $\beta$ -23S-1027r and CR-1282f (Kanzler *et al.*, 2005). In this amplification, the step down PCR program included 10 cycles with denaturation at 94 °C for 30 s, primer annealing at 58 °C for 1 min and elongation at 72 °C for 2 min, followed by 30 cycles with the annealing temperature changed to 53 °C.

### **Analysis of natural bacterial communities**

In order to screen natural bacterial communities for the occurrence of *Betaproteobacteria* exhibiting a similar tandem *rrn* operon structure, we designed two primers,  $\beta$ -5S-30f and  $\beta$ -5S-44f (Supplementary table 1), which specifically target the 5S rRNA gene sequence of all known *Betaproteobacteria*. Each of these primers was combined with either the *Betaproteobacteria*-specific primer  $\beta$ -680r (Overmann *et al.*, 1999), universal primer 907r (Muyzer *et al.*, 1995) or eubacterial primer 1055r (Amann *et al.*, 1995) (Supplementary table 1). The step down PCR program for amplification included 10 cycles with denaturation at 94 °C for 30 s, primer annealing at 58 °C for 1 min and elongation at 72 °C for 2 min, followed by 30 cycles with the annealing temperature set to 53 °C.

All PCR products generated were examined by standard 1.4% (wt/vol) agarose gel electrophoresis and were cloned using the TOPO TA cloning kit (version R; Invitrogen, Carlsbad, CA). Plasmids were extracted with a QIAprep spin miniprep kit (Qiagen), and the presence of inserts was verified by digestion with EcoRI (MBI Fermentas). Two separate clone libraries were established for the Lake Dagow samples obtained in 1996 and 2006.

### **Sequencing and phylogenetic analyses**

PCR products were sequenced by the dideoxynucleotide method (Sanger *et al.*, 1977) using an ABI Prism 3730 genetic analyzer (Applied Biosystems) and the AmpliTaq FS Big Dye Terminator cycle sequencing kit according to the protocol of the manufacturer. The Vector NTI computer package was used for sequence assembly and editing (Invitrogen). Sequencing of the ITS1 region was accomplished by primer walking using four custom designed primers (CR-

ITS1-42f, CR-ITS1-90f, CR-23S-575r, and CR-23S-632r; Supplementary table 1). For covering the complete *rrn* tandem operon, primer walking was conducted with the following primers: CR-23S-2201r, CR-23S-2241r, CR-23S-1288f, CR-23S-1388f, CR-23S-1694f, CR-ITS2-52r (Supplementary table 1). All 16S rRNA gene sequences obtained in the present study were checked for possible chimeras by using the CHIMERA-CHECK online analysis program of the RDP-II database (Maidak *et al.*, 2001). No chimeras were identified.

tRNAs were identified using the program tRNAscan-SE, version 2.21 (Lowe and Eddy, 1997). Phylogenetic relationships were analysed using the software packages ARB (Ludwig *et al.*, 2004) and PHYLIP (Phylogeny Inference Package, version 3.57c; Felsenstein, 1989). Sequences of the phylogenetically closest relatives of the central bacterium and the obtained clones were retrieved from the GenBank database using BLAST version 2.0.4 (Altschul *et al.*, 1997) and imported into the ARB database. Phylogenetic trees were inferred using the maximum likelihood and maximum parsimony algorithms within the ARB package. Additionally, the distance-based methods DNADIST (Kimura) and FITCH were used.

To identify variable branching points, the phylogenetic trees generated were compared in a pairwise fashion employing the COMPARE TOPOLOGY function of the ARB program. Finally, the CONSENSE program implemented in the PHYLIP software package was applied to generate a consensus tree resulting from the three phylogenetic trees. For this comparison, the majority rule was employed. In addition, reproducibility of the branching pattern obtained with the three methods was tested by bootstrap analysis, generating a set of 100 resamplings. In a final step, the consensus tree as well as the bootstrap values were used to correct the maximum likelihood tree. Those branches which were observed to differ between the three tree-building methods and which had only low bootstrap support, were collapsed with deeper branching points to yield a polytomic consensus tree.

### **Coverage and diversity estimates**

We attempted to estimate the diversity of *Betaproteobacteria* with tandem *rrn* operons cooccurring in a single bacterial community. A sample was obtained from the chemocline of Lake Dagow in the year 2006 and a clone library of partial *rrn* operons with a tandem structure was generated as described above. Clonal richness was calculated in EstimateS (Version8.0.0) (Colwell, 2005), using the Chao1 estimator (Chao, 1984). Additionally, we used the abundance based coverage estimator (ACE; Chao and Lee, 1992) to estimate minimum numbers of tandem *rrn* containing  $\beta$ -Proteobacteria in the chemocline of Lake Dagow. Sample order randomisation was set at 50 randomisations, and the coverage estimator was set at 12 (a setting of 2 did not

change the results). Chao analysis was done without bias correction, using the classic formula. All 16S rRNA gene sequences of this clone library were analysed with the Analytic Rarefaction 1.3 program (Holland, 2003).

### **Fluorescence *in situ* hybridisation (FISH)**

Fluorescence *in situ* hybridisation was used to assign environmental 16S rRNA gene sequences of *Betaproteobacteria* to the different bacterial morphotypes present in the chemocline of Lake Dagow with the specific aim to identify sequences of the central heterotrophic symbionts of phototrophic consortia among our sequence collection.

The sequences generated from the first clone library of Lake Dagow were used to design specific FISH probes with the DESIGN PROBES function of the ARB software package. The accessibility of the target sites were checked based on data available for *Escherichia coli* (Fuchs *et al.*, 1998). For probes targeting sites with limited accessibility, corresponding helper oligonucleotides (Fuchs *et al.*, 2000) were designed. Overall, 8 specific probes and 24 helper oligonucleotides were then used (Supplementary table 2) to analyse the chemocline bacterial community present in the chemocline of Lake Dagow in the year 2006. FISH was carried out on white polycarbonate filters (0.2 µm). Of each of the Cy3-labeled probe and the corresponding helper oligonucleotides, twenty nanograms were employed at the appropriate hybridisation stringency (Supplementary table 2). Hybridisation was conducted for 2h at 45 °C. Stringency was tested and optimised by varying the formamide concentrations between 5 and 35%. After counterstaining with 4',6-diamidino-2-phenylindole (DAPI), hybridisations were analysed by epifluorescence microscopy.

### **Nucleotide sequence accession numbers**

The tandem rRNA operon sequence of the central bacterium of "*C. aggregatum*" has been assigned the GenBank accession number EF203797. Partial sequences consisting of identically organized tandem *rrn* operons recovered from the investigated freshwater lakes have been deposited under accession numbers EF203798-EF203865 and EF219476.

### **Acknowledgements**

The authors are indebted to Dr. Hans-Peter Grossart for his kind support during field work and microscopy. We appreciate the samples supplied by Dr. Jesus Garcia-Gil and Dr. Frederic Gich (University of Girona) and Isabella Koch (University of Munich). This work was supported by the Deutsche Forschungsgemeinschaft through grants to J.O. (Ov 20/10-1 and 10-2).

## References

- Acinas, S.G., Klepac-Ceraj, V., Hunt, D.E., Pharino, C., Ceraj, I., Distel, D., and Polz, M.F. (2004) Fine-scale phylogenetic architecture of a complex bacterial community. *Nature* **430**: 551-554.
- Altschul, S.F., Madden, T.L., Schäffer, A.A., Zhang, J., Miller, W., and Lipman, D.J. (1997) Gapped BLAST and PSI-BLAST: a new generation of protein database search programs. *Nucleic Acids Res* **25**: 3389-3402.
- Amann, R., Ludwig, W., and Schleifer, K.-H. (1995) Phylogenetic identification and *in situ* detection of individual microbial cells without cultivation. *Microbiol Rev* **59**: 143-169.
- Ausubel, F.M. (1995) Current protocols in molecular biology. John Wiley, New York. pp. 2.4.4-2.4.5.
- Bosshard, P.P., Santini, Y., Grüter, D., Stettler, R., and Bachofen, R. (2000) Bacterial diversity and community composition in the chemocline of the meromictic alpine Lake Cadagno as revealed by 16S rDNA analysis. *FEMS Microbiol Ecol* **31**: 173-182.
- Caldwell, D.E., and Tiedje, J.M. (1975) A morphological study of anaerobic bacteria from the hypolimnia of two Michigan lakes. *Can J Microbiol* **21**: 362-376.
- Casamayor, E.O., Schäfer, H., Bañeras, L., Pedrós-Alió, C., and Muyzer, G. (2000) Identification of and spatio-temporal differences between microbial assemblages from two neighboring sulfurous lakes: comparison by microscopy and denaturing gradient gel electrophoresis. *Appl Environ Microbiol* **66**: 499-508.
- Chao, A. (1984) Nonparametric estimation of the number of classes in a population. *Scand JStat* **11**:265-270.
- Chao, A., and Lee, S.M. (1992) Estimating the number of classes via sample coverage. *J Am Statist Assoc* **87**:210-217.
- Chao, A, Ma, C.-M., and Yang, M.C.K. (1993) Stopping rules and estimations for recapture debugging with unequal failure rates. *Biometrika* **80**:193-201.
- Chen, H., Lim, C.K., Lee, Y.K., and Chan, Y.N. (2000) Comparative analysis of the genes encoding 23S-5S rRNA intergenic spacer regions of *Lactobacillus casei*-related strains. *Int J Syst Evol Microbiol* **50**: 471-478.
- Colwell, R.K. (2005) EstimateS: Statistical estimation of species richness and shared species from samples. Version 7.5. <http://purl.oclc.org/estimates>.
- Croome, R.L., and Tyler, P.A. (1984) Microbial microstratification and crepuscular photosynthesis in meromictic Tasmanian lakes. *Verh Int Verein Limnol* **22**: 1216-1223.

- Felsenstein, J. (1989) PHYLIP-phylogenetic interference package (version 3.2). *Cladistics* **5**:164–166.
- Fröstl, J.M., and Overmann, J. (1998) Physiology and tactic response of the phototrophic consortium "*Chlorochromatium aggregatum*". *Arch Microbiol* **169**: 129-135.
- Fröstl, J.M., and Overmann, J. (2000) Phylogenetic affiliation of the bacteria that constitute phototrophic consortia. *Arch Microbiol* **174**: 50-58
- Fuchs, B.M., Wallner, G., Beisker, W., Schwippl, I., Ludwig, W., and Amann, R. (1998) Flow cytometric analysis of the *in situ* accessibility of *Escherichia coli* 16S rRNA for fluorescently labeled oligonucleotide probes. *Appl Environ Microbiol* **64**: 4973-4982.
- Fuchs, B.M., Glöckner, F.O., Wulf, J., and Amann, R. (2000) Unlabeled helper oligonucleotides increase the *in situ* accessibility to 16S rRNA fluorescently labeled oligonucleotide probes. *Appl Environ Microbiol* **66**: 3603-3607.
- Gasol, J.M., Jürgens, K., Massana, R., Calderón-Paz, J.I., and Pedrós-Alió, C. (1995) Mass development of *Daphnia pulex* in a sulfide-rich pond (Lake Cisó). *Arch Hydrobiol* **132**:279-296.
- Glaeser, J., and Overmann, J. (2003) The significance of organic carbon compounds for *in situ* metabolism and chemotaxis of phototrophic consortia. *Environ Microbiol* **65**: 5089-5099.
- Glaeser, J., and Overmann, J. (2004) Biogeography, evolution, and diversity of epibionts in phototrophic consortia. *Appl Environ Microbiol* **70**:4821-4830.
- Gorlenko, V.M. (1988) Ecological niches of green sulfur and gliding bacteria. In *Green photosynthetic bacteria*. Olson, J.M., Ormerod, J.G., Amesz, J., Stackebrandt, E., and Trüper, H.G. (eds). Plenum Press, New York, London. p. 257-267.
- Holland, S.M. (2003) Analytic Rarefaction 1.3. <http://www.uga.edu/~strata/software/AnRareReadme.html>
- Kanzler, B.E.M., Pfannes, K.R., Vogl, K., and Overmann, J. (2005) Molecular characterization of the nonphotosynthetic partner bacterium in the consortium "*Chlorochromatium aggregatum*". *Appl Environ Microbiol* **71**: 7434-7441.
- Klepac-Ceraj, V., Bahr, M., Crump, B.C., Teske, A.P., Hobbie, J.E., Polz, M.F. (2004) High overall diversity and dominance of microdiverse relationships in salt marsh sulfate-reducing bacteria. *Environ Microbiol* **6**:686-698
- Krawiec, S., and Riley, M. (1990) Organization of the bacterial chromosome. *Microbiol Rev* **53**: 367-376.
- Lauterborn, R. (1906) Zur Kenntnis der sapropelischen Flora. *Allg Bot* **2**: 196-197.

- Lowe, T.M., and Eddy, S.R. (1997) tRNAscan-SE: a program for improved detection of transfer RNA genes in genomic sequence. *Nucleic Acids Res* **25**: 955-964.
- Ludwig, W., Strunk, O., Westram, R., Richter, L., Meier, H., Yadhukumar, Buchner, A., Lai, T., Steppi, S., Jobb, G., Förster, W., Brettske, I., Gerber, S., Ginhart A.W., Gross, O., Grumann, S., Hermann, S., Jost, R., König, A., Liss, T., Lüßmann, R., May, M., Nonhoff, B., Reichel, B., Strehlow, R., Stamatakis, A., Stuckmann, N., Vilbig, A., Lenke, M., Ludwig, T., Bode, A., and Schleifer, K.-H. (2004) ARB: a software environment for sequence data. *Nucleic Acids Res* **32**: 1363-1371.
- Madrid, V.M., Taylor, G.T., Scranton, M.I., and Chistoserdov, A.Y. (2001) Phylogenetic diversity of bacterial and archaeal communities in the anoxic zone of the Cariaco Basin. *Appl Environ Microbiol* **67**:1663-1674
- Maidak, B.L., Cole, J.R., Lilburn, T.G., Parker, C.T., Saxman, P.R., Farris, R.J., Garrity, G.M., Olsen, G.J., Schmidt, T.M., and Tiedje, J.M. (2001) The RDP-II (Ribosomal Database Project). *Nucleic Acids Res* **29**:173-174.
- Manz, W., Amann, R., Ludwig, W., Wagner, M., and Schleifer, K.H. (1992) Phylogenetic oligodeoxynucleotide probes for the major subclasses of proteobacteria: problems and solutions. *Syst Appl Microbiol* **15**: 593-600.
- Muyzer, G., Hottenträger, S., Teske, A., and Waver, C. (1995) Denaturing gradient gel electrophoresis of PCR-amplified 16S rDNA – a new molecular approach to analyse the genetic diversity of mixed microbial communities. In *Molecular microbial ecology manual*, 2<sup>nd</sup> edition. Akkermans, A.D.L., van Elsas, J.D., and de Bruijn, F.J. (eds.). Kluwer, Dordrecht, Netherlands. pp. 3.4.4.1. – 3.4.4.22.
- Overmann, J., and Tilzer, M.M. (1989) Control of primary productivity and the significance of photosynthetic bacteria in a meromictic kettle lake. Mittlerer Buchensee, West-Germany. *Aquatic Sciences* **51**: 261-278.
- Overmann, J., Tuschak, C., Frösth, J. M., and Sass, H. (1998) The ecological niche of the consortium "*Pelochromatium roseum*". *Arch Microbiol* **169**: 120-128.
- Overmann, J., Coolen, M.J.L., and Tuschak, C. (1999) Specific detection of different phylogenetic groups of chemocline bacteria based on PCR and denaturing gradient gel electrophoresis of 16S rRNA gene fragments. *Arch Microbiol* **172**: 83-94.
- Pfennig, N. (1980) Syntrophic mixed cultures and symbiotic consortia with phototrophic bacteria: a review. In *Anaerobes and anaerobic infections*. Gottschalk, G., Werner, H., and Pfennig, N. (eds). Fischer, Stuttgart, pp. 127-131.

- Rappé, M.S., and Giovannoni, S.J. (2003) The uncultured microbial majority. *Annu Rev Microbiol* **57**: 369-394.
- Sanger, F., Air, G.M., Barrel, G., Brown, N.L., Coulson, C.A., Fiddes, C.A., Hutchinson, C.A. Slocombe, P.M., and Smith, M. (1977) Nucleotide sequence of bacteriophage phi X174 DNA. *Nature* **265**: 687-695.
- Sass, A., Sass, H., Coolen, M.J.L., Cypionka, H., and Overmann, J. (2001) Microbial communities in the chemocline of a hypersaline deep-sea basin (Urania Basin, Mediterranean Sea). *Appl Environ Microbiol* **67**: 5392-5402.
- Srivastava, A.K., and Schlessinger, D. (1990) Mechanism and regulation of bacterial ribosomal RNA processing. *Annu Rev Microbiol* **44**: 105-129.
- Tuschak, C., Leung, M.M., Beatty, J.T., and Overmann J. (2005) The *puf* operon of the purple sulfur bacterium *Amoebobacter purpureus*: structure, transcription and phylogenetic analysis. *Arch Microbiol* **183**: 431-443.
- Vetriani, C., Tran, H.V., and Kerkhof, L.J. (2003) Fingerprinting microbial assemblages from the oxic/anoxic chemocline of the Black Sea. *Appl Environ Microbiol* **69**: 6481-6488.
- Vogl, K., Glaeser J., Pfannes, K.R., Wanner, G., and Overmann, J. (2006) *Chlorobium chlorochromatii* sp. nov., a symbiotic green sulfur bacterium isolated from the phototrophic consortium "*Chlorochromatium aggregatum*". *Arch Microbiol* **185**: 363-372.

**Supplementary table 1.** Oligonucleotide primers used for amplification and sequencing of different portions of the *rrn*-operons of *Betaproteobacteria*

Primer	Sequence (5'-3')	Target	Reference
CR-207r	CGC GCG AGG CCC TCT	16S rDNA	Kanzler <i>et al.</i> , 2005
CR-442f	ACG GAG CGA AAC AGC CTT	16S rDNA	Kanzler <i>et al.</i> , 2005
β-680r	TCA CTG CTA CAC GYG	16S rDNA	Overmann <i>et al.</i> , 1999
907r	CCG TCA ATT CCT TTG AGT TT	16S rDNA	Muyzer <i>et al.</i> , 1995
1055r	AGC TGA CGA CAG CCA T	16S rDNA	Amann <i>et al.</i> , 1995
CR-1282f	CCA TAA AGT CAG TCG	16S rDNA	Kanzler <i>et al.</i> , 2005
CR-ITS1-42f	ATC GGA AGG TGC GGC TGG	ITS1	this study
CR-ITS1-90f	GAC ACC CAC ACT TAT CGG	ITS1	this study
CR-23S-575r	AAT GTA AGT CGC TGA CCC	23S rDNA	this study
CR-23S-632r	ACG CCC TAT TCG GAC TCG	23S rDNA	this study
β-23S-1027r	GCC TCC CCA CTT CGT TT	23S rDNA	Manz <i>et al.</i> , 1992
CR-23S-1288f	AAG GTT TTC TAC GCA ACG	23S rDNA	this study
CR-23S-1388f	ACG TGT AGT GCG ATG TGG	23S rDNA	this study
CR-23S-1694f	TAG GTG AAG TCC CTA GCG	23S rDNA	this study
CR-23S-2201r	TCA AAC TGC CTA CCA TGC	23S rDNA	this study
CR-23S-2241r	TCG AAC TCC TCC GTT ACG	23S rDNA	this study
CR-ITS2-52r	AAC CAA TTT ACG GAG ATG	ITS2	this study
β-5S-30f	CCA CYC CTT CCC WTC CCG	5S rDNA	this study
β-5S-44f	TCC CGA ACA GGA CMG TGA AAC	5S rDNA	this study
CR-5S-55f	GGA CCG TGA AAC ACC TTC	5S rDNA	this study

"CR" denotes primers specific for the central rod-shaped bacterium of "*C. aggregatum*"; "β" indicates primers are specific for *β-Proteobacteria*. Within genes numbers at the end of each primer designation indicate binding position according to *E. coli* numbering. For primers targeting internal described spacers, numbers denote position on the actual sequence of the central bacterium.

**Supplementary table 2.** Fluorescently labelled probes, helper oligonucleotides and hybridisation conditions

Probe or helper <sup>a</sup>	Sequence (5'-3')	T <sub>m</sub> (°C)	Formamide (%)
<b>D1-444</b>	<b>GGC AGA CCT TTT CGC TCC</b>	<b>58.4</b>	<b>35</b>
D1-444-H1	GTA CAA AAG CAG TTT ACA ACC	54.1	
D1-444-H2	GTC ATG AGC CCA CCG TAT TAG	60.0	
D1-444-H3	GGT GCT TAT TCT TAC GGT ACC	58.0	
<b>D2a-454</b>	<b>ATC GTA TTA GGA CAG ACC</b>	<b>51.5</b>	<b>25</b>
D2a-454-H1	GTT TCG TTC CGT ACA AAA G	52.4	
D2a-454-H2	CGG TAC CGT CAT TAG CCC	58.4	
D2a-454-H3	AGC CGG TGC TTA TTC TTA	51.5	
<b>D2b-447</b>	<b>TAA AGA GAG CCT TTT CGC</b>	<b>51.5</b>	<b>5</b>
D2b-447-H1	TCC GTA CAA AAG CAG TTT AC	53.3	
D2b-447-H2	GTC ATG AGC CCC CTG TAT	56.1	
D2b-447-H3	GCT TAT TCT TAC GGT ACC	51.5	
<b>D3-210</b>	<b>CCA TTC GCG CGA GGC CCT</b>	<b>62.9</b>	<b>20</b>
D3-210-H1	GCG AGT CCC CCG CTT TCA TC	63.6	
D3-210-H2	GCT AAT CTG ATA TCG GCC GCT	60.0	
D3-210-H3	GAG CTT TTA CCC CAC CAA ACT	58.0	
<b>D4a-443</b>	<b>TAA AGC CTT TTC GCT CCG</b>	<b>53.8</b>	<b>25</b>
D4a-443-H1	TAC AAA AGC AGT TTA CAA CCC	54.0	
D4a-443-H2	TCA TTA GCC TTA AGT ATT AGT	50.1	
D4a-443-H3	GTG CTT ATT CTT ACG GTA CCG	58.0	
<b>D4b-453</b>	<b>CTT TAT TAG AGC CCA CCG</b>	<b>53.8</b>	
D4b-453-H1	TTT CGT TCC GTA CAA AAG CAG	56.0	
D4b-453-H2	GGT ACC GTC ATT AGC AGA	53.8	
D4b-453-H3	GCC GGT GCT TAT TCT TAC	53.8	
<b>27GS4-208</b>	<b>CAA TCG CGC AAG GCT TTT</b>	<b>53.8</b>	<b>10</b>
27GS4-208-H1	GCA AGT CCC CTG CTT TTA	53.8	
27GS4-208-H2	CTA ATC TGA TAT CGG CCA CTC	56.0	
27GS4-208-H3	AGC TTT TAC CTC ACC AAC TAG	56.0	
<b>27GS4-454</b>	<b>CTT TCC GTA TTA GTT AAA GCT</b>	<b>52.1</b>	<b>10</b>
27GS4-454-H1	TTT TCG CTC CGT ACA AAA G	52.5	
27GS4-454-H2	CTT ACG GTA CCG TCA TTA G	52.5	
27GS4-454-H3	TAG TTA GCG GGT GCT TAT T	52.5	

<sup>a</sup>Numbers indicate 5' - end according to *E. coli* numbering. Fluorescently labelled probes are denoted in bold. Helper oligonucleotides are denoted by the suffix "H".



## Discussion

### Isolation and phylogeny of the epibiont of “*Chlorochromatium aggregatum*”

The phototrophic consortium “*Chlorochromatium aggregatum*” from lake Dagow could be cultivated in the laboratory since 1998 (Fröstl and Overmann 1998). Due to improved cultivation techniques it was possible to isolate the symbiotic epibiont of the consortium in pure culture. The successful isolation was dependent on highly reducing conditions in deep agar media. This is not a unique property of the epibiont, it was also described to be essential for the isolation of two free living green sulfur bacteria, *Chl.* (formerly *Pelodictyon*) *phaeoclathratiforme* DSMZ 5477<sup>T</sup> (Overmann and Pfennig 1989) and a low-light-adapted *Chlorobium* (strain MN1) from the Black Sea (Overmann *et al.* 1992). The major properties of the new organism like gram-negative cell wall, presence of bacteriochlorophyll *c* and chlorosomes, and obligately phototrophic and anaerobic metabolism group the strain CaD within the family *Chlorobiaceae*. The phylogenetic analysis of the full-length 16S rRNA gene obtained confirmed this identification. Strain CaD is related to green sulfur bacteria of group 2 and 3 (group designations according to Imhoff 2003). Since all green sulfur bacteria of these groups belong to the genus *Chlorobium*, strain CaD is classified as a member of this genus. However, no close relationship was found to any strain cultured so far; the highest sequence similarity (94.6 %) was found to the 16S rRNA gene sequence of *Chlorobium phaeobacteroides* III.

### Photosynthetic pigments and physiological properties

Analysis of the carotenoid composition of the epibiont revealed 12 different carotenoids. By comparison to the strains previously investigated, strain CaD thus contains a significantly higher amount of highly hydrophobic carotenoids. Six compounds are unidentified and two of these unidentified compounds so far have only been detected in the epibiont. Specific features are the low concentrations of chlorobactene and the absence of its derivatives OH-chlorobactene glucoside, OH-chlorobactene, OH-chlorobactene glucoside laurate and 1',2'-dihydrochlorobactene. The distinct carotenoid composition of strain CaD suggests that the biosynthetic pathways of carotenoid biosynthesis are different from those found in other green sulfur bacteria.

The restricted range of organic substrates utilized for photomixotrophic growth is in agreement with the very limited physiological flexibility of other green sulfur bacteria. Contrary to the present results, the use of thiosulfate and atypical substrates like glycerol and malate was

reported for a culture obtained from “*C. aggregatum*” five decades ago (Mechsner 1957). It therefore seems to be likely that the earlier cultivation attempts did not result in a culture of the epibiont, but another type of green sulfur bacteria was cultured. 2-Oxoglutarate is known to be essential for the growth of “*C. aggregatum*” in enrichment culture (Frössl and Overmann 1998). After incubation with radioactively labeled 2-oxoglutarate microautoradiographic data demonstrated the incorporation of this substrate by intact consortia (Glaeser and Overmann 2003). Based on our present results, the isolated epibiont is not utilizing 2-oxoglutarate, however. It is therefore concluded that the uptake of 2-oxoglutarate observed for “*C. aggregatum*” is mediated by the central bacterium. Compared to free-living species of green sulfur bacteria which mostly show a pH optimum of 6.8 (Overmann 2001), the pH optimum of growth of the epibiont is slightly shifted towards the alkaline range. This may reflect an adaptation to the close association of the epibiont with the central rod in phototrophic consortia. The present results did not reveal conspicuous differences in the physiology of the epibiont in comparison to free-living green sulfur bacteria and therefore no particular physiological properties of symbiotic green sulfur bacteria could be identified. However it is the first epibiont of phototrophic consortia in pure culture named *Chlorobium chlorochromatii* strain CaD and this strain has a unique carotenoid composition.

Based on the pure culture of of *Chl. chlorochromatii* the molecular basis of symbiotic green sulfur bacteria was investigated.

### **Identification and transcription of candidate symbiosis genes in *Chl. chlorochromatii***

Since the physiology of free-living green sulfur bacteria and symbiotic green sulfur bacteria shows no conspicuous differences, genomic differences of symbiotic green sulfur bacteria and free-living green sulfur bacteria are expected and therefore suppression subtractive hybridization (SSH) should result in sequences specific for symbiosis. In order to reliably identify putative symbiosis-specific genes in the epibiont genome, suppression subtractive hybridization (SSH) included 16 free-living strains of green sulfur bacteria of different physiology (Overmann 2001b) which appeared promising since the members of this group are phylogenetically rather closely related (Overmann and Tuschak 1997).

The results demonstrate that such a mixture of genomic DNA from a larger number of related bacterial strains can be used as driver to recover unique genes of a single tester strain. The unique nature of the putative symbiosis-specific ORFs Cag0614, 0616, 1919 and 1920 were fully confirmed by subsequent *in silico* analyses of the eight available genome sequences of green

sulfur bacteria. SSH also resulted in several gene fragments with similarity to functional genes of free-living green sulfur bacteria. This result is explained by the fact that functional genes of green sulfur bacteria exhibit a larger sequence divergence than the 16S rRNA genes (Figueras *et al.* 2002), as exemplified by the weak dot blot hybridization of the ABC transporter. If sufficiently different, such functional genes will not be depleted during SSH.

Interestingly, the putative symbiosis genes were transcribed constitutively in both “*C. aggregatum*” and *Chl. chlorochromatii* in the free-living state. Therefore, either the regulation is posttranscriptional or expression of the ORFs is not regulated at all. More likely the expression of the ORFs is not regulated because proteins detected by autoradiography were also present in *Chl. chlorochromatii* and “*C. aggregatum*”. Since epibionts seem to be specifically adapted to the life in association with the central bacterium and have never been detected in the free-living state in nature (Glaeser and Overmann 2004), a regulation mechanism for the expression of the three potential symbiosis genes may actually be dispensable.

### **Sequence analysis of Cag0614, Cag0616 and Cag1920**

ORFs Cag0614 and 0616 show similarity to a putative hemagglutinin and contained numerous internal repeats. The high sequence similarity and similar structure of Cag0614 and Cag0616 suggests that these two ORFs arose through a gene duplication event. Contiguous repeats of several hundred amino acids are known for other hemagglutinin-like proteins (Ward *et al.* 1998). In addition, Cag0616 codes three arginyl-glycyl-aspartic acid tripeptides, and one Greek key motif. The RGD motif occurs in proteins (e.g., fibronectin) of the extracellular matrix of mammalian cells, in toxins of plant pathogenic fungi or in surface proteins of certain animal viruses, and mediates adhesion of cell surface receptors (Ruoslathi and Pierschbacher 1986; Isberg and Tran Van Nhie 1994; Tan *et al.* 2001; Senchou *et al.* 2004). In prokaryotes, the RGD motif is present in the integrin-binding proteins of pathogens like *Bordetella pertussis* that attach to mammalian cells (Isberg and Tran Van Nhieu 1994; Kajava *et al.* 2001). Based on their frequent involvement in host-pathogen-interactions, the three RGD tripeptides detected in ORF Cag0616 may participate in the cell-cell-binding of phototrophic consortia.

The Greek key motif is composed of four antiparallel beta strands and occurs as duplicate motif in vertebrate proteins of the  $\beta\gamma$ -crystallin superfamily. In bacteria, this motif was found in the spore coat protein S of *Myxococcus xanthus*, a metalloprotease inhibitor of *Streptomyces* and an extracellular protein of *Yersinia pestis* (Wistow 1990; Rajini *et al.* 2001; Jobby and Sharma 2005). These bacterial proteins have been assumed to participate in the response to stress

conditions. In contrast, the unique occurrence Cag0616 in the symbiotic *Chl. chlorochromatii* indicates that the  $\beta\gamma$ -crystallin-type gene product is involved in the symbiotic interaction. Duplicate Greek key motifs have been shown to bind two calcium ions (Rajini *et al.* 2001). Similarly, the gene product of Cag0616 may be stabilized by binding of  $\text{Ca}^{2+}$  ions.

Since the protein sequence with the closest similarity to Cag0616 was a putative hemagglutinin, we searched for additional properties of the putative gene product of Cag0616. The filamentous hemagglutinin adhesin (coded by *fhaB*) of *Bordetella pertussis* contains a binding site for sulfated glycolipids and a carbohydrate recognition domain besides its two RGD motifs (Kajava *et al.* 2001). Adhesion mediated through the lectine-like activity can be partially blocked by galactose (Isberg and Tran Van Nhieu 1994). In contrast, disaggregation studies did not yield any evidence for the participation of lectines in the cell-cell-interaction in “*C. aggregatum*” (Schlickerrieder 2002; Müller 2003).

Spanning 110,418 and 61,938 bp, respectively, the Cag0614 and Cag0616 are amongst the largest open reading frames known to date. Open reading frames of similar size have only been found in the cyanobacterium *Synechococcus* sp. RS9917 (RS9917\_01402; 84,534 bp). Since known hemagglutinins, like the products of the 10774 bp-long *fhaB* of *B. pertussis* (Domenighini *et al.* 1990) or of the 12,500 and 14,800 bp-long *lspA1* and *lspA2* of *Haemophilus ducreyi* (Ward *et al.* 1998) have been shown to be post-translational processed, only parts of ORFs Cag0614 and 0616 may actually be expressed in the epibiont of phototrophic consortia.

The analysis of ORF 1920 revealed the presence of a bacterial neuraminase repeat (BNR)/Asp box repeat which has been found in more than nine non-homologous protein families, including bacterial ribonucleases, sulfite oxidases, reelin, netrins, some lipoprotein receptors and a variety of glycosyl hydrolases. So far, few experimental data are available concerning the general functions of Asp boxes (Copley *et al.* 2001).

### **Sequence analysis of Cag1919 and calcium binding ability**

Contrary to the RTX-type toxin adenylate cyclase of *B. pertussis* which harbors a N-terminal pore-forming hydrophobic domain and a C-terminal secretion signal (Bauche *et al.* 2006), the gene products of Cag 1919 seems not to be secreted in the same way like RTX toxins and forms no transmembrane helices. Within the putative protein coded by Cag1919, a C-terminal hemolysin type  $\text{Ca}^{2+}$ -binding region with several RTX repeats and a region highly similar to the RTX-region in alkaline protease of *Pseudomonas aeruginosa* were detected. RTX toxins are typically found in Gram-negative pathogenic bacteria and this protein family is characterized by

repetitions of a nonapeptide motif, which includes a GGXGXD consensus motif. The protein family was detected in cytolytic toxins, metallo-dependent proteases, lipases and nodulation-associated proteins (Welch 1995). For the *Pasteurella* leukotoxin, it was demonstrated that the cell-binding domain and the lytic domain could be separated (Cruz *et al.*, 1990). Similarly, the catalytic domain of the adenylate cyclase of *B. pertussis* is also not required for cell binding (El-Azami-El-Idrissi *et al.* 2003). The binding of RTX toxins of pathogenic bacteria to the target cell involves  $\text{Ca}^{2+}$  ions (Ludwig *et al.* 1988; Knapp *et al.* 2003) which are bound at the GGXGDXLX repeats with low affinity (Rose *et al.*, 1995; Lillie *et al.* 2000). Our sequence comparisons and 3D modeling strongly indicates that the Cag1919 gene product forms a C-terminal beta roll which represents a bona fide  $\text{Ca}^{2+}$  binding structure. Based on the results of disaggregation studies (Schlickerrieder 2002; Müller 2003), it appears feasible that the RTX domain encoded by Cag1919 of *Chl. chlorochromatii* is involved in the cell-cell-adhesion between the partner bacteria of phototrophic consortia.

In Gram-negative bacteria,  $\text{Ca}^{2+}$  is also bound within the outer membrane bridging negatively charged phosphate groups of the lipopolysaccharides (LPS). Removal of divalent cations with chelating agents like EDTA can strip a fraction of the LPS from the cell surface and thereby destabilize the outer membrane (Jia *et al.* 2004). Although it cannot be completely excluded that this effect contributes towards the disaggregation of phototrophic consortia, the presence of several  $^{45}\text{Ca}^{2+}$ -binding membrane proteins in the epibiont was clearly demonstrated.

RT-PCR analyses of Cag1919 revealed that this ORF is transcribed over its entire length. The corresponding protein is expected to have a molecular mass of 155 kD, but was not detected by  $^{45}\text{Ca}^{2+}$  autoradiography on SDS gels. A possible reason is the abundance of the protein. At least 2  $\mu\text{g}$  of calcium binding protein can be detected with this method (Maruyama *et al.* 1984), which corresponds to 3% of the membrane proteins fraction. More likely, posttranslational processing and/or limited proteolysis of the Cag1919 gene product would result in the observed pattern of protein bands based on the following reasoning. For the adenylate cyclase toxin CyaA of *B. pertussis* it has been shown that the RTX domain is protected against trypsin proteolysis due to its particular structure (Bauche *et al.* 2006). The smallest  $^{45}\text{Ca}^{2+}$  binding protein detected in the membrane fraction of *Chl. chlorochromatii* had a molecular weight of 22 kD which is exactly the expected size of the RTX domain of Cag1919 (amino acid positions 1319 – 1526). The fact that the smallest protein band yielded the most prominent signal in the membrane fraction of *Chl. chlorochromatii* provides additional evidence for a high stability of this particular protein fragment. Furthermore, posttranslational processing of RTX-type proteins of other Gram-negative bacteria has been demonstrated and similarly may occur in the epibiont (Osicka *et al.* 2004)

### Origin of symbiosis genes of the epibiont

Obligately intracellular bacterial symbionts and pathogens are characterized by a reductive evolution of their genome (Cole *et al.* 2001; van Ham *et al.* 2003). In contrast, the genome size of epibiont *Chl. chlorochromatii* CaD (2.57 Mb) falls within the size range of all sequenced green sulfur bacterial genomes (1.97 – 4.44 Mb; [http://genome.jgi-psf.org/mic\\_home.html](http://genome.jgi-psf.org/mic_home.html)), which is commensurate with the capacity of the epibiont to grow also independently in the free-living state. *Vice versa*, an *in silico* subtractive hybridization analysis of the available genome sequences of green sulfur bacteria identified 188 additional ORFs to be unique for *Chl. chlorochromatii* CaD (data not shown), most of them coding for hypothetical proteins without any homology to sequences in free-living green sulfur bacteria. This number is considerably lower than the numbers of niche-specific genes in high-light-adapted (364 ORFs) and low-light-adapted *Prochlorococcus* strains (923 ORFs) (Rocap *et al.* 2003) and indicates that the adaptation to a symbiosis in phototrophic consortia does not require a large number of additional genes.

Most remarkably, the four putative symbiosis genes showed similarity to different types of virulence factors of typical bacterial pathogens. Genes underlying the adaptation of different evolutionary lineages are either differentially retained from the common ancestor, acquired through gene duplication and divergent evolution, or laterally transferred to an individual lineage from distantly related prokaryotes (Rocap *et al.* 2003). The four symbiosis-specific ORFs of *Chl. chlorochromatii* lack some of the properties thought to be characteristic for horizontally transmitted genes (Lawrence and Roth 1996; Lawrence and Ochman 1998; Jones *et al.* 2003). tRNA genes have been used to localize insertion events but are not present in the vicinity of the four ORFs in *Chl. chlorochromatii*. The G+C content of the symbiosis genes ranges from 42% GC up to 46% GC which is very similar to the *Chl. chlorochromatii* genome average of 44.3 mol% GC and hence cannot serve as evidence of horizontal gene transfer. Also, the codon usage of the symbiosis genes did not differ from that of the entire genome (data not shown).

While the putative gene products of ORFs Cag0614, 0616 and 1920 were only very distantly related to known proteins and could not be studied further, the pronounced similarity to amino acid sequences of the RTX-like protein coded by Cag1919 permitted a detailed phylogenetic analysis. The closest relatives are Ca<sup>2+</sup>-binding proteins from  $\gamma$ - and  $\delta$ -*proteobacteria*, indicating that *Chl. chlorochromatii* acquired at least the RTX-module from proteobacteria via a horizontal gene transfer event. This is further corroborated by the presence of a transposase (Cag1918) in close proximity to Cag1919 and 1920 which also suggests that both ORFs were laterally transferred during the same event.

In conclusion, the different lines of experimental evidence gathered in the present study provide the first indication that genetic modules known from proteobacterial pathogens of eukaryotes have been laterally transferred to nonrelated bacteria and are employed in symbiotic interactions between prokaryotes.

Besides the unique carotenoid composition and the putative symbiosis genes the epibiont of “*C. aggregatum*” shows obvious changes in the cellular morphology. Therefore the ultrastructure of “*C. aggregatum*” was investigated in detail.

### **Symbiosis-specific ultrastructure of the epibiont in “*C. aggregatum*”**

SEM and TEM micrographs revealed up to 150 nm-long hair-like filaments which covered the surface of the epibionts and formed an interconnecting network between the cells of “*C. aggregatum*”. Based on our SEM studies, these filaments occur exclusively on epibionts, suggesting that the interconnected epibionts form an elastic cage which encloses the central bacterium. This conclusion is also supported by the observation that the epibionts stay associated and around the central bacterium when consortia are subjected to shearing forces (by squeezing consortia on a glass slide with a cover slip, or by vacuum filtration of consortia through membrane filters) (Overmann and Schubert 2002).

Recent disgregation experiments with the consortium “*C. aggregatum*” (Schlickenrieder 2002; Müller 2003) demonstrated that cell-cell-aggregation is not susceptible to proteolysis with proteinase K, pepsin, trypsin, chymotrypsin, or to treatment with lysozyme, hyaluronidase,  $\beta$ -glucuronidase, indicating that typical extracellular capsule polysaccharides or easily degradable proteins are not involved in the cell-cell-binding. Extracellular appendages resembling the filaments seen on the epibiont surface have been identified as long carbohydrate chains of lipopolysaccharides (Graham and Beveridge 1990; Lam *et al.* 1992) and may therefore be also involved in the adhesion in phototrophic consortia.

The protuberances seen at the surface of epibionts of intact consortia also appeared at the cell surface of pure cultures of *Chl. chlorochromatii* when entering the stationary phase. The presence of protuberances on symbiotic epibiont cells indicates that their growth rate is strongly limited within phototrophic consortia. In fact, phototrophic consortia in the enrichment cultures exhibit a generation time which is twice as long as that of *Chl. chlorochromatii* growing under optimal conditions in pure culture (Fröstl and Overmann 1998; Chapter 2). It appears reasonable that the physiological activity of the central bacterium is one factor controlling the growth rate of the epibiont.

Underlying a typical outer membrane, peptidoglycan layer and cytoplasmic membrane at the contact site, the epibiont contact layer (ECL) clearly differs in ultrastructure from typical biomembranes. Auto-correlation of cross sections did not reveal a characteristic pattern, whereas oblique sections showed that the ECL is composed of regularly arranged elements, possibly globular proteins. Within "*C. aggregatum*" the ECL was invariably observed in all epibiont cells and always at the site of contact between the epibiont and the central bacterium, indicating that the ECL is an ultrastructure which is essential for symbiosis. In contrast, ECL-like structures were observed only in a small fraction of the cells from pure cultures, suggesting that biosynthesis of this ultrastructure in epibionts is subject to regulation and induced in the symbiotic state. Since chlorosomes were absent at the ECL and these gaps existed exclusively at these positions, intracellular sorting of chlorosomes seem to be likely in the epibiont.

#### **Interior substructures of the central bacterium in "*C. aggregatum*".**

The central bacterium crystalline structure (CBC) was found in varying number and orientation. Since they were primarily cytoplasmic structures their direct involvement in cell-cell adhesion is unlikely. The three dimensional organization of the CBC can be well reconstructed, mainly due to its large size and characteristic pattern in cross sections. Using FFT and auto-correlation, it was determined that the CBC is composed of two symmetrical layers of rather large subunits arranged in a regular hexagonal pattern at a spacing of 9 nm. Neighboring subunits are highly ordered, however, the orientation of the subunit axis ranges from 90° to 70° over larger distances. The crystalline structure of the CBC as well as the size of subunits suggest that the CBC is of a proteinaceous nature. Interestingly, the CBC structurally resembles the chemotaxis receptor Tsr of *Escherichia coli* (Weis *et al.* 2003; Lefman *et al.* 2004; Zhang *et al.* 2004; Zhang *et al.* 2007). In fact, overproduction of Tsr in *E. coli* resulted in internal membrane networks composed of stacks and tubular structures (Lefman *et al.* 2004) which resembled the membranous whirls discovered in the central bacterium of "*C. aggregatum*". However there is a fraction of CBC parallel to the cytoplasmic membrane and/or "central bacterium membrane layers" (CML). Due to resolution limits of ultrathin sections it cannot be shown beyond doubt if/how the CBC and CML are connected to each other. Although small CML look like a small CBC attached to the cytoplasmic membrane, they occur in some variations: i) single lamina (17 nm) and ii) laminae with thickness (30-35 nm) resembling the composition of bilayers typical for CBC. The electron dense line in the axis of symmetry is, however, absent in most CML. FFT and auto-correlation are impeded by the shortness of CML segments and their curvature. Auto-

correlation of tangential sections of CML is very difficult as only a few percent of sectioned consortia show CML that can be identified unequivocally and that are large enough for auto-correlation. As these small CML can occur isolated without contact to CBC and membranous whirls, it could be possible that they represent aggregation subunits of the CBC which have not yet reached final density/crystallinity. Based on the combined information gathered during the present investigation, we propose a model for the formation of CML and CBC. This preliminary model assumes that subunits with hydrophilic and hydrophobic poles are associated to the inner side of the cytoplasmic membrane with the hydrophobic poles oriented toward it. As subunits accumulate, a monolayer develops. Further association of subunits causes the formation of a bilayer, representing a metastable state due to the orientation of hydrophobic poles of one layer to the cytoplasm. When a critical bilayer size is reached, a transitional stage from CML to CBC occurs. The subunits dissociate from the cytoplasmic membrane and flip, re-orientating with their hydrophobic poles facing the bilayer interior and hydrophilic poles facing the cytoplasm. So far, however, possible connections between CML and the CBC could not be investigated due to resolution limits of ultrathin sections.

### **Implications of ultrastructural features**

Although knowledge on the physiology of the central betaproteobacterium so far is still rather limited, experimental data indicate that it incorporates external 2-oxoglutarate (Glaeser and Overmann 2003b). Theoretically, the tight arrangement of cells in phototrophic consortia as observed in SEM micrographs could lead to a diffusion limitation and hence a physiological isolation of the central bacterium. However, our TEM analyses, including the cryo-fixed and cryo-substituted preparations, revealed that considerable intercellular space exists between the cells. Based on volumetric calculations, the central bacterium only occupies 25% of the volume available. Together with the gaps left by the epibiont cells forming the cortex of the consortia, this extracellular space is likely to largely prevent the diffusion limitation of “*C. aggregatum*”.

A conspicuous feature of the intercellular space between the epibionts and the central bacterium were the periplasmic tubules which extended from the outer membrane of the central bacterium towards the cell surface of the epibionts. Together with the numerous papillae, these outer membrane ultrastructures results in a surface enlargement of 300% compared to a smooth membrane, as calculated from TEM tangential sections and SEM micrographs. Based on the close association between the periplasmic tubules and the outer membrane of the epibionts, the two partner bacteria may actually share a common periplasmic space.

Whereas the dimensions of chlorosomes in the epibiont of “*C. aggregatum*” are comparable to those of *Chlorobaculum tepidum* or *Chlorobium* sp. MN1 (Frigaard *et al.* 2003; Fuhrmann *et al.* 1993) their numbers were higher than the values reported for *Cba. tepidum* (200-250 chlorosomes·cell<sup>-1</sup>; Frigaard *et al.* 2003) and reached 150% of this value in symbiotic (374 chlorosomes·cell<sup>-1</sup>) and but only half in the free-living epibionts (121 chlorosomes·cell<sup>-1</sup>). Compared to the size of the cell the chlorosomes per  $\mu\text{m}^2$  cell surface under light saturation are almost equal in free-living epibionts and *Cba. tepidum* (53 respectively 51). Symbiotic epibiont cells grown at limiting light intensities reached coverage of 78 chlorosomes per  $\mu\text{m}^2$  cell surface. Based on these values, the epibiont does not represent one of the extremely low-light adapted members of the Green Sulfur Bacteria (Overmann *et al.* 1992; Fuhrmann *et al.* 1993; Manske *et al.* 2005) which is consistent with the observation that growth of pure epibiont cultures becomes light-saturated only at  $>10 \mu\text{mol}\cdot\text{m}^{-2}\cdot\text{s}^{-1}$  (Chapter 2) in contrast to low-light-adapted relatives which grow light-saturated above  $1 \mu\text{mol}\cdot\text{m}^{-2}\cdot\text{s}^{-1}$  (Overmann *et al.* 1992; Manske *et al.* 2005). Although phototrophic consortia inhabit low-light environments (Overmann *et al.* 1998), their limited adaptation to the *in situ* light intensities does not necessarily represent a disadvantage based on the following reasoning. Green sulfur bacteria are known to excrete considerable amounts of photosynthetically fixed organic carbon which has recently also been confirmed for the epibiont (Pfannes 2007) and it has been suggested that the epibiont supplies the central bacterium with these organic carbon excretion products (Glaeser *et al.* 2003b). Although the rate of anoxygenic photosynthesis per cell decreases under light-limiting conditions, the 16 epibiont cells together may still be able of maintaining a considerable rate of carbon supply for the single central bacterium in phototrophic consortia.

The CBC detected represents one of the most conspicuous ultrastructural elements of phototrophic consortia. It is therefore striking that the phylogenetically non-related multicellular magnetotactic bacteria have crystalline cytoplasmic structures – describes as “striated structures” (Silva *et al.* 2007) – which seem to be identical both in dimension and appearance to the CBC in phototrophic consortia. Although not explicitly described, in TEM micrographs published in Silva *et al.* 2007 a structure which resembles CML can be recognized. Their occurrence in nonrelated bacteria forming multicellular associations suggests that the two structures are involved in prokaryotic cell-cell-interactions.

## Conclusions

In conclusion, the symbiotic green sulfur bacterium *Chlorobium chlorochromatii* strain CaD is the first epibiont of phototrophic consortia in pure culture and this strain has a unique carotenoid composition. The identification and analysis of four genes specific for *Chl. chlorochromatii* provide the first indication that genetic modules known from proteobacterial pathogens of eukaryotes have been laterally transferred to nonrelated bacteria and are employed in symbiotic interactions between prokaryotes. By comparison of intact consortia with epibiont cells in pure cultures, symbiosis-specific subcellular structures could be identified. These structures appear to be specific for phototrophic consortia and are likely to be involved in either the cell-cell-aggregation or in the physiological interaction in this most highly developed symbiosis between prokaryotes.

## References

- Bauche C, Chenal A, Knapp O, Bodenreider C, Benz R, Chaffotte A, Ladant D (2006) Structural and functional characterization of an essential RTX subdomain of *Bordetella pertussis* adenylate cyclase toxin. *J Biol Chem* 281:16914-16926
- Cole ST, Eiglmeier K, Parkhill J, James KD, Thomson NR, Wheeler PR, Honoré N, Garnier T, Churcher C, Harris D, Mungall K, Basham D, Brown D, Chillingworth T, Connor R, Davies RM, Devlin K, Duthoy S, Feltwell T, Fraser A, Hamlin N, Holroyd S, Hornsby T, Jagels K, Lacroix C, Maclean J, Moule S, Murphy L, Oliver K, Quail MA, Rajandream M-A, Rutherford KM, Rutter S, Seeger K, Simon S, Simmonds M, Skelton J, Squares R, Squares S, Stevens K, Taylor K, Whitehead S, Woodward JR, Barrell BG (2001) Massive gene decay in the leprosy bacillus. *Nature* 409:1007-1011
- Copley RR, Russell RB, Ponting CP (2001) Sialidase-like Asp-boxes: sequence-similar structures within different protein folds. *Protein Science* 10:285-292
- Cruz WT, Young R, Chang YF, Struck DK (1990) Deletion analysis resolves cell-binding and lytic domains of the *Pasteurella* leukotoxin. *Mol Microbiol* 4:1933-1939
- Domenighini M, Relman D, Capiou C, Falkow S, Prugnola A, Scarlato V, Rappuoli R (1990) Genetic characterization of *Bordetella pertussis* filamentous haemagglutinin: a protein processed from an unusually large precursor. *Mol Microbiol* 4:787-800
- El-Azami-El-Idrissi M, Bauches C, Loucka J, Osicka R, Sebo P, Ladant D, Leclerc C (2003) Interaction of *Bordetella pertussis* adenylate cyclase with CD11b/CD18. *J Biol Chem* 278:38514-38521
- Figueras JB, Cox RP, Højrup P, Permentier HP, Miller M (2002) Phylogeny of the PscB reaction center protein from green sulfur bacteria. *Photosynthesis Res* 71: 155-164
- Frigaard NU, Chew AGM, Li H, Maresca JA, Bryant DA. (2003) *Chlorobium tepidum*: insights into the structure, physiology, and metabolism of a green sulfur bacterium derived from the complete genome sequence. *Photosynth Res* 78:93-117
- Fröstl J, Overmann J (1998) Physiology and tactic response of "*Chlorochromatium aggregatum*". *Arch Microbiol* 169:129-135
- Fuhrmann S, Overmann J, Pfennig N, Fischer U (1993) Influence of vitamin B<sub>12</sub> and light on the formation of chlorosomes in green- and brown-colored *Chlorobium* species. *Arch Microbiol* 160:193-198
- Glaeser J, Overmann J (2003b) The significance of organic carbon compounds for *in situ* metabolism and chemotaxis of phototrophic consortia. *Environ Microbiol* 5:1053-1063
- Glaeser J, Overmann J (2003b) The significance of organic carbon compounds for *in situ* metabolism and chemotaxis of phototrophic consortia. *Environ Microbiol* 5:1053-1063
- Glaeser J, Overmann J (2004) Biogeography, evolution, and diversity of epibionts in phototrophic consortia. *Appl Environ Microbiol* 70:4821-4830
- Graham LL, Beveridge TJ (1990) Evaluation of freeze-substitution and conventional embedding protocols for routine electron microscopic processing of eubacteria. *J Bacteriol* 172:2141-2149
- Imhoff JF (2003) Phylogenetic taxonomy of the family *Chlorobiaceae* on the basis of 16S rRNA and *fmo* (Fenna-Matthews-Olsen protein) gene sequence. *Int J System Evol Microbiol* 53:941-951

- Isberg RR, Tran Van Nhieu G (1994) Binding and internalization of microorganisms by integrin receptors. *Trends Microbiol* 2:10-14
- Jia W, Zoeiby AE, Petruzzello TN, Jayabalasingham B, Seyedirashti S, Bishop RE (2004) Lipid trafficking controls endotoxin acylation in outer membranes of *Escherichia coli*. *J Biol Chem* 279:44966-44975
- Jobby MK, Sharma Y (2005) Calcium-binding crystallins from *Yersinia pestis*. *J Biol Chem* 280:1209-1216
- Jones H, Ostrowski M, Scanlan DJ (2006) A suppression subtractive hybridization approach reveals niche-specific genes that may be involved in predator avoidance in marine *Synechococcus* isolates. *Appl Environ Microbiol* 72:2730-2737
- Kajava AV, Cheng N, Cleaver R, Kessel M, Simon MN, Willery E, Jacob-Dubuisson F, Locht C, Steven AC. (2001) Beta-helix model for the filamentous haemagglutinin adhesin of *Bordetella pertussis* and related bacterial secretory proteins. *Mol Microbiol* 42:279-292
- Knapp O, Maier E, Polleichtner G, Masin J, Sebo P, Benz R (2003) Channel formation in model membranes by the adenylate cyclase toxin of *Bordetella pertussis*: Effect of calcium. *Biochemistry* 42:8077-8084
- Lam JS, Graham LL, Lightfoot J, Dasgupta T, Beveridge TJ (1992) Ultrastructural examination of the lipopolysaccharides of *Pseudomonas aeruginosa* strains and their isogenic rough mutants by freeze-substitution. *J Bacteriol* 174:7159-7167
- Lawrence J G, Ochman H (1998) Molecular archaeology of the *Escherichia coli* genome. *Proc Natl Acad Sci USA* 95:9413-9417
- Lawrence JG, Roth JR (1996) Selfish operons: horizontal transfer may drive the evolution of gene clusters. *Genetics* 143:1843-1860
- Lefman J, Zhang P, Hirai T, Weis RM, Juliani J, Bliss D, Kessel M, Bos E, Peters PJ, Subramaniam S (2004) Three-dimensional electron microscopic imaging of membrane invaginations in *Escherichia coli* overproducing the chemotaxis receptor Tsr. *J Bacteriol* 186:5052-5061
- Lilie H, Haehnel W, Rudolph R, Baumann U (2000) Folding of a synthetic parallel beta-roll protein. *FEBS Lett* 470:173-177
- Ludwig A, Jarchau T, Benz R, Goebel W (1988) The repeat domain of *Escherichia coli* haemolysin (Hyl A) is responsible for its Ca<sup>2+</sup>-dependent binding to erythrocytes. *Mol Gen Genet* 214:553-561
- Manske AK, Glaeser J, Kuypers MMM, Overmann J (2005) Physiology and phylogeny of green sulfur bacteria forming a monospecific phototrophic assemblage at 100 m depth in the Black Sea. *Appl Environ Microbiol*. 71:8049-8060
- Mechsner K (1957) Physiologische und morphologische Untersuchungen an Chlorobacterien. *Arch Mikrobiol* 26:32-51
- Müller M (2003) Physiologie und Morphologie von phototrophen Konsortien. Diplomarbeit, Universität München
- Osicka R, Prochazkova K, Sulc M, Linhartova I, Havlicek V, Sebo P (2004) A novel “clip-and-link” activity of repeat in toxin (RTX) proteins from gram-negative pathogens. *J Biol Chem* 279:24944-24956

- Overmann J (2001a) Green sulfur bacteria. In: Boone DR, Castenholz RW, Garrity GM (eds) *Bergey's Manual of Systematic Bacteriology* 2nd ed. Springer, New York, pp 601-605
- Overmann J (2001b) Phototrophic consortia. A tight cooperation between non-related eubacteria. In: Seckbach J (ed) *Symbiosis. Mechanisms and model systems*. Kluwer, Dordrecht, pp. 239-255
- Overmann J, Cypionka H, Pfennig N (1992) An extremely low-light-adapted phototrophic sulfur bacterium from the Black Sea. *Limnol Oceanogr* 32:150-155
- Overmann J, Pfennig N (1989) *Pelodictyon phaeoclathratiforme* sp. nov., a new brown-colored member of the *Chlorobiaceae* forming net-like colonies. *Arch Microbiol* 152:401-406
- Overmann J, Tuschak C (1997) Phylogeny and molecular fingerprinting of green sulfur bacteria. *Arch Microbiol* 167: 302-309
- Pfannes KR (2007) Characterization of the symbiotic bacterial partners in phototrophic consortia. Ph.D. Dissertation, Universität München
- Rajini B, Shridas P, Sundari CS, Muralidhar D, Chandani S, Thomas F, Sharma Y (2001) Calcium binding properties of  $\gamma$ -crystallin. *J Biol Chem* 276:38464-38471
- Rocap G, Larimer FW, Lamerdin J, Malfatti S, Chain P, Ahlgren NA, Arellano A, Coleman M, Hauser L, Hess WR, Johnson ZI, Land M, Lindell D, Post AF, Regala W, Shah M, Shaw SL, Steglich C, Sullivan MB, Ting CS, Tolonen A, Webb EA, Zinser ER, Chisholm SW (2003) Genome divergence in two *Prochlorococcus* ecotypes reflects oceanic niche differentiation. *Nature* 424:1042-1046
- Rose T, Sebo P, Bellalou J, Ladant D (1995) Interaction of calcium with Bordetella pertussis adenylate cyclase toxin. Characterization of multiple calcium-binding sites and calcium-induced conformational changes. *J Biol Chem* 270:26370-26376
- Ruoshlati E, Pierschbacher MD (1986) Arg-Gly-Asp: a versatile cell recognition signal. *Cell* 44:517-518
- Schlickerrieder M (2002) Wachstum, Aktivität und Zell-Zell-Interaktion von "*Chlorochromatium aggregatum*". Diplomarbeit, Universität München
- Senchou V, Weide R, Carrasco A, Bouyssou H, Pont-Lezica R, Govers F, Canut H (2004) High affinity recognition of a *Phytophthora* protein by *Arabidopsis* via an RGD motif. *Cell Mol Life Sci* 61:502-509
- Silva KT, Abreu F, Almeida FP, Neumann Keim C, Farina M, Lins U (2007) Flagellar apparatus of south-seeking many-celled magnetotactic prokaryotes. *Microsc Res Tech* 70:10-17
- Tan BH, Nason E, Staeuber N, Jiang W, Monastyrskaya K, Roy P (2001) RGD tripeptide of bluetongue virus VP7 protein is responsible for core attachment to *Culicoides* cells. *J Virol* 75:3937-3947
- van Ham RCHJ, Kamerbeek J, Palacios C, Rausell C, Abascal F, Bastolla U, Fernández JM, Jiménez L, Postigo M, Silva FJ, Tamames J, Viguera E, Latorre A, Valencia A, Morán F, Moya A (2003) Reductive genome evolution in *Buchnera aphidicola*. *Proc Natl Acad Sci* 100:581-586
- Ward CK, Lumbly SR, Latimer JL, Cope LD, Hansen EJ (1998) *Haemophilus ducreyi* secretes a filamentous hemagglutinin-like protein. *J Bacteriol* 180:6013-6022

- Weis RM, Hirai T, Chalah A, Kessel M, Peters PJ, Subramaniam S (2003) Electron microscopic analysis of membrane assemblies formed by the bacterial chemotaxis receptor Tsr. *J Bacteriol* 185:3636-3643
- Welch RA (1995) Phylogenetic analyses of the RTX toxin family. In Roth JA, Bolin CA, Brogden KA, Minion FC, Wannemuehler MJ (eds) *Virulence mechanisms of bacterial pathogens* 2nd ed. ASM press, Washington DC, pp 195-206
- Wistow G (1990) Evolution of a protein superfamily: relationship between vertebrate lens crystallins and microorganism dormancy proteins. *J Mol Evol* 30:140-145
- Zhang P, Bos E, Heymann J, Gnaegi H, Kessel M, Peters PJ, Subramaniam S (2004) Direct visualization of receptor arrays in frozen-hydrated sections and plunge-frozen specimens of *E. coli* engineered to overproduce the chemotaxis receptor Tsr. *J Microsc* 216:76-83
- Zhang P, Khursigara CM, Hartnell LM, Subramaniam S (2007) Direct visualization of *Escherichia coli* chemotaxis receptor arrays using cryo-electron microscopy. *Proc Natl Acad Sci USA* 104:3777-3781



## Summary

The epibiont of the phototrophic consortium “*Chlorochromatium aggregatum*” was isolated in pure culture. This was the first time that a symbiotic green sulfur bacterium was isolated in pure culture indicating, that the symbiosis is not an obligate one with respect to the green sulfur bacterium. The phylogenetic affiliation revealed that the epibiont belongs to the genus *Chlorobium*, accordingly the isolate was named *Chlorobium chlorochromatii* strain CaD. The cells were gram-negative, nonmotile, rod-shaped, and contained chlorosomes. Strain CaD is obligately anaerobic and photolithoautotrophic, using sulfide as electron donor. Physiologically *Chlorobium chlorochromatii* exhibited no conspicuous differences to free-living green sulfur bacteria. The limited number of substrates photoassimilated was the same like in other green sulfur bacteria. The pH optimum was slightly shifted to the alkaline in contrast to free-living green sulfur bacteria, which probably represents an adaptation to the symbiotic association with the central bacterium. Photosynthetic pigments were bacteriochlorophylls *a* and *c*, and  $\gamma$ -carotene and OH-g-carotene glucoside laurate as dominant carotenoids. The unusual carotenoid composition for green sulfur bacteria indicates a different carotenoid biosynthesis in *Chl. chlorochromatii* in comparison to other green sulfur bacteria. The G+C content of genomic DNA of strain CaD is 46.7 mol %. On the basis of 16S rRNA sequence comparison, the strain is distantly related to *Chlorobium* species within the green sulfur bacteria phylum ( $\leq 94.6$  % sequence homology).

The pure culture of *Chl. chlorochromatii* enabled further studies on the molecular basis of the bacterial symbiosis of “*C. aggregatum*”. Suppression subtractive hybridization (SSH) against 16 free-living green sulfur bacteria revealed three different sequences unique to *Chl. chlorochromatii*. Dot blot analysis confirmed that these sequences are only present in *Chl. chlorochromatii* and did not occur in the free-living relatives. Based on the sequence information, the corresponding open reading frames in the genome sequence of *Chl. chlorochromatii* could be identified. Whereas the large ORF Cag0616 showed rather low similarity to a hemagglutinin, ORF Cag1920 codes for a putative calcium-binding hemolysin-type protein. The gene product of ORF Cag1919 is a putative RTX-like protein. Reverse transcriptase PCR of RNA isolated from free-living and symbiotic *Chl. chlorochromatii* demonstrated that all three ORFs are transcribed constitutively. The C-terminal amino acid sequence of Cag1919 comprises six repetitions of the consensus motif GGXGXD and is predicted to form a  $\text{Ca}^{2+}$  binding beta roll structure. The RTX-type protein is most likely involved in cell-cell-adhesion within the phototrophic consortium.  $^{45}\text{Ca}$  autoradiography exhibited calcium-binding proteins in

the membrane fraction of *Chl. chlorochromatii* in the free-living as well as the symbiotic state. On the other hand,  $\text{Ca}^{2+}$  binding proteins were absent in the cytoplasm of *Chl. chlorochromatii* and in both fractions of *Chlorobaculum tepidum*. The proteins detected by autoradiography were considerably smaller in size than predicted from the size of ORF Cag1919. The amino acid sequence of the RTX-type C-terminus coded by Cag1919 is similar to those of a considerable number of RTX-modules in various proteobacterial proteins, suggesting that this putative symbiosis gene has been acquired via horizontal gene transfer from a proteobacterium.

An improved cultivation method to selectively grow intact consortia in a monolayer biofilm was the precondition for understanding the complex interaction between epibionts and the central bacterium on the morphological basis. Therefore detailed ultrastructural investigations combining high resolution analytical SEM, TEM, 3D reconstruction and image analysis were performed to provide a structural model for phototrophic consortia. The coherence of the consortia is most likely achieved by long carbohydrate chains of lipopolysaccharides which interconnect mainly the epibionts and to some extent the central bacterium. Numerous periplasmic tubules, formed from the outer membrane of the central bacterium are in direct contact to the epibionts, resulting in a common periplasmic space which is interpreted to be important for exchange of substances. In the epibionts the attachment site to the central bacterium is characterized by absence of chlorosomes and a single contact layer (epibiont contact layer, ECL) with a thickness of 17 nm attached to the inner side of the cytoplasmic membrane of each epibiont. The ECL is also observed in pure cultures of the epibiont, however, only in about 10-20% of the cells. A striking feature of the central bacterium is the occurrence of hexagonally packed flat crystals (central bacterium crystal, CBC) which are variable in size (up to 1  $\mu\text{m}$  long) and in number (statistically, 1.5 per cell), and are formed by bilayers of subunits with a spacing of 9 nm. Deducing from serial sections, the CBC is interpreted to derive from accumulation of subunits on the inner side of the cytoplasmic membrane (or membranous invaginations), first forming a monolayer (central bacterium membrane layer; CML) and subsequently forming a bilayer of 35 nm, which can be freely orientated within the cytoplasm (CBC). Comparing structural details with published data, the CBC resembles a chemosensor.

# I. Danksagung

An dieser Stelle möchte ich mich bei Herrn Prof. Dr. Jörg Overmann für die Bereitstellung dieses spannenden Themas und die gute wissenschaftliche Betreuung während der Doktorarbeit bedanken.

Großer Dank gilt ebenfalls Herrn Prof. Dr. Gerhard Wanner für die elektronenmikroskopischen Untersuchungen phototropher Konsortien, die interessanten und anregenden wissenschaftlichen Diskussionen. Desweiteren bedanke ich mich bei Ihm und seiner Arbeitsgruppe (insbesondere bei Frau Dr. Elizabeth Schroeder-Reiter und Frau Dobler) für die herzliche Aufnahme und vielfältige Unterstützung.

Der gesamten AG Overmann danke ich aufrichtig für die schöne Zeit während der Doktorarbeit, dabei besonders Frau Dr. Karin Schubert, die im Labor durch ihr umfangreiches Wissen immer einen guten Ratschlag parat hatte. Hervorheben möchte ich auch alle, die mit mir am Konsortienprojekt gearbeitet haben, den Schreibraum oder das Kellerlabor teilten. Der Weg in den Keller wurde mir vor allem durch meine drei ersten Kellerkolleginnen Beate Beahammer, Dr. Katja Sichau und Kerstin Zikeli erleichtert.

Meinen Mitdotorandinnen Ann Manske, Isabella Koch und Kristina Pfannes, die die längste Zeit meiner Doktorarbeit mit mir verbrachten, möchte ich für geteilte Freude und Frust danken.

Der größte Dank gilt meinen Eltern und Geschwistern, die mich nicht nur während meiner Doktorarbeitszeit unterstützt haben.

## II. Lebenslauf

Name:	Kajetan Josef Vogl
Geburtsdatum:	09.09.1975
Geburtsort:	München
09/1982 – 07/1986	Volksschule an der Schulstraße, Eichenau
09/1986 – 06/1995	Städtisches Luisengymnasium, München
06/1995	Abitur
09/1995 – 09/1996	Zivildienst als Pflegediensthelfer auf der Urologischen Station des Kreiskrankenhauses Fürstfeldbruck
09/1996 – 08/2002	Studium der Biologie an der Ludwig-Maximilians-Universität München
11/2001 – 08/2002	Diplomarbeit an der Ludwig-Maximilians-Universität München mit dem Thema "Molekularbiologische und physiologische Charakterisierung phototropher Konsortien und deren Epibionten"
seit 10/2002	Promotion an der Ludwig-Maximilians-Universität München mit dem Thema " <i>Chlorochromatium aggregatum</i> " – molecular basis of a bacterial symbiosis